Immune system modulation in the brain injury of the metallothionein-I/II null mutant mouse

by
Michael W. Pankhurst, BSc(Hons)

Submitted in fulfilment of the
requirements for the Degree of
Doctor of Philosophy

University of Tasmania | January, 2011

Declaration of originality

This thesis contains no material which has been accepted for a degree or diploma by the University or any other institution, except by way of background information and duly acknowledged in the thesis, and to the best of the candidate's knowledge and belief no material previously published or written by another person except where due acknowledgement is made in the text of the thesis, nor does the thesis contain any material that infringes copyright.

Michael W. Pankhurst

Statement of Authority of Access

This thesis may be made available for loan and limited copying in accordance with the Copyright Act 1968.

Michael W. Pankhurst

Abstract

Metallothionein-I/II (MT-I/II) is a 6-7 kDa, cysteine rich, zinc and copper binding protein. MT-I/II null mutant ($^{-/-}$) mice have an altered response to brain injury. Therefore, MT-I/II has been proposed to be a protective protein after brain injury but the mechanism by which it confers protection remains elusive. There is a possibility that MT-I/II has protective actions within the injured brain but MT-I/II also has the capacity to modulate the immune system which plays a role in the progression of brain injury. The aim of this thesis is to investigate the differences in the progression of brain injury between wild type and MT-I/II$^{-/-}$ mice with particular emphasis on the action of MT-I/II in organs peripheral to the central nervous system after brain injury. Using a cryolesion brain injury model, neuron death in MT-I/II$^{-/-}$ mice was prolonged at later stages of the brain injury (7 days post-injury) meanwhile it had ceased in wild type mice. In conjunction with this occurrence, the numbers of T cells infiltrating the injury site were significantly higher in MT-I/II$^{-/-}$ mice at 7 days post-injury. Chemokine mRNA synthesis was analysed to determine if MT-I/II$^{-/-}$ mice had altered chemotactic signals that may affect the rate of T cell infiltration but differences were rarely observed when compared to wild type mice. In MT-I/II$^{-/-}$ mice, circulating leukocytes showed no differences to wild type mice in the relative ratios of lymphocytes, neutrophils, monocytes or T cells. However, the absolute white blood cell count was significantly higher in the blood of MT-I/II$^{-/-}$ mice, but only at 7 days post-injury. MT-I/II$^{-/-}$ mice were also found to have lower levels of the marker of alternatively activated macrophages, Ym1, than wild type mice, both in macrophages in the brain and in monocytes in the blood after brain injury. Therefore, there appear to be several immune system differences between MT-I/II$^{-/-}$ mice and wild type mice after brain injury. To further investigate the role of MT-I/II after brain injury, MT-I and MT-II mRNA levels were quantified by reverse transcriptase PCR. An enzyme-linked immunoassay (ELISA) was developed to measure MT-I/II protein levels in brain and liver after brain injury. Both MT-I and MT-II mRNA levels increase at 1 day post-injury in brain and liver and are decreased by 7 days post-injury. MT-I/II protein in brain was highest at 1 day post-injury but in the liver was maximally expressed at 7 days post injury. This increase in hepatic MT-I/II protein resulted in a higher hepatic zinc content in wild type mice compared to MT-I/II$^{-/-}$ mice. Therefore these results suggest that brain injury induces a hepatic MT-I/II response which may be responsible for modulation of the essential trace metal, zinc after brain injury.

Acknowledgements

First and foremost, I would like to acknowledge my supervisors, Dr Roger Chung, Dr Matthew Kirkcaldie and Professor Adrian West, for their guidance into the work that constitutes the following thesis. Their experience has been invaluable during my candidature.

Shannon Ray, Dr Bill Bennett and Chris Butler deserve acknowledgement for the extra pairs of hands they provided during animal experiments, also to Dr Bill Bennett for lending his expertise in immunohistochemistry and to Chris Butler for his assistance with 4-parameter logistic modelling.

I'd like to thank my parents Dr Tish Pankhurst and Professor Ned Pankhurst for the corticosterone assays they performed and also for their continued support.

Thankyou to Karen Drysdale, Dr Heather McGee, Dr Ros Maley and Mark Cozens for the technical help they provided for the preparation and running of flow cytometry.

Thanks go to Carol Bussey for the provision of albumin buffer and clean clothes and Dr Fiona Poke for providing stimulated EL-4 T cell cDNA samples.

Thankyou to Dr Russel Thompson for providing statistical advice and teaching me the Box-Cox test.

Finally I'd like to acknowledge Dr David Gell and Andrew Measham for the assistance they provided with atomic absorption spectroscopy and Dr Brendan McMorran and Dr Gaetan Burgio for their assistance with the interpretation of haematological data.

List of Abbreviations

$^{-/-}$	Null mutant
$^{+/+}$	Wild type
aaMΦ	Alternatively activated macrophage
APTS	3-aminopropyltriethoxysilane
cAMP	Cyclic adenosine monophosphate
caMΦ	Classically activated macrophage
cGMP	Cyclic guanidine monophosphate
CMe-MT	Carboxyamidomethylated metallothionein
CNS	Central nervous system
DPI	Days post-injury
DTT	Dithiothreitol
EAE	Experimental Autoimmune encephalomyelitis
ELISA	Enzyme-linked immunosorbent assay
GAPDH	Glyceraldehyde phosphate dehydrogenase
HPLC	High-performance liquid chromatography
HRP	Horse raddish peroxidase
IA	Iodoacetamide
IDO	Indoleamine dioxygenase
IFN	Interferon
IgG	Immunoglobulin G
IL	Interleukin
iNOS	Inducible nitric oxide synthase
MT	Metallothionein
MT-I/II	Metallothionein isoforms I and II
MT-III	Metallothionein isoform III
MT-IV	Metallothionein isoform IV
mRNA	Messenger RNA
NT	Neurotrophin
PBMC	Peripheral blood mononuclear cell
RNS	Reactive nitrogen species
ROS	Reactive oxygen species
RT-PCR	Reverse transcriptase-polymerase chain reaction
Th1	Helper T cell type 1
Th2	Helper T cell type 2
TNF	Tumour necrosis factor

Table of Contents

Chapter 1– Introduction

1.0 Overview

Research into brain injury utilising animal models is mostly focused on events that occur within the site of injury or in the surviving tissue proximal to the injured region. This approach is logical and has allowed for the elucidation of several important processes that occur after brain injury that lead to continued cell death. For example, excitotoxicity is one such process that has been identified to account for continued neuron death after brain injury. Excitotoxicity is a self-perpetuating process caused by release of excitatory neurotransmitter from dying neurons that overstimulates surviving neurons in an uncontrolled manner and can cause neuronal exhaustion and death, which leads to further neurotransmitter release and thus exacerbates the problem (reviewed by Werner and Engelhard 2007). This uncontrolled activity in neurons places a large strain on neuronal mitochondria which generate large quantities of reactive oxygen species (ROS) and further contributes to neuronal damage (reviewed by Robertson et al. 2009). Both of these processes are generated by central nervous system (CNS) cells affected by brain injury. Another process that contributes to cell death after brain injury is the inflammatory response which has a component that originates in the injured CNS but is augmented by leukocytes that migrate into the CNS from the circulatory system. Inflammation in the injured brain is primarily mediated by inflammatory cytokines, small secreted signalling molecules, which are initially produced by resident CNS cells such as microglia and astrocytes (Liberto et al. 2004). Leukocytes also produce inflammatory cytokines but the fact that leukocytes are not found in the CNS at the time of injury demonstrates that there can be outside influences on the injured CNS. However, the study of the interaction between the injured CNS and the extraneural organs has received little attention. This is an important consideration because many of the transgenic animal models currently used to identify genes that influence brain injury have the genetic alteration in every cell in the body. The focus of this thesis is the investigation of brain injury in one such transgenic model; the metallothionein-I/II null mutant (MT-I/II$^{-/-}$) mouse. Metallothionein (MT)-I and metallothionein-II are two small zinc binding proteins that are expressed throughout the body that have neuroprotective properties. This introduction describes how MT-I and MT-II may influence the response to brain injury indirectly due to its interaction with the immune system. Furthermore, this interaction has the potential to occur outside the CNS because brain injury activates several processes in extraneural organs that can feedback on the injured brain.

1.1 Cellular arrangement of the immune privileged brain

1.1.1 Cellular Components of the Brain

Neurons are the highly specialised cells responsible for transmitting signals at high-speed around the central and peripheral nervous system. Neurons have a high metabolic rate and require strict control of the extracellular environment to maintain their functions. In addition to neurons, there are several classes of glial cell types in the brain. Astrocytes are the most numerous glial cell type in the brain (Kirchhoff et al. 2001) and their function is to provide metabolic support to neurons and maintain the extracellular environment including homeostasis of ion and extracellular neurotransmitter concentrations (Pekny and Nilsson 2005, Pellerin and Magistretti 1994, Ridet et al. 1997, Yong 1998). Thus, astrocytes are essential for the maintenance of neuronal function and survival in the CNS. In addition, to their support roles, it is becoming clear that astrocytes have influence upon neuronal signalling at synapses (Fellin and Carmignoto 2004, Fields and Stephens-Graham 2002, Vesce et al. 1999). Astrocytes also communicate with each other in response to synaptic activity, with calcium-mediated signals that propagate in extracellular waves rather than aligned along the axon-dendrite paths of neurons (Charles 1998, Guthrie et al. 1999, Vesce 1999). It is hypothesised that these mechanisms regulate the strength of the synaptic signals of neurons and may be an important regulator of synaptic plasticity. Oligodendrocytes are another glial cell type that modulate the speed of axonal signalling of neurons. Oligodendrocytes ensheathe sections of some axons in myelin at regular intervals which enables rapid saltatory conductance of action potentials (reviewed in Sherman and Brophy 2005). In the CNS parenchyma there also exist NG2 proteoglycan expressing ($NG2^+$) progenitor cells. It is poorly understood whether $NG2^+$ cells have a major role in the resting brain, or if they simply lie dormant until they are required to replace lost cells. Recently, it has been shown that there are two populations of $NG2^+$ cells, one with synaptic inputs capable of transmitting action potentials and one that is incapable (Káradóttir et al. 2008). Finally, microglia are considered the resident immune cells of the CNS. The developmental origin of microglia has been controversial with claims they originate from neuroectoderm, mesoderm and directly from the monocyte lineage (reviewed by Kaur et al. 2001). Microglia can be immuno-labelled by many macrophage markers and in certain situations can have very similar functions to macrophages such as phagocytosis and effecting an inflammatory response. In the developing brain, microglia are involved in the programmed cell death and

phagocytosis of neurons that occurs in normal brain development (Upender and Naegele 1999). In the resting brain, microglia are hypothesised to play a role in homeostasis and constantly monitor the CNS parenchyma with mobile, probing processes (reviewed by Hanisch and Kettenmann 2007, Raivich 2005). Microglia, surveying the functional state of synapses under normal brain conditions, may function in termination of dysfunctional synapses (Wake et al. 2009). However, microglia appear to have a greater impact on the CNS in stressful conditions such as injury and disease.

1.1.2 Immune privilege and blood-brain barrier as separate entities

The central nervous system is said to be immune privileged due to its inability to reject tissue allografts (reviewed by Simpson 2006). In most tissues the inflammatory response operates in a very destructive manner that is repaired later by regenerative processes. Regeneration after large scale cell death in the CNS consists almost entirely of replacement of lost tissue with astrocytes, a process known as glial scarring, which prevents the replacement and regeneration of neurons (reviewed by Tan et al. 2005). One possible role for the immune privilege of the CNS is to reduce the risk of inflammatory responses developing in the CNS that have the potential to cause irreversible damage. Investigation of the mechanisms of immune privilege in the CNS has increased in recent years. Previously, the lack of lymphatic vessels in the CNS has been proposed as a mechanism of immune privilege (reviewed by Carson et al. 2006) but it has been known for some time that trafficking of antigens from the CNS to regional lymph nodes does occur (Wekerle et al. 1987). It has since been demonstrated that drainage to cervical lymph nodes occurs via cranial nerves and could account for up to 50% of cerebrospinal fluid drainage in rats and sheep (Boulton et al. 1999, Walter 2006). Therefore the lack of lymphatic vessels in the CNS does not prevent drainage of cerebrospinal fluid to lymph nodes and is unlikely to play a significant part in immune privilege.

The term blood-brain barrier relates to the ability of CNS endothelial cells to prevent unregulated transport or diffusion of blood-borne molecules into the CNS. The blood-brain barrier is often credited as the structure that maintains immune privilege. However, the blood-brain barrier is only one part of the neurovascular unit (figure 1.1). It is actually other aspects of the neurovascular unit that appear responsible for maintaining immune privilege. The primary function of the blood-brain barrier is to maintain homeostasis in the ionic composition of cerebrospinal fluid and exclude

neurotoxic blood-borne molecules (Hawkins & Davis 2005). The blood-brain barrier consists of blood vessel endothelial cells that lack the fenestrations of normal endothelium and express surface proteins such as occludins, claudins and junctional adhesion molecules that form tight junctions between the membranes of endothelial cells to create an impassable barrier to many hydrophilic solutes (Ballabh et al. 2004, Hawkins and Davis 2005). Many molecules require active transport mechanisms to enter the CNS from the blood which allows the endothelial cells of the CNS to regulate the entry of various required metabolites (Pardridge 1998). In addition to providing a barrier to solutes, CNS blood vessel endothelial cells have the potential to regulate the entry of leukocytes into the CNS by altering the expression of surface adhesion molecules that are necessary for circulating leukocytes to anchor to before they can transmigrate across the endothelial layer (reviewed by Ley et al. 2007). Under normal conditions CNS endothelium does not readily allow leukocyte rolling or arrest (Piccio et al. 2002) which may contribute to the lack of leukocyte surveillance of the CNS parenchyma. Surface adhesion molecule expression by CNS endothelial cells is a separate process that helps to maintain immune privilege but is distinctly different to processes that maintain the blood-brain barrier.

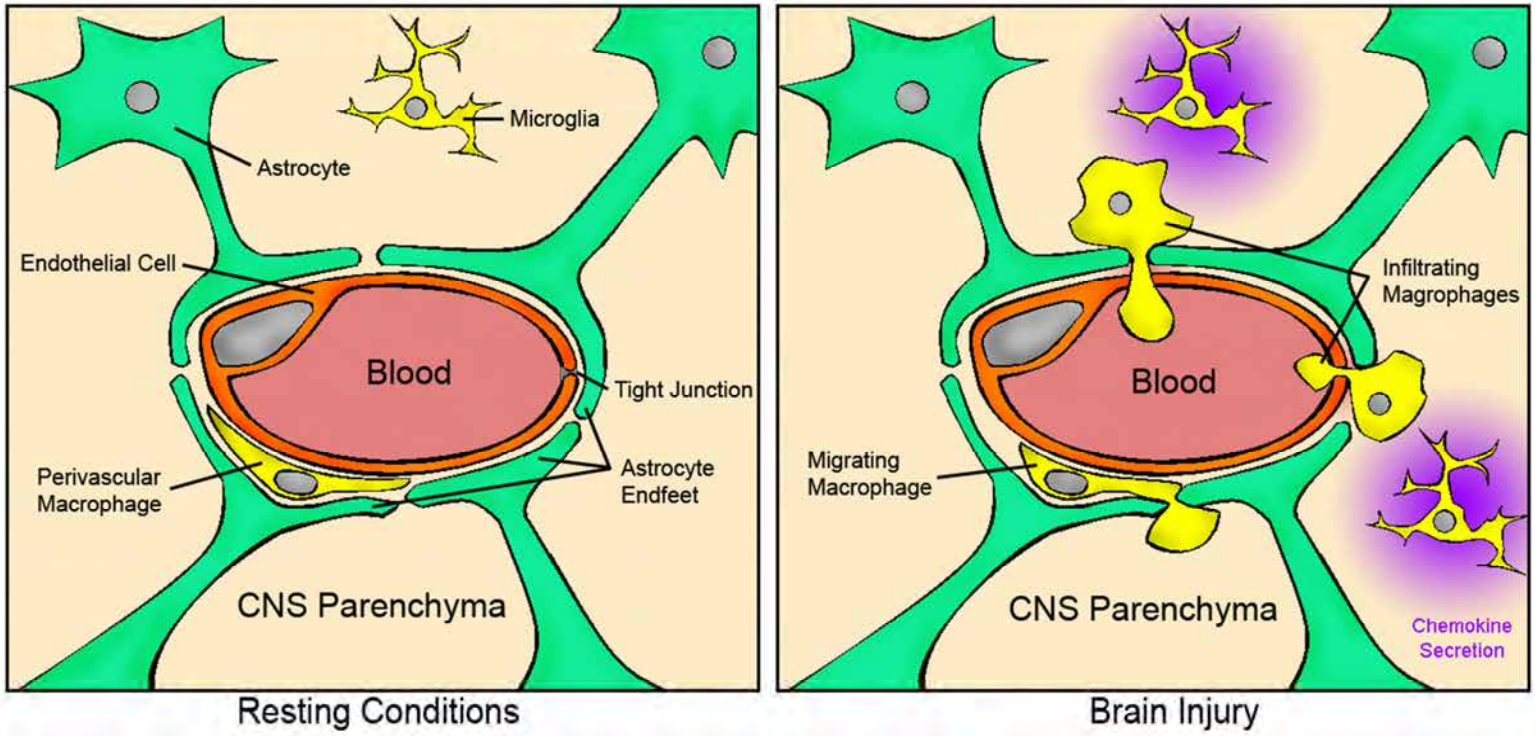

Figure 1.1 Adapted from Guilemin and Brew (2004) and Hawkins and Davis (2005). The neurovascular unit consists of blood vessels lined by endothelial cells and astrocytic endfeet that ensheathe the blood vessels from the abluminal side. The endothelial cells constitute the blood-brain barrier formed by tight junctions that exist wherever endothelial cell membranes meet. Astrocytic endfeet create a second barrier between the CNS parenchyma and the perivascular space known as the glia limitans. The glia limitans demarcates the beginning of the CNS parenchyma. Within the perivascular space reside perivascular macrophages. During brain injury, or other conditions that stimulate CNS inflammation, macrophages other leukocytes not shown here such as neutrophils and T cells, infiltrate the CNS parenchyma. Within the CNS parenchyma microglial secretion of chemokines creates a chemotactic signal that directs leukocyte migration. A consequence of this process is blood-brain barrier breakdown.

1.1.3 Additional mechanisms of immune privilege

Despite the immune privilege of the CNS under normal conditions, there are circumstances which permit leukocytes to migrate across the endothelium of CNS blood vessels. This phenomenon is observed when leukocytes infiltrate the CNS during autoimmune conditions such as multiple sclerosis and the experimental model of multiple sclerosis, experimental autoimmune encephalomyelitis (EAE). The inflammatory response and leukocyte infiltration also occurs in the CNS in response to a range of insults such as infection, physical injury and ischemia. Inflammatory cytokines activate sufficient expression of adhesion molecules on CNS endothelial cells to facilitate leukocyte rolling, arrest and diapedesis (Piccio et al. 2002). However, during CNS inflammation, leukocytes have been observed crossing the CNS endothelium but were retained within the perivascular space suggesting something was excluding these cells from the CNS parenchyma (Bartholomäus et al. 2009). Therefore it is apparent that cells inside the perivascular space encounter a second mechanism by which the CNS maintains immune privilege. T cells, which are important for mediating the adaptive immune response, can cross CNS endothelium but in order to do so, require prior activation via T cell receptor stimulation (Byram et al. 2004, Ling et al. 2006). T cells in the perivascular space require restimulation of their T cell receptor for their exit out of the perivascular space, into the CNS parenchyma (Archambault et al. 2005). Furthermore, continued stimulation of the T cell receptor is necessary for their persistence in the CNS parenchyma (Hickey et al. 1991). For successful T cell activation, the T cell receptor must be ligated to antigen presented on MHC class-II molecules in the presence of the costimulatory molecules B7.1 (CD80) or B7.2 (CD86) on the antigen presenting cell (reviewed in Davis et al. 2003, Dustin and Shaw 1999). In the murine CNS, microglia express low levels of MHC class-II molecules and the costimulatory molecules B7.1 or B7.2 (Santambrogio et al. 2001). It is likely that the low level of MHC class-II expression does not promote T cell persistence in the CNS because of the low capacity to present antigen and support T cell receptor stimulation. Should any T cell receptor stimulation occur, the low levels of costimulatory molecules on the antigen-presenting cell causes the T cell to enter a state of anergy (Becher et al. 2000). Therefore the lack of costimulatory molecule expression by microglia may be a passive mechanism by which immune privilege is maintained. There is however, a population of macrophages within the perivascular space that do express costimulatory molecules (Bartholomäus et al. 2009) which implies that the perivascular space constitutes a less immune privileged region than the CNS parenchyma.

Astrocytes are found throughout the CNS extending processes that cooperatively envelop blood vessels known as astrocytic endfeet (Figure 1.1). This is part of a barrier formed by astrocytes which is abluminal to blood vessels and is also found at meningial borders of the CNS known as the glia limitans. The glia limitans constitutes the edge of the perivascular space and the CNS parenchyma. Like microglia, astrocytes interact with T cells via surface molecules however, astrocytes have the ability to actively suppress the occupation of the CNS by immune cells. Astrocytes do not express MHC class-II costimulatory molecules hence do not support T cell persistence in the CNS (Tontsch and Rott 1993) but astrocytes do express apoptotic ligands such as Fas ligand (Choi et al. 1999) and inhibitory molecules such as CTLA-4 (Gimsa et al. 2004) that have the ability to induce apoptosis in leukocytes and inhibit costimulation of T cells, respectively. Astrocytes are also able to inhibit the secretion of inflammatory cytokines and expression of B7.1 by monocytes when co-cultured *in vitro* (Kostianovsky et al. 2008). When in direct contact with neutrophils, astrocytes suppress neutrophil proliferation and some neutrophils functions (Wie et al. 2010). Therefore cellular contact with astrocytes appears to be important for the suppression of leukocyte function and collectively, astrocytes have the potential to provide a large contribution to the maintenance of immune privilege, due to their large numbers and wide distribution throughout the CNS.

There may be other mechanisms by which immune privilege is maintained which are yet to be discovered. Recently, *in vitro* evidence has been provided for microglial phagocytosis of live neutrophils that infiltrate brain slices (Neumann et al. 2008). It is important to note that immune privilege is a collection of processes that lead to the suppression of immune function in the CNS, not its complete abrogation. This is evident because CNS endothelium has specific transport mechanisms to shuttle cytokines bi-directionally across the blood-brain barrier (reviewed by Banks 2005). This emphasises the idea that the immune system is not excluded from the CNS, but that the CNS regulates the degree to which the immune system operates in the CNS.

1.2 Inflammation of the central nervous system

1.2.1 Inflammation attenuates immune privilege

During inflammation in the CNS, the state of immune privilege begins to break down. Local cytokine production activates an array of inflammatory processes including production of chemokines and matrix metalloproteinases. Cytokine production is able to ellicit changes in the expression of surface markers on CNS endothelium which is one of the requirements for leukocyte infiltration (Piccio et al. 2002). Matrix metalloproteinase secretion causes breakdown of the blood vessel endothelium, and consequently the blood-brain barrier, to facilitate the entry of leukocytes into the CNS (Candelario-Jalil et al. 2009). The initiation of inflammatory processes induces expression of the costimulatory molecules B7.1 and B7.2 and MHC class-II expression on microglia (Aloisi et al. 2000, Santambrogio et al. 2001). Importantly, infiltrating monocyte derived macrophages express MHC class-II, B7.1 and B7.2 surface molecules in the injured CNS (Shechter et al. 2009). The increased presence of costimulatory molecules enables stimulation of the T cell receptor within the injured CNS and reduces the induction of anergic T cells. Hence, the activation of microglia and infiltration of monocytes during CNS inflammation partly counteracts immune privilege.

CNS insults, such as brain injury, that cause the death of astrocytes may alleviate immune suppression because astrocytes normally provide inhibitory signals to leukocytes. The death of an astrocyte would result in loss of the glia limitans and the inhibitory molecules expressed on the astrocyte cell surface. At the border of the affected region, surviving astrocytes extend processes towards the site of injury to re-establish the glia limitans 2-3 days after injury (Faulkner et al. 2004). Re-establishment of the glia limitans has been shown to be important for maintaining immune privilege in surviving CNS tissue and restricting leukocytes to the affected area (Voskuhl et al. 2009). This evidence strongly suggests that the presence of astrocytes is important for the maintenance of immune privilege and that loss of astrocytes from the CNS leads to a loss of immune privilege. The re-establishment of the glia limitans does not necessarily coincide with the re-establishment of the blood-brain barrier which can remain permeant for at least 4 days after injury (Habgood et al. 2007). The consequence of this is that the surviving CNS tissue is not protected from blood-borne neurotoxic molecules or inflammatory mediators from the injury site. Therefore surviving tissue remains susceptible to inflammation-mediated damage for some time after brain injury.

1.2.2 Leukocyte infiltration into the injured CNS

Neuron death occurs over a period of days after brain injury, hence brain injury can be considered as a progression of events that occurs on a scale of days to weeks. During this time, the types of leukocytes that are migrating to, and inhabiting, the injured brain changes as the injury progresses towards resolution (figure 1.2). A major process that facilitates leukocyte infiltration into the injured brain is the production of chemokines in the vicinity of the injury site (Babcock et al. 2003, Ghirnikar and Lee 1996, Ghirnikar et al. 1998, Rhodes et al. 2009, Sandhir et al. 2004). Chemokines are chemoattractant molecules which orchestrate the migration of leukocytes to the area of inflammation via interaction with chemokine receptors on leukocytes (reviewed by Bajetto et al. 2001). Due to their location in the CNS, microglia exhibit the fastest inflammatory response to injury. Astrocytes also undergo a cellular activation which has some inflammatory aspects such as chemokine secretion and enzyme-mediated ROS production (Falsig et al. 2004, Madrigal et al. 2009) but microglia have been shown to become activated at much lower levels of stimulus (Liberto et al. 2004). The first cells expressing activated macrophage markers present in the injured brain are of microglial origin (Denker et al. 2007). Subsequent to the activation of resident CNS cells, the infiltration of neutrophils into CNS injuries is the most rapid of any type of leukocyte but neutrophils do not persist beyond 2 days post-injury, at which time monocytes become the dominant infiltrating leukocyte (Stirling and Yong 2009). T cell infiltration occurs in several waves with an early infiltration within 1 hour (Czigner et al. 2007), followed by a second infiltration at 24 hours (Clausen et al. 2007). However, the maximal T cell occupation of the injured CNS begins to occur about 1 week after the initial injury (Sroga et al. 2003). It warrants mention that it is not known why there are T cells with cognate antigens that are present in the injured CNS because the immune system is able to tolerise proteins found in the CNS (Gregerson et al. 2009). Tolerisation is the process by which the immune system determines which molecules are self-derived and which molecules are exogenous but it is possible that there are CNS derived molecules that are only released into cerebrospinal fluid after CNS injury. Overall, the process is not well understood, but regardless, T cells are found infiltrating the injured CNS. Therefore, the immune response to brain injury is dynamic and varies greatly as time progresses.

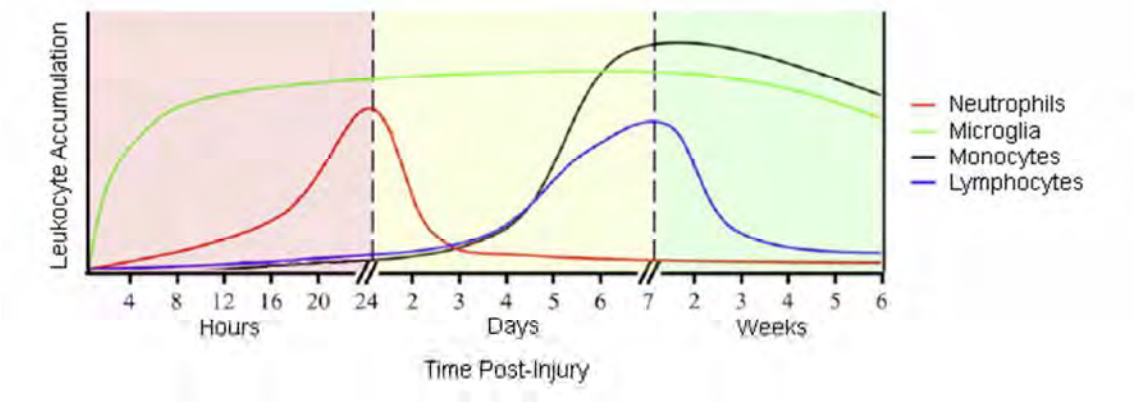

Figure 1.2, compiled by Donnelly and Popovich (2008) to represent the trends observed in leukocyte accumulation during the progression of brain injury from multiple studies in mice. The appearance of activated microglia is the most rapid response to CNS injury. Leukocyte infiltration begins with the appearance of neutrophils and their decline within the first 24-72 hours. At approximately 1 week after injury there is an increase in the occupancy of the CNS by monocytes and lymphocytes.

1.2.3 Effects of inflammation on the injured CNS

The inflammatory response to injury appears to be a trade-off between detrimental and beneficial processes that are evolutionarily coupled. This arises because immune cells must become activated to carry out their beneficial functions but other detrimental processes become active simultaneously. This may explain why the effects of infiltrating immune cells on the injured brain can be contradictory to the effects of immune cells on neurons *in vitro*. Macrophages, derived from activated microglia or infiltrating monocytes, and neutrophils, can participate in the oxidative burst and nitric oxide synthesis. The oxidative burst is an anti-microbial response that accompanies inflammation even in the absence of pathogens and produces ROS and reactive nitrogen species (RNS) via enzymes such as NADPH oxidase and inducible nitric oxide synthase (iNOS) (Alberati-Giani and Cesura 1998, Sankarapandi et al 1998). *In vitro,* ROS/RNS have been shown to cause the death of neurons (Desagher et al. 1996, Hu et al. 1997). Macrophages, astrocytes and T cells can all produce inflammatory cytokines when activated. Inflammatory cytokines generally enhance inflammatory processes such as oxidative burst but increased concentrations of cytokines such as TNF-α can also enhance excitotoxicity (Bezzi et al. 2001). Therefore there are aspects of the inflammatory response that could be considered detrimental to neuronal or glial survival after brain injury.

In contrast, studies to experimentally remove leukocyte sub-populations have yielded results that conflict with this presumed neurotoxicity emanating from leukocytes. For example, neutrophil depletion with monoclonal antibodies to Ly-6C/Ly-6G can worsen the outcome of spinal cord injury (Stirling et al. 2009), mutant *scid* mice that lack functional T cells and B cells have decreased neuron survival after facial motor nerve axotomy (Serpe et al. 1999) and genetic ablation of microglia and monocytes resulted in increased infarct size after stroke (Lalancette-Hébert et al. 2007). Similar results were obtained using transgenic mice that have a null mutation for the inflammatory cytokine TNF-α which had increased infarct volume in an experimental stroke model (Lambertsen et al. 2009). In accordance with these results, transplantation of activated macrophages into an optic nerve injury site has been able to improve nerve regeneration (Lazarov-Spiegler et al. 1996). Therefore, leukocytes have characteristics that are detrimental to neuronal function but also have vital roles to play in the resolution of

injury. A major question from a therapeutic point of view is whether the immune response can be manipulated to attenuate the detrimental processes without removing the beneficial processes.

1.2.4 Therapeutic vaccination for CNS injury

T cells are a large contributor to the pathology of multiple sclerosis and EAE (Martin et al. 1992) which might suggest that T cells would also contribute to the pathology of brain injury. EAE is induced by vaccination with an antigen, usually a myelin-associated protein, and adjuvant, often inactivated mycobacteria, which promotes the formation of a humoral response to the antigen. In contrast to the detrimental effects observed in EAE, this vaccination treatment enhanced the recovery from optic nerve injury when the vaccination was administered at the time of injury (Moalem et al. 1999). In a separate study that aimed to replicate these effects in a spinal cord injury, the vaccination caused no improvement in recovery from injury but EAE occurred as expected (Jones et al. 2004). Therefore the treatment appeared to have beneficial effects only in some instances of CNS injury but the detrimental effects, the induction of EAE, was a reproducible response. This problem was rectified more recently, when a synthetic polymer based on myelin basic protein, glatiramer acetate (also known as copolymer-1, cop-1 and copaxone) was used as the vaccination antigen and was found to improve CNS injury outcome without causing EAE (Kipnis et al. 2003, Skihar et al. 2009). Other polymers based on the structure of myelin basic protein have been used to induce the beneficial effects of T cells in brain injury (Martiñon et al. 2007). Studies using this vaccination technique in transgenic mice lacking helper T cells were unable to reproduce the beneficial effects suggesting that, of all the T cell subtypes, helper T cells are the subtype responsible for the beneficial effects after CNS injury (Serpe et al. 2003). This is supported by the fact that regulatory T cells, which are known to suppress helper T cell responses, have been shown to reduce the efficacy of the vaccination treatment (Kipnis et al. 2002). The original vaccination experiments demonstrated that a CNS specific antigen was required to induce a beneficial effect from T cells (Moalem et al. 1999), suggesting that the vaccination promotes the activation and expansion of helper T cells which are then able to enter the injured CNS and persist there to affect the recovery process. These experiments emphasise the fact that activated helper T cells can have beneficial effects on the injured CNS and that helper T cells can be manipulated to enhance the beneficial effects. A possible mechanism for helper T cell mediated neuroprotection is their ability to produce mRNA for the neurotrophins (NT), NT-1, NT-2, NT-3, NT-4/5 and brain-derived neurotrophic

factor when stimulated *in vitro* (Moalem et al. 2000) and express NT-3 and BDNF mRNA in spinal cord after SCI (Hammarburg et al. 2000). However, this does not explain how the detrimental effects exerted by helper T cells, are overcome.

1.2.5 Th1/Th2 responses in brain injury

Discovery of the ability to attenuate the severity of CNS injuries by increasing T cell numbers was surprising given the pathogenic role of T cells in autoimmune diseases of the CNS. It led to the suggestion that in the CNS, the immune system may be detrimental or beneficial depending on the signals or "context" presented to the immune cells (Schwartz et al. 2006). Furthermore, Hendrix and Nitsch (2007) have proposed that a low Th1/Th2 ratio is beneficial to neural survival after CNS injury. The type-1 helper T cell (Th1) and type-2 helper T cell (Th2) responses are divergent lineages that naïve T cells differentiate into, upon activation and clonal expansion (Mosmann et al. 1986). The Th1 response is a response that mediates the host defence against intracellular pathogens and favours cytolytic and anti-microbial processes such as the oxidative burst. Th1 cells effect this response by producing Th1 cytokines such as interferon-γ (IFN-γ), tumour necrosis factor-α (TNF-α) and IL-2 (Sredni-Kenigsbuch 2002). The Th2 response mediates actions against extracellular pathogens, mainly by stimulating production of antibodies. The prominent Th2 cytokines are IL-4, IL-5 and IL-10 (Sredni-Kenigsbuch 2002). Th1 and Th2 responses always exist together and both processes are required for resolution of infections but the immune system is able to vary the ratio of Th1 to Th2 cells or cytokines according to the requirements for a particular pathogen (de Jong et al. 2002). Th1 and Th2 responses occur in the injured brain and differences in the effects of each phenotype are likely to impact upon the progression of brain injury.

1.2.6 Classical and alternative activation of macrophages in brain injury

In the injured brain, the major cell type responding to Th1 and Th2 cytokines is macrophages which are derived from monocytes and microglia. Th1 cytokines induce what is known as the classically activated macrophage (caMΦ) and Th2 cytokines activate macrophages with a phenotype known as the alternatively activated macrophage (aaMΦ). CaMΦs have a higher antimicrobial capacity due to their ability metabolise arginine into nitric oxide and citruline whereas aaMΦs metabolise arginine into ornithine and urea (Mills et al. 2000). Nitric oxide is a highly reactive, short-lived molecule that is neurotoxic (Hu et al. 1997) which implies that caMΦs have a detrimental effect when activated in the CNS. Conditioned media from caMΦs

transferred to neuron cultures has been shown to be toxic, whereas aaMΦ conditioned media promotes neurite growth (Kigerl et al. 2009). This experiment suggests that caMΦs probably produce soluble neurotoxic molecules in addition to nitric oxide because nitric oxide is rapidly converted to relatively inert nitrates in culture media. Microglia also produce the neurotoxin quinolinic acid and the less toxic kynurenic acid from divergent and competing branches of tryptophan metabolism via the indoleamine 2,3-dioxygenase pathway (Guillemin et al. 2004). Microglia can be induced into a caMΦ phenotype by Th1 cytokines which favours quinolinic acid production whereas aaMΦ induction by Th2 cytokines promotes the production of kynurenic acid at the cost of quinolinic acid production (Kwidzinski and Bechmann 2007, Yadav et al. 2007). *In vitro*, the Th2 cytokine, IL-4 has been demonstrated to induce an alternative activation state in microglia (Zimmer et al. 2003). IL-4 stimulates microglial production of insulin-like growth factor-1 (IGF-1) and reduces the amount of tumour necrosis factor-α (TNF-α) secretion (Butovsky et al. 2005). High levels of TNF-α induce neuronal apoptosis whereas lower levels of TNF-α can promote neuronal survival (Bernadino et al. 2005). IGF-1 is neurotrophic (Laurino et al. 2005, Wilkins et al. 2001), inhibits NO synthesis and reduces blood-brain barrier breakdown after brain injury (Sharma et al. 1998).

In vivo evidence suggests that while both caMΦs and aaMΦs are induced rapidly after spinal cord injury, only the caMΦ response persists for longer than 24 hours after the initial injury (Kigerl et al. 2009). However, in an EAE model a prolonged aaMΦ response was seen to occur (Ponomarev et al. 2007), indicating that a Th2 response and aaMΦ response can persist in the CNS. Interestingly glatiramer acetate, the molecule used to vaccinate animals to enhance the protective T cell response to injury, induces a Th2 response in T cells that enter the CNS (Aharoni et al. 2003). It has also been shown that different strains of mice that have a natural bias towards either Th1 or Th2 responses have different outcomes to CNS insults (Lambertsen et al. 2002). The induction of caMΦ in the CNS may have implications for immune privilege because microglia cultured with Th1 cells or Th1 cytokines leads to increased expression of MHC class-II molecules and B7.1 and B7.2 costimulatory molecules (Aloisi et al. 2000, Séguin et al. 2003). Therefore a caMΦ response in the injured brain may have a higher capacity to support T cells in the injured brain than an aaMΦ response which is the less neurotoxic of the two phenotypes. The study of Th1/Th2 responses and caMΦ/aaMΦ phenotypes has demonstrated that each response has the potential to change the

progression of brain injury. Understanding the effects of leukocytes in the injured brain requires a more complete understanding of how the Th1/Th2 responses and the caMΦ/aaMΦ phenotypes are regulated in the injured CNS.

1.2.7 Peripheral immune response to brain injury

CNS injuries can affect organs peripheral to the CNS. In severe brain injury patients, Zygun et al. (2005) found extraneural organ dysfunction in 89% of cases, and organ failure in 35% of patients. The immune system is often altered by CNS injury with decreased circulating T cell counts within the first week of brain injury (Mazzeo et al 2006) and chronically, spinal cord injury was able to cause a decrease in natural killer cells and an increase helper T cells in circulation more than 3 months after injury (Campagnolo et al. 2008). There are multiple studies showing CNS injury related increases in levels of immune system signalling and effector proteins such as β-2-microglobulin, soluble IL-2 receptor (Lenzlinger et al. 2001), C-reactive protein (McClain et al. 1986), fractalkine (Rancan et al. 2004), IL-6 (McClain et al. 1991), IL-8 (Whalen et al. 2000), tumour necrosis factor (TNF), CC chemokine ligand 5 (CCL5) (Terao et al. 2008), and IL-1 (Ott et al. 1994). While it is possible that these molecules originate from the injured CNS, it has also been shown that donor organs from brain dead patients have elevated expression of cytokines and chemokines (Weiss et al. 2007) which might suggest that extraneural organs contribute to the systemic inflammatory response to brain injury. It is apparent that injury to the CNS affects the functioning of extraneural organs, but whether these organs can influence the outcome of brain injury also needs to be considered. Gris et al. (2008) demonstrated that in rats, spinal cord injury induces a systemic immune response that results in neutrophil recruitment to the lungs and kidneys resulting in inflammatory tissue damage to both organs. Hence the immune response may contribute to the changes seen in extraneural organs after brain injury, although other systems may be involved.

1.2.8 Systemic oxidative stress after brain injury

A rapid change that occurs in extraneural organs after brain injury is increased oxidative stress which can occur within 15 minutes (Shohami et al. 1999). It is not known what triggers this response but redox status inside cells can influence many cellular processes and can profoundly affect immune cell function. Reduced glutathione (GSH) is the main intracellular antioxidant and enzymes are constantly reducing the oxidised form of glutathione (GSSG) which is constantly being oxidised by ROS produced by normal cellular function. Oxidative depletion of GSH suppresses the systemic immune

response to activating stimuli such as endotoxin or bacteria (Wang et al. 1999, Buchmuller-Rouiller et al. 1995). Particularly relevant to the case of brain injury is the fact that in antigen-presenting cells, high cellular GSH content induces Th1 cells and low GSH content induces Th2 cells (Dobashi et al. 2001, Koike et al. 2007, Murata et al. 2002, Peterson et al. 1998). Because T cells need to be activated by antigen-presenting cells in lymphoid organs before they can enter the CNS (Archambault et al. 2005, Byram et al. 2004, Ling et al. 2006), brain injury-induced changes in whole-body redox status could influence the type of helper T cell response induced after injury. Once T cells infiltrate the inflamed CNS, cytokine production by helper T cells could influence the induction of either caMΦs or aaMΦs in the injury site. Such a link has yet to be determined experimentally but there is evidence to support the hypothesis that the immune system can contribute to the progression of brain injury.

1.2.9 Immune responses of extraneural organs after brain injury

The immune system can directly interact with the injured brain because leukocytes are highly mobile cells that migrate towards sites of injury. However there is also evidence that somatic organs can affect the injured brain. Cytokines are expressed in the gastrointestinal tract after brain injury (Bansal et al. 2010, Chen et al. 2008, Feighery et al. 2007). The first organ to be exposed to gut-derived cytokines is the liver via drainage of intestinal capillaries via the hepatic portal vein. Activation of the immune system-related transcription factor NF-κB, has been observed throughout the body after inflammatory insult to the brain, but it occurred predominantly in the liver (Campbell et al. 2008a). Furthermore, the activated liver produces chemokines which contribute to the rate of infiltration of neutrophils and monocytes into the injured brain (Campbell et al. 2002, Campbell et al. 2003, Campbell et al. 2005, Campbell et al. 2007a, Campbell et al. 2007b, Chapman et al. 2009). Specific depletion of liver Kupffer cells and circulating monocytes, but not microglia, was able to attenuate neutrophil infiltration into the injured brain (Campbell et al. 2008b). This is one of the most convincing examples of an extraneural organ responding to brain injury, and this in turn impacting upon the injured brain.

There is increasing evidence that the systemic response to brain injury can have feedback effects on the injured brain. This phenomenon may affect the interpretation of experiments utilising transgenic animals in which the altered gene affects all cells in the animal. The following is an account of the evidence for an extraneural role of

metallothionein-I and –II, two genes identified to be neuroprotective from null mutant, and transgenic over-expressing, mouse experiments.

1.3 Metallothionein (MT) in the injured central nervous system

1.3.1 Metallothionein

Metallothionein (MT) is a 6-7kDa, cysteine rich, metal-binding protein. In a physiological context, metallothionein binds up to 7 zinc ions or 10 copper ions in thiolate clusters (Nielson and Winge 1983, Palumaa et al. 2005). In a physiological context MT-I/II is predominantly found bound to zinc or in various partially zinc-bound forms (Yang et al. 2001). In addition to its zinc binding properties, MT has a very negative redox potential (Maret and Vallee 1998) hence it has strong antioxidant properties. There are four main isoforms of metallothionein. MT-I and MT-II are expressed in most organs in the body and share sufficient homology that they are often considered to be a single species (MT-I/II). MT-III expression is expressed in the brain and MT-IV is expressed only in squamous tissue. MT-I/II is induced by changes in intracellular zinc, extracellular zinc, IL-6 or glucocorticoids (figure 1.3). MT-I/II is highly conserved within the vertebrate classes but the biological function of this protein is still largely unknown. Because highly conserved genes usually represent evolutionarily essential proteins, it was surprising that no overt phenotype was observed in either of the MT-I/II null mutant (MT-I/II$^{-/-}$) mouse strains that have been created (Masters et al 1994, Michalska and Choo 1993). It was not until MT-I/II$^{-/-}$ animals were placed under stressful conditions such as simulated sepsis (Philcox et al. 1995, Waelput et al. 2001), lung injury (Inoue et al. 2005, Takano et al. 2004), ***Helicobacter pylori*** infection (Mita et al. 2008), zinc challenge (Coyle et al. 1995), cadmium toxicity (Masters et al. 1994) and restraint stress (Suzuki et al. 2000) that differences between wild type and MT-I/II$^{-/-}$ mice became apparent. In the case of brain injury, there are numerous documented cases where CNS insults produced a more severe response in MT-I/II$^{-/-}$ mice than wild type (MT-I/II $^{+/+}$) mice (Natale et al. 2004, Penkowa et al. 1999a, Penkowa et al. 1999b, Penkowa et al. 2001, Penkowa et al.2006a, Potter et al. 2007, Potter et al. 2009, Suemori et al. 2006). In accordance with these findings, mice that transgenically over-express MT-I have a less severe outcome from CNS insults (Giralt et al. 2002, Penkowa et al. 2005, van Lookeren Campagne et al. 1999). Cumulatively, these data imply that MT-I/II has a modulatory role under stressful conditions, whereas a definitive role of MT-I/II under resting conditions is yet to be determined.

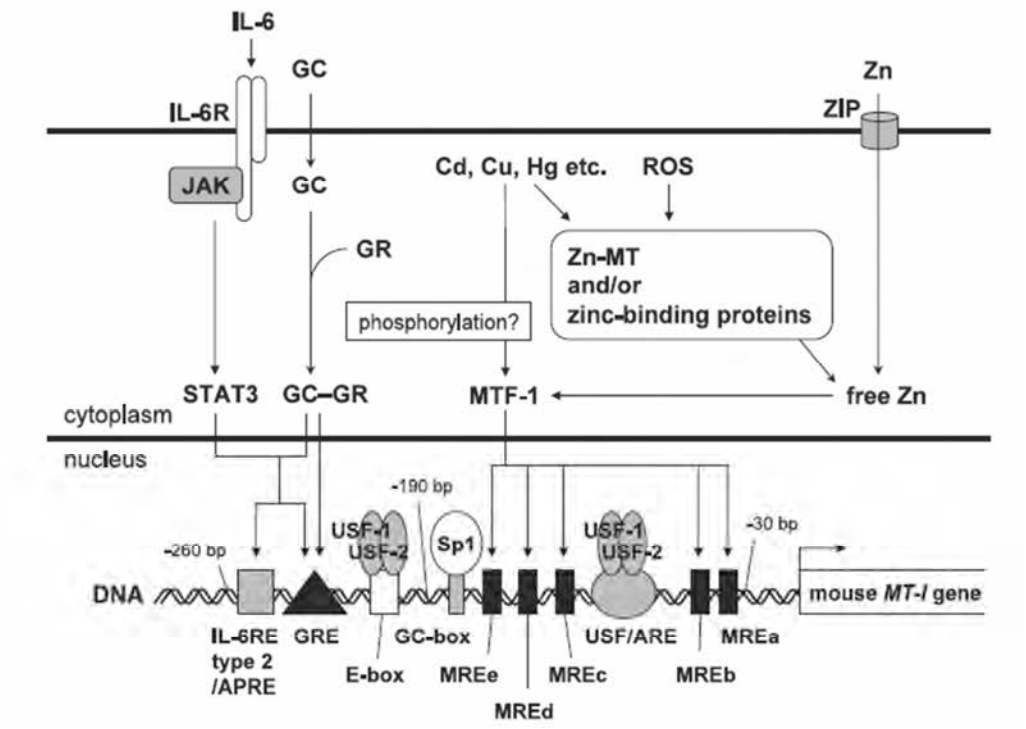

Figure 1.3 Adapted from Kimura and Itoh (2008). Regulation of MT-I occurs via increased intracellular zinc which can arise due to increased extracellular zinc or zinc liberation from proteins by ROS and metals with higher affinity for thiolate clusters than zinc. Free zinc binds to metal transcription factor-1 (MTF-1) which binds to metal response elements (MREs) in the MT-I gene promoter to enhance transcription. Glucocorticoids (GC) and IL-6 can activate glucocorticoid receptors (GR) and the STAT3 pathway, respectively to further enhance MT-I expression. The constitutively expressed transcription factors Sp1, USF-1 and USF-2 are also required for MT-I mRNA transcription but are not involved in the processes that induce MT-I expression.

1.3.2 Putative neuroprotective roles of brain-derived metallothionein

A protective role for MT-I/II after brain injury was first demonstrated ***in vivo*** by Penkowa et al. (1999a) who showed that MT-I/II$^{-/-}$ mice had a larger injury size and a dysfunctional immune response after cryolesion brain injury. Interestingly, mice that were null mutants for MT-III, the brain specific isoform, did not exhibit any alteration to the inflammatory response and actually had greater production of neurotrophins after brain injury (Carrasco et al. 2003). These results demonstrate that the neuroprotective effects of MT are specific to the ubiquitously expressed MT-I and MT-II isoforms, not the brain-specific isoform. After injury to the CNS, MT-I/II expression increases in astrocytes in the vicinity of the injury site (Carrasco et al. 2000, Chung et al. 2004, Penkowa and Moos 1995, Penkowa et al. 1999a, Penkowa et al. 1999b, Penkowa et al. 1999c). An obvious effect that MT-I/II may be having in brain injury is zinc binding. For an individual cell, increasing expression of MT-I/II can protect against zinc toxicity (Palmiter et al. 2004). Zinc is an essential trace metal for a large number of metalloproteins and many cellular functions (reviewed by Cuajunco and Lees 1997, Fraker and King 2004, Lansdown et al. 2007). During brain injury increased oxidative stress is present in the injured brain (Robertson et al. 2009) which has the capacity to liberate zinc from the many zinc binding proteins present in neurons, a process which induces neuronal apoptosis (Aizenman et al. 2000). Zinc also plays a role in membrane depolarisation leading to neuron death (Medvedeaeva et al. 2009). Microglia can induce the release of intracellular free zinc ions in neurons leading to neuronal membrane depolarisation (Knoch et al. 2008). Furthermore, increases in extracellular zinc can activate microglial nitric oxide synthesis and NADPH oxidase activity (Kauppinen et al. 2008) and the RNS/ROS produced could further potentiate neuron death. Astrocytes express MT-I/II whereas neurons do not and astrocytes consequently have a higher tolerance to zinc toxicity (Dineley et al. 2000). Given that MT-I/II is predominantly an intracellular protein with no signal sequence peptide to stimulate secretion, it could be argued that MT-I/II does not have the correct localisation in the CNS to protect neurons. However, there is evidence that astrocytes can protect neurons against increases in extracellular zinc concentration via the expression of MT-I/II which sequesters the free zinc to the astrocyte cytoplasm (Malaiyandi et al. 2004). Such an effect may extend further to prevent the other effects caused by increased free zinc ion concentrations. Astrocytic MT-I/II may also provide protection against oxidative stress because astrocytes cultured from MT-I/II$^{-/-}$ mice are more susceptible to oxidative stress than astrocytes from wild type mice (Suzuki et al. 2000). It is not known if MT-

I/II in the cytoplasm of astrocytes can protect against ROS/RNS generated in neurons or extracellular ROS/RNS generated by the inflammatory response. However, extracellular MT-I/II has been shown to protect cultured neurons against oxidised dopamine products (Gauthier et al. 2008, Køhler et al. 2003) and amyloid-β (Chung et al. 2010, Køhler et al. 2003). Extracellular MT-I/II also promotes neurite extension in neuron cultures and the injured optic nerve (Chung et al. 2003, Chung et al. 2008, Fitzgerald et al. 2007). In human patients with brain injury MT concentrations in the blood are increased (Kukačka et al. 2006) and the concentration is comparable to those used to promote neuron protection and neurite extension *in vitro*. Furthermore, therapeutic application of MT-I/II into the site of brain injury can promote neurite extension *in vivo* (Chung et al. 2003) and reduce quinolinic acid production (Chung et al. 2009). However, extracellular MT-I/II concentrations have never been quantified in the injured brain so it is not known if extracellular MT-I/II concentrations increase sufficiently to act via an extracellular mechanism. Despite the comprehensive research into the role of MT-I/II in astrocytes and neurons in the injured brain, one aspect of MT-I/II that has not received attention is the role of MT-I/II expressed in organs outside the CNS following brain injury.

1.3.3 Zinc and metallothionein in the peripheral response to brain injury

Metallothionein is implicated in zinc homeostasis due to its ability to bind zinc and to be induced rapidly in response to a wide variety of stimuli. Dietary zinc deficiency has been shown to increase neuronal cell death in a rat model of brain injury (Penkowa et al. 2001a, Yeiser et al. 2002) suggesting that zinc availability is important for the injury response. In brain injured patients, serum zinc levels were found to be severely depressed compared to healthy controls upon admission, with a steady increase towards normal levels over the 16-day experimental period (McClain et al. 1986). In the same study, urinary excretion of zinc did not increase until later in the experimental period, hence excretion of zinc was not an explanation for the depressed plasma zinc at the time of admission. It should be mentioned that pancreatic secretion and subsequent faecal excretion of zinc is another method by which zinc is removed from the body (Walsh et al. 1994) but it is not known if the pancreas alters the rate of zinc secretion after brain injury. Plasma zinc or free zinc is not necessarily an informative measure of zinc status because much of the zinc in biological systems is bound to proteins or is associated with plasma membranes (Lansdown et al. 2007) but altered plasma zinc concentration is probably indicative of altered zinc homeostasis. Increases in serum IL-6 (McClain et al. 1991) and C-reactive protein (McClain et al. 1986) indicate that the acute phase

response is activated during brain injury. The acute phase response is a systemic response to injury or infection and primarily accomplished by the liver that functions to augment immune system pathways, induce glucocorticoid secretion, and decrease serum zinc and iron concentration (reviewed by Heinrich et al. 1990). Induction of liver MT-I/II expression as part of the acute phase response has been hypothesised as the cause of decreased serum zinc after brain injury (Ott et al. 1994). Induction of hepatic MT-I/II expression occurs in a range of conditions such as burn injury (Cho et al. 2004, Ding et al. 2002, Zhou et al. 2003), restraint stress (Hernández et al. 1999, Jacob et al. 1999), increased plasma zinc concentration (Coyle et al 1995, Zhou et al. 2004), fasting and septic challenge with LPS (Philcox et al. 1995, De et al. 1990). An increase in liver zinc levels and decreased plasma zinc levels coincide with increased hepatic MT-I/II expression in wild type mice but not MT-I/II$^{-/-}$ mice, indicating that MT-I/II in the liver is capable of sequestering zinc from circulation (Philcox et al. 1995, Coyle et al. 1995). It has been suggested that zinc in the body exists in several compartments, with most compartments defined as an organ due to the fact that the rate of zinc influx and efflux varies between organs (Wastney and House 2008). Figure 1.4 demonstrates how a few zinc compartments may affect zinc homeostasis before and after brain injury. The induction of liver MT-I/II after brain injury has not been confirmed experimentally but could be important given the multitude of zinc dependent processes that could affect the resolution of brain injury if zinc homeostasis is disrupted. The possible consequences of increased hepatic MT-I/II expression include altered zinc trafficking, increased antioxidant resistance and downstream consequences of both of these phenomena.

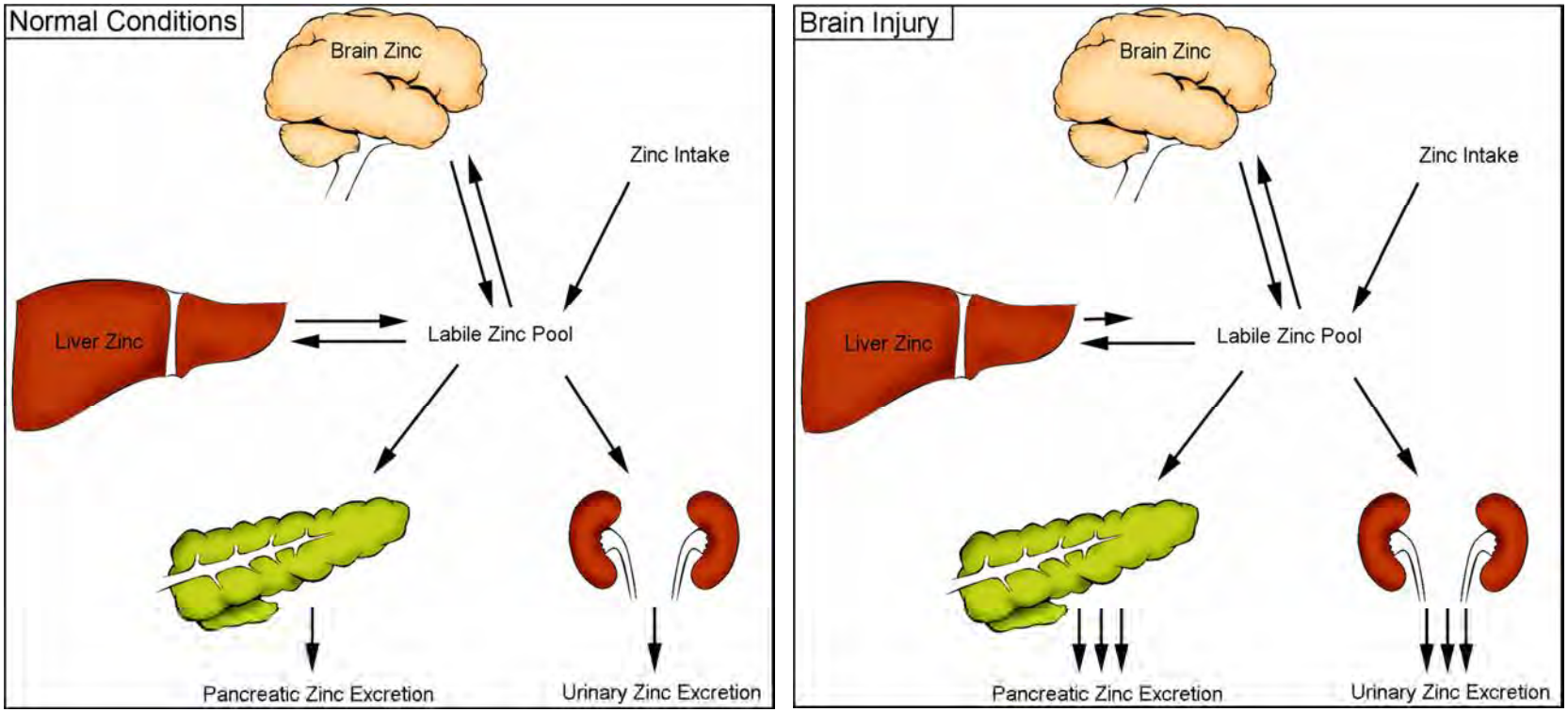

Figure 1.4 Proposed model of zinc homeostasis under normal conditions (left) and after brain injury (right). At steady state, there is constant cycling of zinc between the labile zinc pool and the organs. The labile zinc pool is also affected by dietary zinc absorption, pancreatic zinc secretion and urinary zinc uptake. After brain injury it is proposed that urinary zinc excretion increases and that zinc is sequestered in the liver due to increased hepatic MT-I/II expression. It is not known how zinc intake and zinc traffic to, and from, the brain will be affected by brain injury. It is also possible that pancreatic zinc secretion and faecal excretion is altered by brain injury but this has not been studied. The combination of changes in zinc trafficking are likely to be responsible for decreases in the labile zinc pool and plasma zinc levels after brain injury.

1.3.4 Influence of zinc on immune system function

Changes to the quantities of zinc in various compartments will affect zinc availability to various systems. The immune system is an important system that may be affected by zinc shifts after brain injury. For example, severe zinc deficiency in rodents results in thymic atrophy and disruption to haematopoiesis (DePasque-Kardieu and Fraker 1979, DePasque-Kardieu and Fraker 1980, King and Fraker 2000, King and Fraker 2002, King et al. 2005). Moderate zinc deficiency inhibits the production of Th1 cytokines by helper T cells without affecting production of the Th2 cytokines causing a Th2 shift (Prasad et al. 2007). MT-I/II may play a role in preventing this process because, helper T cells isolated from MT-I/II$^{-/-}$ mice expressed higher levels of IFN-γ when exposed to Th1 inducing conditions than wild type mice but showed no difference in cytokine expression when exposed to Th2 conditions (Huh et al. 2007). In contrast to zinc deficiency, zinc supplementation to raise zinc levels in humans enhances leukocyte responses to activating stimuli (Aydemir et al. 2006). Increases in labile cellular zinc in monocytes can affect production of cAMP and cGMP in the complex phosphodiesterase system that ultimately leads to decreases in production of the inflammatory cytokines TNF-α and IL-1β (reviewed by Haase and Rink 2007). Therefore increases and decreases in zinc availability can affect the function of the immune system and it is possible that MT-I/II plays a role in modulating some of these effects. For example, zinc can directly induce macrophage-colony stimulating factor production in fibroblasts from wild type mice but not in MT-I/II$^{-/-}$ mice (Kanekiyo et al. 2002a). Furthermore, MT-I/II can affect the activity of iNOS, a metalloenzyme that requires zinc because macrophages isolated from MT-I/II$^{-/-}$ mice have lower iNOS activity when stimulated compared to wild type mice (Itoh et al. 2005). Therefore, zinc status affects the immune system and there is a possibility MT-I/II can influence these interactions.

1.3.5 Putative immune system regulatory roles for systemic metallothionein

There is some evidence that the immune system of MT-I/II$^{-/-}$ mice has some inherent differences when compared to wild type mice. NF-κB is an important transcription factor for activation of immune responses (Blackwell and Christman 1997). Studies using various MT-I/II$^{-/-}$ cell lines have determined that MT-I/II inhibits NF-κB activation when in the cytoplasm, but MT in the nucleus enhances DNA binding of NF-κB (Butcher et al. 2004, Kanekiyo et al. 2002b, Sakurai et al. 1999). This paradox might be explained by the fact that under certain conditions, metallothionein can translocate almost completely to the nucleus (Spahl et al. 2003). Therefore on a cellular

level MT-I/II$^{-/-}$ mice might have an altered immune response. *In vivo*, MT-I/II$^{-/-}$ mice show increased immunoglobulin production in response to antigen, increased numbers of lymphoid cells in the spleen and decreased numbers of circulating helper T cells (Crowthers et al. 2000). T cells isolated from MT-I/II$^{-/-}$ mice have a reduced proliferative response when stimulated by concanavalin A compared to T cells in wild type mice (Mita et al. 2002). Further experiments suggest that circulating extracellular MT-I/II suppresses the ability of B cells to produce antibodies in response to foreign antigen (Canpolat and Lynes 2001, Lynes et al. 1993), yet paradoxically, extracellular MT-I/II can stimulate B cell proliferation (Borghesi et al. 1996). To further confuse matters, both MT-I/II$^{-/-}$ and transgenic MT-I over-expressing mice have increased host-defence against the bacterium *Listeria monocytogenes* compared to wild type mice (Emeny et al. 2009). The often contradictory findings with regard to the effect of MT-I/II on the immune system likely arise from multiple mechanisms by which the presence or absence of MT-I/II can affect immune function. These processes are not completely understood but could relate to the zinc-binding capacity, antioxidant properties or the cellular localisation of MT-I/II. Therefore, the altered immune response to brain injury in MT-I/II$^{-/-}$ mice could be the result of inherent differences in immune system functioning when compared to wild type mice. Intraperitoneal injection of MT-I/II can reduce the symptoms of EAE in rats (Penkowa and Hidalgo 2000) and intraperitoneal injection of MT-I/II after brain injury results in a response to brain injury in MT-I/II$^{-/-}$ mice that is similar to that of wild type mice (Penkowa et al. 2006b). Therefore systemically administered exogenous MT-I/II can affect the immune response to brain injury but it is still not understood how endogenously expressed MT-I/II affects the immune response to brain injury.

1.4 Project Aims

The mechanism by which MT-I/II imparts protection to the injured CNS is difficult to elucidate. MT-I/II may be able to directly increase the survival rate of neurons under high zinc concentration or oxidative stress but *in vivo* brain injury models suggest that there is a strong immune component to the action of MT-I/II in CNS insults. Given the zinc binding properties of MT-I/II, it is surprising that the role of zinc in the phenomena observed in CNS injury models with MT-I/II$^{-/-}$ and transgenic MT-I over-expressing mice has not been investigated in detail. Another important factor to consider in the study of MT-I/II$^{-/-}$ and transgenic MT-I over-expressing mice is that MT-I/II is

normally expressed in most tissues, not just the brain, and the method used to knock-out or knock-in MT does not distinguish between cell types. The present thesis details a system wide approach to investigating the function of MT-I/II after brain injury. The project aims were:

1) To utilise a cryolesion brain injury model to administer an aseptic cortical lesion to MT-I/II$^{-/-}$ and wild type mice.
2) To assess immune system response to brain injury in MT-I/II$^{-/-}$ mice after brain injury to determine whether MT-I/II may be altering the peripheral immune response to have beneficial effects upon the injured brain.
3) To develop an ELISA to quantify MT-I/II expression after brain injury and assess MT-I/II-mediated zinc trafficking in the liver.

Chapter 2 – Cryolesion Injury Characterisation

2.1 Introduction

A wide range of methods exist to administer experimental brain injury to rodents including penetrating injuries, skull impact injuries, fluid percussion injuries, cranial nerve axotomy and cryolesion. Cryolesion injury, defined here as the injury resulting from application of a cold instrument to the external surface of the skull, has several advantages as an experimental model of brain injury. Because it is possible to perform the injury through the intact skull, the injury is aseptic, the CNS remains separated from the lymphatic system and stress to the animal is reduced. This minimises the confounding factors that can affect the progression of the inflammatory and regenerative responses to injury. One of the criticisms for the experimental use of cryolesion to induce brain injury is that it does not mimic any clinically relevant form of brain injury. However, it does produce a well-defined injury site, initiates a robust glial response and leads to the infiltration of leukocytes. In addition, to the injury caused to the brain all animals have also effectively received open wounds that may be subjected to infection or exposure to endotoxin. Nonetheless, the experimental procedure remains appropriate, even though it may affect the function of the immune system, because many head trauma patients have attained additional injuries. For these reasons cryolesion is a useful model for the study of inflammation after brain injury. Many experimental injury models require craniotomy which results in mixing of lymph and cerebrospinal fluid and carries the risk of infection which may exacerbate the inflammatory response of the CNS. The cryolesion model avoids craniotomy and is useful to study how non-CNS organs can affect CNS injury progression because surgical disturbance to other tissues is minimal.

Cortical cryolesion by direct application of dry ice to the surgically exposed skull has been used extensively in the study of brain injury in MT-I/II$^{-/-}$ mice (Giralt et al. 2002, Penkowa et al. 1999a, Penkowa et al. 2006a, Penkowa et al. 2006c). Other injury models used in the study of MT-I/II$^{-/-}$ mice include kainic acid injection into the hippocampus (Carrasco et al. 2000), systemic injection of the glial specific toxin 6-aminonicotinamide (Penkowa et al. 1999b) and surgical ablation of the occipital cortex (Natale et al.2004, Potter et al. 2007, Potter et al. 2009). MT-I/II$^{-/-}$ mice given these treatments showed greater neural death and an increased inflammatory response to injury with one exception; 6-aminonicotinamide caused a decrease in inflammatory cells inhabiting the injury site and this was likely due to the fact that 6-aminonicotinamide is also toxic to rapidly dividing cells such as the bone marrow cells

that produce leukocytes (Penkowa et al 1999b). The inflammatory response to brain injury, particularly the infiltration of leukocytes into the injured brain, is likely to play an important role in the detrimental effects caused by MT-I/II null mutation.

Dry ice is often used as the freezing agent for cryolesion brain injury in MT-I/II$^{-/-}$ mice however, heat transfer by direct application of dry ice to a warmer surface can be disrupted by the Leidenfrost effect (Leidenfrost 1966); an insulating effect caused by sublimation of dry ice which creates a cushion of gas between the dry ice and warmer surface. Because this effect could interfere with even heat transfer between the skull and the dry ice pellet, a different method of administering cryolesion was utilised. This chapter characterises a cryolesion injury caused by heat-transfer from the mouse skull and underlying cortex to a liquid nitrogen-cooled steel rod. Histology and immunohistochemistry were used to quantify neuron death and define the injury site in wild type and MT-I/II$^{-/-}$ mice based on several characteristic hallmarks of brain injury. Once the injury site was defined cell counts for neutrophils, macrophages and T cells within the injury site were conducted to objectively compare the cellular infiltrate in MT-I/II$^{-/-}$ mice and wild type mice.

2.2 Methods

2.2.1 Animals

All procedures involving animals were approved by the Animal Experimentation Ethics Committee of the University of Tasmania and were consistent with the Australian Code of Practice for the Care and Use of Animals for Scientific Purposes. Breeding stock for 129SI/SvImJ mice and MT-I/II$^{-/-}$ mice of the strain 129S7/SvEvBrd-*Mt1*^{tm1Bri} *Mt2*^{tm1Bri}/J (Masters et al. 1994) were obtained from Jackson Laboratories. The 129S1/SvImJ strain is reported by Jackson Laboratories to be a very close genetic match to the 129S7/SvEvBrd-Mt1^{tm1Bri}Mt2^{tm1Bri}/J strain. However, the records for the back-crosses of the original MT-I/II -/- mouse strain are incomplete so it is difficult to guarantee the adequacy of the 129S1/SvImJ strain as a control strain although it is commonly used in the prevailing literature. Male mice from both strains were housed with food and water ***ad libitum*** with 12/12 hour light/dark cycling. Mice of both strains were age-matched within the age-range of 12-24 weeks old. Mice were divided evenly into groups for the time points of 0, 1, 3 and 7 days post-injury (DPI). Animals within these groups were randomised and placed in numbered cages to blind the strain of the mouse from the researchers. Each mouse was housed in an individual cage for at least 3 days prior to injury surgery. Experiments were conducted with 7 animals per treatment

group (i.e. mice of the same strain and time-point of euthanasia) and total number of experimental size of 56 mice.

2.2.2 Cryolesion brain injury

The cryolesion injury method was adapted from Ling et al. (2006). Mice were fitted with an anaesthesia mask and 2-3% Isoflurane (Veterinary Companies Australia) vaporised in pure oxygen was delivered to the animal at 0.6 L/min. A 3 mm diameter, 50 mm long steel rod, insulated at one end, was cooled to equilibrium in liquid nitrogen. The scalp of the animal was shaven and swabbed with 70% isopropanol. A sagittal incision through the scalp was used to expose the cranium and the non-insulated end of the steel rod was then applied directly to the skull for 6 seconds, 4 mm anterior of lambda and 2 mm right of the midline. The skin was sutured and the animal was allowed to recover back in its original cage. Mortality rate was less than 1% but a few animals showed signs of seizure within the first 24 hours after the application of the cryolesion injury. These animals were euthanized and excluded from the study. Animals were euthanized for tissue collection at 1, 3 and 7 DPI. Zero time-point animals were housed identically to injured mice for at least 3 days but did not undergo surgery before euthanasia.

2.2.3 Paraffin embedding

Mice were euthanised with an overdose of Nembutal (9 mg per mouse) delivered via intraperitoneal injection. Mice were transcardially perfused with 0.01 M phosphate buffered saline (PBS, Medicago), brains were dissected out of the skull and immersion post-fixed in 4% paraformaldehyde for 24 hours. Brains were cut square in the coronal plane within 1 mm anterior and posterior to the injury site. Uninjured control brains were cut similarly to obtain the same region where the injury site was located in the injured animals. Blocks were placed in tissue cassettes for dehydration for 30 minutes in 70% ethanol solution followed by 30 minutes in 90% ethanol, three 30 minute submersions in 100% ethanol and three 30 minute submersions in 100% xylene. Brains were paraffin infiltrated by immersion in paraffin heated to 65-70°C for 30 minutes then were transferred to two successive 65-70°C paraffin solutions under 15 psi vacuum then 25 psi vacuum. Brains were then removed from their cassettes and embedded in moulds for microtome sectioning. Coronal sections were cut at a thickness of 5 µm on a microtome (Microm) and mounted onto APTS coated slides in a 42°C water bath. Sections were cured to slides by incubation at 50°C for 1-2 hours in an oven. Section-bearing slides were dewaxed by 3 washes in 100% xylene then rehydrated in 2 washes

in 100% ethanol, 1 wash in 90% ethanol, 1 wash in 70% ethanol, each for one minute, and final rehydration in distilled water.

2.2.4 Fluoro-jade C staining for neuron death

Fluoro-jade C (Chemicon) is a neuron-specific marker of dead and degenerating neurons. Staining was carried out according to the protocol of Schmued et al. (2005) whom demonstrated that fluoro-jade C labels both apoptotic and necrotic neuron death without discrimination. Rehydrated, slide-mounted sections were immersed in 0.06% potassium permanganate solution for 10 minutes. The slides were rinsed for 2 minutes in distilled water then immersed in 0.0001% fluoro-jade C, 0.01% acetic acid solution for 10 minutes. The slides were rinsed twice in distilled water for 5 minutes then were air-dried before they were coverslipped with Di-N-Butylphthalate in xylene mounting medium (Merck).

2.2.5 Immunohistochemistry

Before staining, antigen retrieval was undertaken in 0.01M citrate buffer, pH 6, in a pressure cooker for 10 minutes. Primary antibodies used were 1:1000 rabbit polyclonal anti-GFAP (Dako) for astrocytes, 1:100 rat monoclonal NIMP-R14 to neutrophil (Abcam) for neutrophils, 1:500 goat polyclonal anti-Iba1 (Abcam) for microglial and microglial/monocyte derived macrophages and 1:100 rabbit polyclonal anti-CD3 (Abcam) was used for T cells. All antibodies were diluted with 0.3% Triton-X 100 (Sigma) solution in PBS. Blocking with serum-free protein block (Dako) was required for CD3 staining and was applied for 30 minutes before application of primary antibodies. The diluted NIMP-R14 antibody solution contained 10% normal goat serum (Vector Labs) as a blocking reagent. Biotinylated goat anti-rat IgG (Invitrogen), biotinylated goat anti-rabbit IgG (Invitrogen) or donkey anti-goat IgG (Santa Cruz) secondary antibodies, were applied to sections according to primary antibody used, for 1 hour at room temperature. Avidin-biotin complex (Vector Labs) was used as the detection reagent and was applied to sections for 15 minutes followed by 2 rinses in PBS. Nickel enhanced 3'3-diaminobenzidine (DAB, Vector Labs) was used as the chromogen and was applied at the manufacturer's specified concentration for 8 minutes. Slides were then rinsed in distilled water for at least 5 minutes. Nuclear Fast Red (Sigma) was used as a counterstain for NIMP-R14 and Iba1 stained sections and was applied for 2 minutes or 30 seconds, respectively. The sections were rinsed thoroughly in tap water then dehydrated in graded alcohol solutions (70% ethanol, 90% ethanol,

100% ethanol, 100% xylene, 100% xylene, 1 minute each) and were coverslipped with Di-N-Butylphthalate in xylene mounting medium.

2.2.6 Cell counting strategy

Low power, 10x objective images were taken of the injury site for sections stained for fluoro-jade C, NIMP-R14, Iba1 and CD3. Fluoro-jade C counts were conducted for all positively labelled cells in the injury site and at lower depths in the un-injured CNS parenchyma. To standardise cell counts, fluoro-jade C counts were divided by the linear width of the injury in the section plane at the upper cortical surface in millimeters. NIMP-R14, Iba1 and CD3 positive cells were only counted within the injury site, the border of which was determined by methods described in the results section of this chapter. Cell counts within the injury site were standardised to the area of the injury site in that section in mm^2. Cell counts were conducted blinded to the strain of the mouse.

2.2.7 Statistical analysis

Statistical analysis was conducted using SPSS software v16.0 (SPSS Inc.). Homogeneity of variances between groups within each data set was determined with Levene's test. For data sets with heterogeneous variances between groups, the Box-Cox test was used to determine the appropriate transformation. All comparisons between wild type and MT-I/II$^{-/-}$ mice were conducted with 2-way ANOVA on the factors of time after injury and strain of mouse. Statistically significant differences in the factor of time were differentiated with Tukey's B post-hoc test. Statistically significant differences in the interaction between time and strain required a different approach to determine statistically significant groups. Single factor ANOVA was carried out on the data where data points from the same strain at each time point were considered to be a single group. Tukey's B post-hoc test on the 1-way ANOVA was used to identify the differences shown to exist in the 2-way ANOVA.

2.3 Results

2.3.1 Histological delineation of the cryolesion injury site

Investigation of the injury site at 1 DPI revealed few nuclear fast red-stained nuclei in the more dorsal levels of the injury site indicating few cells remain in the injury site (figure 2.1). As time progressed, the number of nuclear fast red-stained nuclei in the injury site increased indicating cell migration was occurring. The nuclei that could be observed near the injury border were pyknotic indicating the presence of cells

undergoing apoptosis (see figure 2.4A). For analysis of the injury site, a reliable method was required to designate the border separating the injured tissue and surviving tissue. Up-regulation of glial fibrillary acidic protein (GFAP) is a well-defined indicator of astrogliosis and is a useful indicator of brain injury (reviewed by Eng et al. 2000). Most of the astrocytes in the uninjured cortex were not immunoreactive for GFAP however, $GFAP^+$ astrocytes can be observed in the cingulum and deep cortical white matter which constitute the ventral layers of the cortex (figure 2.2B). This indicates that there is regional variation in GFAP expression in quiescent astrocytes. GFAP immunoreactivity after injury was not apparent in the cortex until 3 DPI (figure 2.1). Isomorphic reactive astrocytes have increased expression of GFAP but no change in cellular morphology and all reactive astrocytes observed at 3 DPI were of this phenotype. Anisomorphic reactive astrocytes obtain a polarity in their GFAP expression with fibrils aligned perpendicular to the injury border. Anisomorphic reactive astrocytes were evident at 7 DPI at the border to the injury site and isomorphic reactive astrocytes were still present in the parenchyma further from the injury (figure 2.1 E,F). No obvious differences in GFAP expression were found between wild type and MT-I/$II^{-/-}$ mice at any time point. The division between the injured tissue and anisomorphic reactive astrocytes was seen as a physiologically relevant demarcation between the injury and surviving tissue. However the lack of GFAP expression at 1 DPI and the lack of anisomorphic astroglia segregating injured and surviving tissue at 3 DPI required a method to demarcate the injury border which did not rely on patterns of GFAP staining. At 7 DPI the nuclear fast red-stained injury site contains visibly disrupted tissue integrity which does not extend into the domain of the anisomorphic reactive astrocytes at the border of the injury site. This disrupted tissue integrity is also found at 1 and 3 DPI but anisomorphic reactive astrocytes are not present at the injury border at these time-points to indicate whether tissue disruption is a physiologically accurate demarcation of the injury site. However, at 1 and 3 DPI pyknotic nuclei, indicative of apoptotic cells, are found in the lesion site but rarely outside the region of disrupted tissue. Therefore, in this study the border of the injury site was defined according to the integrity of the extracellular matrix, identified by nuclear fast red background staining. This definition encompasses the region of interest which is the lesion site and penumbra which will henceforth be collectively referred to as the “injury site”.

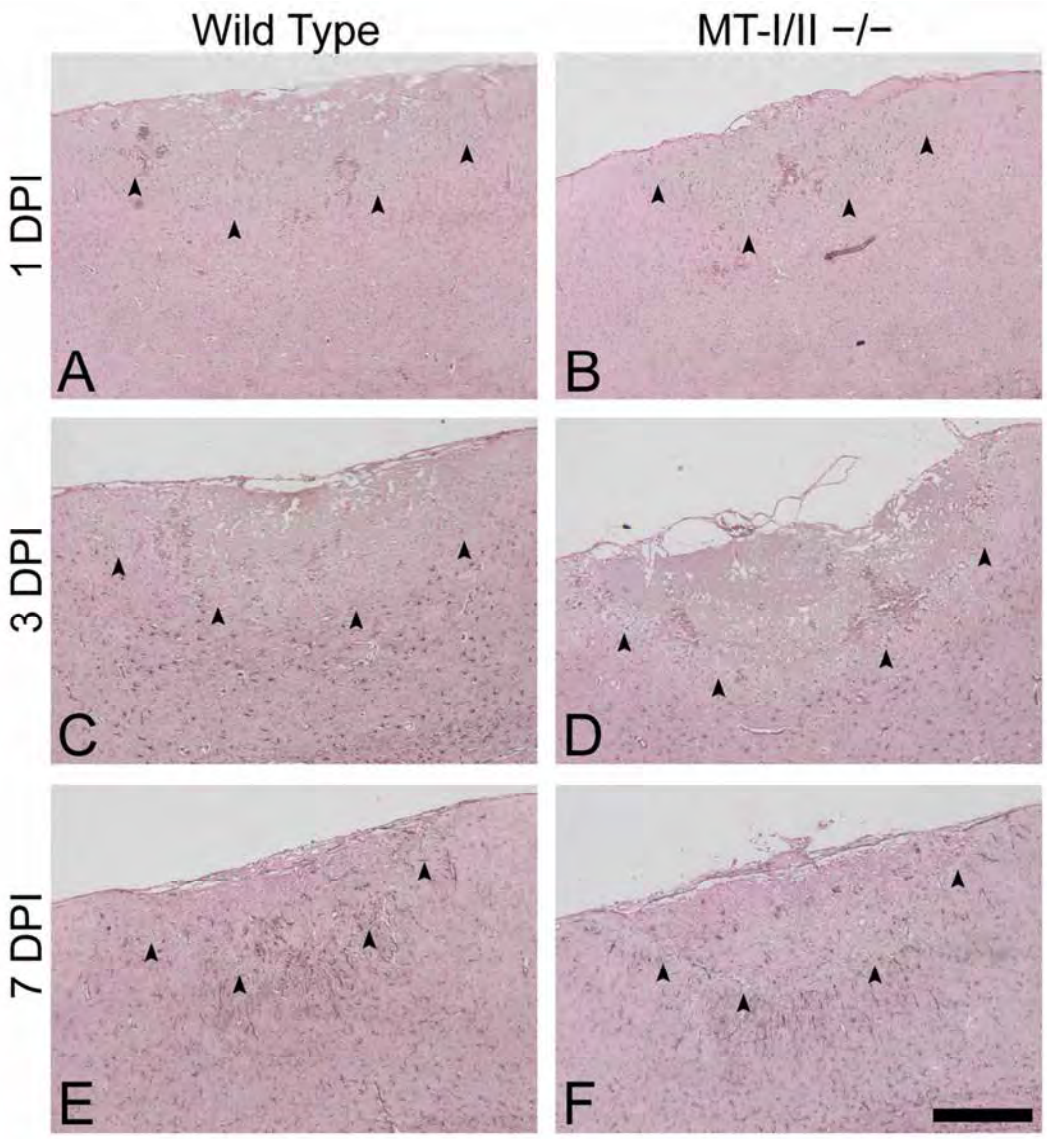

Figure 2.1. Glial fibrillary acidic protein (GFAP) immunoreactivity in the injury sites of wild type (**A**,**C**,**E**) and MT-I/II$^{-/-}$ mice (**B**,**D**,**F**). GFAP staining is absent from the injured cortex at 1 DPI (**A** and **B**). GFAP immunoreactivity is increased at 3 DPI (**C** and **D**) with isomorphic astrocytes visible in the uninjured parenchyma. At 7 DPI (**E** and **F**) GFAP immunoreactivity is increased further and anisomorphic astrocytes are now present at the lesion border, extending processes towards the injured tissue. Arrowheads indicate the injury border defined by a loss of tissue integrity which divides area containing pyknotic nuclei and the area occupied by surviving astrocytes (Scale bar = 400 μm).

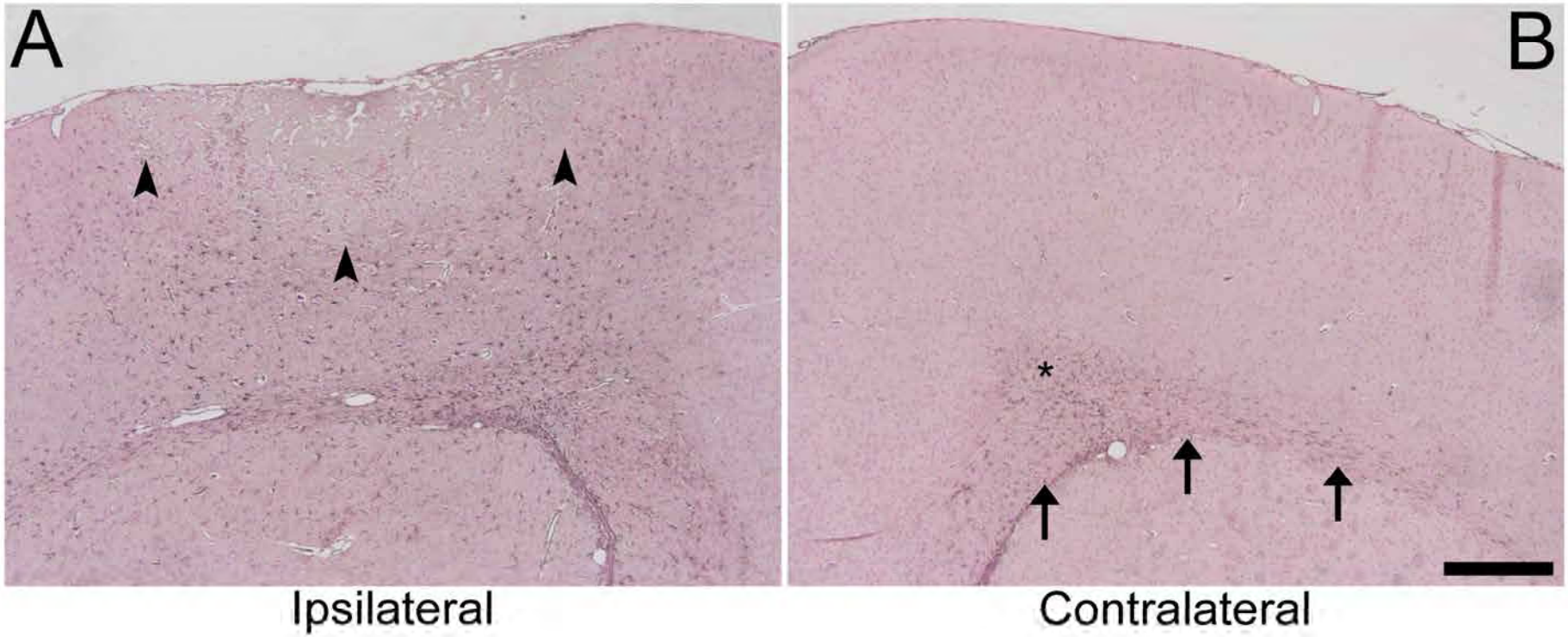

Figure 2.2 GFAP expression the ipsilateral (**A**) and contralateral (**B**) hemispheres of the cryolesioned cortex from a wild type mouse at 3 DPI. DAB immunohistochemical staining for GFAP in the contralateral hemisphere is confined to the deep cortical white matter (arrows) and cingulum(asterisk); astrocytes in the cortex are not immunolabelled for GFAP. In the ipsilateral hemisphere GFAP expression in the deep cortical white matter and cingulum is increased and GFAP expression in the upper layers of the cortex beneath the injury border (arrowheads) becomes apparent (Scale bar = 400 μm).

2.3.2 Comparison of cortical cryolesion injury in MT-I/II$^{-/-}$ and wild type mice

The cross-sectional area of the injury site in the section with the widest injury site was used as a comparative measure of injury size. The area of the injury did not change significantly from 1-3 DPI but declined significantly from 3-7 DPI in both wild type mice and MT-I/II$^{-/-}$ mice (Figure 2.3 A). However, no significant differences were observed between the strains at any time-point (P(strain) = 0.152, P(time) < 0.001, P(interaction) = 0.889). Quantification of neuron death with fluoro-jade C labelling revealed the highest degree of cell death at 1 DPI. In wild type mice the number of fluoro-jade C labelled cells decreased from 1-3 DPI and again at 3-7 DPI. MT-I/II$^{-/-}$ mice had a similar decrease in Fluoro-jade C labelled cells from 1-3 DPI compared to wild type mice. In contrast to wild-type mice, the amount of cell death did not differ between 3 and 7 DPI in the injury site of MT-I/II$^{-/-}$ mice. This was indicated by significantly greater numbers of fluoro-jade C labelled cells in MT-I/II$^{-/-}$ mice than wild type mice at 7 DPI (by 2-way ANOVA; P(interaction) = 0.022. The significant difference at 7 DPI was revealed by 1-way ANOVA with Tukey's B post-hoc test).

2.2.3 Qualitative assessment of inflammatory cell infiltration into mouse cryolesion

Neutrophils, identified with NIMP-R14 antibody, were predominantly found to occupy the necrotic and degenerating regions of the injury site (figure 2.4). Neutrophil infiltration occurred predominantly at 1 DPI and was found to be diminished at 3 DPI and almost absent from injured brains at 7 DPI. Microglia and monocyte derived macrophages were identified with Iba1 immunoreactivity (figure 2.5). Activated, ramified microglia were present at the injury border and in surviving CNS parenchyma at 1 DPI. At 3 DPI ramified microglia were still present at the injury border and in surviving parenchyma. Additionally, amoeboid macrophages of microglial or monocyte origin were beginning to enter lower levels of injury site at 3DPI. This pattern was observed at 7 DPI except the number of amoeboid macrophages in the injury site had increased and macrophages occupied both the injury border and the upper levels of the injury site. T cells were identified by CD3 immunoreactivity and were found in similar numbers at 1 and 3 DPI and showed maximal infiltration at 7 DPI (figure 2.6). T cells also occupied the same regions as Iba1^{+} cells at each time point. All images shown are from the brains of wild type mice but qualitative assessment revealed no obvious differences in wild type and MT-I/II$^{-/-}$ brains.

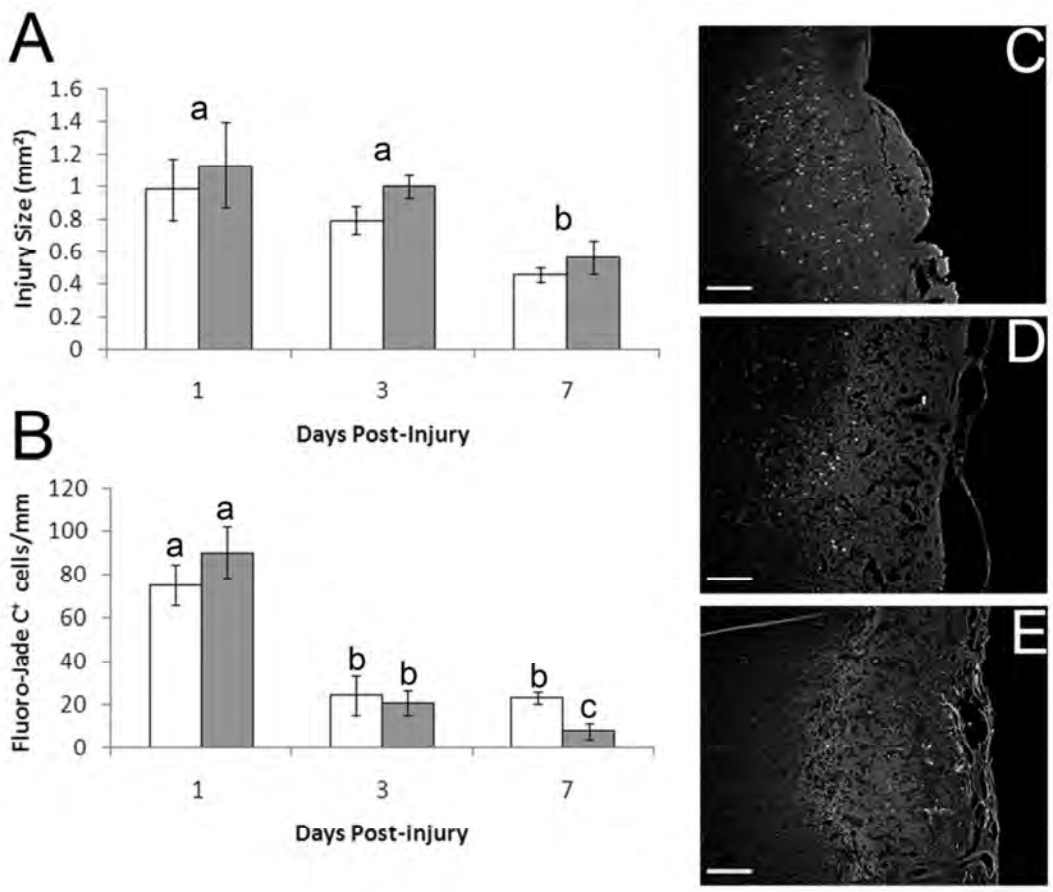

Figure 2.3 Quantification of injury size and neuron death after cryolesion injury in wild type (grey bars) and MT-I/II$^{-/-}$ mice (white bars). (**A**) Injury size was quantified by measurement of the area of the injury in sections taken from the widest point of the injury. Time-points sharing letters indicates a lack of statistically significant difference as determined by 2-way ANOVA with Tukey's B post-hoc test on the factor of time post-injury (n=5-7, error bars=SEM). (**B**) Neuron death was identified by fluoro-jade C labelling. Fluorojade-C^{+} cells were counted in the injury site and the surrounding tissue. Counts were standardised per linear mm (width) of the injury site. Lower case letters indicate significance determined by 1-way ANOVA with SNK post-hoc test. Time-points sharing letters indicates lack of statistically significant difference. n=5-7, error bars=SEM. Representative images of fluoro-jade C staining from wild type animals at 1 (**C**),3 (**D**) and 7 (**E**) DPI demonstrate the distribution of positively labelled neurons in the injury site and surrounding parenchyma. Fluoro-jade C background staining increases at later time points but the number of positively labelled cell bodies decreases (Scale bars = 200 μm).

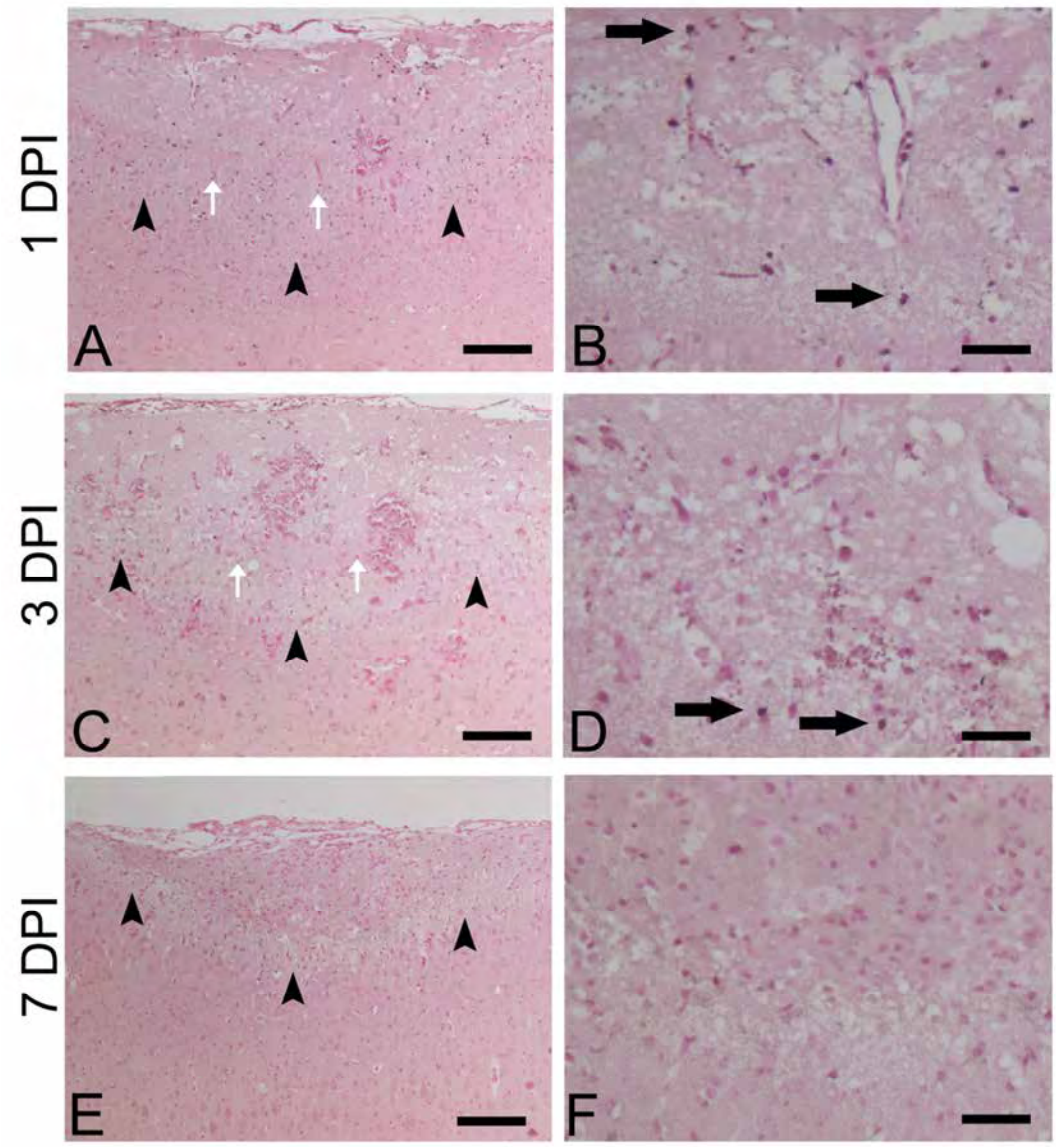

Figure 2.4 Neutrophil staining in the injury site of wild type mice with NIMP-R14 antibody with nuclear fast red counterstain. Arrowheads in the low power images designate the border of the injury site (**A**,**C**,**E**) and black arrows in the high power images indicate neutrophils (**B**,**D**,**F**). Higher power images were taken at the border of the injury site. The brain injury at 1 DPI (panels **A** and **B**) has the highest quantity of neutrophil infiltration compared to 3 DPI (panels **C** and **D**) and 7 DPI (panels **E** and **F**). At 1 DPI few non-neutrophil cells are present in the injury site evidenced by lack of DAB-negative nuclear fast red stained nuclei. Pyknotic nuclei in the fringe of the injury site are indicated by white arrows (panels **A** and **C**). The dense accumulations of red to pink cells visible within the injury site at 3 DPI are red blood cells (Scale bars = 200 μm (**A**,**C**,**E**), 50 μm (**B**,**D**,**F**)).

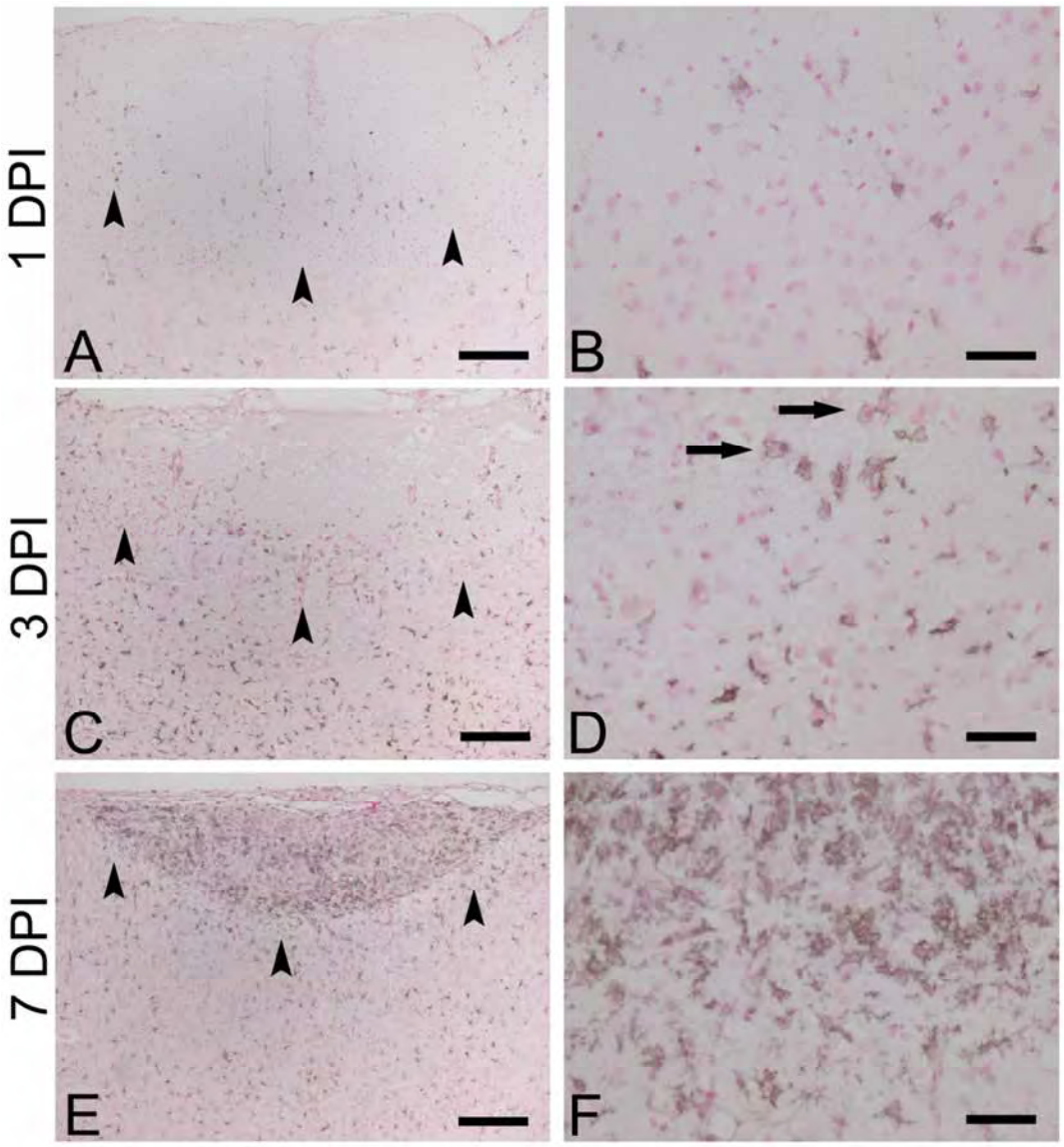

Figure 2.5 Activated microglia and macrophages labelled with Iba1 antibody within the cryolesion injury site of wild type mice. Arrowheads in the low power images designate the border of the injury site (**A**,**C**,**E**) and higher power images were taken at the border of the injury site (**B**,**D**,**F**). At 1 DPI (panels **A** and **B**) minimal microglial activation is present in the uninjured parenchyma with little Iba1 immunoreactivity found within the injury site. At 3DPI (panels **C** and **D**) microglial activation in the uninjured parenchyma is markedly increased and amoeboid macrophage-like Iba1 positive cells (arrows) are beginning to infiltrate the injured tissue at the injury border. At 7 DPI (panels **E** and **F**) the cellular infiltrate into the injury site has increased greatly and many Iba1 positive cells are found within (Scale bars = 200 μm (**A**,**C**,**E**), 50 μm (**B**,**D**,**F**)).

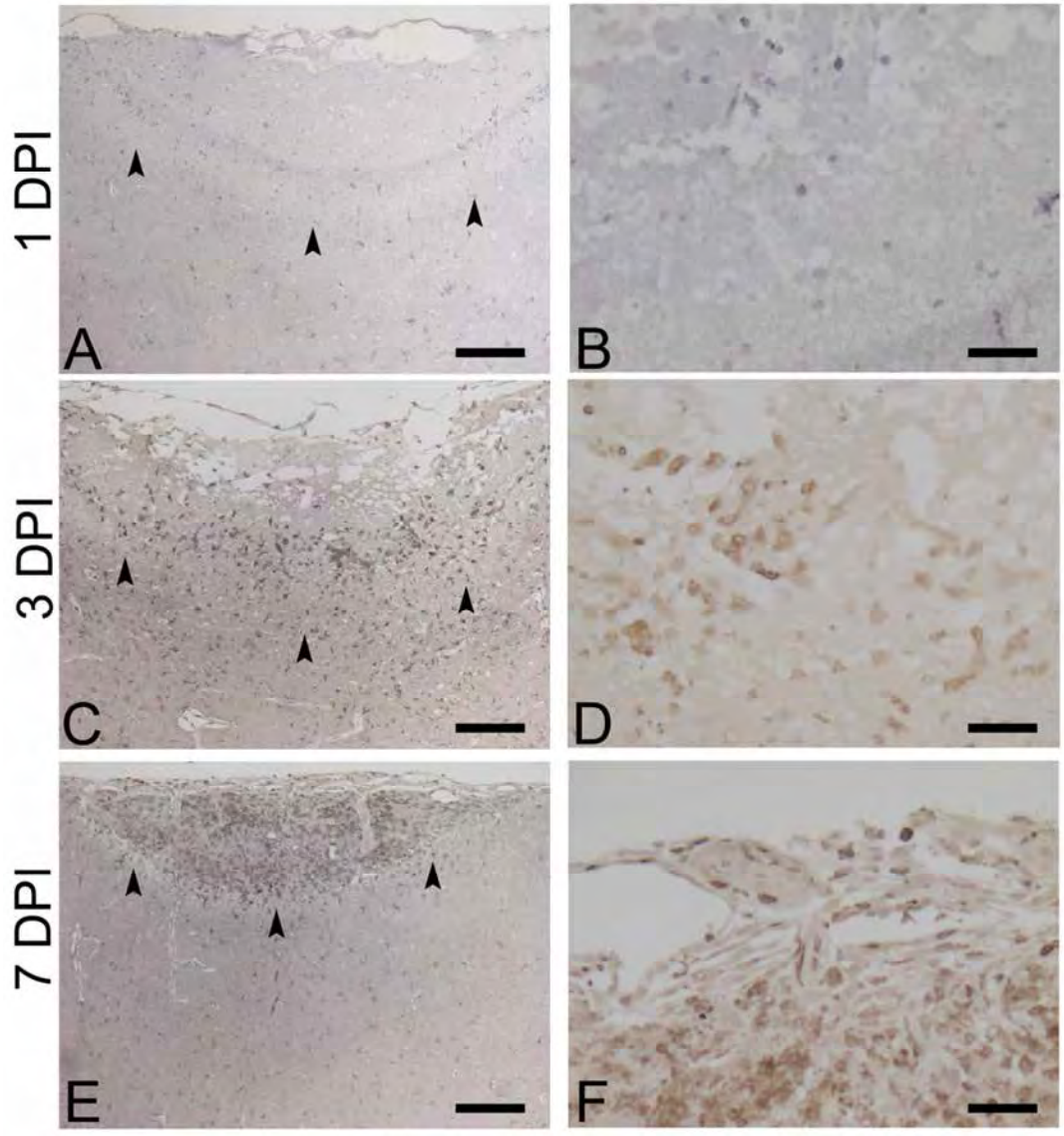

Figure 2.6 T cells labelled with anti-CD3 antibody within the cryolesion injury site of wild type mice. Arrowheads in the low power images designate the border of the injury site (**A**,**C**,**E**) and higher power images were taken at the border of the injury site (**B**,**D**,**F**). T cells are present within the injury site from 1 DPI (panels **A** and **B**), steadily increase in number at 3 DPI (panels **C** and **D**) and continue to increase up to 7 DPI (panels **E** and **F**). At all time points T cells are found predominantly within the injury site compared to CD3 positive cells in the uninjured tissue (Scale bars 200 μm (**A**,**C**,**E**), 50 μm (**B**,**D**,**F**)).

2.3.4 Quantitative comparison of leukocyte infiltration into mouse cryolesion

Leukocyte infiltration into the cryolesion at 1, 3 and 7 DPI was quantified to determine if there was any relationship between leukocyte numbers and the sustained neuron death at 7 DPI in MT-I/II$^{-/-}$ mice (figure 2.7). No significant differences were found between neutrophil numbers in the injury site of wild-type and MT-I/II$^{-/-}$ mice at 1, 3 or 7 DPI (P(strain) = 0.835, P(time) < 0.001, P(interaction) = 0.833). Iba1^{+} cells within the injury site were quantified and no significant differences in microglia/macrophage numbers were found between MT-I/II$^{-/-}$ and wild type mice were observed at any time point (P(strain) = 0.253, P(time) < 0.001, P(interaction) = 0.616). There was no difference between T cell numbers in the injury site of wild type and MT-I/II$^{-/-}$ mice at 1 and 3 DPI. However the density of T cells was found to be significantly higher in MT-/I/II $^{-/-}$ mice than in wild type mice at 7 DPI by ~55% (by 2-way ANOVA P(interaction) = 0.002 and the significant difference at 7 DPI was revealed by 1-way ANOVA with Tukey's B post-hoc test). Of the time points examined, 7 DPI was observed to have the highest level of immune cells occupying the injury site. Neutrophil numbers were maximal at 1 DPI and were comparable to microglia and T cell numbers at this time point. The maximal density of neutrophils which occurred at 1 DPI was ~6-fold lower than macrophage and T cell numbers at their maximum density which occurred at 7 DPI. Therefore neutrophils were never the most prevalent leukocyte in the cryolesioned brain in terms of cell number. Macrophages and T cells dominated the injury site at 3 and 7 DPI.

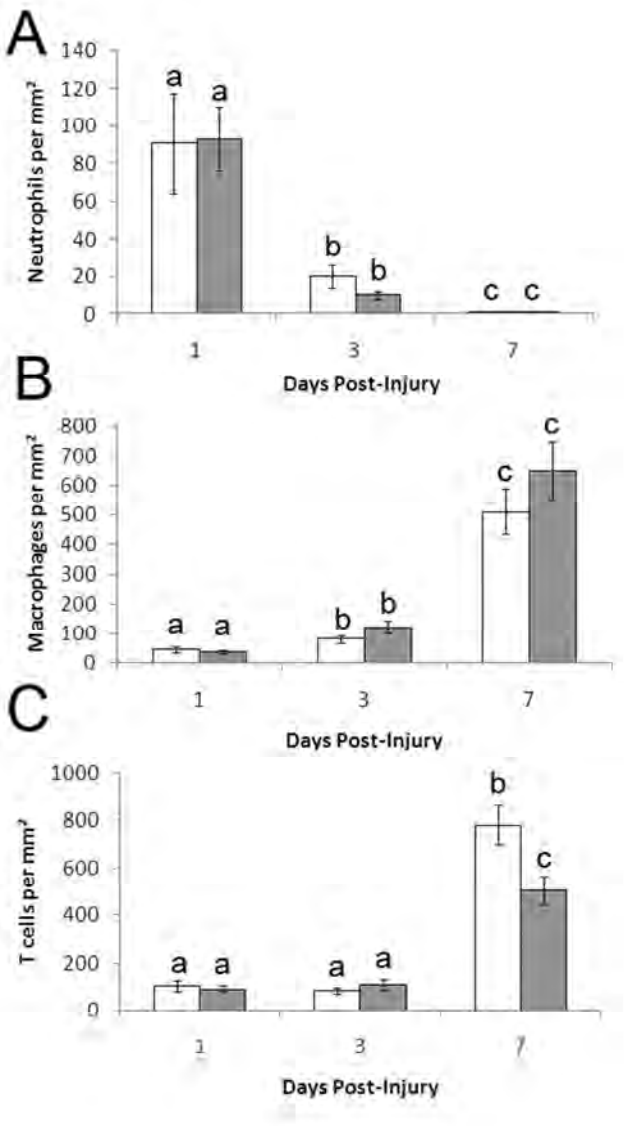

Figure 2.7 Leukocyte counts in sections of the injury site of MT-I/II$^{-/-}$ mice (white bars) and wild type mice (grey bars) standardised to injury area. Neutrophil numbers (**A**) were determined by NIMP-14 immunoreactivity. Microglial and monocyte derived macrophages numbers (**B**) were determined by Iba1 immunoreactivity. T cell numbers (**C**) were determined by CD3 immunoreactivity. Lower case letters indicate significance determined by 1-way ANOVA with Tukey's B post-hoc test. Time-points sharing letters indicates a lack of statistically significant difference (n=5-7, error bars=SEM).

2.4 Discussion

The major experimental aim of this chapter was to develop a method to deliver an aseptic closed-head injury to the CNS. The adoption of a liquid nitrogen-cooled steel rod to administer cortical cryolesion to MT-I/II$^{-/-}$ and wild type mice resulted in a reproducible and well-defined injury site. Using this method, no differences in lesion size were observed between wild type and MT-I/II$^{-/-}$ mice. Significant increases in neuron death and T cell infiltration were apparent in MT-I/II$^{-/-}$ mice, but only at 7 DPI. The fluoro-jade C data show that for wild type mice, the injury has transitioned from a degenerative phase observed at 1-3 DPI, to a regenerative phase by 7 DPI. The macrophage and T cell density in the injury site was highest at 7 DPI suggesting that these cells may influence the recovery from brain injury after the degenerative period has ceased in wild type mice. It would also appear that the injured brain of MT-I/II$^{-/-}$ mice is not transitioning to a regenerative state in the same manner as wild type mice based on the fluoro-jade C and immune cell temporal distribution.

2.4.1 Neuron death and T cell infiltration is altered in MT-I/II$^{-/-}$ mouse brain injury

Prolonged neuron death and increased T cell infiltration in the injury site were major differences observed between MT-I/II$^{-/-}$ mice and wild type mice. It is possible that the two phenomena are related because neurons can directly trigger microglial activation ***in vitro*** (Sudo et al. 1998) which can lead to the inflammatory processes that promote the infiltration of T cells. Additionally, T cells have been shown to directly cause neuron death ***in vitro*** (Giuliani et al. 2003). From the present data it is not possible to determine whether neuron death and T cell infiltration are related in MT-I/II$^{-/-}$ mice but the fact that they both differed from wild type mouse levels at 7 DPI, but no other time points, presents the possibility that the two events are linked. A latent period before increased neuron death in MT-I/II$^{-/-}$ mice compared to wild type mice has been reported previously (Natale et al. 2004). However, increased neuron death in MT-I/II$^{-/-}$ mice has also been observed within 24 hours of brain injury (Penkowa et al. 1999a). One of the criticisms of the study by Penkowa et al. (1999a) is that neuron death was assessed by counting neuron-specific enolase labelled neurons immediately adjacent to the injury border. This approach assumes that neuron numbers in the region of interest were identical in wild type mice and MT-I/II$^{-/-}$ mice before the injury occurred. Because, in their study, the injury site was larger in MT-I/II$^{-/-}$ mice, the border of the injury site would be at different depths in wild type mice and MT-I/II$^{-/-}$ mice and therefore the counts for surviving neurons may have been conducted in different layers

of the cortex. It is well known that there are large differences in the density and distribution of neurons in different layers of the cortex (DeFelipe et al. 2002). The present study avoids these problems because the injury size did not differ between the strains at any time point and neuron death was measured directly.

In light of this, the important question becomes: why do MT-I/II$^{-/-}$ mice have an increased injury size in dry ice induced cortical lesions compared to the liquid nitrogen induced lesion used in the present study? The cryolesion model presented here consists of a 6 second freeze with a steel rod cooled to approximately −196°C which is sufficient to cause damage to neural tissue but the temperature of the cortex is only lowered momentarily, whereas cryolesion by dry ice (−78°C) requires application to the skull for 90 seconds (Penkowa and Moos 1995). The dry ice cryolesion induced a high degree of haemorrhage which was determined by both a visible accumulation of haemoglobin in the injury site and immunohistochemical staining for extravasation of albumin within 30 minutes of injury (Penkowa and Moos 1995). Albumin extravasation was not investigated in the present study, but substantial numbers of red blood cells in the injury site were not found until 3 DPI (most evident in figure 2.4). The dry ice cryolesion also produced a lesion with an irregular shape (Penkowa and Moos 1995) which may affect the ability to compare injury size in histological sections. In the present study, the affected surface of the cryolesioned brain was consistently circular in shape (personal observation) and had some bruising but the haemorrhaging was not to the extent observed by Penkowa and Moos (1995). Therefore the two methods of administering cryolesion injury differ considerably and therefore the sequelae of the injury is also likely to differ which may explain differences in the activation of the macrophage response to the injury.

The level of T cell infiltration into MT-I/II$^{-/-}$ mouse cryolesions has not been compared to wild type mice before. However it has been shown that transgenic over-expression of MT-I in mice leads to decreased T cell infiltration into the CNS after cryolesion or kainic acid injection to the hippocampus (Giralt et al. 2002, Penkowa et al. 2005). Systemic injection of MT-II protein after brain injury causes decreases in T cell infiltration in wild type and MT-I/II$^{-/-}$ mice (Giralt et al. 2002, Penkowa et al. 2006b) which might suggest that extracellular MT-I/II can affect the T cell response to brain injury. Similarly, the T cell infiltrate into the CNS of mice with EAE is greater in MT-I/II$^{-/-}$ mice than in wild type mice (Penkowa et al. 2003). It is not known if MT-I/II is

required to enter the brain to affect the infiltration of T cells into the injury site. However, it has been shown that injection of MT into mice and rats alters the numbers of macrophages and T cells in the spleen and bone marrow (Giralt et al. 2002, Penkowa and Hidalgo 2000). Increased plasma concentration of MT has been observed in patients with traumatic brain injury (Kukačka et al. 2006), which gives credence to the hypothesis that extracellular MT could influence the progression of brain injury indirectly by modulating the immune system.

2.4.2 Injury-site neutrophil and macrophage numbers are not altered in MT-I/II$^{-/-}$ mice

Comparison of neutrophil infiltration into the injured CNS of wild type and MT-I/II$^{-/-}$ mice has not been previously reported. Because neutrophils showed the lowest infiltration cumulatively over the 7 day experimental period and were mostly absent from injury sites at 7 DPI, they probably do not contribute to the altered levels of cell death and T cell infiltration in MT-I/II$^{-/-}$ mice at 7 DPI. The finding that numbers of macrophages in the injury site did not differ between the MT-I/II$^{-/-}$ mice and wild type mice is in contrast to previous studies that show higher numbers in MT-I/II$^{-/-}$ mice after injury (Penkowa et al 1999a, Potter et al. 2007, Potter et al. 2009). However, in experimental brain injury induced by systemic 6-aminonicotinamide injection and hippocampal injection of kainic acid, numbers of cells expressing macrophage markers in the CNS of MT-I/II$^{-/-}$ mice were lower than wild type mice (Penkowa et al. 1999b, Carrasco et al. 2000). Therefore different injury models can vary greatly in the response they elicit from microglia and macrophages.

An important question regarding the technique of cell counting for macrophages using immunohistochemistry is whether the technique adequately identifies all microglia and monocytes present, or labels only a subset of the most activated cells in the injury site. Because microglia express macrophage markers at lower levels when quiescent (Denker et al. 2007, Sedgwick et al. 1991, Stirling and Yong 2008), the observations of differences in macrophages in previous studies may represent different activation states of microglia in MT-I/II$^{-/-}$ mice rather than differences in microglial cell density. In the present study sufficient numbers of cells could not be isolated from the cryolesion injury site to assess microglia/macrophage activation by flow cytometry (data not shown). However all macrophage counts were confined to the injury site in the present study. Given the fact that the injury site is almost devoid of cells at 1 DPI, any cells expressing macrophage markers must either derive from infiltrating monocytes or activated microglia that have migrated to the injury site. Because macrophage

migration requires activation, the cells found in the injury site have all undergone activation and are likely to be expressing macrophage markers strongly.

2.4.3 Conclusion

The cryolesion injury model developed for assessing the response to injury induces a reproducible lesion with a substantial infiltration of immune cells. The increase in T cell infiltration into the lesion site at 7 DPI in MT-I/II$^{-/-}$ mice is consistent with several other studies and is of interest due to the potential for MT-I/II to affect brain injury by modulating T cell responses. It warrants mention that in the studies reviewed by Donnelly and Popovich (2008), the function of the immune system may persist for some time after the 7 DPI time point used in these experiments and it remains possible that additional differences in the immune function of MT-I/II -/- mice may become apparent as the brain injury progresses further. Subsequent chapters of this thesis seek to elucidate some of the mechanisms by which MT-I/II$^{-/-}$ mice have an altered immune response to brain injury.

Chapter 3 – MT-I/II$^{-/-}$ Mouse Immune Response to Brain Injury

3.1 Introduction

In the previous chapter, the level of T cell infiltration into the injured brain of MT-I/II$^{-/-}$ mice was found to be significantly greater than in wild type mice, seven days after injury. There are three aspects of the immune response to brain injury that may provide plausible explanations for this difference between MT$^{-/-}$ and wild type mice; (1) altered chemotactic signals that initiate extravasation of leukocytes into the cryolesion injury site, (2) differences in the numbers of circulating leukocytes before and after injury, or (3) the activation phenotype of leukocytes entering the injured CNS. A multi-tier approach was designed to investigate these processes, both in the injured brain, and in organs outside the CNS.

3.1.1 The role of chemokines in the inflammatory response to brain injury

Chemokines are essential for leukocyte diapedesis, the process by which leukocytes leave blood vessels and enter tissues (reviewed by Ley et al. 2007). Chemokines in the site of brain injury are generally up-regulated and orchestrate immune cell migration into the injury site. There are two basic chemokine sub-sets, the CXC (α-chemokines) which act upon CXC chemokine receptors and CC (β-chemokines) which act on CC chemokine receptors (for review see Bajetto et al. 2001). Chemokine gradients within inflamed tissues provide a chemotactic signal that direct leukocytes and tissue resident immune cells to migrate to the affected area. Certain chemokines, known as arrest chemokines, activate leukocytes in the blood which induces cell-membrane molecule changes that cause firm adhesion of activated leukocytes to the endothelial wall allowing extravasation into tissues (Anacuta et al. 2003, Baltus et al. 2005, Gerszten et al. 1999, Ley 2003, Smith et al. 2005). Plasma chemokine levels are known to increase in response to brain injury and are thought to influence leukocyte infiltration into the CNS parenchyma (Rancan et al. 2004, Terao et al. 2008, Lumpkins et al. 2008). The liver has been proposed to be a major source of chemokines found in plasma after brain injury because hepatic expression of chemokines increases after inflammation in the brain (Campbell et al. 2002, Campbell et al. 2003, Campbell et al. 2005, Campbell et al. 2007a, Campbell et al. 2007b, Chapman et al. 2009). Furthermore, interfering with chemokine signalling via specific depletion of circulating monocytes and Kupffer cells, or by inhibiting hepatic NF-κB activation, attenuates the rate of leukocyte infiltration into the injured CNS (Campbell et al. 2008a, Campbell et al. 2008b). For these reasons, the expression of chemokines in both brain and liver of MT-I/II$^{-/-}$ mice were assessed in this chapter.

3.1.2 Circulating leukocytes in MT-I/II$^{-/-}$ and wild type mice

A common assumption regarding the use of null mutant mice in brain injury experiments is that the control strain and null mutant have the same baseline levels of relevant parameters before brain injury. Under resting conditions, blood T cell counts have been found to be lower in MT-I/II$^{-/-}$ mice compared to wild type mice (Crowthers et al. 2000) but a lack of variation between the two strains has been observed in other experiments (Huh et al. 2007). In both studies the MT-I/II$^{-/-}$ mice were bred on the 129SI/SvImJ background. It is possible that differences in the leukocyte populations in MT-I/II$^{-/-}$ mice only arise under certain conditions, as do many of the differences observed between wild type and MT-I/II$^{-/-}$ mice. In this chapter the ratios and absolute numbers of circulating leukocytes in MT-I/II$^{-/-}$ mice and wild type mice were compared before and after injury.

3.1.3 Th1/Th2 responses after brain injury

The process by which leukocytes are activated after injury is not well understood but cytokines are thought to play a primary role. It is also known that T cells are activated in peripheral lymphoid organs before they enter the injured brain (Ling et al. 2006). There are examples of differences in response to brain injury or cerebral ischemia where Th1 and Th2 biased strains of mice exhibit altered pathology after the insult (Kipnis et al. 2003, Lambertsen et al. 2002). Th1 cytokines induce classically activated macrophages (caMΦs) and Th2 cytokines induce alternatively activated macrophages (aaMΦs) (reviewed by Gordon 2003). Recent evidence has shown that aaMΦs are less neurotoxic than caMΦs (Kigerl et al. 2009). Evidence also suggests that MT-I/II$^{-/-}$ mouse helper T cells have a Th1 bias (Huh et al. 2007) and that monocytes from MT-I/II$^{-/-}$ mice have phenotype more characteristic of classically activated macrophages than wild type mice (Emeny et al. 2009). In this chapter, attempts to assess the Th1/Th2 ratio and quantify the aaMΦ response in wild type and MT-I/II$^{-/-}$ mice after cryolesion to the cerebral cortex were undertaken.

Thus, cytokine expression, chemokine expression, blood leukocyte concentrations and alternative activation of macrophages were all investigated in this chapter. The underlying aim was to provide an explanation for the prolonged neuron death and increased T cell infiltration at 7 DPI in MT-I/II$^{-/-}$ mice detailed in the previous chapter.

3.2 Methods

3.2.1 Animals and cryolesion brain injury

Animal housing and cryolesion injury were conducted as per the method outlined in chapter 2.2. Experiments were conducted with either 7 animals per treatment group (i.e. mice of the same strain and time-point of euthanasia) and total number of experimental size of 56 mice or 6 animals per group and 48 animals per treatment group.

3.2.2 Isolating leukocytes and peripheral blood mononuclear cells (PBMCs) from whole blood

Blood was obtained from mice by cardiac puncture with syringes containing EDTA (3 mg per ml of blood). Blood was diluted 1:4 in PBS supplemented with 2% foetal calf serum (FCS, Gibco) and overlaid onto tubes containing 2 ml of histopaque at room temperature. Histopaque 1119 (Sigma) was used to obtain leukocytes and Histopaque 1083 (Sigma) was used to obtain peripheral blood mononuclear cells (PBMCs). Centrifugation of the tubes at 700*g* for 30 minutes was used to isolate the required cell population on the density gradient. The cells from the density interface were removed by aspiration with a Pasteur pipette and were transferred to separate tubes. The cells were pelleted by centrifugation at 10 000*g* for 1 minute. The supernatant was removed and 1 ml of PBS-2%FCS was used to resuspend the cells and rinse away any remaining Histopaque. The cells were pelleted by centrifugation and the supernatant was removed so the cells could be used for RNA isolation or flow cytometry staining.

3.2.3 Quantitative reverse-transcriptase PCR (RT-PCR)

Mice were transcardially perfused with PBS. The brain injury site was dissected out of the brain using a 3 mm biopsy punch and frozen in liquid nitrogen. Liver samples from the left lobe were dissected out of mice and frozen in liquid nitrogen. To lyse PBMCs, 250 μl of TRI reagent (Sigma) was added to cell pellets. Liver samples were first ground to a fine powder under liquid nitrogen and approximately 50 mg of tissue was homogenised with an Ultra-Turrax mechanical homogeniser (IKA) in 250 μl of TRI reagent. Brain biopsies were homogenised whole by Ultra-Turrax in 250 μl of TRI reagent. RNA was extracted from TRI reagent according to manufacturer specification. RNA concentration was determined by optical density and 1 μg of RNA from each sample was used to synthesise cDNA with the Superscript III reverse transcriptase system (Invitrogen). RNA samples were treated with 1 unit of DNase I (Sigma) at 37°C in first strand buffer (Invitrogen) followed by heat-inactivation at 75°C for 10 minutes

and annealing of mRNA to oligo-DT primer (6.9 μM) at 70°C for 5 minutes. mRNA was reverse-transcribed to cDNA in a solution containing first strand buffer (Invitrogen), 5 units/μl Superscript III reverse transcriptase (Invitrogen), 0.01 M dithiothreitol (Invitrogen) and 1.125 mM dNTP (Promega) in a total volume of 20 μl. The reaction was incubated at 42°C for 50 minutes followed by enzyme heat-inactivation at 70°C for 15 minutes. Real-time PCR was conducted to quantify concentration of various cDNA transcripts using Quantitect SYBR green PCR master mix (Qiagen) on the Corbett Rotorgene-6000 as described by (Brettingham-Moore et al. 2005). The initial melt phase was set to 95°C for 900 seconds followed by cycling which consisted of 95°C for 15 seconds and 60°C for 60 seconds then acquiring data to cycling A, Channel 1. PCR cycling was conducted for 45 cycles and melt curves were generated from 60°C to 95°C holding for 5 seconds at every 1°C increment and acquiring data to cycling A, Channel 1. Primers (sets are listed in table 3.1) were used at a final concentration of 1 μM. Standard curves were created by serial dilution of known quantities of each PCR product. From the standard curve the cDNA copy number could be determined from the number of PCR cycles required to reach a given fluorescence threshold (C_T). GAPDH was found to be highly variable between animals in liver so β-actin was used as the house keeping gene for liver samples (data not shown). GAPDH was used as the house keeping gene in brain injury samples because β-actin is a structural protein that is likely to undergo changes during brain injury due to the high degree of tissue remodelling occurring in the injury site. For each transcript of interest, the mRNA copy number was divided by the copy number of the house keeping gene to standardise the data set.

Table 3.1 Oligonucleotide primer sets used for quantitative RT-PCR of brain and liver samples after cryolesion brain injury.

Primer		Sequence (5' - 3')	Product length
GAPDH	Fwd	CCCAGAAGACTGTGGATGG	80
	Rev	GGATGCAGGGATGATGTTCT	
β-actin	Fwd	GTCCACCTTCCAGCAGATGT	260
	Rev	AGGGAGACCAAAGCCTTCAT	
CCL2	Fwd	AGGTCCCTGTCATGCTTCTG	249
	Rev	TCTGGACCCATTCCTTCTTG	
CCL3	Fwd	CCTCTGTCACCTGCTCAACA	217
	Rev	CAGGAAAATGACACCTGGCT	
CCL5	Fwd	CCCTCACCATCATCCTCACT	220
	Rev	CACTTCTTCTCTGGGTTGGC	
CXCL1	Fwd	AGACTGCTCTGATGGCACCT	290
	Rev	TGCACTTCTTTTCGCACAAC	
CXCL2	Fwd	AGTGAACTGCGCTGTCAATG	308
	Rev	CATCAGGTACGATCCAGGCT	
TNF-α	Fwd	CTCTTCAAGGGACAAGGCTG	253
	Rev	CGGACTCCGCAAAGTCTAAG	
IL-6	Fwd	CCGGAGAGGAGACTTCACAG	134
	Rev	CAGAATTGCCATTGCACAAC	
IFN-γ	Fwd	ACTGGCAAAAGGATGGTGAC	212
	Rev	GACCTGTGGGTTGTTGACCT	
IL-4	Fwd	TCAACCCCCAGCTAGTTGTC	184
	Rev	TCTGTGGTGTTCTTCGTTGC	
Ym1	Fwd	ACAATTTAGGAGGTGCCGTG	324
	Rev	CCAGCTGGTACAGCAGACAA	

3.2.4 Haemocytological analysis

Blood was obtained by cardiac puncture with syringes containing EDTA (3 mg per ml of blood). From each animal 250 µl whole blood was analysed in an Advia 120 haemocytological analyser (Siemens). Samples showing a high degree of platelet clumping as determined by the haemocytological analyser or anomalous cell distribution on forward and side scatter plots compared to the majority of samples were excluded from the data set.

3.2.5 Flow cytometry for $CD3^+CD4^+$ helper T cells

10^6 leukocytes were used for each batch of staining. Leukocytes were stained with a combination of 1 µg/ml APC-conjugated hamster IgG1 anti-mouse CD3e (BD Biosciences) and 1 µg/ml PE-conjugated rat IgG2a anti-mouse CD4 (BD biosciences) in 200 µl PBS-2%FCS at 4°C for 15 minutes. The cells were pelleted by centrifugation, and washed twice by resuspension in PBS-2%FCS followed by centrifugation to pellet. The pellet was resuspended in a fixation solution consisting of 2% paraformaldehyde, 4% D-glucose, 0.03% sodium azide and 0.01M PBS for storage. Staining procedures were also carried out for isotype control antibodies, PE-conjugated rat IgG2a (BD Biosciences) and APC-conjugated hamster IgG1 (BD Biosciences), which were applied at the same concentration as the specific antibodies to unstained cells. Samples were assayed by flow cytometry (BD Canto II flow cytometer) and were analysed using BD FACS Diva software v6.1.1. A quadratic gate was applied to the scatter plots of CD3 versus CD4 fluorescence to identify $CD3^+CD4^+$ and $CD3^+CD4^-$ T cells which were expressed as a percentage of all leukocytes. The distinction between positive and negative staining was determined by the upper fluorescence of isotype control stained cells. All thresholds and gates were applied on this basis.

3.2.6 Flow cytometry for $CD4^+CD25^+FoxP3^+$ naturally occurring regulatory T cells

10^6 PBMCs were used for each batch of staining. Naturally occurring regulatory T cells were stained with the mouse regulatory T cell staining kit # 2 (eBioscience). PBMCs in a volume of 100 µl were stained with a combination of 1.25 µg/ml FITC-conjugated rat IgG2a anti-mouse CD4 (clone RM45, eBioscience) and 0.6 µg/ml PE-conjugated rat IgG1 anti-mouse CD25 (clone PC61.5, eBioscience) in flow cytometry staining buffer (eBioscience) at 4°C for 30 minutes. The cells were pelleted by centrifugation, and washed twice by resuspension in flow cytometry staining buffer followed by centrifugation to pellet. The pellet was resuspended in 1 ml fixation solution (eBioscience) for 30 minutes at 4°C. The cells were pelleted by centrifugation and the

supernatant was removed. Cell permeabilisation was conducted by washing twice with resuspension in permeabilisation buffer (eBioscience) followed by centrifugation to pellet. After removal of the supernatant, the cells were incubated in 100 µl of 5 µg/ml Fc Block (affinity purified anti-mouse CD16/32 antibody, BD Bioscience) for 15 minutes at 4°C. The cells were pelleted by centrifugation and the supernatant was removed followed by addition of 5 µg/ml APC anti-mouse FoxP3 antibody (clone FJK16s) for 30 minutes at 4°C. The cells were washed twice by resuspension in permeabilisation buffer followed by centrifugation to pellet. The pellet was resuspended in 200 µl of PBS containing 0.03% sodium azide for storage. Isotype control antibodies, PE-conjugated rat IgG2a (BD Biosciences) and PE-conjugated rat IgG1 (BD Biosciences), were applied to the cells in the same manner as specific antibodies. Single colour staining for each antibody was also carried out to enable compensation for spectral overlap during multicolour flow cytometry. Samples assayed by flow cytometry (BD Canto II flow cytometer) and were analysed using BD FACS Diva software v6.1.1. To identify naturally occurring regulatory T cell populations, a gate was applied to cells expressing CD4. Cells within the $CD4^+$ gate were analysed with a quadratic gate applied to the scatter plots of CD25 versus FoxP3. $CD4^+CD25^+FoxP3^+$ cells are expressed as a percentage of $CD4^+$ cells. The distinction between positive and negative staining was determined by the upper fluorescence of isotype control stained cells. All thresholds and gates were applied on this basis.

3.2.7 Plasma and brain cytokine assay

Blood was collected from mice via cardiac puncture with heparinised syringes (20 µl of 5000 units/ml heparin, Sigma) and Halt protease inhibitor cocktail (Thermo Scientific) was added to each blood sample. Plasma was obtained after centrifugation of blood for 5 minutes at 14000*g*. Plasma samples were diluted four-fold with PBS and assayed with a cytometric bead array mouse Th1/Th2/Th17 cytokine kit (BD Biosciences). The assay was run according to specification on a Canto II flow cytometer (BD Biosciences) and analysis was conducted using FCAP Array software v1.0.1 (Soft Flow Inc).

IL-4 and IFN-γ in brain were assayed with ELISA kits (R&D Systems). Brain samples were obtained using a 3 mm biopsy punch and frozen in liquid nitrogen. Protein was obtained by Ultra-Turrax homogenisation in 150 mM NaCl, 20 mM Tris-HCl, 1% Igepal, pH 7.6 with EDTA-free Halt-protease inhibitor cocktail (Thermo Scientific). Samples were centrifuged at 10 000*g* for 10 minutes and the supernatant was retained for assay. Protein content was determined by Bradford assay (Bradford 1976). Samples

were diluted to a standard 0.1 mg/ml total protein concentration and were assayed according to kit specification.

3.2.8 Statistical analysis

Homogeneity of variances between groups within each data set was determined with Levene's test. The Box-Cox test was used to determine the appropriate transformation for data sets with heterogeneous variances between groups. All comparisons between wild type and MT-I/II$^{-/-}$ mice were conducted with 2-way ANOVA on the factors of time after injury and strain of mouse. Statistically significant differences in the factor of time were differentiated with Tukey's B post-hoc test. Statistically significant differences in the interaction between time and strain required a different approach. Single factor ANOVA was carried out groups classified by injury time point and strain combined. Tukey's B post-hoc test on the 1-way ANOVA was used to identify the differences shown to exist in the 2-way ANOVA.

3.3 Results

3.3.1 MT-I/II$^{-/-}$ mouse chemokine expression in brain is not different to wild type mice post-brain injury

Chemokine mRNA was quantified to compare the chemoattractant capacity of the injury site between MT-I/II$^{-/-}$ and wild type mice (figure 3.1). No significant differences in expression of the chemokines CCL2, CCL3, CCL5, CXCL1 or CXCL2 were observed between the two strains of mice. However, the mRNA of all chemokines tested changed following brain injury, and there were several distinctly different temporal patterns observed. CXCL1 (figure 3.1A, P(strain) = 0.495, P(time) < 0.001, P(interaction) = 0.650), CXCL2 (figure 3.1B, P(strain) = 0.125, P(time) < 0.001, P(interaction) = 0.848) and CCL2 (figure 3.1C, P(strain) = 0.267, P(time) < 0.001, P(interaction) = 0.223) all show sharp increases in expression at 1 DPI. Expression of these chemokines declined to near resting levels at 3 DPI and continued to decrease towards 7 DPI. Similarly, CCL3 mRNA shows a rapid increase at 1 DPI but levels had decreased by 3 and 7 DPI, although it remained significantly elevated above resting levels (figure 3.1D, P(strain) = 0.213, P(time) < 0.001, P(interaction) = 0.618). Most chemokines tested peak early after brain injury but CCL5 mRNA expression gradually increased and was greatest at the 7 day time point. CCL5 mRNA expression was significantly up-regulated at 1 and 3 DPI but its expression was approximately 4-fold higher at 7 DPI, than at 1 and 3 DPI (figure 3.1E, P(strain) = 0.621, P(time) < 0.001,

P(interaction) = 0.876). Therefore, the data show that there are temporal differences in the expression profiles of different chemokines after brain injury but the expression profile of these chemokines does not differ between wild type and MT-I/II$^{-/-}$ mice after brain injury.

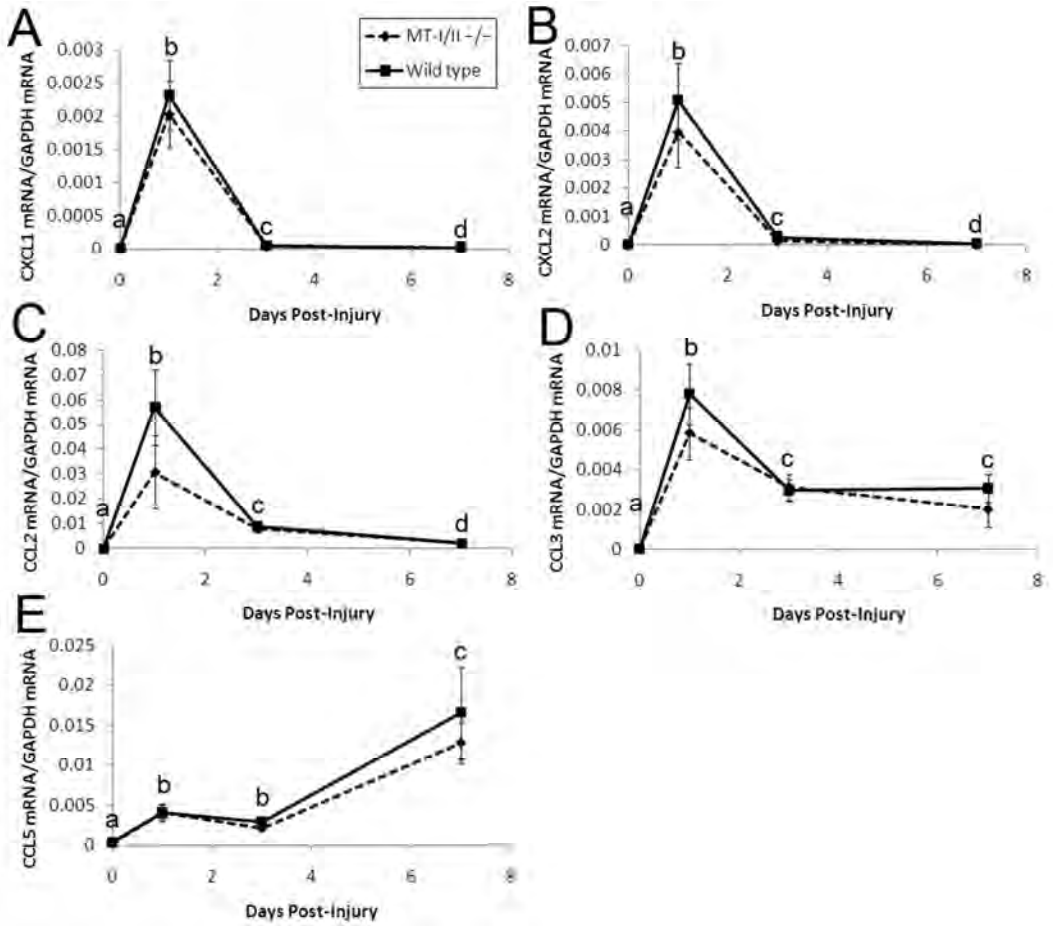

Figure 3.1 Chemokine mRNA expression in the injury site of wild type mice (solid lines) and MT-I/II$^{-/-}$ mice (dashed lines) after brain injury. 2-way ANOVA did not determine any significant differences in expression of any of the chemokines between wild type and MT-I/II$^{-/-}$ mice. A similar pattern of expression occurred for CXCL1 (**A**), CXCL2 (**B**) and CCL2 (**C**) with a marked increase in expression at 1 DPI followed by a large decrease at 3 DPI and a further decrease at 7 DPI that did not return to normal over the 7 day period. CCL3 (**D**) also increased sharply at 1 DPI but expression levels were only slightly decreased at 3 and 7 DPI. CCL5 (**E**) expression was increased at 1 and 3 DPI but showed a large increase at 7 DPI. Significant differences were determined by 2-way ANOVA with Tukey's B post-hoc test on the factor of time; groups that share lower case letters are not significantly different from each other. For all graphs; n=6-7, Error bars=SEM.

3.3.2 MT-I/II$^{-/-}$ and wild type mouse chemokine expression in liver is similar after brain injury

Liver chemokine expression has been shown to contribute to leukocyte infiltration into the injured brain (Campbell et al. 2008a, Campbell et al. 2008b). To investigate this further, brain-injury induced expression of chemokine mRNA in the liver of wild type and MT-I/II$^{-/-}$ mice was determined using quantitative RT-PCR (figure 3.2). CCL3 mRNA and CXCL2 mRNA could not be detected in liver before or after cryolesion brain injury. CXCL1 mRNA expression did not change significantly between time-points and genotypes (figure 3.2A, P(strain) = 0.422, P(time) = 0.127, P(interaction) = 0.119). CCL2 mRNA expression was increased significantly in liver after brain injury, but did not differ between strains (figure 3.2B, P(strain) = 0.718, P(time) < 0.001, P(interaction) = 0.730). In contrast to CCL2 mRNA expression in the injured brain, hepatic CCL2 was not significantly increased until 3 DPI and remained at the same level at 7 DPI. Hepatic CCL5 mRNA was detectable but did not reliably or reproducibly show any deviation from the resting levels after brain injury (data not shown). CCL3 and CXCL2 mRNA was rarely detected in the liver of either strain of mouse during the course of the experiment (data not shown). Overall there were no robust differences in chemokine expression between the mouse strains.

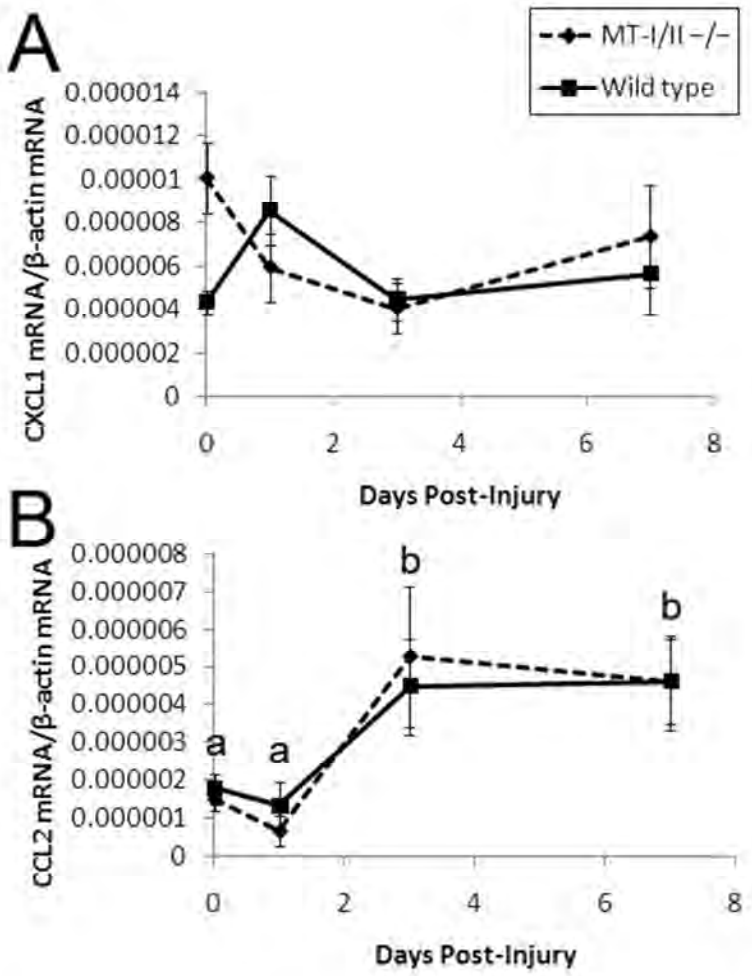

Figure 3.2 Chemokine mRNA expression in liver after brain injury. (**A**) CXCL1 mRNA expression is not significantly up-regulated in wild type mice as determined by 2-way ANOVA. (**B**) CCL2 mRNA expression is significantly increased at 3 and 7 DPI as determined by 2-ANOVA but no significant difference between strains occurred. Lower case letters indicate statistically significant differences based on the factor of time determined by Tukey's B post-hoc test. For all graphs; n=6-7, Error bars=SEM.

3.3.3 Circulating leukocyte numbers are increased in MT-I/II$^{-/-}$ mice at 7 days post-injury

A haemocytological analyser was used to determine whether differences in absolute numbers of white blood cells in MT-I/II$^{-/-}$ mice and wild type mice might account for differences in leukocyte infiltration rates into the cryolesion affected tissue (figure 3.3A). Leukocyte counts from whole peripheral blood did not significantly change after brain injury in wild type mice at 0 (uninjured), 1, 3 or 7 DPI. MT-I/II$^{-/-}$ mice showed no significant changes in leukocyte numbers in whole peripheral blood from 0-3 DPI but had significantly higher leukocyte counts at 7 DPI compared to uninjured controls and wild type mice at 7DPI (*P*(interaction) = 0.026). Due to the significant interaction in the 2-way ANOVA, 1 way ANOVA was conducted with grouping on the basis of time and strain combined into a single factor. The ANOVA remained significant (*P* = 0.026) and Tukey's B post-hoc test revealed that absolute leukocyte counts in MT-I/II$^{-/-}$ mice at 7 DPI were statistically higher than wild type mice at 7 DPI. There was no significant effect of time after injury or strain of mouse on the numbers of circulating neutrophils (figure 3.3B, *P*(strain) = 0.103, *P*(time) = 0.095, *P*(interaction) = 0.206), lymphocytes (figure 3.3B, *P*(strain) = 0.073, *P*(time) = 0.473, *P*(interaction) = 0.374) or monocytes (figure 3.3B, *P*(strain) = 0.294, *P*(time) = 0.075, *P*(interaction) = 0.081).

Because the haemocytological analyser did not differentiate between sub-classes of lymphocytes, flow cytometry was used to determine if relative ratios of T cells were equal in MT-I/II$^{-/-}$ mice and wild type mice. No significant differences between MT-I/II$^{-/-}$ mice and wild type mice were observed at any time point for CD3^{+}CD4^{+} helper T cells (figure 3.4A) or CD3^{+}CD4^{-} T cells which most likely consist of cytotoxic T cells (data not shown). It is interesting to note that T cell numbers were decreased slightly, but significantly at 7 DPI which inversely correlates with the increase in T cell infiltration into the brain at 7 DPI (chapter 2.3.4). However, using the data for absolute leukocyte counts to convert the T cell percentages into absolute T cell numbers revealed an average increase of 16% in MT-I/II$^{-/-}$ mice at 7DPI compared to uninjured mice. In contrast, wild type mice absolute T cell numbers showed an average decrease of 26% at 7 DPI compared to uninjured animals.

CD4^{+}CD25^{+}FoxP3^{+} naturally occurring regulatory T cell numbers were also investigated due to their ability to modulate the functions of helper T cells during CNS insults (Johnson et al. 2007, Kipnis et al. 2004, Liesz et al. 2009). The fraction of the CD4^{+} T cell population that consisted of CD4^{+}CD25^{+}FoxP3^{+} naturally occurring

regulatory T cells was not significantly different at 3 or 7 DPI between wild type and MT-I/II$^{-/-}$ mice (figure 3.4C).

Cryolesion brain injury does not appear to affect the relative ratios of various types of leukocytes after brain injury but there is an increase in the absolute number of circulating leukocytes 7 days after brain injury in MT-I/II$^{-/-}$ mice that is not observed in wild type mice at 7 DPI.

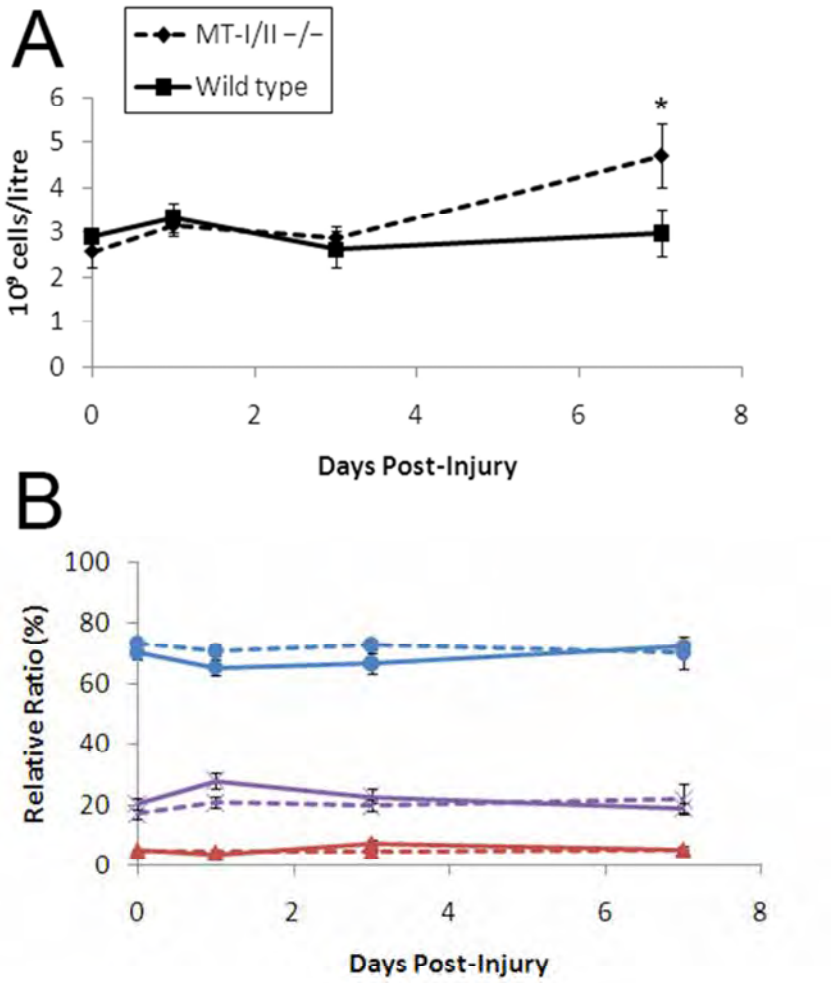

Figure 3.3 Circulating leukocyte counts after brain injury were obtained with the Advia 120 haemocytological analyser. Absolute cell numbers (**A**) show an increase at 7 DPI in MT-I/II$^{-/-}$ mice which was significantly different to all other groups of mice as determined by 2-way ANOVA with Tukey's B post-hoc test. Relative ratios of leukocytes (**B**) were compared between wild type mice (solid lines) and MT-I/II$^{-/-}$ mice (dashed lines) for lymphocytes (●), neutrophils (×) and monocytes (▲). No significant differences were found between strains for any cell type and no significant changes over time were found for any cell type by 2-way ANOVA. For all graphs; n=4-6, error bars=SEM.

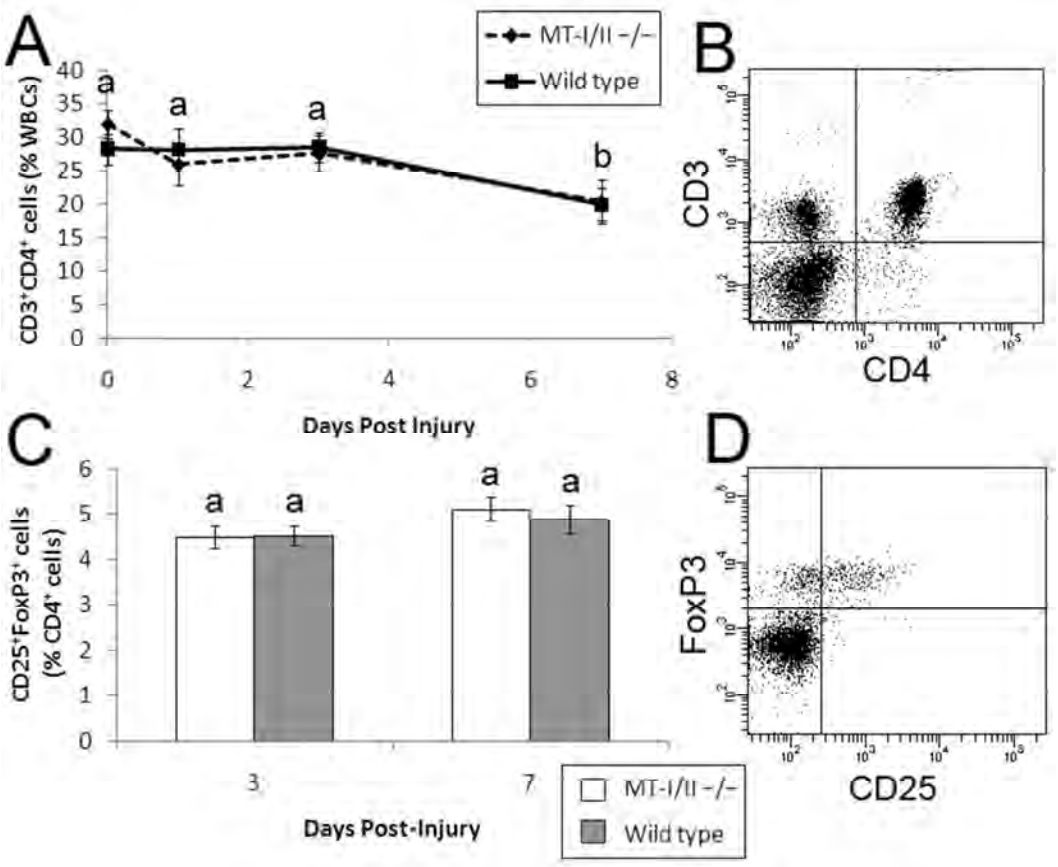

Figure 3.4 $CD4^+$ T cell ratios after brain injury were assessed by flow cytometry for CD3 and CD4 labelled cells shown in a representative scatter plot (**B**). Temporal changes in $CD4^+$ T cell ratios after brain injury are present but no significant differences between wild type (solid line) and MT-$I/II^{-/-}$ mice (dashed line) were found (**A**). Lower case letters indicate statistically significant differences based on the factor of time determined by ANOVA with Tukey's B post-hoc test, n=6-7, error bars=SEM. The $CD4^+$ cell gated population revealed the ratios of $CD25^+$ and $FoxP3^+$ naturally occurring regulatory T cells (**D**). At 3 and 7 DPI no significant differences were observed between wild type mice (grey bars) and MT-$I/II^{-/-}$ mice (white bars) (**C**), n=7, error bars=SEM.

3.3.4 MT-I/II$^{-/-}$ and wild type mouse cytokine expression does not differ in brain post-brain injury

To assess the inflammatory response in the cryolesion injury site, mRNA levels for the cytokines TNF-α, IL-6, IL-4 and IFN-γ were all assessed by quantitative RT-PCR. TNF-α mRNA levels were significantly elevated at 1 DPI and returned to normal levels at 3 and 7 DPI and no significant difference between strains was found (figure 3.5A, P(strain) = 0.187, P(time) < 0.001, P(interaction) = 0.178). IL-6 mRNA was also significantly increased in the cryolesion site at 1 DPI but a decrease in mRNA was observed at 3 and 7 DPI that remained increased above basal IL-6 mRNA expression levels (figure 3.5B, P(strain) = 0.634, P(time) < 0.001, P(interaction) = 0.392). No mRNA expression was found in the injury site for IL-4 or IFN-γ after cryolesion. Both of these transcripts were detectable in the positive control, mRNA from the EL-4 mouse T cell line that had been stimulated with calcium ionophore and phorbol ester for 6 hours (data not shown). Hence, of the measurable cytokines tested, no differences were found in mRNA quantity between wild type and MT-I/II$^{-/-}$ mice.

3.3.5 Cryolesion brain injury did not induce robust systemic cytokine production

After brain injury, IL-4 and IFN-γ protein was undetectable by ELISA in the injured brain of wild type and MT-I/II$^{-/-}$ mice (data not shown). Plasma concentrations of Th1/Th2 cytokines were assessed by fluorescent flow cytometric multiplex assay. A summary of the results is shown in table 3.2, which demonstrates that the presence of detectable plasma cytokines was a rare event after injury. IL-4 and IL-6 were not detected during the experiment and INF-γ, TNF-α and IL-10 were detected rarely and showed no discernable pattern between wild type and MT-I/II$^{-/-}$ mice. Similarly, the Th1 cytokine, IL-2 could not be detected consistently in plasma and was detected in a fraction of wild type and MT-I/II$^{-/-}$ mice at 1 and 3 DPI (figure 3.6). At 7 DPI however, only MT-I/II$^{-/-}$ mice had detectable plasma concentrations of IL-2 with 4 out of 6 animals exhibiting detectable expression of IL-2. No wild type animals had detectable levels of IL-2 at 7 DPI. Statistical analysis could not be conducted on this data set due to the high proportion of animals with plasma IL-2 concentrations lower than the detection limit. While the data set was incomplete, IL-2 signalling after brain injury appeared to be prolonged in MT-I/II$^{-/-}$ mice compared to wild type mice after brain injury.

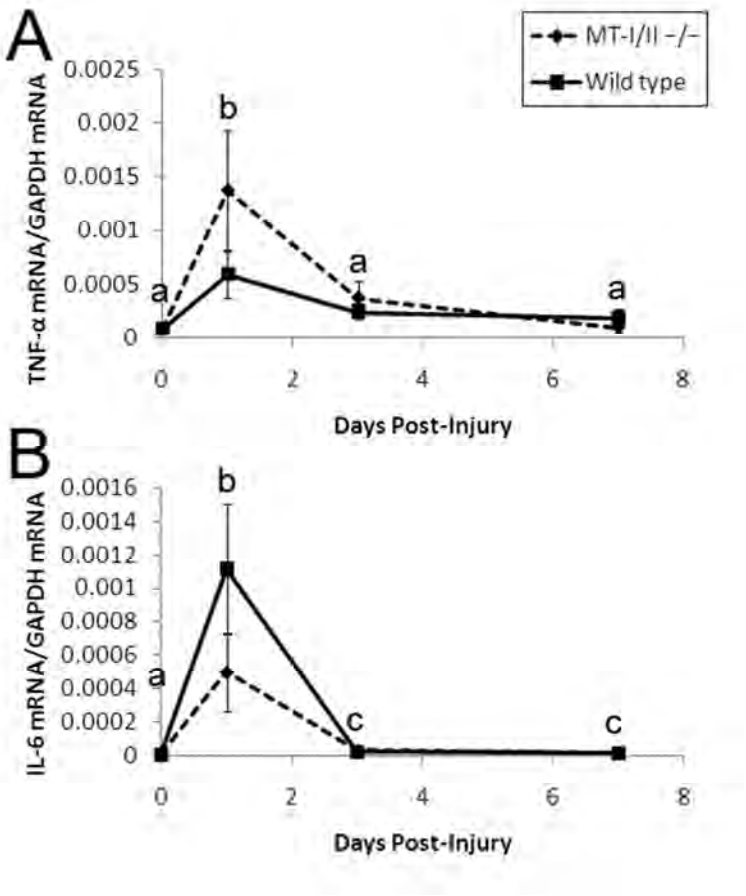

Figure 3.5 Cytokine mRNA expression in the injury site of wild type mice (solid lines) and MT-I/II$^{-/-}$ mice (dashed lines) after brain injury. (**A**) 2-way ANOVA with Tukey's B post-hoc test reveals that TNF-α mRNA production was significantly up-regulated at 1DPI and returns to normal by 3 DPI. TNF-α mRNA expression was not significantly different between wild type and MT-I/II$^{-/-}$ mouse strains. (**B**) 2-way ANOVA with Tukey's B post-hoc test reveals that IL-6 mRNA production was significantly increased at 1 DPI and began to decrease at 3 and 7 DPI but was still significantly higher than uninjured IL-6 expression. IL-6 mRNA expression was not significantly different between wild type and MT-I/II$^{-/-}$ mouse strains. For all graphs; n=6-7, Error bars=SEM.

Table 3.2. Plasma cytokine detection in MT-I/II$^{-/-}$ mice after brain injury. Displayed for each time point are the number of mice that had detectable levels of each cytokine/total number of mice. The maximum concentration detected (pg/ml) for of each cytokine at each time point is also shown.

		IL-2	IL-4	IL-6	IFN-γ	TNF-α	IL-17A	IL-10
Theoretical Detection limit (pg/ml)		0.4	0.12	5.6	2	3.6	3.2	67.2
Wild type mice								
0DPI	Number of Detectable Samples	0/6	0/6	0/6	0/6	0/6	0/6	0/6
	Maximum Concentration Detected	-	-	-	-	-	-	-
1DPI	Number of Detectable Samples	2/7	0/7	0/7	1/7	1/7	0/7	0/7
	Maximum Concentration Detected	12.56	-	-	6.27	20.1	-	-
3DPI	Number of Detectable Samples	4/7	0/7	0/7	1/7	0/7	0/7	0/7
	Maximum Concentration Detected	11.54	-	-	4.7	-	-	-
7DPI	Number of Detectable Samples	0/7	0/7	0/7	1/7	0/7	0/7	0/7
	Maximum Concentration Detected	-	-	-	8.31	-	-	-
MT-I/II$^{-/-}$ mice								
0DPI	Number of Detectable Samples	0/7	0/7	0/7	1/7	0/7	0/7	0/7
	Maximum Concentration Detected	-	-	-	4.7	-	-	-
1DPI	Number of Detectable Samples	2/7	0/6	0/6	2/6	2/6	1/6	0/6
	Maximum Concentration Detected	13.16	-	-	8.62	12.24	6.81	-
3DPI	Number of Detectable Samples	2/7	0/6	0/6	2/7	1/6	1/6	1/6
	Maximum Concentration Detected	16.66	-	-	8.52	6.27	8.84	404.1
7DPI	Number of Detectable Samples	4/6	0/6	0/6	2/6	0/6	0/6	0/6
	Maximum Concentration Detected	12.15	-	-	12.78	-	-	-

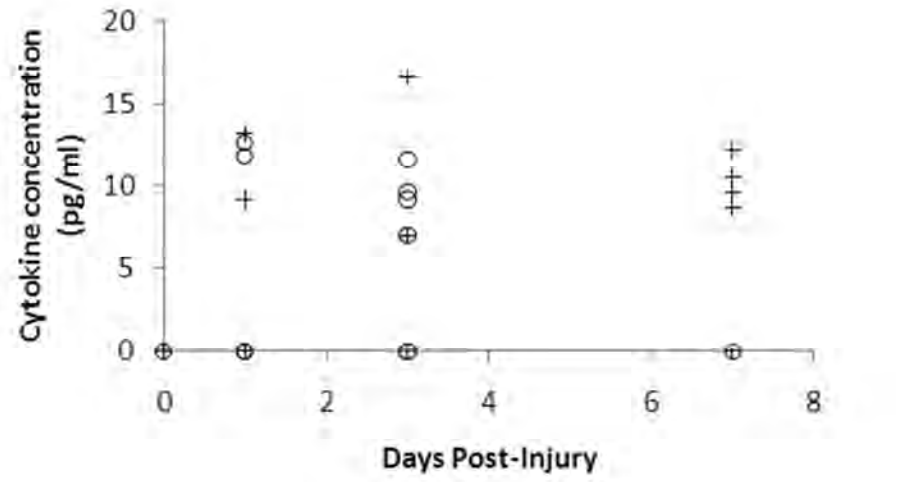

Figure 3.6 Scatter plot showing detectable plasma IL-2 concentrations in MT-I/II$^{-/-}$ mice (+) and wild type mice (○) after brain injury. Values below the detection limit (0.4 pg/ml) were arbitrarily given concentrations of zero. Increases in IL-2 in plasma after injury were sporadic with few animals posting detectable concentrations. At 7 DPI only MT-I/II$^{-/-}$ mice have detectable levels of plasma IL-2. n=7 for all groups except wild type mice at zero DPI and MT-I/II$^{-/-}$ mice at 7 DPI for which n=6.

3.3.6 MT-I/II$^{-/-}$ mice have decreased expression of the alternative activation marker Ym1

IL-4 and IFN-γ mRNA and protein was undetectable in the brain and detection of IL-4 and IFN-γ protein in the plasma was not reliable enough to determine the Th1/Th2 ratio of MT-I/II$^{-/-}$ mice and wild type mice. To circumvent this problem the marker of alternative activation Ym1 was used to assess the Th2-dependent alternative activation response of macrophages. In the brain, Ym1 was significantly increased at 1 DPI in both strains of mouse but Ym1 was significantly higher in wild type mice at all time-points, including uninjured mice (figure 3.7A, P(strain) < 0.001, P(time) < 0.001, P(interaction) = 0.053). Using this method, it is impossible to determine whether the Ym1 is derived from the CNS-resident microglia or infiltrating monocytes because both cell types can contribute to the pool of activated macrophages in the injury site. RT-PCR was able to determine Ym1 levels in monocytes circulating in peripheral blood (figure 3.7B). At 1 and 3 DPI, Ym1 mRNA was found in significantly higher levels in peripheral blood mononuclear cells (PBMCs) from wild type mice compared to MT-I/II$^{-/-}$ mice. MT-I/II$^{-/-}$ PBMCs showed no significant change in Ym1 mRNA expression over time after cryolesion brain injury (P(time) = 0.083, P(strain) < 0.001 P(interaction) = 0.220). Wild type mice express significantly more Ym1 in the injury site and in circulating monocytes than MT-I/II$^{-/-}$ mice.

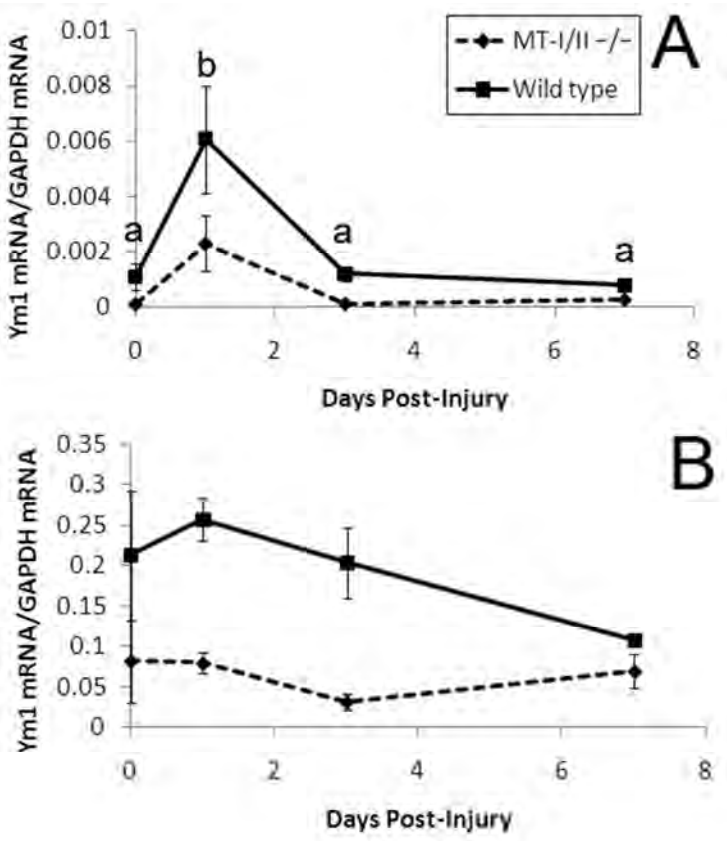

Figure 3.7 (**A**) Ym1 expression in the injury site of wild type and MT-I/II$^{-/-}$ mice after brain injury. Ym1 mRNA expression is significantly greater in the injury site of wild type mice than in MT-I/II$^{-/-}$ mice at all time-points as determined by 2-way ANOVA. Lower case letters indicate statistically significant differences based on the factor of time determined by Tukey's B post-hoc test, n=6-7, error bars=SEM. (**B**) Ym1 expression in PBMCs of wild type and MT-I/II$^{-/-}$ mice after brain injury. Ym1 mRNA expression is significantly greater in the PBMCs of wild type mice than in MT-I/II$^{-/-}$ mice at all time-points as determined by 2-way ANOVA but no significant changes were found over time, n=6, error bars=SEM.

3.4 Discussion

The results in this chapter describe attempts to identify the cause of increased T cell infiltration into the injured CNS of MT-I/II$^{-/-}$ mice. MT-I/II$^{-/-}$ mice were found to have more circulating white blood cells than wild type mice at 7 DPI, which may translate into increased numbers of T cells available for infiltration into the injured CNS. Wild type mice were found to have greater expression of the aaMΦ marker Ym1 in PBMCs and the brain injury site. The activation phenotype of macrophages may play a role in facilitating the persistence of T cells that enter the CNS and in the activation of T cells before they enter the CNS. The ability of MT-I/II$^{-/-}$ mice to produce an appropriate inflammatory response via cytokine production and a chemotactic response via chemokine production was also studied, and no differences were identified in the expression profiles of either cytokine or chemokine mRNA transcripts after brain injury.

3.4.1 Brain injury and MT-I/II deficiency alters the numbers of circulating leukocytes

Prior studies have found MT-I/II$^{-/-}$ mice to have altered numbers of circulating T cells in basal conditions in comparison to wild type mice (Crowthers et al 2000). However, other studies have reported no significant differences in circulating leukocyte numbers (Huh et al. 2007). This discrepancy may reflect differences in MT-I/II$^{-/-}$ mice that occur only under certain physiological or environmental conditions. The present study supports this proposition, demonstrating that basal circulating leukocyte counts in MT-I/II$^{-/-}$ mice were not different to wild type mice until the system was disrupted, in this case by brain injury. After brain injury, the level of leukocytes was not significantly altered in wild type mice but, in MT-I/II$^{-/-}$ mice at 7 DPI, there was a significant increase in absolute leukocyte numbers. Interestingly, the increase in absolute leukocyte counts occurred without changes in the ratios of lymphocytes, monocytes or neutrophils. This implies that each of the cell types are increasing proportionately to each other in MT-I/II$^{-/-}$ mice at 7 DPI. It was interesting that in both strains of mice, the proportion circulating leukocytes that were helper T cells declined with time after injury. One possibility is that circulating T cell numbers decreased as they were recruited to the injury site. An important distinction between the two strains of mice is that the increased leukocyte numbers at 7 DPI in MT-I/II$^{-/-}$ mice resulted in a net increase in T cells despite the proportionate decrease relative to the total leukocyte population. Because circulating leukocyte numbers did not change in wild type mice there was a net decrease in circulating T cells. A hypothesis synthesised from these

findings is that larger numbers of T cells in circulation of MT-I/II$^{-/-}$ mice could be responsible for the increased numbers of T cells in the injury site relative to wild type mice, as described in Chapter 2.

3.4.2 Phenotype of activated leukocytes is altered in MT-I/II$^{-/-}$ mice after brain injury

Two pieces of evidence suggest that MT-I/II$^{-/-}$ mice have a Th1 skew and a reduced aaMΦ response after brain injury in comparison to wild type mice; 1) persistence of the Th1 cytokine, IL-2, in the plasma of MT-I/II$^{-/-}$ mice but not wild type mice after brain injury, and 2) the comparatively lower quantity of Ym1 mRNA in brain and PBMCs of MT-I/II$^{-/-}$ mice after brain injury. Previously, it has been reported that peripheral circulating T cells isolated from MT-I/II$^{-/-}$ mice have an increased Th1 cytokine response compared to wild type mice, but show no difference in Th2 cytokine responses (Huh et al. 2007). Unfortunately the cryolesion did not induce a sufficient helper T cell cytokine response to allow accurate detection and measurement of Th1 and Th2 cytokines in the injured brain. Both immunoassay for cytokine protein and RT-PCR for cytokine mRNA failed to detect IFN-γ and IL-4 which are Th1 and Th2 cytokines, respectively. Quantitative RT-PCR was able to detect mRNA for TNF-α and IL-6 and while they are associated with the Th1 and Th2 response respectively, both are also produced by astrocytes and microglia (reviewed by Liberto et al. 2004) which may explain why mRNA for these particular cytokines was detectable. Due to relatively small numbers of leukocytes in the injury biopsy and the presence of mRNA or protein from glia, it as not possible to specifically determine the cytokine expression profile of infiltrating leukocytes within the injury site.

As an alternative to investigating the Th1/Th2 response, the aaMΦ response was analysed because it was suspected that macrophages and microglia would produce a substantial proportion of the cytokine mRNA found in the injury site biopsy. Ym1 is induced by IL-4 via the stat6 pathway (Welch et al. 2002) and expression of Ym1 mRNA has been shown to be a reliable marker of aaMΦs (Raes et al. 2002). Ym1 is not expressed in neurons or astrocytes but is expressed in microglia and other monocyte derived cells in the CNS (Hung et al. 2002). IL-4 dependent increases in Ym1 have been demonstrated during EAE indicating that the alternative activation response does take place in the CNS (Ponomarev et al. 2007). Although the Th2 cytokine IL-4 is a strong regulator of Ym1 expression, there is evidence that Ym1 itself can positively regulate the Th2 response (Arora et al. 2006, Cai et al. 2009). Therefore, the higher Ym1 expression in wild type mice before injury may predispose them to have a slight

Th2 bias when compared to MT-I/II$^{-/-}$ mice. The caMΦ response to CNS injury has been demonstrated to dominate the aaMΦ response and *in vitro*, caMΦs cause neuron death whereas aaMΦs are neurotrophic (Kigerl et al. 2009). Macrophage numbers were not different between the two strains of mice therefore lower Ym1 expression in MT-I/II$^{-/-}$ mice could indicate a greater caMΦ response which may explain the increased neuron death observed in MT-I/II$^{-/-}$ mice (see Chapter 2). Furthermore, the Th1 cytokines that induce classically activated macrophages can also induce increases in microglial expression of MHC class-II molecules and the B7.1 and B7.2 costimulatory molecules required for T cells to persist in the CNS parenchyma (Aloisi et al. 2000, Séguin et al. 2003). Hence, a shift towards caMΦs in MT-I/II$^{-/-}$ mice may allow greater numbers of T cells to persist in the CNS after brain injury than in wild type mice. Typically, classical activation is associated with higher production of reactive oxygen species and there is evidence that circulating monocytes in MT-I/II$^{-/-}$ mice have an increased capacity for oxidative burst (Emeny et al. 2009). Microglia in the adult CNS are likely derived from hematopoietic origin (Hess et al. 2004) and the fact that Ym1 expression is higher in the PBMCs and brain before injury might indicate that the difference between Ym1 expression in MT-I/II$^{-/-}$ mice arises before the macrophage lineage cells enter the CNS.

To determine if there is a definite Th1 skew during CNS insults in MT-I/II$^{-/-}$ mice, future studies to isolate T cells from the injury site for *in vitro* analysis or *in vivo* studies using experimental models that cause a large influx of T cells into the CNS such as EAE may be more useful than the cryolesion injury model. However, an advantage of the cryolesion injury model is that the effects that it imparts on the immune system are slight which suggests that the robust difference in Ym1 expression is a fundamental difference between MT-I/II$^{-/-}$ mice and wild type mice.

The use of MT-I/II$^{-/-}$ mice to determine the effects of brain injury has revealed repeatedly that there are differences in the response to brain injury but the mechanism by which MT-I/II affects this response remains unclear. It is possible that one of the reasons for this is that little is known about when and where MT-I/II is expressed after brain injury. Similarly, the results of this chapter do not indicate how MT-I/II affects the aaMΦ response after brain injury. One hypothesis that has not received attention is that the zinc binding capacity MT-I/II may play a role maintaining zinc homeostasis after brain injury, thus affecting immune system function. Altered zinc homeostasis is

one of the effects that brain injury has systemically (McClain et al. 1986) and zinc deficiency can inhibit Th1 responses but not Th2 responses (Prasad et al. 2000). Under certain stressful conditions hepatic MT-I/II expression increases (Cho et al. 2004, Coyle et al 1995, Ding et al. 2002, Hernández et al. 1999, Jacob et al. 1999, Philcox et al. 1995, Swapan et al. 1990, Zhou et al. 2003) and has been shown to alter zinc homeostasis (Philcox et al. 1995, Coyle et al. 1995). The potential for the interaction between zinc and hepatic MT-I/II expression to affect the progression of brain injury requires further investigation and is the subject of chapter 5.

3.4.3 Inflammatory and chemotactic signalling is unaltered in MT-I/II$^{-/-}$ mouse brain injury

To investigate the signalling mechanisms that underlie the elevated leukocyte infiltration into the injured brain of MT-I/II$^{-/-}$ mice, the expression profile of key cytokines and chemokines was assessed. Analysis of the inflammatory cytokines IL-6 and TNF-α reveals that the ability of the injured CNS to launch an inflammatory response is not significantly different in MT-I/II$^{-/-}$ mice and wild type mice. Similarly, expression of mRNA for the chemokines CCL2, CCL3, CCL5, CXCL1 and CXCL2 were not significantly different between the two strains of mice. Based on this information, there does not appear to be a difference in the ability of the CNS resident cells to recruit leukocytes in MT-I/II$^{-/-}$ mice which adds further support to the idea that MT-I/II may act peripherally to alter brain injury progression. However, hepatic chemokine expression does not appear to differ greatly between wild type and MT-I/II$^{-/-}$ mice except for a slight increase in hepatic CCL5 mRNA expression at 3 DPI in MT-I/II$^{-/-}$ mice. The increase in CCL5 mRNA was not observed when the experiment was repeated which suggests that altered hepatic CCL5 expression is not a cause of the altered progression of brain injury in MT-I/II$^{-/-}$ mice. The cause of the increase in hepatic CCL5 expression is unknown but brain injury is known to induce recruitment of leukocytes to the liver (Campbell et al. 2003) and increased liver expression of CCL5 in MT-I/II$^{-/-}$ mice may have been the result of a similar occurrence. Hence the observed increase in hepatic CCL5 mRNA at 3DPI in MT-I/II$^{-/-}$ mice may have been a real difference but the fact that it was not reproducible suggests that it is a secondary effect, not the primary cause of the altered response to brain injury in MT-I/II$^{-/-}$ mice. An aspect of leukocyte extravasation that has not been addressed by this thesis and requires further study is the expression of adhesion molecules on the endothelium of CNS blood vessels. Endothelial cell adhesion molecule expression changes during CNS insults and is known to affect the ability of leukocytes to enter the CNS (Piccio et al. 2002).

Variation in the expression of chemokine receptors on T cells in MT-I/II$^{-/-}$ mice also warrants investigation because the ability to respond to chemokines may affect the rate of T cell infiltration into the CNS when the chemokine response is unchanged. This hypothesis predicts that an alteration in MT-I/II$^{-/-}$ mice that occurs outside the CNS but could affect the progression of brain injury.

An interesting facet of the study of chemokine expression in the brain and liver is the correlation between chemokine expression and infiltration of the various leukocyte types into the injured CNS. Chemokines have been found to be induced rapidly within 24 hours of brain injury (Babcock et al. 2003, Sandhir et al. 2004). In the present study, CXCL1, CXCL2 and CCL2 were all rapidly expressed and quickly returned to near basal levels. CXCL1 and CXCL2 are both chemoattractive to neutrophils (Bozic et al. 1995, Lee et al. 1995) so their up-regulation at 1 DPI when neutrophil numbers in the injury site are maximal is not surprising. CCL2 is commonly perceived to be a monocyte attracting chemokine but its expression peaks well before infiltrating monocyte numbers peak, by which time CCL2 expression has severely declined. There is some evidence that CCL2 can act synergistically with CXCL chemokines to increase the rate of neutrophil infiltration (Gouwy et al. 2004) and may explain the early expression of CCL2 after cryolesion injury.

CCL5 and CCL3 were both elevated when numbers of macrophages and T cells were most numerous in the injury site. CCL5 is capable of inducing migration of monocytes and T cells across an *in vitro* blood-brain barrier model (Ubogu et al. 2006a, 2006b) and CCL3 can act similarly on T cells (Man et al. 2008). Late increases in CCL5 mRNA expression have been observed previously after 7 DPI in spinal cord injuries (Jones et al. 2005) and CCL5 protein expression has been observed in brain injuries as late as 12 DPI (Ghirnikar et al. 1998). CCL2 expression in the liver was up-regulated later after injury when macrophages and T cells were at their greatest density in the injury site. Arrest chemokines produced in the liver have been shown to contribute to the infiltration of neutrophils and macrophages into brain injuries (Campbell et al. 2003, Campbell et al. 2005, Campbell et al. 2007a, Campbell et al. 2007b, Campbell et al. 2008b) and CCL2 does function as an arrest chemokine (Gerszten et al. 1999). Therefore it is possible that CCL2 expressed in the brain is affecting neutrophil infiltration early after injury whereas hepatic CCL2 is expressed when monocytes and T cells are entering the injured brain and may leukocyte infiltration later after injury.

Studies involving CCL2 $^{-/-}$ mice have revealed differences in the number of cells expressing macrophage markers in the brain, after brain injury (Semple et al. 2010) and after stroke (Hughes et al. 2002) but these differences did not occur until 4 weeks after brain injury and 2 weeks after stroke. The observation that hepatic chemokines are induced at later time points after brain injury provides further evidence that somatic organs affected by brain injury can also have affects on the injured brain. However, hepatic chemokine production after brain injury does not appear to be a cause of altered brain injury progression in wild type and MT-I/II$^{-/-}$ mice in the experiments undertaken in this thesis.

3.4.4 Conclusion

Three aspects of leukocyte infiltration were investigated in MT-I/II$^{-/-}$ mice in an attempt to identify the cause of increased T cell infiltration at 7 DPI. The chemoattractant signals investigated in MT-I/II$^{-/-}$ mice were normal when compared to wild type mice and are probably not responsible for the altered T cell infiltration. Circulating leukocyte numbers were found to be increased in MT-I/II$^{-/-}$ mice at 7 DPI which may explain increased T cell infiltration in MT-I/II$^{-/-}$ mouse injury sites. There is also evidence that MT-I/II$^{-/-}$ mice are prone to have a higher caMΦ to aaMΦ ratios compared to wild type mice, and this may affect activation and restimulation of T cells that enter the brain. The higher neurotoxicity of caMΦs may also explain the continued neuron death experienced by MT-I/II$^{-/-}$ mice at 7 DPI. Many of the important changes observed in MT-I/II$^{-/-}$ mice are occurring at 7 DPI. To determine whether MT-I/II derived from non-CNS organs is involved in mediating changes in brain injury progression, more information is required on the expression of MT in non-CNS tissues after brain injury.

Chapter 4 – Enzyme-Linked Immunosorbent Assay (ELISA) for MT-I/II

4.0 Introduction

Many methods of assay for metallothionein (MT) in biological samples exist, including radio-immunoassay (RIA), cadmium/haemoglobin affinity (Cd/Haem) assay or silver/haemoglobin affinity (Ag/Haem) assay, capillary electrophoresis coupled to HPLC, electrochemical methods and enzyme-linked immunosorbent assay (ELISA) (reviewed by Dabrio et al. 2002). Capillary electrophoresis and HPLC are perhaps the most accurate of the assays for MT and have the advantage of distinguishing different isoforms of MT. However this technique requires specialised equipment and technical knowledge. The metal binding assays are most accurate when MT is at high concentrations, but fail to differentiate between the different MT isoforms and other proteins that bind metals with high affinity. For example, Cd/Haem assay of liver homogenates from MT-I/II$^{-/-}$ mice, which would not be expected to contain any of the four MT isoforms, display some metal binding capacity which indicates that there is some residual metal binding capacity possibly due to other metalloproteins (Zhou et al. 2004). RIA is accurately quantitative and can be specific to the MT-I/II isoforms (Gasull et al. 1993) but it is time consuming and technically complicated. ELISA is a relatively uncomplicated and rapid process that can be adopted by laboratories without the requirement for specialist equipment or technical expertise (for description of the ELISA technique see figure 4.1). ELISA for MT has been used extensively with user-generated antibodies (Apostolova et al. 1998, Chan et al. 1992, Grider et al. 1990, Sullivan et al. 1998, Swierzcek et al. 2004, Tang et al. 1999, Thomas et al. 1986, Liu et al. 2000). However, these techniques are not readily transferable between laboratories due to variation in the generation of polyclonal antibodies.

The E9 monoclonal mouse anti-MT immunoglobulin G (IgG) is a commercially available antibody that is specific to the MT-I and MT-II isoforms (Skabo et al. 1997). It has been used to measure MT-I/II by both competitive and direct ELISA in non-murine biological samples (Hirauchi et al. 1999, Milnerowicz and Bizon 2010, Szitányi et al. 1996). The E9 antibody can detect mouse MT-I/II by ELISA in samples obtained from mouse cell lines (Butcher et al. 2003) but difficulties arise when the E9 antibody is used to detect MT-I/II in mouse tissues. Secondary antibodies will bind to endogenous mouse immunoglobulins which can not be distinguished from the E9 primary antibody. Recently a competitive ELISA has been used to quantify MT in mouse tissue samples (Emeny et al. 2009) with the use of the commercially available, UC1MT mouse monoclonal anti-MT antibody which was first described by Lynes et al. (1993).

However, there are no published data pertaining to the presence or absence of matrix effects in ELISA using this antibody. It has been demonstrated that the UC1MT antibody binds to MT-I and MT-II (Lynes et al. 1993) but it is not known if brain-specific MT-III isoform will cross-react with the antibody, which is an important consideration for assay of MT-I/II in the brain.

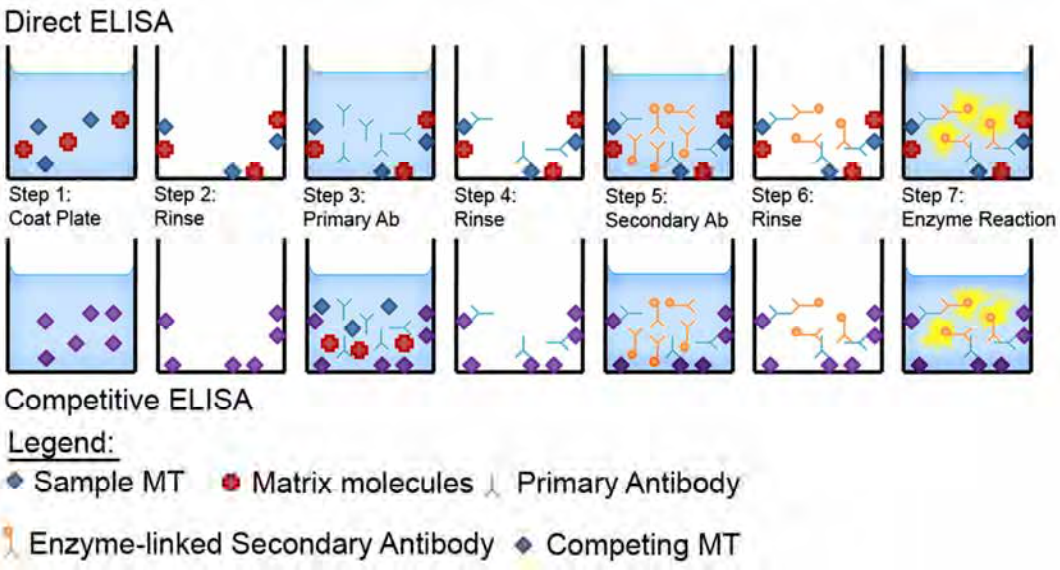

Figure 4.1 Schematic of MT assay by direct enzyme-linked immunosorbent assay (ELISA) technique (top) and competitive ELISA technique (bottom). Both methods involve the same steps but they differ in how the antibody interacts with the MT sample to be assayed. Direct ELISA requires adsorption (coating) of the sample with an unknown quantity of MT to a microplate well followed by incubation with a primary antibody, incubation with an enzyme-linked secondary antibody and then application of a chromogenic substrate for the conjugated enzyme. The absorbance reading of the well is directly proportional to the quantity of MT in the sample added to the well in step 1. The competitive ELISA is slightly different because a known quantity of MT is adsorbed to the substrate in the first stage then, in a later step, the sample containing an unknown quantity of MT is added along with the primary antibody. The MT adsorbed onto the microplate competes with the soluble MT in the sample for primary antibody and only the primary antibody that binds to substrate-bound MT will remain in the well after the rinsing step. MT in the sample will attract a proportion of the primary antibody which remains in solution and is removed during rinsing. After the rinsing step the secondary antibody is applied to the plate followed by the chromogenic enzyme-substrate. The absorbance reading for competitive ELISA is inversely proportional to the quantity of MT in the sample. A major difference in the direct and competitive ELISA techniques is that the matrix molecules, the other molecules found in the MT sample, are also adsorbed onto the microwell plate in direct ELISA but not in competitive ELISA.

The term “matrix effects” relates to the complex and variable mixture of proteins, carbohydrates, lipids, urea, small molecules and salts found in biological samples that can interfere with the assay (Swierzcek et al. 2004). In the history of MT ELISA development matrix effects have been poorly investigated. The traditional method of determining the presence of matrix effects is construction of displacement curves. Like standard curves, displacement curves involve the serial dilution and assay of a known quantity of assay antigen, in this case MT. A standard curve is often constructed by dilution of antigen in a buffered saline solution whereas displacement curves are constructed using tissue samples that contain little or no antigen of interest. When matrix effects are present they can displace antibody binding from substrate bound antigen and result in a curve non-parallel to the standard curve. The first MT ELISA developed by Thomas et al. (1986) found that serum sample displacement curves did not parallel the standard curve, indicating the presence of matrix effects. Displacement curves were used to validate the use of ELISA to measure MT in human blood cells (Sullivan et al. 1998). Swierzcek et al. (2004) used activated charcoal to remove organic molecules from human urine and created displacement curves in the resulting fluid to validate an MT ELISA. Few other published studies address this issue and none of these studies have reported testing for matrix effects in MT ELISA using a commercially available antibody. Displacement curves are essential for validation of ELISAs because they are an effective method for identifying the presence of non-specific interference with the assay.

In addition to matrix effects, one of the problems that confounds immunoassay of MT is the fact that the protein has a propensity to aggregate, particularly at high concentrations and under oxidising conditions (Haase & Maret 2004, Zangger et al. 2001). MT aggregation can also occur purely by hydrophobic interactions but there has been limited study into this phenomenon (Hou et al. 2000). Oxidation-induced MT aggregation is more widely documented and involves the formation of disulphide bonds between cysteine residues of MT (Zangger et al. 2001). However due to the complexity of biological samples, it is likely that in addition to self-polymerisation, MT forms disulphide bonds with a variety of proteins with similarly oxidised cysteine residues. Aggregation of MT can affect the affinity of anti-MT antibodies to a given quantity of MT which can alter the accuracy of ELISA (Tang et al. 1999). ELISA has also been found to estimate significantly less MT in the liver samples than Ag/Haem assay when MT concentrations with one implication being that there is a phenomenon that masks

MT from immunoassay (Chan et al. 1992). Filtration steps have been used to further purify monomeric and aggregated MT (Hirauchi et al. 1999, Tang et al 1999), which can help determine the degree of aggregation of MT but will also remove all MT bound to higher molecular weight molecules. Therefore a method capable of reversing any nonspecific disulphide linkages between MT and other molecules formed as a result of oxidative processes would be advantageous to ELISA for MT.

The first aim of this chapter was to develop an ELISA for the measurement of MT in mouse tissue and plasma using commercially available antibodies. The second aim of this chapter was to develop a method of reversing the disulphide linkage formation of MT in tissue samples to allow accurate quantification of MT. The issue of the formation of disulphide linkages by MT has been encountered previously during electrophoresis of MT by SDS-PAGE. Disulphide linkages formed by MT and a heterogeneous array of proteins results in MT bands at several different molecular weights. The problem can be solved by reduction of disulphide bonds to two separate sulfhydryl groups, followed by modification of these sulfhydryl groups via alkyl halide substitution reaction to prevent further oxidation of cysteines (Kimura et al. 1991, Shaw et al. 1991). The carboxyamidomethylation reaction is described in figure 4.2. Carboxyamidomethylation was attempted as a sample preparation for preserving, and returning MT to its monomeric form before ELISA.

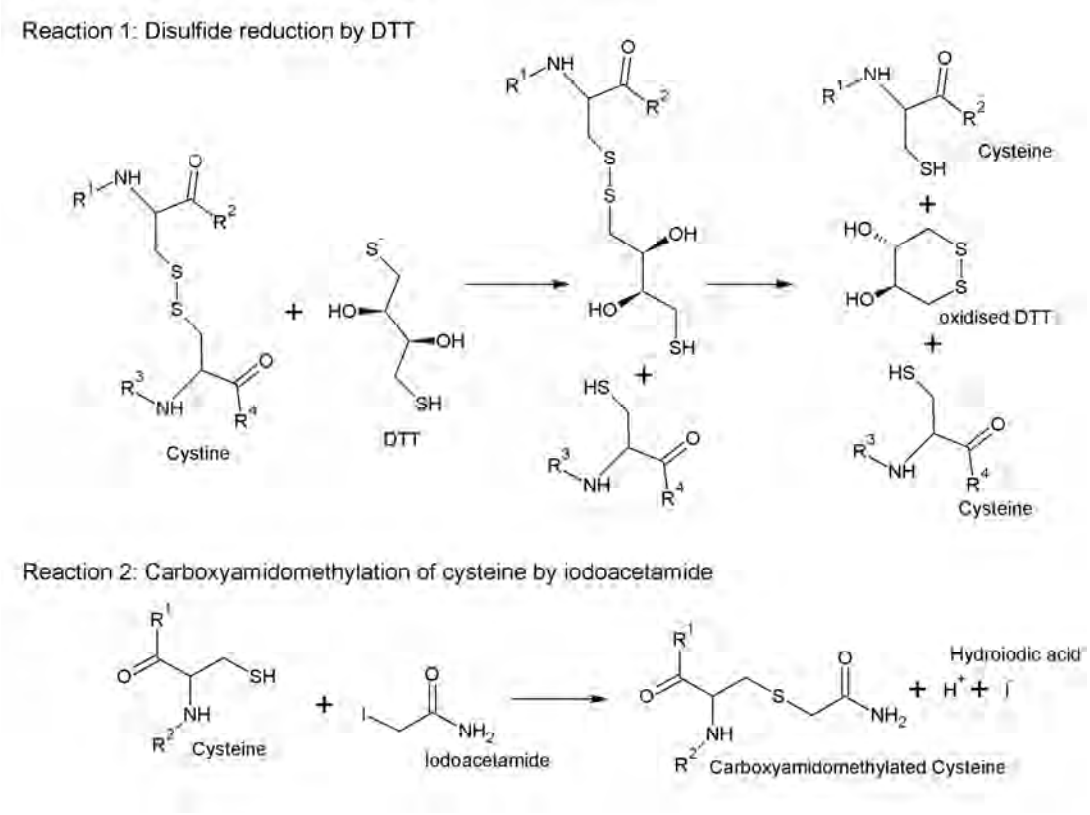

Figure 4.2 Carboxyamidomethylation of cysteine. The reaction is a two step process. In the first step which occurs at high temperature, dithiothreitol (DTT) is required to reduce any cystine that has formed via disulfide bonding. In the second step of the reaction iodoacetamide replaces the hydrogen atom in the thiol group via substitution reaction to form carboxyamidomethylated cysteine with hydroiodic acid as the by-product.

4.2 Materials and Methods

4.2.1 Direct (E9 antibody) ELISA

Nunclon delta surface microplate wells (Nunc) were coated with 25 µl of MT-I/II-containing samples and 25 µl of 50 mM Na_2CO_3 and incubated overnight at 4°C on an orbital shaker. All subsequent stages took place at room temperature. Endogenous peroxidases were quenched with 3% hydrogen peroxide (Merck) in ELISA wash buffer (0.05% Tween-20 in 0.01M PBS) for 5 minutes at room temperature. Following a 5 minute rinse in wash buffer, wells were blocked with 150 µl casein solution (2.5%, pH 7.4) for 30 minutes. The wells were washed again in wash buffer for 5 minutes. Primary antibody (E9 mouse anti-MT-I/II IgG, Dako) was diluted 1:1000 in ELISA wash buffer and applied to wells and incubated for 1 hour. The plate was rinsed for 5 minutes, 3 times with wash buffer. Horse radish peroxidase-conjugated secondary antibody (goat anti-mouse IgG-HRP conjugate, Dako) was diluted 1:1000 in ELISA wash buffer and applied to each well in 50 µl aliquots and incubated for 1 hour. To amplify the signal a biotinylated secondary antibody was also tested (biotinylated goat anti-mouse IgG, Zymed) and was diluted 1:1000 in ELISA wash buffer and applied to each well in 50 µl aliquots and incubated for 1 hour followed by 3 rinses in wash buffer and application of either ABC reagent (Vector labs) or HRP-streptavidin conjugate (Biosource). The plate was rinsed for 5 minutes, 3 times with wash buffer. TMB peroxidase substrate (KPL) was incubated in the wells in 50 µl aliquots for 1 hour. The reaction was terminated by addition of 50 µl of 1 M phosphoric acid and the absorbance of the microplate wells were measured at 450 nm. Standard curves were generated (section 4.2.4) and were used to calculate MT-I/II concentrations in the assayed samples (section 4.2.5).

4.2.2 Competitive (E9 antibody) ELISA

Nunclon delta surface microplate wells (Nunc) were coated with 50 µl of 100 ng/ml Zn_7MT-IIA (HPLC-purified rabbit MT-IIA conjugated to 7 Zn^{2+} ions, Bestenbalt, Estonia), 50 mM Na_2CO_3 and incubated overnight at 4°C on an orbital shaker. All subsequent stages took place at room temperature. Following a 5 minute rinse in wash buffer, wells were blocked with 150 µl casein solution (2.5%, pH 7.4) for 30 minutes. The wells were washed again in wash buffer for 5 minutes. For the competitive step, samples were applied to the plate first, in triplicate or quadruplicate, in 50 µl aliquots. Then the primary antibody (E9 mouse anti-MT-I/II IgG, Dako) was diluted 1:5000 in ELISA wash buffer and applied to the wells in 50 µl aliquots. This competition step

was incubated for 1 hour. The plate was rinsed for 5 minutes, 3 times with wash buffer. Secondary antibody (goat anti-mouse IgG-HRP conjugate, Dako) was diluted 1:10 000 in ELISA wash buffer, applied to each well in 50 µl aliquots and incubated for 1 hour. The plate was rinsed with wash buffer for 5 minutes, 3 times. TMB peroxidase substrate (KPL) was incubated in the wells in 50 µl aliquots for 1 hour. The reaction was terminated by addition of 50 µl of 1 M phosphoric acid and the absorbance of the microplate wells were measured at 450 nm. Standard curves were generated (section 4.2.4) and were used to calculate MT-I/II concentrations in the assayed samples (section 4.2.5).

4.2.3 Competitive (UC1MT antibody) ELISA

Nunclon delta surface microplate wells (Nunc) were coated with 50 µl of 100 ng/ml Zn_7MT-IIA, 50 mM Na_2CO_3 and incubated overnight at 4°C on an orbital shaker. All subsequent stages took place at room temperature. Following a 5 minute rinse in wash buffer, wells were blocked with 150 µl casein solution (2.5%, pH 7.4) for 30 minutes. The wells were washed again in wash buffer for 5 minutes. For the competitive step, samples were applied to the plate first, in triplicate or quadruplicate, in 50 µl aliquots. Then the primary antibody (UC1MT mouse anti-MT IgG, Assay designs) was diluted 1:5000 in ELISA wash buffer and applied to the wells in 50 µl aliquots. This competition step was incubated for 1 hour. The plate was rinsed with wash buffer for 5 minutes, 3 times. Secondary antibody (goat anti-mouse IgG-HRP conjugate, Dako) was diluted 1:5000 in ELISA wash buffer and applied to each well in 50 µl aliquots and incubated for 1 hour. The plate was rinsed with wash buffer for 5 minutes, 3 times. TMB peroxidase substrate (KPL) was incubated in the wells in 50 µl aliquots for 1 hour. The reaction was terminated by addition of 50 µl of 1 M phosphoric acid and the absorbance of the microplate wells were measured at 450 nm. Standard curves were generated (section 4.2.4) and were used to calculate MT-I/II concentrations in the assayed samples (section 4.2.5).

4.2.4 Standard curves

Standard curves were created and run within each ELISA to calibrate the assay. Lyophilised Zn_7MT-IIA was dissolved in MilliQ water at a concentration of 1 mg/ml. These stock solutions were diluted in ELISA wash buffer in maximum-recovery microcentrifuge tubes (Axygen) to create the top standard, usually at 1 or 10 µg/ml. Serial dilution from the top standard was conducted with each step constituting a 4-fold

dilution in ELISA wash buffer in maximum-recovery tubes. Standards were kept on ice while the rest of the ELISA samples were prepared.

4.2.5 Displacement curves

Tissue samples were obtained to test for matrix effects in the various formats of MT ELISA. Tissue samples were obtained from MT-I/II$^{-/-}$ mice so that no endogenous MT-I/II was present in the sample. Brain and liver were ground to a fine power in a mortar and pestle under liquid nitrogen. The powdered tissue was homogenised in 150 mM NaCl, 20 mM Tris-HCl, 1% Igepal, pH 7.6 with EDTA-free Halt-protease inhibitor cocktail (Thermo Scientific) with an Ultra-Turrax mechanical homogenizer (IKA). Samples were centrifuged at 10 000*g* for 10 minutes and the supernatant was retained for assay. Protein concentration was obtained by Bradford assay (Bradford 1976). MT-I/II$^{-/-}$ mouse urine and rat brain homogenate prepared as above were also tested for matrix effects. Matrix solutions for displacement curves were constructed by diluting tissue samples in ELISA wash buffer to give a range of solutions with varied total protein content. Zn_7MT-IIA serial dilutions were conducted in the matrix solutions in the same manner as for standard curves. Displacement curves and standard curves were conducted simultaneously for direct comparison.

4.2.6 4-parameter logistic modelling

ELISA standard curves were sigmoidal so 4-parameter logistic modelling was used to calculate sample MT concentrations from the observed absorbance values. The following formula from Findlay and Dillard (2007) was used to fit a 4-parameter logistic model to the standard curves generated by the various ELISA formats:

$$\boldsymbol{Y = D + \frac{(A - D)}{\left(1 + \left(\frac{x}{C}\right)^{B}\right)}}$$

where, Y is the absorbance response, A is the lower asymptote of the curve, B is the slope of the linear phase of the curve, C is the concentration of MT at the inflection point of the curve and D is the upper asymptote of the curve. The standard curves did not always include concentrations of MT at the upper limit of the assay. In these cases the relevant value for the asymptote had to be estimated. The slope of the linear phase often had to be altered to improve the fit of the model to the standard curve. R^2 was calculated for the model and was used to find the best fit for values which had to be estimated. The model was then used to derive the concentration of MT in tissue samples (data shown in chapter 5).

4.2.7 Western blot

SDS-PAGE and protein transfer to nitrocellulose membranes was conducted with the Mini-Protean II Cell (Novex). 20 µl sample was added to 7µl of Nupage 4x LDS sample buffer (Invitrogen) and samples were heated at 95ºC for 5 minutes. Samples were loaded onto Tris buffered 10% bis-acrylamide gels (Invitrogen) and underwent electrophoresis in NuPage MES running buffer (Invitrogen) at 200 volts for 40 minutes at room temperature. Proteins were transferred to nitrocellulose in NuPage transfer buffer with 10% methanol (Invitrogen) for 1 hour at 30 volts at room temperature. The membrane was blocked with 5% skim milk powder in PBS-T (0.1% Tween-20, 0.01M PBS) for 1 hour. The membrane was probed with E9 anti-MT-I/II antibody (Dako) diluted 1:500 in PBS-T containing 2.5% skim milk powder for 1 hour at room temperature followed by two washes for 10 minutes in PBS-T. Goat anti-mouse IgG-HRP secondary antibody (Dako) was diluted 1:1000 in PBS-T and applied to the membrane for 1 hour at room temperature. The membrane was washed twice for 10 minutes in PBS-T. Pico-west chemiluminescent substrate (Pierce) was applied to the blot for 5 minutes at room temperature before the excess was removed then the membrane was exposed to photographic film for 1-5 minutes in an autoradiographic cassette and the film was developed.

4.2.8 Heat treatment of Zn_7MT-IIA to test heat stability

Zn_7MT-IIA solutions were made up to 10 µg/ml in MilliQ water. A control Zn_7MT-IIA solution was kept on ice for the duration of the experiment and received no heat treatment or centrifugation. Two samples were prepared for heat treatment, with and without the addition of 1 µl of β-mercaptoethanol (Sigma) per 100 µl of sample. Samples were heated at 90°C for 10 minutes followed by centrifugation at 10 000*g* for 10 minutes. The control and heat-treated samples were analysed by western blot.

4.2.9 Iodoacetamide mediated carboxyamidomethylation of Zn_7MT-IIA

Carboxyamidomethylation was carried out on Zn_7MT-IIA samples in PBS and MT-I/II$^{-/-}$ mouse plasma. Plasma was first diluted 1:3 with PBS before addition of Zn_7MT-IIA. To reverse any cystine disulphide bonds present in the samples, 80 µl of 0.2 M dithiothreitol (DTT, Sigma) was added to the samples followed by heating to 100°C for 5 mins then allowing to cool to room temperature. To carboxyamidomethylate the free thiol groups in the sample, 120 µl of 1 M iodoacetamide was added to the samples which were then heated to 50°C for 15 minutes. Upon cooling, the samples were centrifuged at 10 000*g* for 10 minutes to remove any precipitated species. A Zn_7MT-IIA control which was stored on ice for the duration of the carboxyamidomethylation

reaction was also centrifuged to remove any MT-IIA aggregates. The supernatant was analysed by western blot, direct E9 antibody ELISA and competitive E9 antibody ELISA.

4.2.10 pH titration of the iodoacetamide reaction in artificial plasma

The volume of the iodoacetamide reaction was scaled-up by a factor of 10 and conducted on a BSA buffer to simulate the protein and thiol content of plasma given that albumin is a large proportion of blood protein. The buffer consisted of 4% BSA, 8.3 mM D-glucose, 118 mM NaCl, 4.7 mM KCL, 1.2 mM KH_2PO_4, 1.2 mM Mg_2SO_4 and 25 mM $NaHCO_3$. To prevent decreases in pH, all reaction solutions were buffered with a combination of MES and Tris buffers. No MT was added to the BSA buffers. In 15 replicate tubes, 1 ml of BSA buffer, 3 ml of DTT reaction buffer (0.2 M DTT, 100 mM Tris, 100 mM MES, pH 9) was added and the resulting solution was heated to 100°C for 5 minutes. The tubes were allowed to cool to room temperature before the pH of the solution was measured. The tubes were divided into 3 groups that received 1 ml of 1 M iodoacetamide, 0.5M MES at a pH of either 6, 7 or 8. The reactions were heated to 50°C for 15 minutes then allowed to cool before the pH of each reaction was measured. An adjustment buffer (1 ml) was added to each solution containing 0.3 M DTT, 0.5 M MES at pH of either 5, 6, 7, 8.2 or 8.9. The solutions were again heated to 50°C for 15 minutes and were allowed to cool to room temperature before the final pH measurement. After pH measurement 3 samples were chosen that had a final pH of 4.76, 5.48 and 6.48. The supernatant from each sample was divided into two aliquots and HPLC-purified, carboxyamidomethylated MT-IIA was added to one of these aliquots to give a final concentration of 80 μg/ml MT. These samples were then assayed by competitive MT ELISA (E9 antibody clone) and compared to PBS with and without 80 μg/ml carboxyamidomethylated MT-IIA.

4.2.11 Direct (UC1MT antibody)ELISA to compare MT-IIA and MT-III cross-reactivity

Nunclon delta surface microplate wells (Nunc) were coated with 50 μl of standard curves for Zn_7MT-IIA and Zn_7MT-III (HPLC-purified human MT-III conjugated to 7 Zn^{2+} ions, Bestenbalt, Estonia) which were made up in 50 mM Na_2CO_3 and incubated overnight at 4°C on an orbital shaker. All subsequent stages took place at room temperature. Following a 5 minute rinse in wash buffer, wells were blocked with 150 μl casein solution (2.5%, pH 7.4) for 30 minutes. The wells were washed again in wash buffer for 5 minutes. UC1MT primary antibody was diluted 1:1000 in ELISA wash buffer and applied to wells and incubated for 1 hour. The plate was rinsed for 5

minutes, 3 times with wash buffer. Horse radish peroxidase (HRP)-conjugated secondary antibody (goat anti-mouse IgG-HRP conjugate, Dako) was diluted 1:5000 in ELISA wash buffer and applied to each well in 50 µl aliquots and incubated for 1 hour. The plate was rinsed for 5 minutes, 3 times with wash buffer. TMB peroxidase substrate (KPL) was incubated in the wells in 50 µl aliquots for 1 hour. The reaction was terminated by addition of 50 µl of 1 M phosphoric acid and the absorbance of the microplate wells were measured at 450 nm.

4.3 Results

4.3.1 Metallothionein ELISA with the E9 antibody

Commercially available antibodies raised in non-murine species were sought to avoid problems with cross reactivity of primary antibodies. The following commercially available MT-I/II antibodies were tested for ability to detect MT by western blot; rabbit anti-FL-61 polyclonal IgG (Santa Cruz), rabbit anti-MT polyclonal IgG (Genway), mouse anti-MT monoclonal IgG, Clone E9 (Dako). Neither of the rabbit polyclonal antibodies was able to detect Zn_7MT-IIA by western blot, whereas the E9 antibody robustly detected Zn_7MT-IIA by this method (data not shown). Therefore use of a mouse-derived primary antibody for the development of an MT-I/II ELISA with commercially available reagents was unavoidable. The E9 antibody was able to produce a reliable standard curve when used as the primary antibody in direct ELISA (figure 4.3A). Of the detection systems used, the highest sensitivity was acquired with a biotinylated anti-mouse IgG secondary antibody combined with streptavidin-HRP conjugate. HRP-conjugated anti-mouse IgG and biotinylated anti-mouse IgG secondary antibody combined with ABC reagent were less sensitive. Competitive ELISA with the E9 antibody was also tested (figure 4.3B) but the assay was much less sensitive than the direct ELISA and was deemed not sensitive enough for effective detection of MT in mouse tissue.

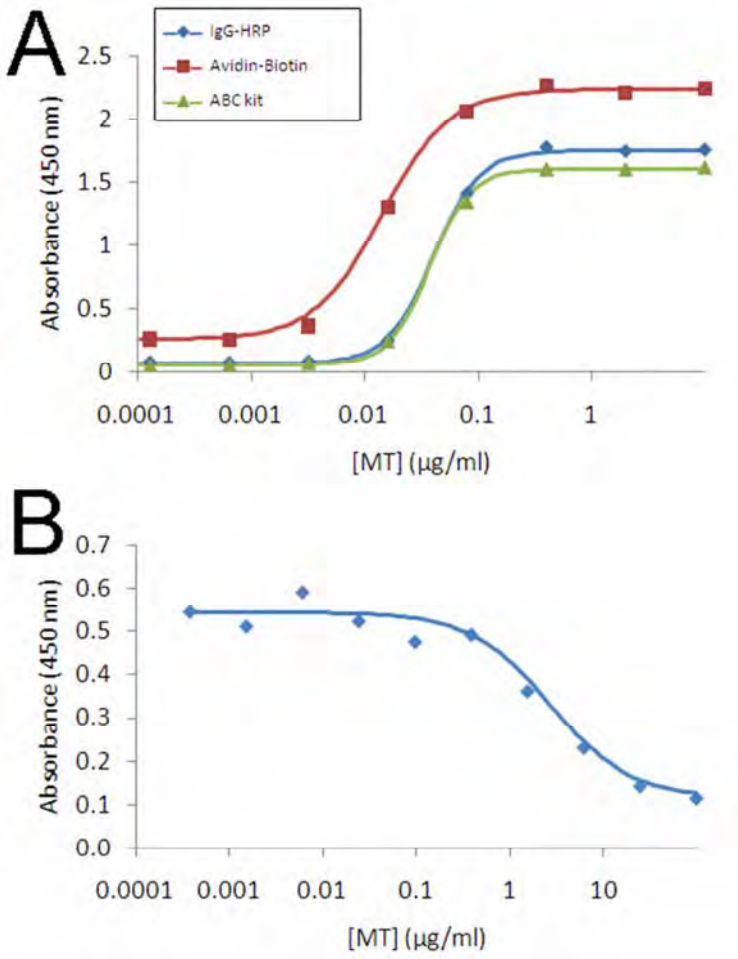

Figure 4.3 Standard curves for direct MT ELISA (**A**) and competitive MT ELISA (**B**) both conducted with the E9 antibody clone and fitted with a 4-parameter logistic curve. Three secondary antibody detection systems were trialled for the direct ELISA; HRP-conjugated secondary antibody (blue), biotinylated secondary antibody with HRP-conjugated streptavidin (red) and biotinylated secondary antibody with ABC (green). Competitive ELISA was conducted with HRP-conjugated secondary antibody. The direct ELISA was more sensitive than the competitive ELISA by two orders of magnitude. All data points were collected in triplicate, the mean is displayed.

4.3.2 Metallothionein detection in mouse plasma by western blot

The E9 antibody is a mouse IgG which is detected following binding to antigen on the blotting membrane with an enzyme-linked anti-mouse IgG secondary antibody. These secondary antibodies were expected to react with endogenous antibodies in tissue samples. Figure 4.4A demonstrates the high degree of non-specific high molecular weight staining that was observed in MT-I/II$^{-/-}$ mouse plasma samples (lanes 2 and 3). The two 14 kDa bands that are visible in the plasma samples are not MT-IIA dimers because the same band is present in the sample without any Zn_7MT-IIA added (lane 3). A 7 kDa band was resolved in the plasma sample with Zn_7MT-IIA added (lane 2) but this band was not present in the MT-free plasma sample (lane 3). This indicates that despite the non-specific staining, monomeric Zn_7MT-IIA is still detectable in mouse samples. However, the intensity of the MT band present in the Zn_7MT-IIA seeded plasma sample is considerably reduced compared to the control Zn_7MT-IIA which was dissolved in PBS even though the initial concentrations of Zn_7MT-IIA in these samples were identical (10 μg/ml). It is apparent that monomeric Zn_7MT-IIA is being lost from the plasma sample, possibly through disulphide linkages formed between cysteine residues on MT and higher molecular weight species. Western blot can differentiate between monomeric Zn_7MT-IIA and nonspecific binding or aggregated MT-IIA based on the molecular weight of immunopositive bands. ELISA does not have the ability to differentiate between molecules of different sizes leading to a diminished ability to identify false positive readings. To assay MT-I/II by direct ELISA, a method was sought to remove endogenous IgG and related antibody binding proteins, while retaining MT-I/II in solution.

4.3.3 Heat stability of Zn_7MT-IIA

MTs are reported to be highly heat stable compared to most other proteins, a property previously exploited to separate MT-I/II from protein solutions (Summer and Klein 1991). However, in these applications MT-I/II was often experimentally bound to metals other than zinc, which might influence its heat stability, prompting assessment of recovery of Zn_7MT-IIA after heat treatment. Zn_7MT-IIA in PBS was heated to 90°C for 10 minutes in the presence or absence of β-mercaptoethanol, a reducing agent (Figure 4.4B). Comparison of untreated Zn_7MT-IIA (lane 1) to heat treated Zn_7MT-IIA without β-mercaptoethanol (lane 2) and Zn_7MT-IIA with β-mercaptoethanol (lane 3) reveals a reduction in monomeric Zn_7MT-IIA at 7 kDa after heat treatment. Furthermore some high molecular weight immunoreactivity is visible which, may indicate formation of large complexes of aggregated MT. This high molecular weight immunoreactivity is

visible in all lanes suggesting that Zn_7MT-IIA forms aggregates without heat treatment but the level of high molecular weight immunoreactivity increases with heat-treatment. The recovery of monomeric Zn_7MT-IIA from heat treatment was not high enough for the technique to be incorporated into a quantitative assay. Heat treatment appears to accelerate the rate of MT-IIA aggregation so the prevention of MT aggregation was investigated as a possible solution to this problem.

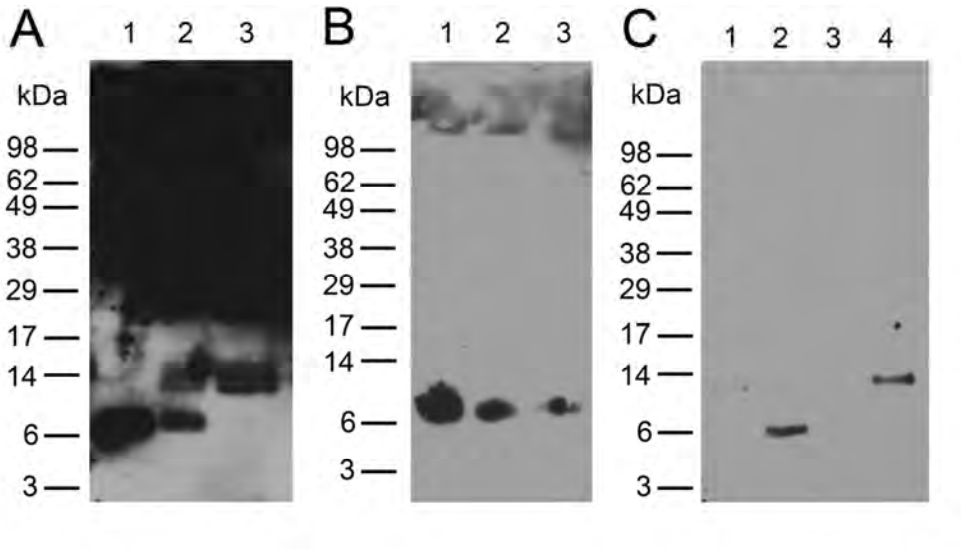

Figure 4.4 Western blots demonstrate the instability of MT in various solutions. Monomeric MT is a 7 kDa protein. (**A**) Zn_7MT was seeded into MT-I/II$^{-/-}$ mouse plasma to assess the recovery of MT. A high degree of immunoreactivity can be seen at higher molecular weights but an immunoreactive band is present at 7 kDa. Lane 1, Zn_7MT in PBS; lane 2, Zn_7MT in MT-I/II$^{-/-}$ mouse plasma; lane 3 MT-I/II$^{-/-}$ mouse plasma without any Zn_7MT added. (**B**) Zn_7MT is unstable when heated to 90°C. Lane 1, unheated Zn_7MT; lane 2, 90°C heat-treated Zn_7MT; lane 3, 90°C heat-treated Zn_7MT with β-mercaptoethanol. (**C**) Carboxyamidomethylation of Zn_7MT in MT-I/II$^{-/-}$ mouse plasma removes the binding at high molecular weights. Lane 1, Zn_7MT in PBS; lane 2, Zn_7MT in PBS after carboxyamidomethylation; lane 3, MT-I/II$^{-/-}$ mouse plasma after carboxyamidomethylation reaction without MT; lane 4, Zn_7MT seeded in to MT-I/II$^{-/-}$ mouse plasma followed by carboxyamidomethylation reaction.

4.3.4 Carboxyamidomethylation of Zn_7MT-IIA

Aggregation of MT occurs via disulphide linkages formed between MT molecules under oxidative conditions (Zangger et al. 2001) and disulphide linkages are also expected to occur between MT and other cysteine-containing proteins in tissue samples. Iodoacetamide is an alkylating agent that binds covalently to free thiol groups and is used to prevent MT from forming disulphide cystine linkages. Samples were first heated with DTT to reduce any disulphide bonds to free thiols then were treated with iodoacetamide to produce carboxyamidomethylated MT which does not bind metals and is no longer able to form disulfide bonds. After iodoacetamide treatment of Zn_7MT-IIA (Figure 4.4C, lane 2), western blot revealed a single band of 7 kDa size which differed from untreated Zn_7MT which produced a band of lower intensity at 14 kDa which is consistent with the possibility of the formation of a MT-IIA dimer (lane 1). The untreated Zn_7MT-IIA was kept on ice during the carboxyamidomethylation reaction and centrifuged to remove aggregated MT-IIA. The lower intensity compared to the carboxyamidomethylated MT-IIA suggests that this time frame was sufficient to allow spontaneous aggregation of Zn_7MT-IIA however no high molecular weight bands were observed possibly because they were removed by centrifugation. The carboxyamidomethylation reaction was also applied to plasma from MT-I/II$^{-/-}$ mice, both with and without the addition of a known quantity of Zn_7MT-IIA. The reaction applied to MT-free mouse plasma (lane 3) was able to remove all non-specific staining previously observed in mouse plasma. The carboxyamidomethylation of MT-I/II$^{-/-}$ mouse plasma containing 50 µg/ml of Zn-MT-IIA was able to recover MT from solution albeit in dimeric form suggesting that some disulphide bonds were still present (lane 4). Therefore iodoacetamide treatment can preserve MT-I/II concentrations in mouse tissue samples and remove endogenous proteins that bind to anti-mouse IgG secondary antibody.

4.3.5 Carboxyamidomethylation reaction inhibits the direct ELISA for MT

The compatibility of iodoacetamide treatment of samples with the ELISA was assessed. MT-I/II$^{-/-}$ mouse plasma with and without Zn_7MT-IIA seeded into it underwent the iodoacetamide reaction and was assayed by direct ELISA (figure 4.5A). HPLC-purified Zn_7MT-IIA and HPLC-purified carboxyamidomethylated MT-IIA, both commercially obtained (Bestenbalt), were dissolved in PBS and left untreated to serve as positive controls. It is important to note that the HPLC-purified carboxyamidomethylated MT-IIA contains none of the reagents or products of the carboxyamidomethylation reaction. Figure 4.5A shows that the Zn_7MT-IIA and carboxyamidomethylated MT-IIA positive

controls were detectable by ELISA demonstrating that the E9 antibody retains its affinity for MT-IIA with carboxyamidomethylated cysteine residues. The negative control registered a low absorbance reading, as expected. However the samples containing Zn_7MT-IIA that had undergone reaction with iodoacetamide failed to register an increased absorbance reading above the negative-control. Therefore some component of the iodoacetamide reaction appears to be interfering with the direct ELISA. The components of the carboxyamidomethylation reaction are in contact with the ELISA plate only during the coating step and are rinsed away before subsequent steps in the ELISA. Western blot of the post-reaction Zn_7MT-IIA from the previous experiment confirmed that the MT-IIA remains in solution and retains the ability to bind antibody after reaction with iodoacetamide (figure 4.4C) therefore it can be inferred that it is the coating step of the ELISA that is being affected by the iodoacetamide reaction.

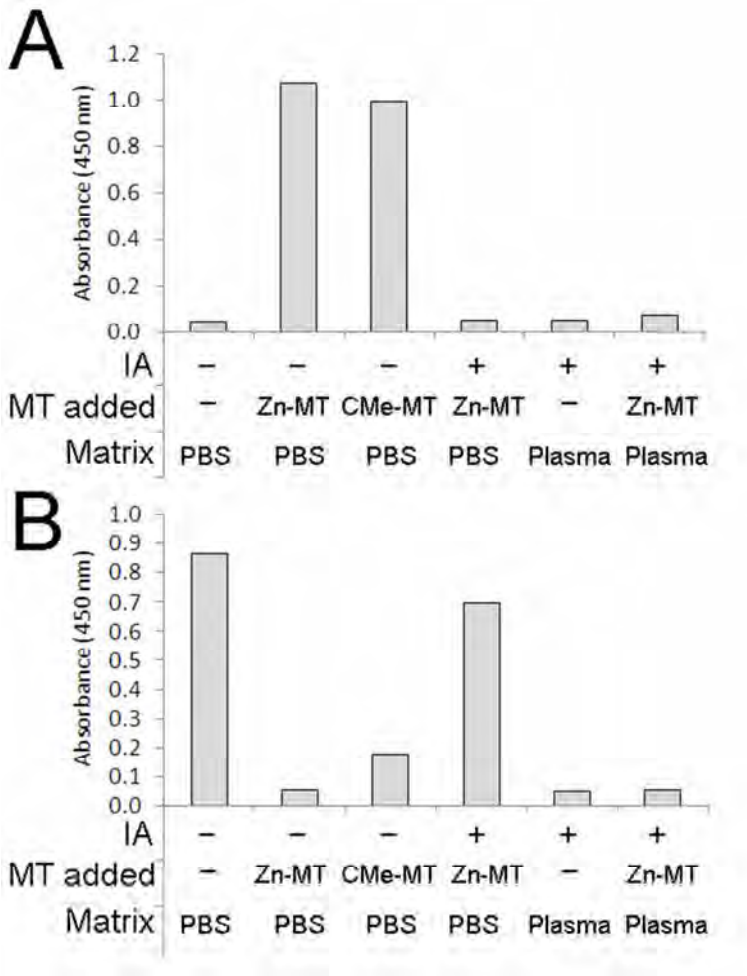

Figure 4.5 Direct MT-I/II ELISA (**A**) and competitive MT-I/II ELISA (**B**), both with the E9 antibody, to test efficacy of the assays for iodoacetamide treated samples. Samples either underwent carboxyamidomethylation with iodoacetamide (IA) or were left untreated. Before the addition of iodoacetamide, some samples were seeded with HPLC-purified Zn7MT-IIA or HPLC-purified carboxyamidomethylated MT-IIA CMe-MT, both commercially obtained. The remaining samples served as negative controls. All untreated samples were prepared in PBS whereas the IA treated samples were prepared in both PBS and MT-I/II$^{-/-}$ mouse plasma. Each sample was assayed in duplicate and the data are expressed as means.

4.3.6 Carboxyamidomethylation reaction inhibits the competitive ELISA for MT

During competitive ELISA, samples to be assayed are not present at the time of MT coating to the substrate. The treated samples, along with the primary antibodies, are added to the microplate wells at a later stage in the protocol. To circumvent the problems encountered with coating in the direct ELISA, the compatibility of iodoacetamide treatment and competitive ELISA was assessed (figure 4.5B). The sample preparation for the competitive ELISA was identical to that used for the direct ELISA (section 4.3.5). The negative control prepared in PBS registered a high absorbance reading in the ELISA due to a lack of competition for substrate bound Zn_7MT-IIA, as expected. Both positive controls containing HPLC-purified Zn_7MT-IIA or HPLC-purified carboxyamidomethylated MT-IIA registered a low absorbance reading indicating that they were competitively reducing E9 antibody binding to the substrate bound Zn_7MT-IIA. When Zn_7MT-IIA dissolved in PBS was treated with iodoacetamide, the MT-IIA in the sample was unable to competitively reduce the absorbance reading for the assay indicating that the iodoacetamide was also interfering with the competitive ELISA. The absorbance reading for Zn_7MT-IIA dissolved in plasma and treated with iodoacetamide did produce a low absorbance reading but the validity of this reading is questionable because the iodoacetamide plasma sample containing no MT-I/II had a similar absorbance reading. With no interference, a plasma sample containing no MT-I/II would be expected to give an absorbance reading equivalent to the PBS negative control. Therefore iodoacetamide treatment interferes with the competitive ELISA but the result of this interference differs between PBS and mouse plasma as the sample matrix.

4.3.7 The iodoacetamide reaction decreases the sample pH

The carboxyamidomethylation reaction results in the addition of a carboxyamidomethyl group to the sulphur atom of cysteine residues and the loss of a hydrogen ion from the thiol group and an iodide ion from iodoacetamide (see figure 4.2). Because hydroiodic acid is a strong acid, it has the capacity to strongly affect the pH of the solution as the carboxyamidomethylation reaction proceeds and more acid is produced. The pH of the iodoacetamide treated samples was investigated as a putative cause of interference in direct and competitive ELISA for MT-I/II. An artificial plasma solution containing a physiological albumin concentration and no MT-I/II was used as a substrate for the iodoacetamide reaction. The pH of the reaction was measured at various stages of the process in order to devise a method to adjust the pH back to neutral. The carboxyamidomethylation reaction was allowed to proceed with initial pH at 6, 7 or 8.

The pH of the samples after the iodoacetamide treatment is displayed in table 4.1. After the carboxyamidomethylation reaction was completed the pH was adjusted with MES buffered solutions at pH 5, 6, 7, 8.2 and 8.9. Figure 4.6 shows that higher initial pH and higher pH in the adjustment solutions results in a final pH closer to neutral.

Table 4.1 The pH of the sample after the iodoacetamide reaction, before the addition of the adjustment buffer. The iodoacetamide was buffered with MES at pH 6, 7 or 8 and added to the samples with heating. Even with MES buffer the pH of the sample decreased substantially. Data are presented as mean ± SEM (n=5).

pH of Iodoacetamide buffer	pH of sample after iodoacetamide reaction
6	5.59 ± 0.20
7	6.29 ± 0.12
8	6.57 ± 0.11

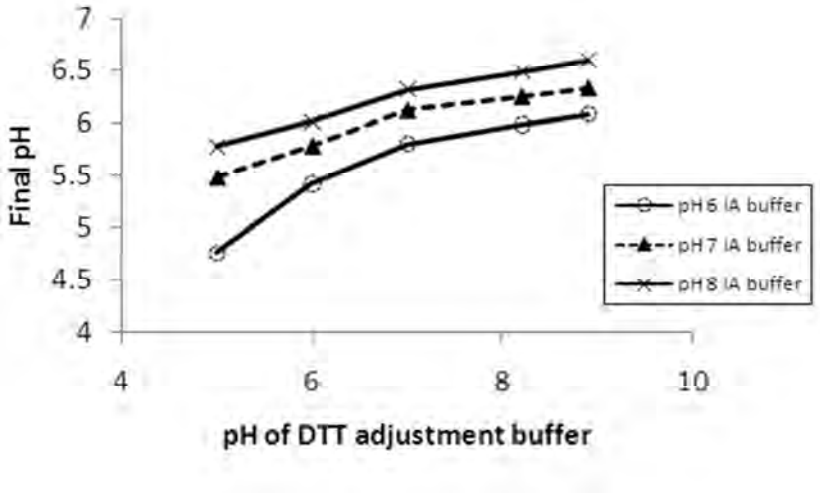

Figure 4.6 A titration of the carboxyamidomethylation reaction was conducted on artificial plasma with buffers at different pH. The 3 different buffers containing iodoacetamide with pH 6, 7, or 8 were added during the second step of the carboxyamidomethylation reaction. There were 5 different adjustment buffers containing DTT at pH 5, 6, 7, 8.2 and 8.9 that were added after the carboxyamidomethylation reaction. These adjustment buffers were designed to raise the final pH towards neutral (x-axis). The final pH of the carboxyamidomethylation is plotted on the y-axis. No MT was present in any of the samples (n=1).

4.3.8 Buffering the iodoacetamide reaction as a potential solution to ELISA inhibition

From the previous experiment, reactions with final pH or 4.76, 5.48 and 6.48 were chosen to be spiked with commercially obtained HPLC purified, carboxyamidomethylated MT with a final concentration of 80 µg/ml. An MT-free aliquot was also retained. All samples were assayed by competitive ELISA and compared to PBS with and without 80 µg/ml of HPLC purified, carboxyamidomethylated MT (figure 4.7). Across the pH ranges, in samples containing MT, signal was low in the competitive ELISA as expected. However, in the carboxyamidomethylated samples without MT, decreased signal was observed suggesting that primary antibody binding is being inhibited. Therefore, the samples containing MT are not reliable because low signal could be the result of either competition for primary antibody or interference to antibody binding to the substrate. The unexpected result was that increasing the pH towards neutral had a greater effect at inhibiting antibody binding to the substrate. Therefore the iodoacetamide reaction without buffering interferes with the assay but returning the pH towards neutral further increased the interference.

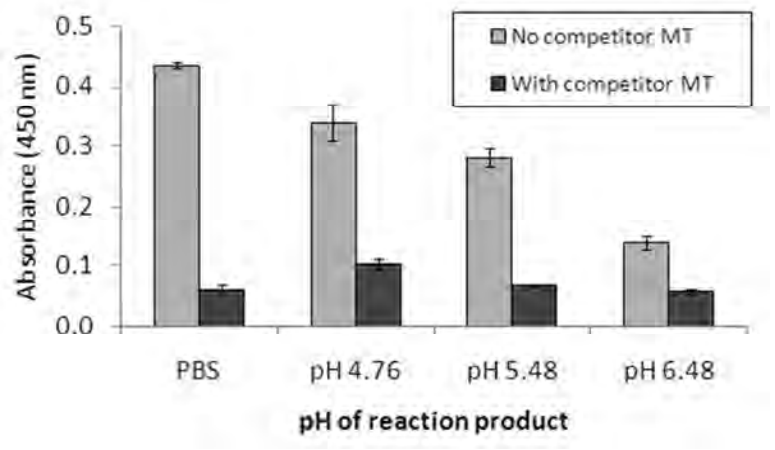

Figure 4.7 Competitive ELISA on the reaction product of the carboxyamidomethylation reaction after pH adjustment. Samples from the titration experiment were chosen according to their final pH and were run on ELISA with or without the addition of HPLC-purified, carboxyamidomethylated MT-IIA (10 µg/ml final concentration). Compared to 10 µg/ml HPLC-purified, carboxyamidomethylated MT-IIA in PBS, all reaction products have reduced absorbance readings. If no interference was occurring in the ELISA, samples with no competitor HPLC-purified, carboxyamidomethylated MT-IIA should have equal absorbance to HPLC-purified, carboxyamidomethylated MT-IIA dissolved in PBS. Each sample was assayed in triplicate (error bars=SEM).

4.3.9 Optimisation of competitive ELISA with UC1MT antibody

The interference obtained with iodoacetamide indicated that a new approach to ELISA was required to allow quantification of MT-I/II in mouse tissues without non-specific interference. During the course of the work described above using the E9 antibody, a competitive ELISA to assay MT-I/II in mouse tissue with the commercially available UC1MT mouse monoclonal antibody was published (Emeny et al. 2009). However, the sensitivity of the ELISA was not published nor was any evidence of matrix effects assessed.

With the use of the UC1MT antibody, the optimal conditions for competitive ELISA were assessed with a chequerboard ELISA with 100 ng/ml competitor MT coating concentration (Figure 4.8A). Similar results were obtained with a 1µg/ml competitor MT coating concentration in terms of maximum immunoreactivity and sensitivity (data not shown) but 100 ng/ml coating concentration was chosen because it was more cost-effective. HPLC-purified Zn_7MT and HPLC-purified carboxyamidomethylated MT were trialled as the coated antigen. Binding of UC1MT to carboxyamidomethylated MT-IIA appeared to be substantially greater than binding to Zn_7MT-IIA (data not shown). The objective of competitive ELISA is to compete soluble antigen with coated antigen hence, Zn_7MT-IIA was chosen as the coated antigen because lower concentrations of soluble MT will be more able to compete with the less immunoreactive form of coated MT. Primary and secondary antibody dilutions of 1:5000 were chosen from the results of the chequerboard ELISA because this combination appeared to have the highest sensitivity of the combinations tested. Therefore 100 ng/ml Zn-MT-IIA was used to coat plates for competitive ELISA with primary antibody dilution of 1:5000 and a secondary antibody dilution of 1:5000. A standard curve was conducted in quadruplicate for the competitive ELISA using these chosen conditions (figure 4.8B). This ELISA has a lower detection limit of approximately 4-10 ng/ml MT-I/II in the original sample or 0.2-0.5 ng per well (see figures 4.8 and 4.9).

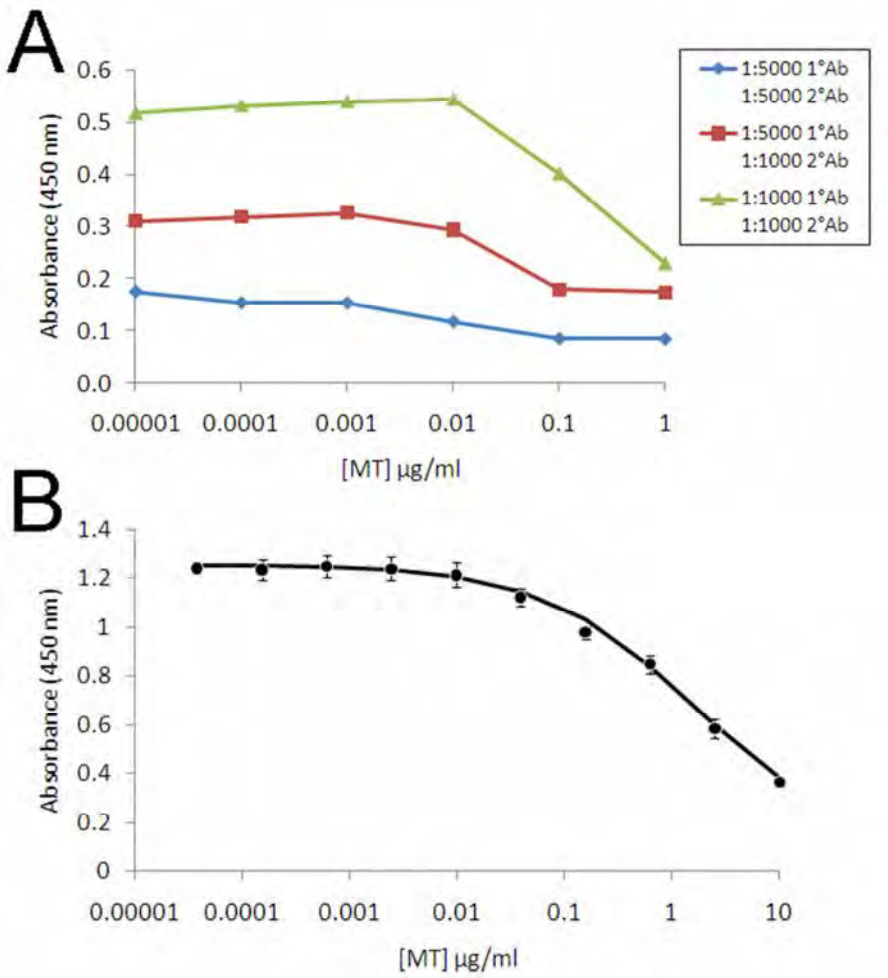

Figure 4.8 (**A**) Chequerboard ELISA for MT was conducted using the competitive technique with the UC1MT antibody clone. The chequerboard determined that the ELISA reached a plateau at lower sample MT concentrations when the primary antibody (1°Ab) and secondary antibody (2°Ab) concentrations were lower. (**B**) Standard curve for competitive MT ELISA conducted with the UC1MT antibody clone diluted 1:5000 and secondary antibody diluted 1:5000. The increased absorbance for this antibody concentration in (**B**) compared to (**A**) is due to a longer incubation time for the TMB substrate step in (1 hour for **B** versus 10 mins for **A**). The curve has been fitted to a 4-parameter logistic model (R^2=0.96). Data are expressed as the mean of 4 replicates (error bars=SEM).

4.3.10 Displacement curves to assess matrix effects in mouse tissue with UC1MT ELISA

Displacement curves are designed to test non-specific displacement of the antibody from the substrate bound antigen. If matrix effects are present in the tissue of interest they will alter the slope of the displacement curve. Displacement curves were created by serial dilution of Zn-MT-IIA in homogenate samples of varying protein concentration and compared to a standard curve created in wash buffer. Previous experience with displacement curves in competitive ELISA suggested that 0.1 mg/ml total protein concentration would be an acceptable total protein concentration. Figure 4.9 demonstrates that at concentrations of 0.1 mg/ml and 0.01 mg/ml, homogenates from both brain and liver did not exert matrix effects on the UC1MT competitive ELISA. This is evident because the displacement curves are parallel to the standard curve which indicates that the primary antibody is not being displaced from its antigen when liver or brain proteins are present. Therefore with an absolute detection limit of 4 ng/ml and a total protein content of 0.1 mg/ml, the lower detection limit for UC1MT ELISA in brain and liver is 40-100 ng/mg of total protein. For comparison, two examples of matrix effects are shown in MT-I/II$^{-/-}$ mouse urine assayed by E9 antibody direct ELISA, and in rat brain assayed by E9 antibody competitive ELISA (figure 4.10). In both cases, the least dilute substrate was able to cause the greatest deviation from the gradient of the linear phase of the standard curve. Therefore MT-I/II can be quantified by competitive ELISA with UC1MT antibody in mouse liver and mouse brain homogenates but not in mouse urine or rat brain homogenate.

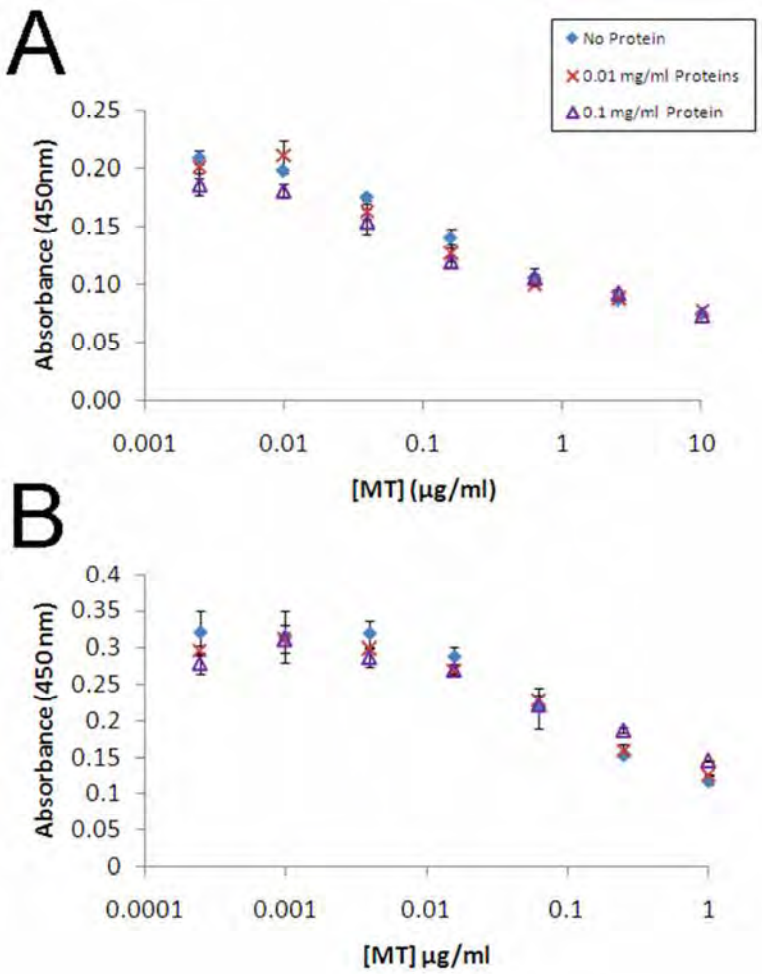

Figure 4.9 Displacement curves for Zn_7MT-IIA in MT-I/II$^{-/-}$ mouse brain homogenate (**A**) and MT-I/II$^{-/-}$ mouse liver homogenate (**B**). Displacement curves constructed in solutions with protein content of 0.01 mg/ml and 0.1 mg/ml are parallel to the standard curve constructed in PBS containing no protein for both liver homogenate and brain homogenate. Therefore no matrix effects were observed at these concentrations. Data are expressed as the mean of 3 replicates (error bars=SEM).

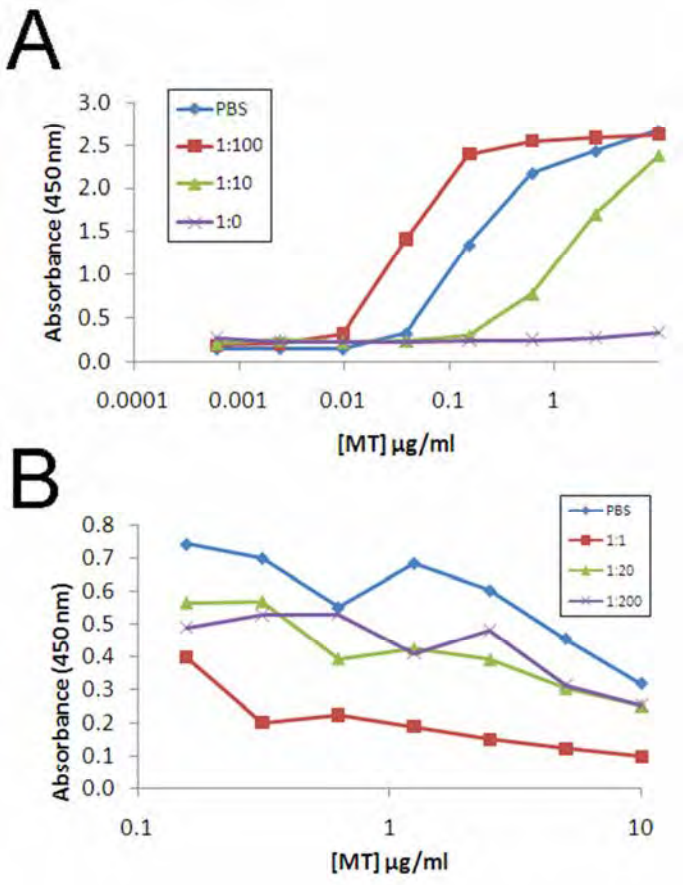

Figure 4.10 Examples of displacement curves that indicate the presence of matrix effects. (**A**) Direct MT ELISA conducted with the E9 antibody clone in various dilutions MT-I/II$^{-/-}$ mouse urine indicates vastly different gradients in the displacement curves generated compared to the standard curve. Hence mouse urine produces matrix effects for MT ELISA conducted with the E9 antibody clone. Data are expressed as the mean of 3 replicates. (**B**) Displacement curves were prepared in rat brain homogenate and competitive ELISA with the UC1MT antibody clone was conducted. Protein content was not assayed for these samples but the matrix effects persisted after 1:200 dilution of the homogenate. Rat brain contains MT-I/II which may interfere with the position of the displacement curve on the x-axis but the curve would still be parallel to the standard curve if matrix effects were not present. Data are expressed as the mean of duplicate assays.

4.3.11 Specificity of the UC1MT antibody for MT-I/II and MT-III

It has previously been shown that UC1MT exhibits equal binding to MT-I and MT-II (Lynes et al. 1993), however it is not known if UC1MT cross-reacts with MT-III. MT-III would have been present in brain homogenate from MT-I/II$^{-/-}$ mice and did not appear to be affecting the UC1MT competitive ELISA based on the displacement curves. However, there may be situations where MT-III concentrations change, therefore the affinity of the UC1MT antibody for MT-IIA and MT-III was compared by direct ELISA (figure 4.11). There was a slight increase in the absorbance of MT-III standard curve between 7-70 µg/ml which may indicate a small amount of cross-reactivity of UC1MT with MT-III. However the direct ELISA was able to detect Zn_7MT-IIA at concentrations 4 orders of magnitude lower than MT-III. Therefore when used in a competitive ELISA the contribution of MT-III to the competition for the UC1MT antibody will be negligible unless MT-III concentrations are many orders of magnitude greater than MT-I/II concentrations.

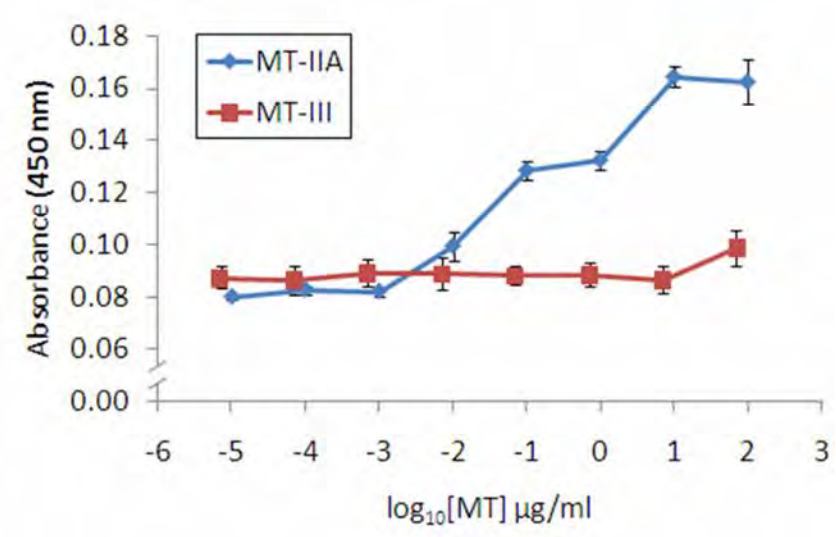

Figure 4.11 Cross-reactivity of the UC1MT antibody for MT-III was tested by direct ELISA. Comparison of the standard curves for Zn_7MT-IIA (blue lines) and Zn_7MT-III (red lines) demonstrate some immunoreactivity may occur when MT-III concentrations are high but UC1MT detects Zn_7MT-IIA at concentrations 4 orders of magnitude lower than Zn_7MT-III. Data are expressed as the mean of triplicate experiments (error bars = SEM).

4.4 Discussion

The data presented herein demonstrate that the commercially available, UC1MT antibody is capable of detecting MT-I/II in samples derived from mouse tissues using competitive ELISA. Outcomes from western blotting determined that direct ELISA was not suitable because the anti-mouse secondary antibodies do not distinguish between the primary antibody and an endogenous component of mouse isolates, most likely IgGs; both the E9 and UC1MT antibodies are mouse IgGs. Competitive ELISA avoids the non-specific binding issues because proteins in the tissue sample are not adsorbed onto the microplate. Only the UC1MT antibody was suitable for competitive ELISA because the E9 antibody was not able to generate an ELISA with high enough sensitivity to quantify physiological quantities of MT. Carboxyamidomethylation of Zn_7MT-IIA was attempted to try to prevent MT aggregation or formation of complexes between MT and higher molecular weight proteins and it appeared that this technique may have removed endogenous proteins that were interfering with specific MT detection. However it was demonstrated that the iodoacetamide reaction is incompatible with both direct and competitive ELISA. It was also determined that the required heat treatment and processing of samples is likely to affect accurate quantitation of MT.

4.4.1 Analysis of displacement curves

UC1MT has been used to quantitate MT-I/II in mouse tissues previously but the authors did not publish displacement curves to verify a lack of interference in the assay (Emeny et al. 2009). The authors did show that samples from MT-I/II$^{-/-}$ mice did not exhibit the increases in MT-I/II that were observed in wild type mice after experimental manipulation. However, the absence of signal in the absence of MT does not eliminate the possibility of interference. Molecules in the sample matrix that do not themselves give a false positive reading, can interfere with various stages of immunoassays and lead to overestimation or underestimation of the analyte (Selby 1999, Span et al. 2003). By creating dilution curves in analyte free matrix, information about the affinity of the antibody for the antigen for a given matrix can be derived. Matrix effects can not easily be controlled for because they can vary under different conditions. Serial dilution is a method for assessing the presence of matrix effects in individual samples and has been used to identify matrix effects that occur in a sub-set of patients in clinical immunoassays (Emerson et al. 2003). Interactions between endogenous antibodies and primary antibodies are large contributors to interference in immunoassays and are a

potential cause of the variation in matrix effects observed in different patients (Ismail et al. 2002). Therefore, assaying samples from in-bred mouse strains requires the generation of displacement curves each time a new mouse strain is analysed. The lack of interference in the displacement curves for UC1MT ELISA demonstrate that MT-I/II content in murine liver and brain samples of up to 0.1 mg/ml total protein content can be assayed.

4.4.2 Carboxyamidomethylation of MT

Initially, carboxyamidomethylation was attempted as a method for preserving monomeric MT in tissue samples and showed promise in removing nonspecific interactions between anti-mouse IgG secondary antibody and endogenous mouse proteins. The technique has been used successfully to prevent aggregation of MT when the detection method is western blotting (Kimura et al. 1991). However, the reagents or products of this reaction disrupt both antigen adsorption to microplates and antibody binding in ELISAs. Before western blotting, SDS-PAGE separates the proteins from lower molecular weight species that include iodoacetamide, DTT and hydroiodic acid before the adsorption and antibody binding steps. The formation of hydroiodic acid and the consequent decrease in pH is the most likely cause of interference in ELISA. The rationale behind this observation comes from the fact that the reaction with MT in the absence of plasma protein resulted in underestimation of MT concentration in the ELISA but did not abolish antibody binding to the substrate. The iodoacetamide reaction in the presence of plasma protein, with or without MT, resulted in abolishment of antibody binding to the substrate indicating that the reaction with plasma caused greater disruption to the ELISA. The reason for this may be that plasma has a higher protein content and contains many thiol groups that can react with iodoacetamide, with each carboxyamidomethylation of a thiol group causing formation of hydroiodic acid. Hence acid formation would be higher in the reactions containing plasma and likely explains why the reactions with plasma had a greater inhibitory effect on the ELISA. Antigen coating to the microplate and antibody-antigen interactions are both non-covalent interactions that are pH dependent. Attempts to rectify the decrease in pH did not improve the problem. One hypothesis is that by adding buffers to the samples the salt concentration is increased with higher pH adjustment solutions containing more salts. Increases in ionic solutes can decrease the amount of non-covalent binding of protein in a solution and immunoglobulins are so-called for their propensity to aggregate at high salt concentrations. A second hypothesis to explain the failure of pH adjustment to return antibody binding to iodoacetamide treated samples is that DTT is

more active as a disulphide reducing reagent at high pH. Antibodies contain an essential disulphide linkage between the heavy and light chains of the protein. DTT may be responsible for reducing this bond, thereby abolishing the binding capacity of the antibody. β-mercaptoethanol, which has a similar action to DTT, can similarly interfere with MT ELISA (Tang et al. 1999). Both iodoacetamide and DTT must be in excess of all thiols in the sample for complete carboxyamidomethylation to occur. Therefore reducing the concentrations will reduce the efficacy of the carboxyamidomethylation reaction. Due to the nature of the interaction between the products of the carboxyamidomethylation reaction and ELISA and the lack of heat stability of Zn_7MT-IIA, carboxyamidomethylation does not appear to be a suitable method to prevent MT forming higher molecular weight complexes via disulfide bonds. To accurately measure total MT in tissues an ELISA-compatible approach is still required.

4.4.3 Heat stability of Zn_7MT-IIA

Zn_7MT-IIA was lost from solution when heated to 90°C for 10 minutes most likely due to MT aggregation. This step is required for MT assays such as the Cd/Haem and Ag/Haem methods which rely on the heat stability of MT to separate it from less heat-stable proteins (Summer and Klein 1991). However, it is possible that Cd-MT and Ag-MT complexes are more heat stable than the native Zn-conjugated form of MT due to the higher affinity of MT for cadmium and silver. For example it has been shown that cadmium bound MT is more resistant to metal stripping than zinc bound MT in response to NO (Khatai et al. 2004). In future studies, cadmium treatment of MT-containing tissue samples may be an applicable method of preventing aggregation of MT. However, this will require careful implementation because cadmium-bound forms of MT have been shown to have different levels of immunoreactivity than to zinc-bound MT via ELISA (Chan et al. 1992). Therefore cadmium addition must result in complete replacement of zinc bound to MT and must be in excess to MT and any other cadmium binding proteins that could compete for cadmium. However, the concentration of the added cadmium must not increase the salt concentration in the sample to a level that interferes with non-covalent binding to the microplate required for the ELISA.

4.4.4 Conclusions

The UC1MT antibody has been used before to quantify MT in liver and spleen by ELISA in mouse tissue (Emeny et al. 2009) although it was incompletely characterised. The optimisation of this technique described here allows 100-fold less antibody to be

used and 200-fold less MT for adsorption to the substrate compared to the previous report. The presence of matrix effects was examined and it was discerned that a solution containing up to 0.1 mg/ml protein can be assayed from either mouse brain or liver. The original application for MT-I/II ELISA was to determine if MT-I/II levels in mouse plasma after brain injury were similar to the increase in plasma MT observed in brain injured patients (Kukačka et al. 2006). Due to the high protein content of plasma and relatively low levels of MT expected in plasma this aim was not possible with the currently developed UC1MT ELISA. Measurement of urine MT levels as an approximate measure of MT in circulation was also not possible because matrix effects interfere with the ELISA. It should be noted that prevention of MT aggregation was not compatible with ELISA, however few other studies have attempted to address this issue and a viable solution for MT immunoassays has yet to be developed. A consequence of this is that ELISA may underestimate the quantity of metallothionein but it will still be a useful and conservative measure of comparative increases in MT expression within biological samples. MT in liver is a reliable indicator of systemic MT-induction and the use of the ELISA technique to quantify brain injury-induced MT expression in brain and liver is the subject of chapter 5.

Chapter 5 – Hepatic MT-I/II Induction Post-Brain Injury

5.1 Introduction

Multiple studies with MT-I/II$^{-/-}$ mice and transgenic MT-I over-expressing mice have shown that MT-I/II may have a beneficial role in the recovery from brain injury (Natale et al. 2004, Penkowa et al. 1999a, Penkowa et al.1999b, Penkowa et al.2001, Penkowa et al.2006a, Potter et al. 2007, Potter et al. 2009, Suemori et al. 2006). Because the techniques used to ablate or increase MT-I/II expression were not targeted to specific tissues (Masters et al. 1994, Palmiter et al. 1993), the actual source or the site of action of MT-I/II in this protective context is not known. There is evidence that MT-I/II regulates the inflammatory response to stress or injury, hence the production of MT-I/II outside the CNS may be capable of influencing the recovery process within the injured brain.

It is well reported in the literature that stress can induce expression of MT-I/II in the liver. Specifically, hepatic MT-I/II expression has been demonstrated in response to burn injury (Cho et al. 2004, Ding et al. 2002, Zhou et al. 2003), restraint stress (Hernández et al. 1999, Jacob et al. 1999), zinc challenge (Coyle et al 1995, Zhou et al. 2004), fasting and simulated sepsis with LPS challenge (Philcox et al. 1995, Swapan et al. 1990). The induction of liver MT-I/II expression has been shown to cause increases in hepatic zinc content, a response that does not occur in MT-I/II$^{-/-}$ mice (Cho et al. 2004, Coyle et al. 1995, Ding et al. 2002, Philcox et al. 1995, Zhou et al. 2003). The process of hepatic MT-I/II mediated zinc sequestration has been proposed to explain alterations in plasma zinc concentrations in brain-injured patients (Ott et al. 1994). Hepatic MT-I/II has not been quantified after brain injury although increased concentrations of MT have been detected in the blood of patients with head injury (Kukačka et al. 2006) but it is not known if this MT originates from the brain or an extraneural source. Dietary zinc deficiency preceding experimental brain injury in rats has been shown to cause greater microglial activation and neuron death compared to injured rats on zinc-sufficient diets (Penkowa et al. 2001, Yeiser et al. 2002). There is also a positive association between zinc supplementation after hospital admission and neurologic recovery rate in head injured patients (Young et al. 1996). Given the ability of zinc to cause microglial reactivity (Kauppinen et al. 2008), alter Th1/Th2 ratios (Prasad et al. 2007) and the ability of zinc deficiency to reduce immune system function (DePasquale and Fraker 1979, DePasquale and Fraker 1980, King and Fraker 2000, King and Fraker 2002, King et al. 2005), there is potential for MT-I/II to modulate the immune system via its role in zinc homeostasis. This relationship may be responsible

for some of the differences in the response to brain injury in wild type and MT-I/II$^{-/-}$ mice (see chapters 2 and 3).

MT-I and MT-II gene expression is inducible by increased intracellular free zinc concentrations, IL-6 and glucocorticoids (reviewed by Kimura & Itoh 2008). Altered zinc homeostasis (McClain et al. 1986), raised concentrations of IL-6 in serum (McClain et al. 1991) and increased glucocorticoid availability (Savaridas et al. 2004) have all been observed in patients after brain injury. The aim of this chapter was to determine if hepatic MT-I/II expression was up-regulated after cryolesion brain injury. Subsequent aims were to determine the mechanism by which hepatic MT-I/II expression is induced and to determine if hepatic MT-I/II expression has the capacity to sequester zinc to the liver, after brain injury.

5.2 Methods

5.2.1 Animals

Animal housing was identical to the methods outlined in chapter 2.2. However, extra care was taken to maintain a consistent routine around the animals. Each mouse was housed in the experimental facility for at least 1 week prior to any surgical procedure. Maintenance tasks were conducted in the animal room at between 9:00 am and 11:00 am every day to acclimatise the animals to human activity before the day of surgery and during the recovery period. These precautions were taken to minimise confounding factors for assay of stress hormones in the animals after cryolesion injury. Experiments were conducted with either 7 animals per treatment group (i.e. mice of the same strain and time-point of euthanasia) and total number of experimental size of 56 mice or 6 animals per group and 48 animals per treatment group.

5.2.2 Cryolesion brain injury and sham surgery

Cryolesion surgery was conducted as outlined in chapter 2.2. Sham injury surgery was identical to cryolesion injury in every regard except that the steel rod was not cooled in liquid nitrogen before application to the skull. Note that zero time point animals were always untreated and hence differ from sham injured animals. Zero time point animals never received cryolesion surgery or sham surgery.

5.2.3 Quantitative reverse-transcriptase PCR (RT-PCR)

The methods for isolating RNA from liver and brain injury biopsies, the synthesis of cDNA and the real-time PCR protocols are outlined in chapter 3.2. Table 5.1 details the

primer sequences and the PCR product lengths. GAPDH was used as the housekeeping gene in brain biopsy samples and β-actin was used as the housekeeping gene in liver samples for reasons discussed in chapter 3. Samples from MT-I/II$^{-/-}$ mice were able to be analysed for MT-I and MT-II mRNA transcripts because the MT-I and MT-II inactivation strategy involved the insertion of premature stop codons into each gene which was expected to prevent protein translation but not RNA transcription. The MT-I and MT-II mRNA transcripts from MT-I/II$^{-/-}$ mice differ slightly from wild type mice due to the insertion of the short DNA sequences containing the premature stop codons. The MT-I and MT-II primer sets were designed to bind to the cDNA for the transcripts from both wild type and MT-I/II$^{-/-}$ mice. Primer binding to sequences distal to the transgenic inserts for the MT-I/II$^{-/-}$ mouse cDNA transcripts is demonstrated in figure 5.1. The product lengths for the MT-I and MT-II cDNA transcripts are 216 and 171 base pairs, respectively, in MT-I/II$^{-/-}$ mice.

Table 5.1 Oligonucleotide primer sets used for quantitative RT-PCR of brain and liver samples after cryolesion brain injury. Product lengths for wild type mice are shown. Product lengths for GAPDH and β-actin in MT-I/II$^{-/-}$ mice are the same as for wild type mice but the PCR products for the MT-I and MT-II sequences are slightly longer due to the transgenic inserts.

Primer		Sequence (5' - 3')	Product length
GAPDH	Fwd	CCCAGAAGACTGTGGATGG	80
	Rev	GGATGCAGGGATGATGTTCT	
β-actin	Fwd	GTCCACCTTCCAGCAGATGT	260
	Rev	AGGGAGACCAAAGCCTTCAT	
MT-I	Fwd	GCTGTCCTCTAAGCGTCACC	193
	Rev	AGGAGCAGCAGCTCTTCTTG	
MT-II	Fwd	CAAACCGATCTCTCGTCGAT	150
	Rev	AGGAGCAGCAGCTTTTCTTG	

MT-I mRNA

```
  1 tctgcactcc gcccgaaaag tgcgctcggc tctgccaagg acgcggggcg cgtgactatg
 61 cgtgggctgg agcaaccgcc tgctgggtgc aaacccttg cgcccggact cgtccaacga
121 ctataaagag ggcaggctgt cctctaagcg tcaccacgac ttcaacgtcc tgagtacctt
181 ctcctcactt actccgtagc tccagcttca ccagatctcg gaatggaccc caactgctcc
241 tgctccaccg gatagGTACC AATTATCCGc ggctcctgca cttgcaccag ctcctgcgcc
301 tgcaagaact gcaagtgcac ctcctgcaag aagagctgct gctcctgctg tcccgtgggc
361 tgctccaaat gtgcccaggg ctgtgtctgc aaaggcgcGC GATGTAACGG TCACATCACC
421 cgcggacaag tgcacgtgct gtgcctgatg tgacgaacag cgctgccacc acgtgtaaat
481 agtatcggac caacccagcg tcttcctata cagttccacc ctgtttacta aacccccgtt
541 ttctaccgag tacgtgaata ataaaagcct gtttgagtct aaaaaaaaaa aaaaaaaaaa
601 aaaaaaaaaa aaaaaaaaaa aaaaa
```

MT-II mRNA

```
  1 ggtcgtgcgc aggcccaggg gcgtgtgctg gccatatccc ttgagccaga aaaagggcgt
 61 gtgcaggcgg cgggggcgcg tgcatggtgc cttccacccg ggcggagctt ttgcgctcga
121 cccaatactc tccgctataa aggtcgcgct ccgcgtgctt ctctccatca cgctcctaga
181 actcttcaaa ccgatctctc gtcgatcttc aaccgccgcc tccactcgcc atggacccca
241 actgctcctg tgcctccgat ggatcCACGG TTGACTAAGG TAGATCctgc tcctgcgctg
301 gcgcctgcaa atgcaaacaa tgcaaatgta cttcctgcaa gaaaagctgc tgctcctgct
361 gccccgtggg ctgtgcgaag tgctcccagg gctgcatctg caaagaggct tccgacaagt
421 gcagctgctg tgcctgaagg ggggcggagg ggtccccaca tctgtgtaaa tagaccatgt
481 agaagcctag ccttttttgt acaaccctga ctcgttctcc acaacttttt ctataaagca
541 tgtaactgac aataaaagcc gttgacttga ttaattc
```

Figure 5.1 cDNA for the MT-I and MT-II mRNA transcripts from MT-I/II$^{-/-}$ mice compiled from (genbank accession numbers NM_013602.3 and NM_008630.2 and Masters et al. 1994). Underlined text designates the forward primer sequence and sequence complementary to the reverse primer. The blue text indicates the transgenically inserted bases that contain the premature stop codons. Premature stop codons are coloured red and the start codons have been coloured green.

5.2.4 UC1MT competitive ELISA

Brain biopsies and liver samples were ground to a fine power in a mortar and pestle under liquid nitrogen. The powdered tissue was homogenised in 150 mM NaCl, 20 mM Tris-HCl, 1% Igepal, pH 7.6 with EDTA-free Halt-protease inhibitor cocktail (Thermo Scientific) with an Ultra-Turrax mechanical homogenizer (IKA). Samples were centrifuged at 10 000*g* for 10 minutes and the supernatant was retained for assay. Protein concentration was obtained by Bradford assay (Bradford 1976).

Zn_7MT-IIA (HPLC-purified rabbit MT-IIA conjugated to 7 Zn^{2+} ions, Bestenbalt, Estonia) was coated to a 96-well microplate (Nunc) in 50 mM Na_2CO_3 solution at 4 °C overnight on an orbital shaker. All subsequent stages took place at room temperature. Following a 5 minute rinse in wash buffer, wells were blocked with 150 µl casein solution (2.5%, pH 7.4) for 30 minutes. The wells were washed again in wash buffer for 5 minutes. Zn_7MT-IIA standards were serially diluted by a factor of 4 in ELISA wash buffer to create standard curves. Mouse tissue homogenates or plasma samples were diluted in wash buffer to achieve a protein concentration of 0.1 mg/ml. Samples were applied to the plate in triplicate or quadruplicate in 50 µl aliquots first. Primary antibody (UC1MT mouse anti-MT-I/II, Assay designs) was diluted 1:5000 (200ng/ml, final concentration) in ELISA wash buffer and applied to sample- or standard-containing wells. This competition step was incubated for 1 hour. The plate was rinsed for 5 minutes, 3 times with wash buffer. Secondary antibody (Dako, Goat anti-mouse IgG-HRP conjugate) was diluted 1:2000 in ELISA wash buffer and applied to each well in 50 µl aliquots and incubated for 1 hour. The plate was rinsed for 5 minutes, 3 times with wash buffer. TMB peroxidase substrate (KPL) was incubated in the wells in 50 µl aliquots for 1 hour. The reaction was terminated with 50 µl of 1 M phosphoric acid and the absorbance of the microplate was measured at 450 nm. A standard curve was generated from the rabbit MT-IIA standard solutions which allowed calculation of MT-I/II content in tissue sample solutions. Calculation of sample MT-I/II concentrations from the standard curve was conducted with 4-parameter logistic modelling as outlined in chapter 4. The MT-I/II concentration of samples with absorbance readings less than or equal to the asymptote for the lower limit of the assay could not be quantified. These data points were assigned a value equal to the ELISA detection limit, as a conservative estimate for statistical analysis.

5.2.5 Radioimmunoassay for corticosterone

Blood was obtained from mice at 0, 1, 3 or 7 DPI via cardiac puncture with syringes containing 20 µl of 5000 units/ml heparin solution (Sigma). Blood was centrifuged at 14 000*g* for 5 minutes to obtain plasma which was snap-frozen in liquid nitrogen for storage. Assay of plasma corticosterone was conducted by Prof. N.W. Pankhurst and Dr P.M. Pankhurst as described in Pankhurst et al. (2008). Corticosterone was extracted from 50 µl of plasma with 1 ml of ethyl acetate in a polycarbonate tube. The tube was centrifuged at 2000*g* for 5 minutes then 50 µl of the supernatant was transferred to a separate tube and the solvent was evaporated overnight. To each sample tube, 200 µl of ^{3}H-corticosterone solution (1,2,6,7-^{3}H(N)-corticosterone, PerkinElmer Life Sciences, 0.02 µCi/ml; 70-100 Ci/mmol in PBS containing 0.1% gelatin) was added followed by the addition of 200 µl polyclonal rabbit anti-corticosterone antibody in PBS-1% gelatin (Sigma, diluted to give 40-50% binding of ^{3}H-corticosterone in the absence of a competitor). This competitive step was incubated overnight at room temperature. Unbound corticosterone was removed from antibody-bound corticosterone by addition of 200 µl of dextran coated charcoal solution (0.05% dextran, 0.5% charcoal, 0.1% gelatin in PBS) for 10 minutes followed by decantation of the supernatant into scintillation vials. To each vial, 4ml of Ecolite scintillation cocktail was added and the radioactivity of the samples was counted on a scintillation counter. Standard solutions of unlabelled corticosterone were prepared by serial dilution in assay buffer and were added directly to assay tubes. A standard curve was generated to calculate the concentration of corticosterone in each sample. All samples and standards were assayed in duplicate. Extraction efficiency for mouse plasma was determined by adding a known quantity of ^{3}H-corticosterone to plasma samples pooled from several mice. Extraction with ethyl acetate was conducted and scintillation counts were compared to solutions of ^{3}H-corticosterone of equivalent original concentration that had not undergone extraction. The extraction efficiency was determined to be 84.5% hence the radioimmunoassay determined-concentration of all samples was adjusted by a factor of 1.18.

5.2.6 Liver zinc assay by atomic absorption spectroscopy

Liver samples from uninjured and injured mice were dissected out and freeze-clamped in liquid nitrogen. Each sample was ground to a fine power under liquid nitrogen with a mortar and pestle. The powdered liver was homogenised in 1 ml of MilliQ water with a Potter-Elvehjem homogeniser. The homogenate was transferred to a pre-weighed tube and was lyophilised. The gross weight of the tube was measured after lyophilisation to

calculate the net weight of the sample. Lyophilised liver samples were dissolved in 3.5 ml of 70% nitric acid (Trace select, Fluka) by heating to 70°C for 1 hour. The samples were further diluted with 3 ml of MilliQ water. Centrifugation at 2000*g* for 20 minutes was required to remove a floating layer of insoluble matter and a small quantity of protein that precipitated in some samples with the decrease in acid concentration. Before centrifugation 0.5 ml of 30% hydrogen peroxide (Trace select, Fluka) was added to each sample to oxidise any thiols present in the protein precipitate and thereby restrict its zinc binding capacity. The infranatant from each sample was obtained for each sample taking care to avoid aspiration of the pellet. Zinc concentration in each sample was assayed on an atomic absorption spectrometer (GBC Avanta Σ). Zinc concentration of the sample solutions was determined by comparison to the absorbance of zinc sulphate standard solutions prepared in 35% nitric acid and 2.14% hydrogen peroxide in MilliQ water.

5.2.7 Statistical analysis

Homogeneity of variances between groups within each data set was determined with Levene's test. The Box-Cox test was used to determine the appropriate transformation for data sets with heterogeneous variances between groups. Comparisons of MT-I and MT-II mRNA, MT-I/II protein expression and liver zinc content were conducted by 1-way ANOVA with Tukey's B post-hoc test. The comparison of corticosterone between wild type and MT-I/II$^{-/-}$ mice was conducted with 2-way ANOVA on the factors of time after injury and strain of mouse. Statistically significant differences in the factor of time were differentiated with Tukey's B post-hoc test.

5.3 Results

5.3.1 MT-I and MT-II induction in brain post-cryolesion brain injury

MT-I and MT-II mRNA were increased 5.0 ($P < 0.001$) and 32.6 fold ($P < 0.001$), respectively, at 1 DPI in wild type mice (figure 5.2). At 3 and 7 DPI, MT-I and MT-II mRNA are no longer significantly elevated from basal levels. In MT-I/II$^{-/-}$ and wild type mice, MT-I and MT-II mRNA increased to similar levels in response to cryolesion injury. It is interesting to note that MT-I/II$^{-/-}$ mice had significantly lower levels of MT-I mRNA than wild type mice at 0, 3 and 7 DPI when MT-I was at basal levels. MT-II mRNA was also significantly lower in MT-I/II$^{-/-}$ mice compared to wild type mice at 1 and 3 DPI. UC1MT ELISA demonstrated that MT-I/II protein in the vicinity of the lesion was increased, albeit with a high degree of variability, at 1 DPI. MT-I/II

protein remained at an intermediate concentration at 3 and 7 DPI (figure 5.3). Except for one outlier, the uninjured mice recorded MT-I/II concentrations at the detection limit of the ELISA so it is not possible to determine a definitive basal concentration of MT-I/II protein in mouse cortex or the relative increase in MT-I/II protein in injured versus uninjured mice. Regardless, the data demonstrate that MT-I/II is up-regulated after injury in the cryolesion injury site.

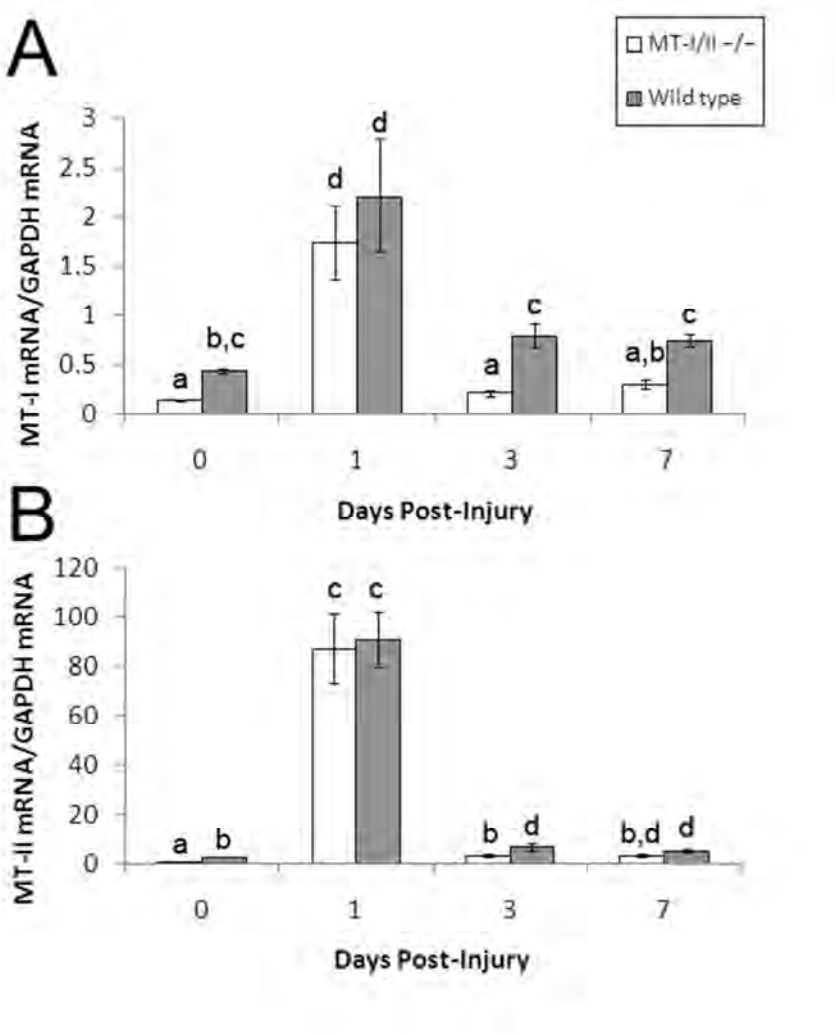

Figure 5.2 MT-I and MT-II mRNA induction in the injury site was quantified by RT-PCR. (**A**) MT-I mRNA increased to a similar extent in MT-I/II$^{-/-}$ and wild type mice at 1 DPI. MT-I mRNA was not increased significantly from basal expression at other time points but the resting levels and 3 and 7 DPI levels in MT-I/II were lower than wild type mice. (**B**) MT-II mRNA was increased a 1 DPI to the same level in wild type and MT-I/II$^{-/-}$ mice. MT-II mRNA decreased from 1-3 DPI but was still significantly higher than resting levels in wild type mice. In uninjured mice and mice at 3 DPI there was a significant difference between wild type and MT-I/II$^{-/-}$ mice. Significant differences were determined by 1-way ANOVA with Tukey's B post-hoc test; groups that share lower case letters are not significantly different from each other (for both graphs; n=6-7, error bars=SEM). These results are representative of a second repeat of this experiment.

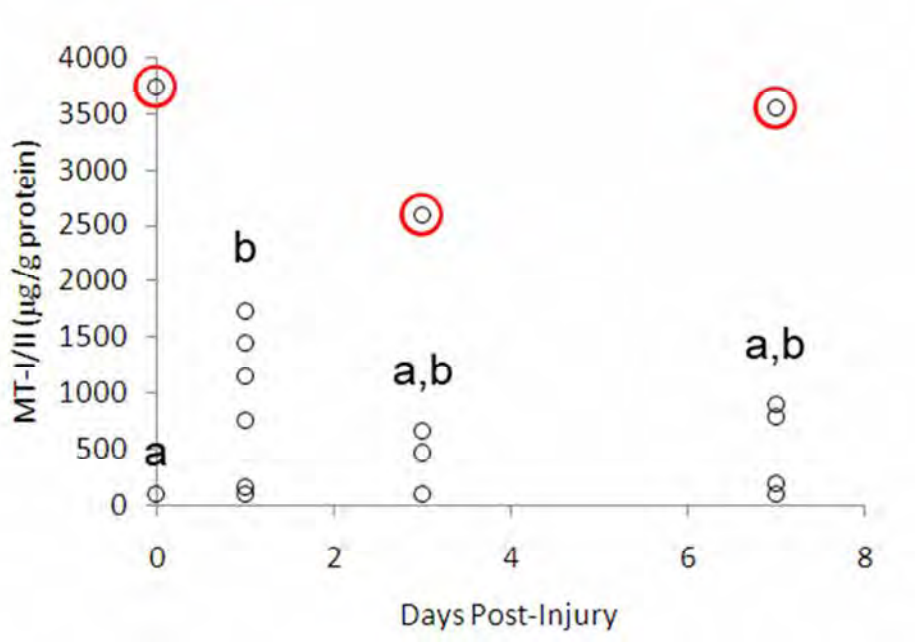

Figure 5.3 MT-I/II protein levels in the cryolesion injury site of wild type mice were assayed by UC1MT ELISA. The expression of MT-I/II protein was highly variable in the cryolesion injury site and three data points (circled in red) were treated as outliers and excluded from statistical analysis. MT-I/II expression was significantly elevated at 1 DPI then decreased at 3 and 7 DPI but remained higher than resting concentrations. Significant differences were determined by 1-way ANOVA with Tukey's B post-hoc test; groups that share lower case letters are not significantly different from each other (n=5-7, error bars=SEM).

5.3.2 MT-I and MT-II induction in liver post-cryolesion brain injury

Similar to the injured brain, wild type mice showed a 4.9 fold increase in MT-I mRNA at 1 DPI in the liver, followed by subsequent decreases at 3 and 7 DPI (figure 5.4A, $P < 0.001$). MT-II mRNA was significantly increased at 1 DPI but was maximal at 3 DPI with a 40.4 fold increase in expression over uninjured levels (figure 5.4B, $P < 0.001$). Unlike the situation in the brain, the level of liver MT-I and MT-II mRNA expression was similar in uninjured wild type and MT-I/II$^{-/-}$ mice. However, at the time points when hepatic MT-I and MT-II mRNA was highly expressed in wild type mice after injury (1-3 DPI), MT-I/II mRNA levels in MT-I/II$^{-/-}$ mice were significantly attenuated. UC1MT ELISA was used to quantify the changes in hepatic MT-I/II protein after brain injury (figure 5.5). The temporal profile of MT-I/II protein expression is shifted such that maximal protein expression occurs much later than maximal MT-I and MT-II mRNA expression. During the experimental period, MT-I/II protein expression was highest at 7 DPI which does not preclude that hepatic MT-I/II expression may increase further at later time-points. These results demonstrate that hepatic MT-I/II protein expression is a late event after brain injury in the present cryolesion model.

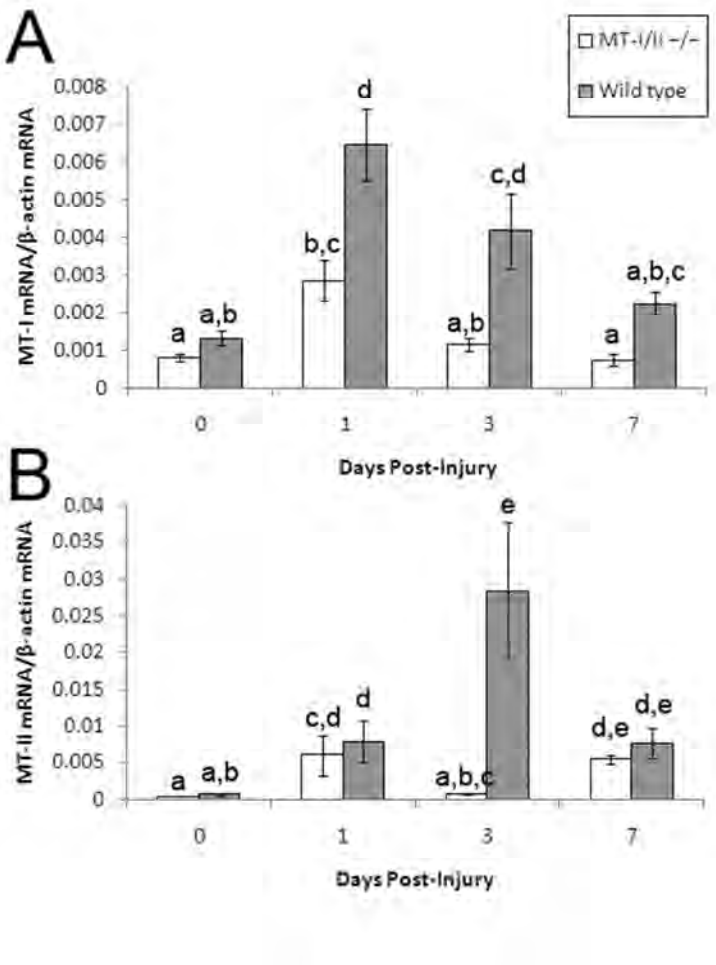

Figure 5.4 Expression of MT-I and MT-II mRNA in the liver of wild type and MT-I/II$^{-/-}$ mice after brain injury was quantified by RT-PCR. (**A**) MT-I mRNA expression showed its greatest increase at 1 DPI and 3 DPI in wild type mice. MT-I mRNA expression also increased in MT-I/II$^{-/-}$ mice at 1 DPI, but not 3DPI and was significantly lower than wild type mice at both 1 and 3 DPI. (**B**) MT-II mRNA was increased at 1 DPI in wild type mice but was at peak levels at 3 DPI. MT-I/II$^{-/-}$ mice were unable to increase MT-II mRNA levels to the same extent as wild type mice at 3 DPI but did have similar levels of MT-II mRNA expression to wild type mice at all other time points. Significant differences were determined by 1-way ANOVA with Tukey's B post-hoc test; groups that share lower case letters are not significantly different from each other (for both graphs; n=6-7, error bars=SEM). These results are representative of a second repeat of this experiment.

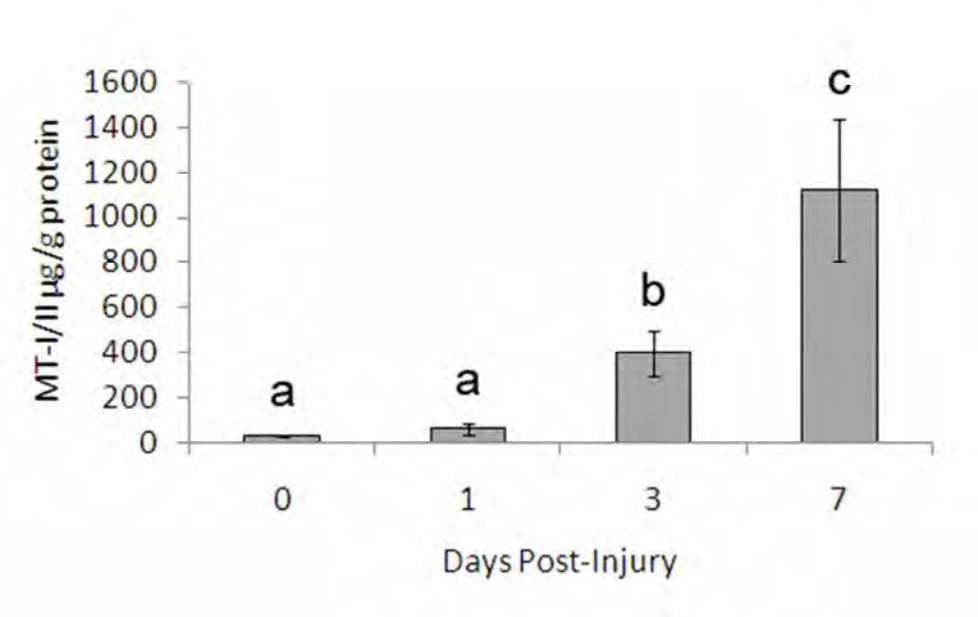

Figure 5.5 Liver MT-I/II protein levels after cryolesion injury to the brain were assayed by UC1MT ELISA in wild type mice. Hepatic MT-I/II protein levels were not increased until 3 DPI and showed a further increase at 7 DPI. Significant differences were determined by 1-way ANOVA with Tukey's B post-hoc test; groups that share lower case letters are not significantly different from each other (n=7, error bars=SEM).

5.3.3 Plasma corticosterone concentration increases after cryolesion brain injury

The glucocorticoid, corticosterone, is the primary stress hormone in rodents, and has an analogous role to cortisol in humans (Sorrells et al. 2009). Corticosterone levels were assayed to determine the potential for glucocorticoid signalling to influence hepatic MT synthesis after brain injury (figure 5.6). 2-way ANOVA revealed no significant difference between plasma glucocorticoid concentrations in wild type and MT-I/II$^{-/-}$ mice at any time point before or after injury. However there were significant changes in corticosterone over time, after injury (figure 5.6A, P(strain) = 0.300, P(time) = 0.002, P(interaction) = 0.260). Figure 5.6B shows the pooled data from both strains of mice which, with twice as many samples per time-point, better demonstrates the changes in corticosterone expression over time. Both cryolesion-injured mice and sham-operated animals have significantly increased plasma corticosterone concentrations compared to uninjured animals but the sham and injured animals were not significantly different at 1 DPI. This indicates that the stress of sham surgery alone is sufficient to increase the plasma corticosterone concentration and that cryolesion to the cortex does not additively increase this. Due to the fact that sham injury induces an increase in plasma corticosterone, sham injury was utilised to assess the ability of glucocorticoids to induce hepatic MT-I/II in the absence of brain injury. Figure 5.7 demonstrates that sham operated animals had no increase in hepatic MT-I mRNA or MT-II mRNA over the seven day experimental period. Therefore, observed increases in plasma corticosterone in the absence of brain injury do not appear to be able to induce hepatic MT-I/II expression.

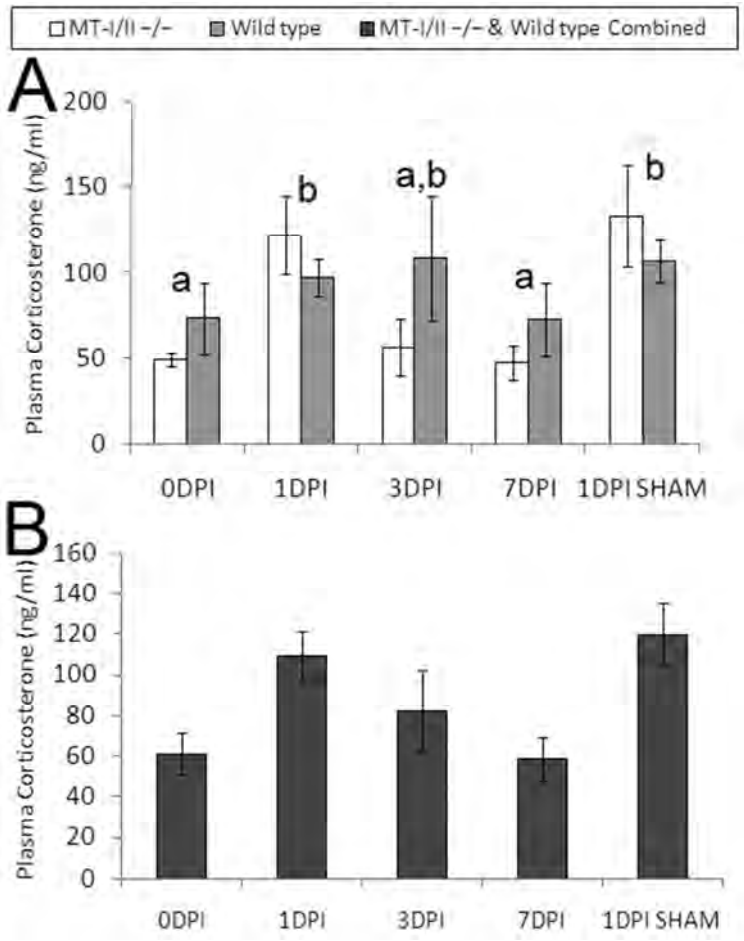

Figure 5.6 Corticosterone concentrations in plasma after cryolesion injury to the brain were assayed by RIA in wild type and MT-I/II$^{-/-}$ mice. Graph (**A**) shows the data separated between wild type and MT-I/II$^{-/-}$ mice. Significant differences were determined by 2-way ANOVA with Tukey's B post-hoc test on the factor of time; groups that share lower case letters are not significantly different from each other (n=5-6, error bars=SEM). No significant differences in plasma corticosterone were found at any time-point between the wild type and MT-I/II$^{-/-}$ strains. Graph (**B**) is an alternative representation of the data set with data for both strains of mice pooled at each time point (n=11-12, error bars=SEM). Plasma corticosterone concentrations are increased equally 1 day after mice receive cryolesion injury or sham surgery.

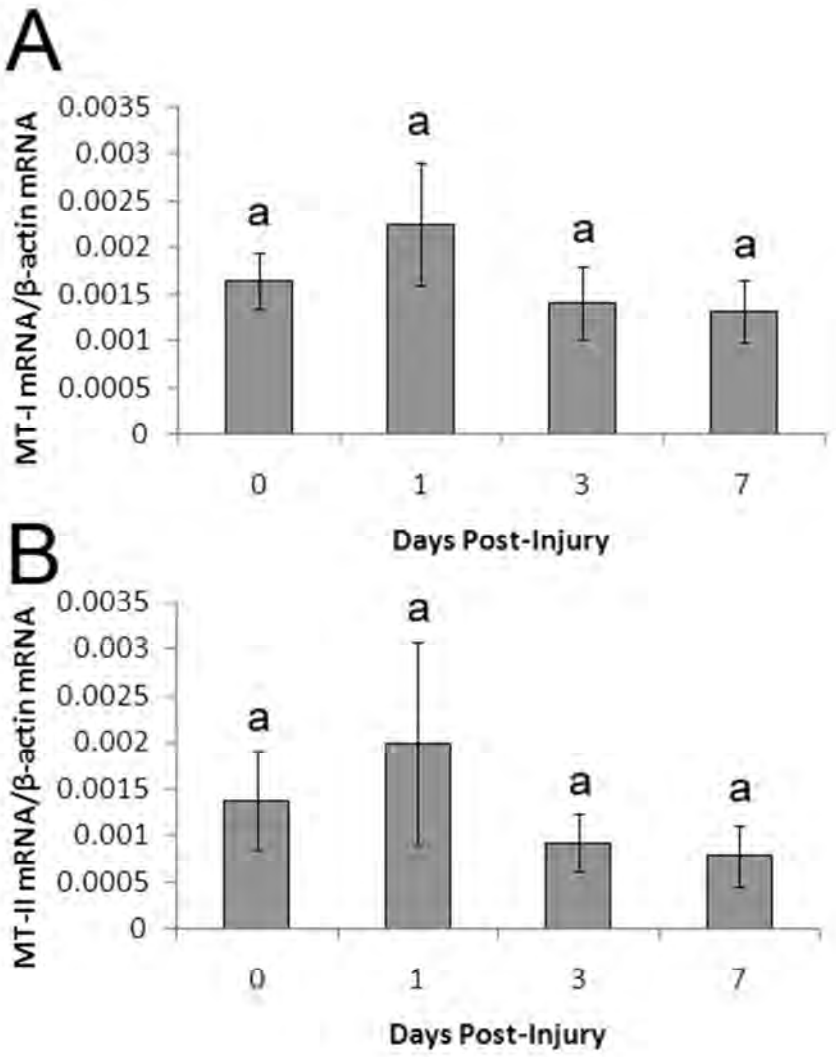

Figure 5.7 Expression of MT-I and MT-II mRNA in the liver of wild type mice after sham surgery was quantified by RT-PCR. Hepatic MT-I mRNA (**A**) and MT-II mRNA (**B**) expression does not change significantly after sham surgery (n=5, error bars=SEM). Significant differences were determined by 1-way ANOVA with Tukey's B post-hoc test; groups that share lower case letters are not significantly different from each other (for both graphs; n=5, error bars=SEM).

5.3.4 Liver zinc post-injury

Liver zinc was assayed by atomic absorption spectroscopy in MT-I/II$^{-/-}$ and wild type mice. Brain injury caused a slight decrease in liver zinc content at 1 and 3 DPI in both strains of mouse (figure 5.8, $P < 0.001$). The liver zinc content in wild type and MT-I/II$^{-/-}$ mice was only significantly different at 7 DPI with liver zinc levels being 15.2% higher in wild type mice, a similar level to that seen in uninjured mice. MT-I/II$^{-/-}$ mice at 7 DPI had a similar zinc content to mice at 1 and 3 DPI. Therefore, the difference in liver zinc content between wild type and MT-I/II$^{-/-}$ mice occurred when hepatic MT-I/II protein levels were highest in wild type mice.

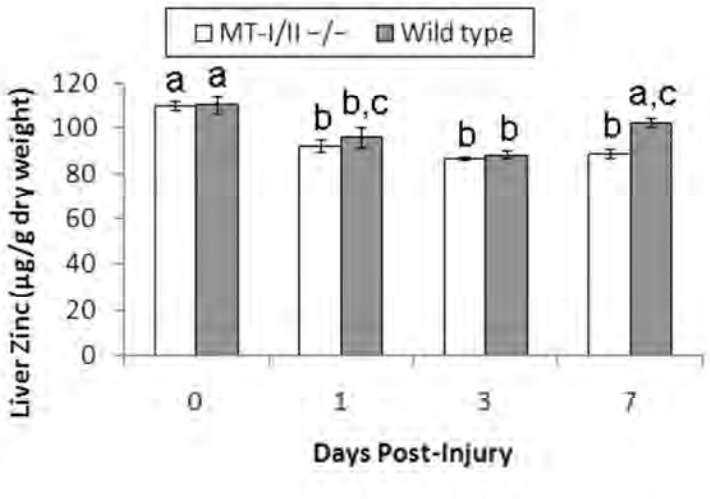

Figure 5.8 Liver zinc content was measured by atomic absorption spectroscopy. Liver Zinc content was decreased in both wild type and MT-I/II$^{-/-}$ mice at 1 and 3 DPI. 1-way ANOVA revealed significantly higher hepatic zinc in wild type than MT-I/II$^{-/-}$ mice at 7 DPI (n=5-6, error bars=SEM). Groups that share lower case letters are not significantly different from each other as determined by Tukey's B post-hoc test on the factor of time after injury.

5.4 Discussion

The data presented here demonstrate that MT-I/II expression is induced, not only in brain following brain injury, but also in the liver. Interestingly, there is a distinct temporal difference between the induction of MT-I/II expression in the brain and liver. In the brain, MT-I/II protein expression is induced rapidly after injury and begins to recede after 24 hours. However, liver MT-I/II protein is maximally induced at later time-points after injury. Maximal hepatic expression of MT-I/II at 7DPI in wild type mice coincided with 15.2% greater liver zinc content compared to MT-I/II$^{-/-}$ mice. This suggests that MT-I/II can participate in regulation of zinc homeostasis when it is expressed in the liver after brain injury. The inability of MT-I/II$^{-/-}$ mice to express hepatic MT-I/II protein after brain injury may affect zinc-dependent processes after brain injury.

5.4.1 Hepatic MT-I/II induction post-brain injury

Increases in intracellular free zinc concentration, glucocorticoid receptor activation and IL-6 mediated STAT3 signalling are the three direct mechanisms that are capable of inducing MT-I/II at the transcriptional level (reviewed by Kimura and Itoh 2008). Intraperitoneal zinc injection has been shown to directly induce hepatic MT-I/II in mice (Coyle et al. 1995, Zhou et al. 2004). Restraint stress in rodents can induce hepatic MT-I/II expression which suggests that glucocorticoids or IL-6 can increase hepatic MT-I/II synthesis independently of zinc (Jacob et al. 1999). IL-6 $^{-/-}$ mice have been shown to be less capable of increasing hepatic MT synthesis in response to restraint stress and the glucocorticoid receptor inhibitor, RU486, can inhibit hepatic MT-I/II synthesis (Hernández et al. 2000). IL-6 $^{-/-}$ mouse studies have also shown that there is a partial requirement for IL-6 in normal MT-I/II induction in the injured CNS (Penkowa et al. 1999c). In chapter 3 of the present thesis, IL-6 mRNA was found to be up-regulated in the injury site after injury but IL-6 protein was not detected in plasma by cytokine assay. Therefore IL-6 may participate in induction of MT-I/II expression in the brain but was not required to induce hepatic MT-I/II synthesis. Many cytokines induce MT-I/II but it is thought that this occurs via stimulation of local IL-6 synthesis in the target tissue (De et al. 1990). In the cryolesion model, plasma cytokine levels were not found to increase consistently and no IL-6 mRNA expression was detectable in the liver of mice after injury which suggests that cytokines were not responsible for the increased liver MT-I/II expression observed after brain injury. Therefore IL-6 does not appear to be required for hepatic MT-I/II expression in mice after cryolesion injury. Notably

however, IL-6 has been shown to increase in human plasma after brain injury (McClain et al. 1991), therefore IL-6 may have the capacity to influence hepatic MT-I/II expression in a clinical setting or in other animal models where plasma IL-6 levels do increase.

Plasma corticosterone concentration was assayed to determine if increases could be responsible to induction of hepatic MT-I/II synthesis. Both cryolesion and sham surgery led to increases of corticosterone to equivalent levels, in both conditions. The fact that sham surgery was incapable of inducing liver MT-I/II despite the fact that corticosterone was increased suggests that corticosterone alone is not responsible for inducing hepatic MT-I/II expression. It warrants mention that corticosterone can enhance zinc mediated increases in MT synthesis in hepatocytes *in vitro* (Coyle et al. 1993) which implies that the increased plasma corticosterone concentrations after cryolesion injury could enhance the pre-existing expression of hepatic MT-I/II. Pharmacological corticosterone administration has been shown to induce MT synthesis in the brain (Beltramini et al. 2004) therefore it is possible that corticosterone, and IL-6, play a role in MT-I/II expression in the brain injury site. In the present model, IL-6 was found to be unlikely to play a role in hepatic MT-I/II induction and increased corticosterone alone does not lead to increased hepatic MT-I/II levels but an enhancing role of corticosterone on hepatic MT-I/II transcription can not be excluded without pharmacological inhibition of the glucocorticoid receptor. An interesting possibility is that the changes in MT-I and MT-II mRNA levels arise due to differences in mRNA stability. A combination of changes in mRNA stability and mRNA expression may account for the fact that maximal MT-I and MT-II mRNA levels precede maximal MT-I/II protein levels in the liver post-brain injury.

5.4.2 Hepatic MT-I/II and zinc homeostasis

Changes in zinc homeostasis are difficult to observe *in vivo* due to the diverse range of molecules that bind zinc within an organism. To further complicate matters, increases in free zinc are rapidly rectified by MT-I/II expression which in turn, is induced by free zinc itself. For this reason, altered zinc homeostasis was not directly assessed in the present study. The induction of liver MT-I and MT-II mRNA was rapid, occurring within 24 hours of injury, hence a rapid process is required for the zinc mediated induction of liver MT-I/II to be possible. Oxidative stress is one rapidly occurring process that can displace zinc from metalloproteins, effectively increasing the free zinc concentration inside the affected cell which initiates MT-I/II transcription (Giles et al.

2002). Head injury to rats has been shown to induce a whole body oxidative stress within 15 minutes of the injury (Shohami et al. 1999) which may represent a rapid method by which zinc homeostasis is altered in non-CNS organs after brain injury. In addition to a rapid change in zinc homeostasis, a prolonged change in zinc homeostasis is also required to explain the maximal expression of MT-II mRNA at 3 DPI. It has been proposed that the hypermetabolic and hypercatabolic state that is induced by brain injury is responsible for release of zinc from muscle breakdown (McClain et al. 1986). In the present study, the decreases in hepatic zinc levels after injury are evidence of altered zinc homeostasis because for zinc to leave the liver it must first transition from protein or membrane associated zinc to free zinc before it can be transported out of cells and into circulation. Therefore, this increase in cytoplasmic free zinc may be responsible for the induction of hepatic MT-I/II after brain injury.

5.4.3 MT-I/II expression may be self-regulated

In the present study, MT-I/II$^{-/-}$ mice had lower levels of MT-I and MT-II mRNA transcripts in the brain than wild type mice when at basal levels but were able to mount a normative MT-I and MT-II expression profile in response to brain injury. The inverse was true in the liver with MT-I/II$^{-/-}$ mice having similar levels of MT-I and MT-II mRNA to wild type mice when at basal expression levels but MT-I/II$^{-/-}$ mice were unable to mount the same response to injury as wild type mice. Therefore it is possible that the presence of MT-I/II protein has an auto-regulatory effect upon the level of MT-I and MT-II mRNA expression. MT-I/II, itself represents a source of protein bound zinc that can be liberated by oxidative stress and has been shown to be responsible for zinc release when nitric oxide levels increase (Khatai et al. 2004, Spahl et al. 2003). MT-I/II has also been shown to donate or remove zinc molecules to, and from, zinc-dependent enzymes (Jacob et al. 1998, Maret et al. 1999, Krężel and Maret 2008) or transcription factors (Zeng et al. 1991), affecting their activity. MT-I/II expression has been shown to inhibit the zinc-mediated activation of the transcription factor NF-κB (Kim et al. 2003). Hence MT-I/II may be able to buffer zinc availability to metalloproteins or affect transcription factor activity. It is interesting that the relationship between the quantity of MT-I/II protein being expressed and the expression of MT-I and MT-II mRNA in MT-I/II$^{-/-}$ mice is inverted in the brain and liver. It is possible that zinc trafficking is very different in the two organs which may affect how zinc is utilised to regulate MT-I/II induction.

One caveat in the use of MT-I/II$^{-/-}$ mice to study MT-I/II self-regulation is that while the MT-I/II$^{-/-}$ mice do produce MT-I and MT-II transcripts, these have been altered due to the inserts that produce the premature stop codons (Masters et al. 1994). Processes known collectively as nonsense-mediated mRNA decay exist to remove abnormal transcripts (reviewed by Amrani et al. 2006) which may explain reduced MT-I and MT-II mRNA levels in MT-I/II$^{-/-}$ mice. However the fact that lowered MT-I and MT-II mRNA levels in MT-I/II$^{-/-}$ mice only occurs under certain conditions argues against a non-specific degradation of the transgenic MT-I and MT-II mRNAs which would be expected to occur continuously as a part of normal transcriptome maintenance.

5.4.4 Zinc homeostasis post-brain injury

More than two decades ago, McClain et al. (1986) observed decreases in plasma zinc and activation of the acute phase response occurring simultaneously after head injury. It was later postulated that the activation of the acute phase response lead to hepatic MT-I/II up-regulation which was the cause of decreased plasma zinc concentration (Ott et al. 1994). In principle the up-regulation of hepatic MT-I/II has the ability to sequester free zinc from plasma (Cho et al. 2004, Coyle et al 1995, Ding et al. 2002, Philcox et al. 1995, Zhou et al. 2003). However whether this occurs after brain injury had never been tested experimentally, to the best of my knowledge. The current findings indicate that while hepatic MT-I and MT-II mRNA levels increase within 24 hours of brain injury, significant increases in protein occur from 3 to 7 DPI and possibly at later time-points that were not assayed in this study. The highest hepatic MT-I/II protein concentration coincided with a higher liver zinc content in wild type mice compared to MT-I/II$^{-/-}$ mice which occurred at 7 DPI. Previously, Coyle et al. (1995) demonstrated that wild type mice injected intraperitoneally with zinc sulphate have a 60% increase in hepatic zinc content within 16 hours whereas MT-I/II$^{-/-}$ mice injected with zinc have no change in hepatic zinc content, meanwhile plasma zinc levels and urinary excretion of zinc were higher in MT-I/II$^{-/-}$ mice. By comparison, the difference in zinc content in the liver of MT-I/II$^{-/-}$ mice and wild type mice after brain injury was smaller in magnitude but it should be noted that no exogenous zinc apart from the normal dietary zinc was being introduced into the animal's system. Therefore, hepatic sequestration of zinc in wild type mice may be having significant effects on the labile zinc pool of the animal after brain injury. Therefore zinc dependent processes may differ in wild type and MT-I/II$^{-/-}$ mice at 7 DPI. Increases in urinary excretion of zinc with the passage of time after brain injury has been observed previously (McClain et al. 1986) and may explain the decreases we observed in hepatic zinc after brain injury. To investigate the effect of

MT-I/II on zinc homeostasis after brain injury further, more information is required in regard to zinc availability in cells and plasma and zinc excretion/secretion after brain injury. A major question to be answered is what causes zinc homeostasis to change after brain injury?

5.4.5 Conclusion

This study demonstrates that MT-I/II is induced in the liver after brain injury. The factor that induces hepatic MT-I/II was not identified but IL-6 does not appear to be required and corticosterone alone is insufficient. Therefore a zinc-mediated mechanism appears likely and a component of the observed response may reflect MT-I/II protein regulating the expression of its own gene, indirectly via localised changes in zinc concentration. The data presented here demonstrate not only that MT-I/II can be induced in a non-CNS organ after brain injury, but also that MT-I/II has the potential to influence zinc homeostasis in the entire organism. Future study is required to determine if hepatic MT-I/II expressed after brain injury alters zinc homeostasis in a feedback manner that affects the progression of brain injury.

Chapter 6 – Age-dependent changes to the blood of the MT-I/II$^{-/-}$ mouse

6.1 Introduction

The following chapter describes an interesting and unexpected finding that arose during the study of MT-I/II in brain injury. During haematological analysis of leukocytes after brain injury, it was found that there are some differences in the red blood cell numbers of MT-I/II$^{-/-}$ mice in comparison to wild type mice. These findings are interesting because the fact that the absence of MT-I/II affects erythrocyte numbers is suggestive of a specific zinc regulatory role of MT-I/II *in vivo*.

Erythropoiesis is the process by which erythrocytes are produced and is a divergent branch of the haematopoiesis that occurs in the bone marrow. Hematopoietic stem cells give rise to all of the various types of blood cells. Erythropoiesis requires the differentiation of hematopoietic stem cells into erythroid progenitor cells. Erythroid progenitor cells undergo several stages of differentiation before they give rise to the erythroblasts that, through further stages of differentiation, produce circulating erythrocytes (reviewed by Testa et al. 2004). One of the final steps in the development of an erythrocyte before it enters circulation is the enucleation of the cell which signifies the cessation of protein synthesis for the rest of the erythrocyte life span. The remnants of ribosomal RNA in newly formed erythrocytes can still be found in the cytoplasm for 1-2 days after enucleation and this property is used to identify the very young erythrocytes which are known as reticulocytes. In humans the mean life span of an erythrocyte is 120 days but in mice the mean erythrocyte life-span is a much shorter 50 days (Saxena & Khandelwal 2009). Erythropoiesis occurs continuously to replace aging erythrocytes which are constantly being removed from circulation by phagocytic splenic macrophages (Bennet and Kay 1981). The main mechanism by which erythropoiesis is regulated is by the production of the cytokine erythropoietin which is produced in the kidneys and to a lesser extent in the liver and its secretion is up-regulated under hypoxic conditions (reviewed by Moritz et al. 1997).

Erythropoietin is primarily released from the kidneys to stimulate erythropoiesis in bone marrow. Erythropoietin has been shown to induce MT synthesis in an erythroleukemic cell line (Abdel-Mageed et al. 2003) and in human cord blood precursor cells (Rahman and De Ley 2001), suggesting a role for MT in erythropoiesis. MT is inducible in red blood cell (RBC) precursor cells upon zinc treatment (Rahman et al. 2000). Deficiency of zinc, the main physiological ligand of MT-I/II, leads to a decrease in erythrocyte formation in rats (Hendy et al. 2001, Morgan et al. 1995). Deficiency of copper,

another physiological ligand of MT-I/II, often leads to anaemia and neutropenia indicating that copper has a role in haematopoiesis (reviewed by Danks 1988, Mually et al. 2004). Erythrocytes express several zinc transporters that are regulated according to nutritional zinc levels (Ryu et al. 2008), presumably to maintain constant zinc concentrations, suggesting that zinc is not only important for erythropoiesis, but that an optimal zinc level exists. The ability of MT to bind to zinc and copper may be a further mechanism to maintain zinc levels during the development of erythrocytes.

MT-I/II$^{-/-}$ mice have been shown to have a greater susceptibility to cadmium induced anaemia than wild type mice but there was no difference in erythrocyte numbers or haemoglobin content in control mice from both strains (Liu et al. 1999). In this chapter an age-dependent decrease in blood haemoglobin content is identified in MT-I/II$^{-/-}$ mice. MT-I/II$^{-/-}$ mice that were the same age as those used in the study by Liu et al. (1999) were not substantially different to wild type mice in their blood parameters. However, there was an age-dependent decrease in haemoglobin levels in wild type and MT-I/II$^{-/-}$ mice that affected MT-I/II$^{-/-}$ mice at a younger age. Zinc sulphate was administered to young wild type and MT-I/II$^{-/-}$ mice to investigate the plausibility of the hypothesis that a zinc-dependent mechanism was involved.

6.2 Materials and Methods

6.2.1 Animals

129SI/SvImJ mice and 129S7/SvEvBrd-*Mt1*^{tm1Bri} *Mt2*^{tm1Bri}/J (Masters et al. 1994) were housed as detailed in chapter 2. For the first experiment male mice of each strain were used and were 6 months of age at time of sampling (n=6). The mice received no experimental treatment in this experiment. In the second experiment 3 month-old male mice from each strain were given either no treatment or were injected with 5 micrograms of zinc (as zinc sulphate) per gram of body weight each day for five successive days (n=5). A saline injection was not used because of the potential to cause stress that could lead to induction of hepatic MT-I/II in the wild type mice. For the third experiment only female mice were available at an age above 1 year. Female mice from both strains were from 13 to 16 months of age and received no experimental treatment before blood sampling (n=6).

6.2.2 Haematological analysis

Blood was obtained by cardiac puncture with syringes containing EDTA (3 mg per ml of blood). From each animal, 250 µl whole blood was analysed in an Advia 120 haematological analyser (Siemens). A list of the blood parameters and their abbreviations can be found in table 6.1.

6.2.3 Zinc analysis of hepatic zinc

Liver zinc content was analysed in 3 month old mice treated with or without zinc by atomic absorption spectroscopy according to the methods outlined in chapter 5.

6.2.4 Giemsa staining of blood smears.

Blood collected by cardiac puncture with syringes containing EDTA was smeared onto microscope slides and allowed to dry. The dry blood smear was fixed with a few drops of methanol which were allowed to dry. The fixed slides were stained in Giemsa stain for 10 minutes then were rinsed in tap water and allowed to dry. Di-N-Butylphthalate in xylene was used to mount coverslips onto the slides.

6.3 Results

6.3.1 Differences in blood between 6 month-old wild type and MT-I/II$^{-/-}$ mice

At 6 months of age MT-I/II$^{-/-}$ mice had 12% fewer red blood cells (RBCs) and 27% fewer reticulocytes in circulation compared to wild type mice (Table 6.1). In MT-I/II$^{-/-}$ mice, the decrease in reticulocyte count as a percentage of all RBCs is greater than the decrease in RBCs alone which determines that reduction in reticulocytes is greater than the reduction in mature RBCs. Consistent with these observations, haematocrit and blood haemoglobin were also lower in MT-I/II$^{-/-}$ mice compared to wild type mice.

On an individual cell basis, RBCs from MT-I/II$^{-/-}$ mice were slightly macrocytic with a 5% increase in mean corpuscular volume (MCV). Corpuscular haemoglobin (CH) was increased in MT-I/II$^{-/-}$ mice but the mean corpuscular haemoglobin concentration (MCHC) measure, which takes cell size into account indicates that the difference in CH between wild type and MT-I/II$^{-/-}$ mice is due to increased MCV in MT-I/II$^{-/-}$ mice. There was no difference in haemoglobin distribution width (HDW) between RBCs from either strain indicating haemoglobin concentration per cell was relatively constant between the RBCs of each strain. However the red cell volume distribution width (RDW) of MT-I/II$^{-/-}$ mice was 4% higher than in wild type mice indicating a slight anisocytosis.

Table 6.1 Blood parameters from 6 month-old wild type and MT-I/II$^{-/-}$ mice. Statistically significant differences were determined by Student's t-test. P-value ranges are denoted by the following symbols; (*) $p<0.05$, (**) $p<0.01$, (***) $p<0.001$. Data are expressed as the mean of the group (n=6) ± SEM.

Parameter	Abbreviation	MT-I/II$^{-/-}$	Wild type
Red Blood Cell Count (x10^{12} cells/L)	RBC	9.73 ± 0.13***	11.04 ± 0.24
Reticulocyte Count (x10^{9} cells/L)	Retic#	197.9 ± 19.4**	270.3 ± 9.2
Percent Reticulocytes (%)	%Retic	2.028 ± 0.182*	2.456 ± 0.050
Haemoglobin (g/L)	HGB	146.2 ± 1.5**	157.6 ± 3.1
Haematocrit (L/L)	HCT	0.492 ± 0.004**	0.536 ± 0.010
Mean Corpuscular Volume (fL)	MCV	50.68 ± 0.48**	48.48 ± 0.18
Mean Corpuscular Haemoglobin (pg)	MCH	15.02 ± 0.16**	14.3 ± 0.09
Mean Corpuscular Haemoglobin Concentration (g/L)	MCHC	296.6 ± 1.0	295.2 ± 2.63
Cellular Haemoglobin Concentration Mean (g/L)	CHCM	277.8 ± 1.6	276.8 ± 2.1
Corpuscular Haemoglobin (pg)	CH	14.08 ± 0.6**	13.42 ± 0.07
Reticulocyte Haemoglobin Content (pg)	CHr	16.18 ± 0.16**	15.56 ± 0.07
Red Cell Volume Distribution Width (%)	RDW	12.66 ± 0.23*	12.16 ± 0.06
Haemoglobin Distribution Width (g/L)	HDW	14.08 ± 0.18	14.42 ± 0.19
White Blood Cell Count (x10^{9} cells/L)	WBC	2.56 ± 0.36	2.9 ± 0.11
Platelet Count (x10^{9} cells/L)	PLT	1025.6 ± 29.8	1043.8 - 36.3
Mean Platelet Volume (fL)	MPV	5.18 ± 0.16	5.14 ± 0.26

6.3.2 Differences in blood between 3 month-old wild type and MT-I/II$^{-/-}$ mice

A second experiment was devised to test the effect of altering zinc levels in the mice to assess the impact on erythrocytes. However, in the control animals of this experiment, there were no differences in red blood cell counts, reticulocyte counts or haemoglobin levels between wild type and MT-I/II$^{-/-}$ mice (Table 6.2). The obvious difference between this experiment and the previous experiment is that the mice were 3 months younger in the second experiment. There were some minor differences between the strains in the second experiment in that wild type mice had significantly smaller mean RBC cell volume and consequently, a lower corpuscular haemoglobin content reading. Wild type mice also had a higher HDW and RDW indicating a greater degree of variability in erythrocyte volume and haemoglobin content per RBC than MT-I/II$^{-/-}$ mice. None of these parameters in wild type mice were altered by the zinc injection treatment. Overall, the differences in untreated 3 month old wild type and MT-I/II$^{-/-}$ mice were not substantially different and ultimately, the quantity of circulating haemoglobin was equivalent in the two strains.

Zinc sulphate was injected intraperitoneally into wild type and MT-I/II$^{-/-}$ mice over 5 days to determine if zinc challenge would alter the blood parameters in MT-I/II$^{-/-}$ mice and wild type mice differentially. It is interesting to note that the liver zinc content was not different between wild type and MT-I/II$^{-/-}$ mice and was not increased after 5 days of zinc injections (figure 6.1). Despite the lack of differences between 3 month-old MT-I/II$^{-/-}$ and wild type control mice, MT-I/II$^{-/-}$ mouse blood had a decrease in RBC count and haemoglobin levels after zinc treatment that did not occur in zinc-treated wild type mice. Interestingly, there was a significant effect of the zinc treatment in decreasing haematocrit from both strains of mice. The decrease in haematocrit was larger in zinc injected MT-I/II$^{-/-}$ mice but was not significantly different from zinc injected wild type mice. Zinc also caused a decrease in the platelet cell volume in both MT-I/II$^{-/-}$ and wild type mice without affecting absolute platelet number.

One of the more profound changes that occurred after zinc administration was the increase in the number of circulating leukocytes. This affect occurred in both wild type and MT-I/II$^{-/-}$ mice indicating that the response was zinc-dependent but MT-I/II-independent. Analysis of the various leukocyte subtypes however, did not reveal any significant changes in the relative % of each subtype (Table 6.3). This suggests that all sub-sets of leukocytes, except monocytes, are increasing in the blood simultaneously to

cause the increase in total blood leukocyte count. In addition to the effects of zinc treatment, MT-I/II$^{-/-}$ mice were found to have a lower percentage of neutrophils and higher percentage of circulating lymphocytes than wild type mice, an effect that was zinc-independent. These data demonstrate that zinc administration can affect several aspects of the blood cell populations. However, the only factors that were dependent on the ability to synthesise MT-I/II and increased zinc levels were those related to the number of red blood cells.

Table 6.2 Blood parameters from 3 month-old wild type and MT-I/II$^{-/-}$ mice. Mice were either untreated or were injected with zinc for 5 days before blood sampling. Statistically significant effects were determined by 2-way ANOVA on the factors of mouse strain and experimental treatment. For parameters with a significant interaction term, 1-way ANOVA with Tukey's B post-hoc test was conducted to determine significant differences. Groups that share the superscripts (a) and (b) or (*) and (†) are not significantly different from each other. Data are expressed as the mean of the group (n=5) ± SEM.

Parameter	Control		Zinc Injected		P-Value
	MT-I/II$^{-/-}$	Wild type	MT-I/II$^{-/-}$	Wild type	
WBCs	2.96 ± 0.34†	3.08 ± 0.57†	4.26 ± 0.38*	4.52 ± 0.39*	0.002
RBCs	10.37 ± 0.12^{a}	10.56 ± 0.16^{a}	9.56 ± 0.13^{b}	10.42 ± 0.12^{a}	< 0.001
Retic#	199.04 ± 27	223.32 ± 20	226.78 ± 15	205.32 ± 15	0.629
%Retic	1.92 ± 0.26	2.12 ± 0.19	2.37 ± 0.15	1.97 ± 0.15	0.298
HGB	158.8 ± 2.9^{a}	157.0 ± 2.9^{a}	140.6 ± 5.4^{b}	152.2 ± 0.7^{a}	0.003
HCT	0.542 ± 0.008†	0.54 ± 0.011†	0.502 ± 0.005*	0.522 ± 0.004*	0.001
MCV	52.26 ± 0.75†	51.16 ± 0.61*	52.26 ± 0.32†	49.94 ± 0.40*	0.003
MCH	15.34 ± 0.22	14.9 ± 0.18	14.74 ± 0.64	14.62 ± 0.151	0.428
MCHC	293.8 ± 1.0	291 ± 1.5	281.8 ± 10.6	292.6 ± 0.8	0.318
CHCM	281 ± 1.3	279.6 ± 0.7	279.6 ± 1.0	280.4 ± 0.8	0.623
CH	14.7 ± 0.16†	14.28 ± 0.14*	14.6 ± 0.08†	13.98 ± 0.10*	<0.001
CHr	15.92 ± 0.07	15.88 ± 0.10	15.88 ± 0.11	15.64 ± 0.10	0.146
RDW	11.76 ± 0.09^{a}	12.7 ± 0.27^{b}	12.38 ± 0.12^{a,b}	12.08 ± 0.21^{a,b}	0.007
HDW	14.92 ± 0.20†	15.28 ± 0.22*	14.88 ± 0.07†	15.56 ± 0.26*	0.010
PLT	804.0 ± 23	856.4 ± 40	810.4 ± 27	782.4 ± 40	0.377
MPV	5.00 ± 0.04†	5.12 ± 0.08†	4.88 ± 0.02*	4.96 ± 0.06*	0.011

Table 6.3 Circulating leukocyte percentages in 3 month-old wild type and MT-I/II$^{-/-}$ mice. Mice were either untreated or were injected with zinc for 5 days before blood sampling. Statistically significant effects were determined by 2-way ANOVA on the factors of mouse strain and experimental treatment. Groups that share the superscripts (*) and (†) are not significantly different from each other. Data are expressed as the mean of the group (n=5) ± SEM.

% Leukocytes	Control		Zinc Injected		P value
	MT-I/II$^{-/-}$	Wild type	MT-I/II$^{-/-}$	Wild type	
Neutrophils	12.98 ± 0.44†	20.14 ± 2.34*	16.18 ± 1.02†	19.38 ± 0.96*	0.001
Lymphocytes	78.98 ± 0.99*	72.46 ± 2.71†	77.3 ± 2.07*	74.16 ± 1.02†	0.010
Monocytes	5.32 ± 0.67†	4.8 ± 0.57†	3.34 ± 0.70*	3.48 ± 0.31*	0.006
Eosinophils	2.34 ± 0.22	2.16 ± 0.45	2.68 ± 0.40	2.66 ± 0.31	0.601
Basophils	0.16 ± 0.04	0.18 ± 0.02	0.22 0.07	0.14 ± 0.08	0.710

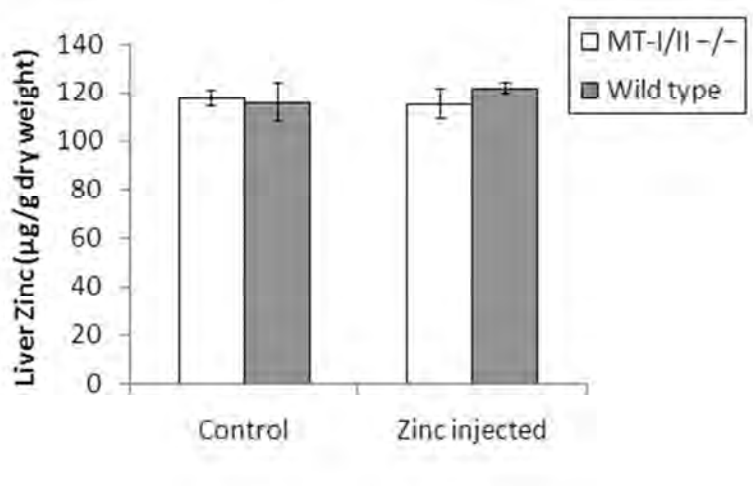

Figure 6.1 Hepatic zinc content after 5 days of zinc injections in 3 month-old wild type and MT-I/II$^{-/-}$ mice as determined by atomic absorption spectroscopy (n=5, error bars = SEM). No statistically significant differences were obtained by 2-way ANOVA on the factors of mouse strain and experimental treatment.

6.3.3 Differences in blood between 1 year-old wild type and MT-I/II$^{-/-}$ mice

To further investigate the effect of age on blood haemoglobin content in MT-I/II$^{-/-}$ mice, blood was analysed from wild type and MT-I/II$^{-/-}$ mice that were older than 1 year of age. Female MT-I/II$^{-/-}$ mice that were around 1 year of age were not significantly different from age-matched female wild type mice on any of the blood parameters measured except for CHCM (Table 6.4). Comparison of the changes in erythrocyte number and blood haemoglobin content over time reveals that age causes a decrease in both parameters in both mouse strains (figure 6.2). However the difference between MT-I/II$^{-/-}$ and wild type mice lies in the age at which erythrocyte numbers and blood haemoglobin content decreases. Both parameters are already decreased in MT-I/II$^{-/-}$ mice by 6 months of age whereas they are not decreased in wild type mice until some point between 6 and 12 months of age. In wild type mice there is a slight increase in erythrocyte counts from 3 to 6 months of age but the key factor that determines the capacity of the blood to transport oxygen is haemoglobin content which is stable over the 3 to 6 month period. At 3 months of age MT-I/II$^{-/-}$ mice have normal haemoglobin levels compared to wild type mice but by 6 months of age this value is reduced to a level only found in wild type mice when they are around 1 year of age. The MHCH values, which are a measure of cellular haemoglobin content standardised for cell size, are similar for mice of both strains at all ages (Tables 6.1, 6.2, 6.4). Morphologically there were no differences between erythrocytes and reticulocytes from wild type and MT-I/II$^{-/-}$ mice at 3 months of age and 1 year of age (figure 6.3). There was also no difference in morphology of erythrocytes or reticulocytes after zinc treatment in either wild type or MT-I/II$^{-/-}$ mice.

Table 6.4 Blood parameters from 1 year-old wild type and MT-I/II$^{-/-}$ mice. Statistically significant differences were determined by Student's t-test. P-value ranges are denoted by the following symbols; (*) $p<0.05$, (**) $p<0.01$, (***) $p<0.001$. Data are expressed as the mean of the group (n=6) ± SEM.

Parameter	MT-I/II$^{-/-}$	Wild type
WBC	2.97 ± 0.13	3.60 ±0.51
RBC	9.93 ± 0.24	10.30 ± 0.14
Retic#	191.7 ± 16.1	177.9 ± 14.9
Retic%	1.95 ± 0.22	1.73 ± 0.16
HGB	142.8 ± 5.0	145.8 ± 2.6
HCT	0.50 ± 0.01	0.51 ± 0.01
MCV	50.3 ± 0.486	49.1 ± 0.433
MCH	14.40 ± 0.22	14.15 ± 0.14
MCHC	285.5 ± 1.3	288.7 ± 1.0
CHCM	273.8 ± 0.6 ***	278.8 ± 1.1
CH	13.78 ± 0.14	13.65 ± 0.10
CHr	15.43 ± 0.22	15.47 ± 0.10
RDW	13.28 ± 0.44	12.98 ± 0.26
HDW	16.53 ± 0.61	15.85 ± 0.18
PLT	820.5 ± 29.4	936.17 ± 80.5
MPV	5.17 ± 0.09	5.68 ± 0.30

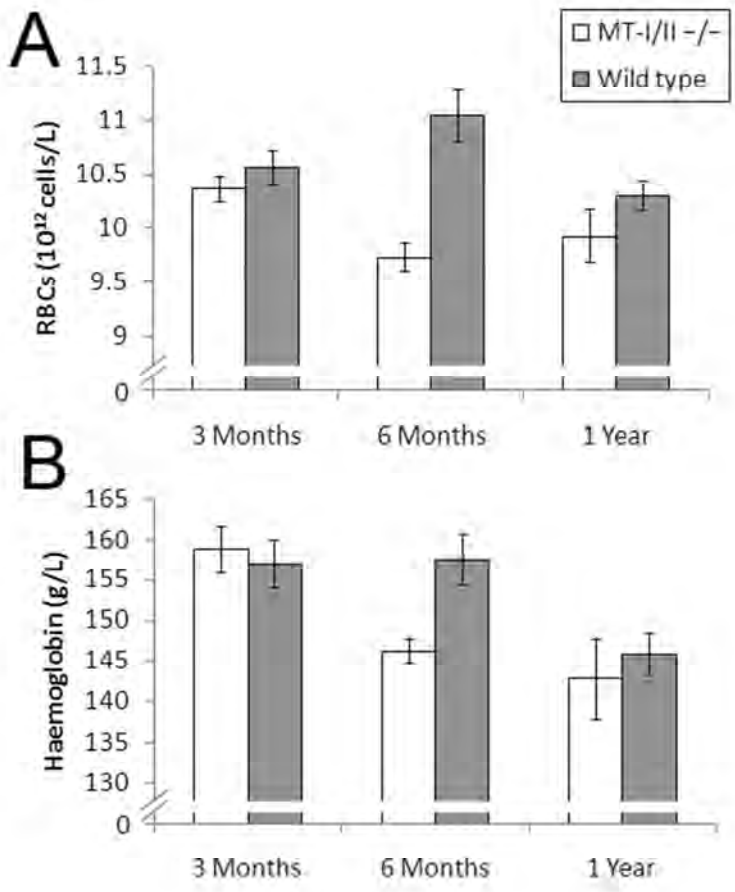

Figure 6.2 Changes in RBC counts (**A**) and blood haemoglobin content (**B**) in wild type and MT-I/II$^{-/-}$ mice with age. RBC counts and blood haemoglobin content decrease in both groups with age but the decreases occur earlier in MT-I/II$^{-/-}$ mice than wild type mice. To generate these graphs data were compiled from all three experiments (n=5-6, error bars = SEM).

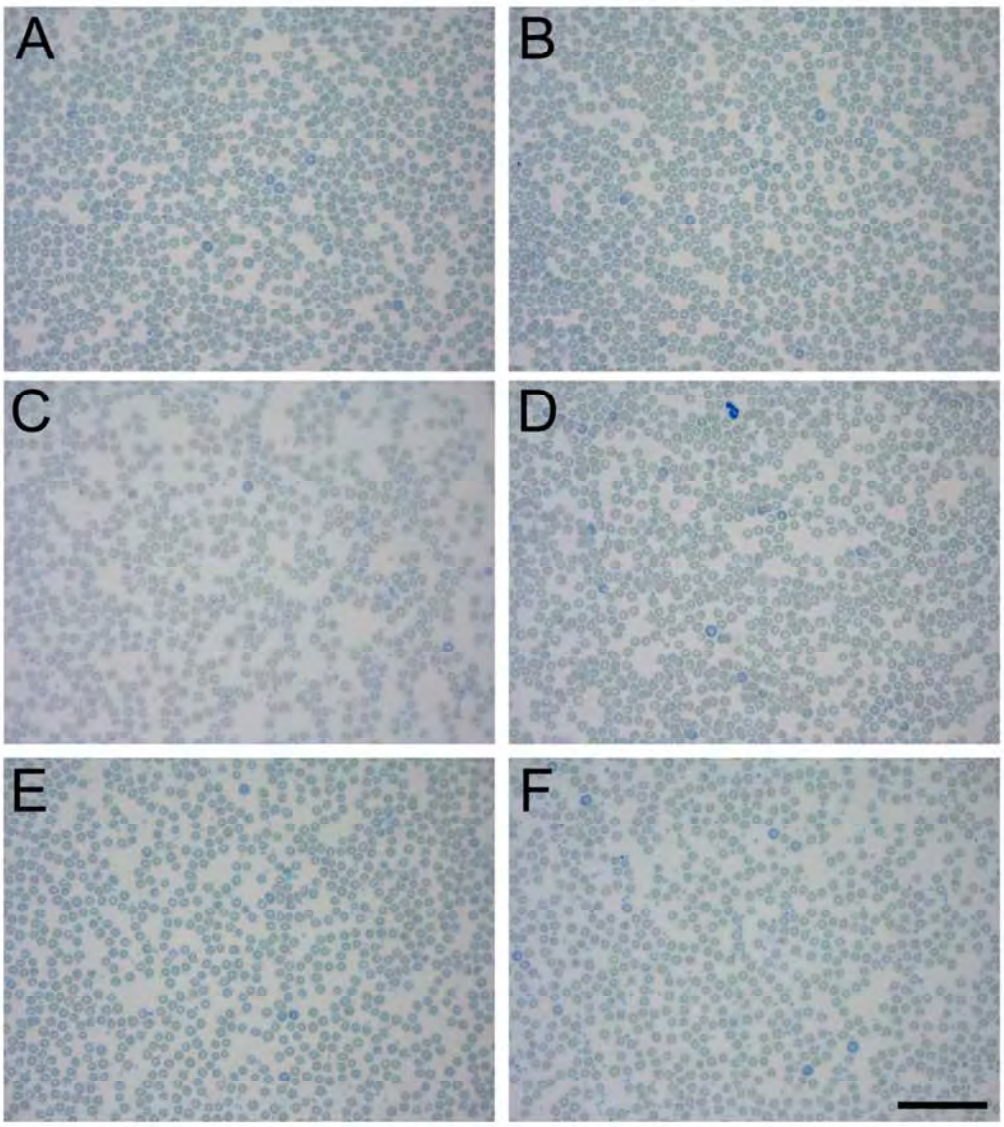

Figure 6.3 Giemsa stain of blood smears of wild type and MT-I/II$^{-/-}$ blood were assessed for differences in cellular morphology of erythrocytes (lightly stained enucleated cells) and reticulocytes (dark blue enucleated cells). Blood from untreated 3 month-old wild type mice (**A**), untreated 3 month-old MT-I/II$^{-/-}$ mice (**B**), zinc treated 3 month-old wild type mice (**C**), zinc treated 3month-old MT-I/II$^{-/-}$ mice (**D**), untreated 1 year-old wild type mice (**E**) and untreated 1 year-old MT-I/II$^{-/-}$ mice (**F**) revealed no overt differences. Images are representative of each experimental group, scale bars=50 μm.

6.4 Discussion

The results presented herein demonstrate an age-dependent decrease in red blood cells and blood haemoglobin content in MT-I/II$^{-/-}$ mice that is accelerated compared to wild type mice. The fact that the reticulocytes, the more immature blood cells, showed the greatest decrease in number, suggests that erythropoiesis is the process affected by the absence of MT-I/II as the animals age. Younger MT-I/II$^{-/-}$ mice did not show a decrease in RBCs and haemoglobin relative to young wild type mice but systemic administration of zinc was able to recapitulate the anaemia observed in older MT-I/II$^{-/-}$ mice. The fact that wild type mice were protected from zinc-mediated decreases in blood haemoglobin and RBC numbers suggests that MT-I/II plays a role in zinc homeostasis in a manner that is important for normal blood function. Increases in the circulating leukocyte counts caused by zinc treatment is also of interest because it mimics the effect observed in MT-I/II$^{-/-}$ mice, 7 days after cryolesion brain injury (see chapter 3).

6.4.1 Zinc and erythropoiesis

Several lines of evidence suggest that zinc is important for erythropoiesis. Zinc deficiency in rats has been shown to cause a decrease in erythrocyte formation or blood haemoglobin content (Hendy et al. 2001, Morgan et al. 1995) hence it can be inferred that zinc is necessary for erythropoiesis. The zinc efflux transporter, ZnT1 and the zinc influx transporters, Zip8 and Zip10 were demonstrated by Ryu et al. (2008) to be expressed on erythrocytes. The results of this study also suggested that erythrocyte precursor cells vary zinc transporter expression to maintain an optimal zinc concentration. Because erythrocytes are enucleated cells, the proteins that they carry are indicative of the protein expression that was occurring during erythropoiesis, suggesting that zinc regulatory mechanisms are occurring at the erythroblast stage. When zinc supplementation was administered to humans it led to increases in MT-I/II in erythrocytes and MT-I/II was shown to have a very short half-life in circulating erythrocytes (Grider et al. 1990). MT-I/II is not taken up by erythrocytes (Tanaka et al. 1985) hence MT-I/II is probably exerting effects in erythroblasts or early in the RBC life span, rather than in mature erythrocytes. Indeed, MT-I/II expression increases in an erythroleukemic cell line treated with erythropoietin (Abdel-Mageed et al. 2003), which demonstrates that MT-I/II is up-regulated in conjunction with erythropoiesis. It is possible that MT-I/II has a zinc sequestering role that maintains the cellular zinc content required for erythropoiesis. This is supported by rapid zinc and MT-I/II accumulation

in the bone marrow of rats after acute blood loss or phenylhydrazine-induced anaemia, two conditions that stimulate erythropoiesis (Huber and Cousins 1993).

In the present study, it was interesting to find that there was no difference in the reticulocyte numbers after zinc administration in wild type and MT-I/II$^{-/-}$ mice. It has previously been shown that a single zinc injection at the dose used in these experiments induces hepatic MT-I/II zinc sequestration within 14-16 hours (Coyle et al. 1995, Saito and Kojima 1997). In a study by Kelly et al. (1996), zinc administration over 7 days was capable of increasing liver MT-I/II expression but the dose was ramped up each day. The body primarily regulates zinc by altering the rate of zinc absorption in the intestine, the rate of zinc excretion in urine and pancreatic secretion of zinc (Walsh et al. 1994). In the present study, the daily zinc dose was constant and the liver zinc content was the same in MT-I/II$^{-/-}$ mice at wild type mice after 5 days of treatment which suggests that this amount of time is sufficient for MT-I/II independent zinc homeostasis mechanisms to be instated. For this reason it can not be concluded that reticulocytes were not affected in the early stages of zinc treatment in MT-I/II$^{-/-}$ mice because these cells only remain in the reticulocyte phase for 1-2 days and would have matured to erythrocytes after 5 days of zinc treatment.

6.4.2 Hypothesis for age-dependent anaemia in MT-I/II$^{-/-}$ mice

In humans zinc deficiency increases in elderly populations due to a reduced dietary zinc intake but is also thought to be influenced by metabolic changes that affect zinc homeostasis (reviewed by Vasto et al. 2007). Studies in mice using radioactive ^{65}Zn as a tracer have shown that zinc uptake declines with age and zinc secretion/excretion increases with age (He et al. 1991) and mice older than 1 year of age have reduced plasma zinc concentrations compared to 8 week old mice (Wong et al. 2009). Little is known about zinc distribution in aging MT-I/II$^{-/-}$ mice but zinc distribution in the liver is altered in MT-I/II$^{-/-}$ mice perinatally, another period when zinc distribution is undergoing changes (Lau and Cherian 1998). Therefore MT-I/II may play a larger role in regulating zinc as the animals age and become more susceptible to zinc deficiency.

In addition to zinc, MT-I/II also binds copper and copper has been shown to be important for regulating iron transport into transferrin due to its requirement in the ferroxidase protein, ceruloplasmin (Fox 2003). For this reason, anaemias caused by copper deficiency are often hypochromic, but the anaemia observed in MT-I/II$^{-/-}$ mice was not indicating that haemoglobin synthesis, and therefore iron transport, was normal in MT-I/II$^{-/-}$ mice.

Oxidative stress is thought to increase the rate of erythrocyte clearance from circulation (reviewed by Kiefer & Snyder 2000). MT-I/II can act as an antioxidant (Maret and Vallee 1998) but MT-I/II is only present in erythrocytes for a short time after they enter circulation (Grider et al. 1990) and is not present in the older erythrocytes that are more prone to macrophage phagocytosis. However zinc and copper are essential for the function of the antioxidant protein Cu/Zn superoxide dismutase. Cu/Zn Superoxide dismutase null mutant mice are anaemic compared to wild type mice, a difference caused by increased erythrocyte clearance that is amplified with age (Iuchi et al. 2007). The role of MT-I/II may be to sequester zinc and copper to erythrocyte precursors for metalloproteins such as Cu/Zn superoxide dismutase.

To determine the mechanism by which MT-I/II protects against anaemia with age several processes require investigation. Measurement of zinc and copper in bone marrow and erythrocytes from wild type and MT-I/II$^{-/-}$ mice with age via atomic absorption spectroscopy is straight-forward but was not possible in the present study because EDTA, a zinc and copper chelator, was used as the anticoagulant for blood samples and bone marrow was not collected. The rate of erythrocyte clearance can be assessed by removing erythrocytes from an animal, adding a fluorescent label, and then reinjecting them back into the animal (Suzuki and Dale 1987). Following this procedure in MT-I/II$^{-/-}$ mice, observation of numbers of labelled cells over time can be assessed by flow cytometry to determine the rate of erythrocyte clearance which can be compared to that of wild type mice. Finally, to assess the role of MT-I/II in erythropoiesis, isolation of hematopoietic stem cells from bone marrow would be useful for *in vitro* experiments to determine differentiation occurs similarly in MT-I/II$^{-/-}$ and MT-I/II $^{+/+}$ cells in normal conditions and in zinc deficiency or zinc excess.

6.4.3 Zinc-induced leukocytosis

The leukocytosis induced by zinc treatment was of interest due to the similarity to the increased leukocyte numbers observed in MT-I/II$^{-/-}$ mice at 7 DPI. Alterations to leukocyte production during haematopoiesis have been shown to occur during zinc deficiency (King and Fraker 2000, King and Fraker 2002) which may account for the observations of the present study. However, the effect was shown to occur in both wild type and MT-I/II$^{-/-}$ mice which is in contrast to the effect of zinc on erythrocyte numbers which only affected MT-I/II$^{-/-}$ mice. It is suspected that zinc homeostasis is disrupted after brain injury and that MT-I/II may play a role in modulating changes in

zinc, or perhaps causing changes in zinc. Therefore the possibility that MT-I/II can modulate zinc in certain situations but has no effect in other circumstances suggests that study of MT-I/II$^{-/-}$ phenotypes requires a greater understanding of zinc-dependent processes. The present study could be improved by a better understanding of where zinc is shuttled to within the body when systemic zinc levels increase and where the zinc is preferentially retained when systemic zinc levels decline.

6.4.4 Conclusion

The data presented herein suggest that MT-I/II can affect the hematopoietic system, particularly the erythropoietic branch. These data are interesting because they provide a system in which MT-I/II$^{-/-}$ mice have an altered phenotype in the absence of experimental manipulation to the mice. The levels of blood haemoglobin and erythrocyte cell number in MT-I/II$^{-/-}$ mice may not be low enough to be considered anaemia in a clinical context but MT-I/II does appear able to affect the rate of red blood cell production. Future experiments are required to determine if MT-I/II is more important when the requirement for red blood cell production is greater for example, in animals with acute blood loss. The requirement for MT-I/II in erythropoiesis may become more pronounced when dietary zinc is altered or when zinc homeostasis is disrupted in conditions such as the acute phase response. Brain injury exerted no effect on erythrocyte numbers or haemoglobin levels in the blood (data not shown) but it is interesting to note that administration of zinc to wild type and MT-I/II$^{-/-}$ mice alike had an effect on leukocyte numbers similar to brain injury in MT-I/II$^{-/-}$ mice at 7 DPI.

Chapter 7 – Discussion

One of the key findings in this body of work was that MT-I/II$^{-/-}$ mice exhibit elevated levels of neuronal death at 7DPI in comparison to wild type mice, in an experimental model of brain injury. The results presented in this thesis chronicle an attempt to determine the mechanism responsible for this, by focussing upon whether MT-I/II$^{-/-}$ mice have an altered inflammatory response to brain injury. MT-I/II expressed in the injured brain itself is possibly the most obvious location for MT-I/II to have an effect after injury due to its proximity to the injured cells. However, MT-I/II is a protein expressed in many organs in mice (Iszard et al. 1995), and the role of this protein remains unclear (Palmiter 1998). It is not implausible however, that MT-I/II expressed peripherally to the injured CNS may have systemic effects that influence the progression of brain injury, and this was a hypothesis that was tested in this thesis. Immune system function is known to be affected by MT-I/II, and alteration to the immune response to injury has been suggested to explain some of the differences in the injured brain of MT-I/II$^{-/-}$ mice. However, as the inflammatory response to brain injury progresses, the location where MT-I/II interacts with the cells of the immune system is unclear. It is also interesting that zinc homeostasis has not been studied extensively in MT-I/II$^{-/-}$ mice after brain injury, given that MT-I/II is primarily a zinc binding protein. The experiments detailed in the present thesis provide evidence that MT-I/II is involved in a systemic response to brain injury which may affect the resolution of the injury.

7.1.1 Alterations in neuron death in the cryolesioned MT-I/II$^{-/-}$ mouse brain occur at 7 DPI

After injury, an increased rate of neuron death between wild type and MT-I/II$^{-/-}$ mice was only evident at 7 DPI. Between the published studies that investigate the rate of neuron death after brain injury in MT-I/II$^{-/-}$ mice, there is variability in the time after injury that MT-I/II$^{-/-}$ mice to show a difference compared to wild type mice (Natale et al. 2004, Penkowa et al. 1999a). The reason for these differences is not obvious but it does suggest that the ability of MT-I/II to provide neuroprotection depends upon specific conditions in the injury site which vary in different experimental brain injury models. It has been shown *in vitro* that MT-I/II may protect neurons against oxidised dopamine products in neuron cultures (Gauthier et al. 2008, Køhler et al. 2003) and amyloid-β (Chung et al. 2010, Køhler et al. 2003) but for this to occur *in vivo* requires extracellular MT-I/II to reach concentrations of approximately 1 μg/ml. MT-I/II is a cytoplasmic protein with no secretory signal sequence and is not expressed in neurons. There is currently no quantitative data to determine whether extracellular MT-I/II concentration increases in cerebrospinal fluid after brain injury.

Under oxidative stress, MT-I/II is protective to cultured astrocytes which are the main MT-I/II-expressing cell type in the CNS (Suzuki et al. 2000). Therefore, it is most likely that astrocytes receive some protection from the MT-I/II that they synthesise but it is not known if astrocytic MT-I/II confers protection to other cell types in the injured brain. A protective effect of MT-I/II that prevents astrocyte death could promote neuron survival indirectly because neurons are highly reliant on trophic support from astrocytes (Pekny and Nilsson 2005, Pellerin and Magistretti 1994, Ridet et al. 1997, Yong 1998). In the present study the rate of neuron death was only different in MT-I/II$^{-/-}$ mice after the peak period of neuron death suggesting that the injury site of MT-I/II$^{-/-}$ mice was failing to enter the regenerative phase or there was an underlying detrimental process that was failing to resolve. One of the defining characteristics of transgenic mice over-expressing MT-I/II and MT-I/II$^{-/-}$ mice during CNS insults is an inverse correlation between the level of MT-I/II present in the system and the degree of inflammation in the CNS (Natale et al. 2004, Giralt et al. 2002, Penkowa et al. 1999a, Penkowa et al. 1999b, Penkowa et al. 2001, Penkowa et al. 2005, Penkowa et al. 2006a, Potter et al. 2007, Potter et al. 2009, Suemori et al. 2006). In the present study it was interesting to find that the time when inflammatory cells were at highest density in the injury site coincided with the time that neuron death was significantly higher in MT-I/II$^{-/-}$ mice compared to wild type mice. It is possible that elevated levels of neuronal death at 7DPI in MT-I/II$^{-/-}$ mice are linked to the inflammatory response to brain injury.

7.1.2 Alterations in T cell infiltration of the cryolesioned MT-I/II$^{-/-}$ mouse brain occur at 7 DPI

Part of the inflammatory response in the injured brain is generated within the CNS itself by microglia and astrocytes (reviewed by Liberto et al. 2004). However leukocytes can infiltrate the brain after brain injury and can therefore, affect its progression. The number of activated macrophages is commonly found to differ between wild type and MT-I/II$^{-/-}$ mice after CNS insults but was not found to be different in the present experiments. Therefore the alterations to the microglial/macrophage response in MT-I/II$^{-/-}$ mice appear to be dependent on the type of injury model used, or the methods used for quantification. The cryolesion injury model used to induce brain injury in this thesis appears to have a relatively low severity. This is evident because plasma cytokine levels did not rise substantially, hepatic cytokine expression was absent and the brain injury itself did not increase plasma corticosterone levels further than the increase caused by sham surgery alone. Despite the inability of the injury to produce a

measurable systemic cytokine response, there were significantly higher numbers of T cells infiltrating the injured CNS of MT-I/II$^{-/-}$ mice than wild type mice. T cells are activated and expand peripherally before they enter the injured CNS (Byram et al. 2004, Ling et al. 2006). MT-I/II has the potential to modulate the function of T cells and antigen presenting cells (Borghesi et al. 1996, Borghesi and Lynes 1996, Mita et al. 2002, Youn et al. 1995, Youn and Lynes 1999), hence its expression outside the CNS may affect T cell activation; a process that occurs outside the CNS.

Similar to the rate of neuron death, T cell infiltration into the injury site of MT-I/II$^{-/-}$ mice was only elevated above that of wild type mice at 7 DPI. The increase in T cell infiltration in MT-I/II$^{-/-}$ mice coincided with an increase in the number of leukocytes circulating in the blood at 7 DPI. An increased number of T cells in circulation provides a larger pool of T cells that can be recruited to the injury site in MT-I/II$^{-/-}$ mice. This evidence suggests that after brain injury, a change in the immune system of MT-I/II$^{-/-}$ mice is occurring before the leukocytes enter the injured CNS.

7.1.3 Altered ratio of caMΦs and aaMΦs in MT-I/II$^{-/-}$ mice

In addition to changes in leukocyte numbers in MT-I/II$^{-/-}$ mice after brain injury, is the possibility that the individual leukocytes may behave differently in MT-I/II$^{-/-}$ mice after injury. Activated macrophages fall under two major categories; classically activated (caMΦ) and alternatively activated (aaMΦ). Ym1 mRNA expression is used as a marker of alternative activation in macrophages (Raes et al. 2002) and has been reported to be indicative of aaMΦs in the CNS (Ponomarev et al. 2007). In the present study, both in the brain and PBMCs, Ym1 mRNA expression was consistently higher in wild type mice compared to MT-I/II$^{-/-}$ mice. This phenomenon was in occurrence before and after injury suggesting that there is a predisposition for MT-I/II$^{-/-}$ mice to produce less Ym1 mRNA. One interpretation of these data is that wild type mice have a certain ratio of aaMΦs to caMΦs which in MT-I/II$^{-/-}$ mice is more biased towards caMΦs. Current evidence suggests that in the CNS, caMΦs are detrimental to neuronal survival whereas aaMΦs are pro-regenerative (Kigerl et al. 2009). Therefore it is possible that a difference in the ratio of caMΦs to aaMΦs in MT-I/II$^{-/-}$ mice affects neuronal survival after brain injury. MT-I/II may influence the aaMΦ to caMΦ ratio in a range of ways. Firstly, helper T cells isolated from MT-I/II$^{-/-}$ mice have been shown to have a Th1 shifted Th1/Th2 ratio (Huh et al. 2007) and Th1/Th2 responses have a strong influence on the ratio of caMΦs to aaMΦs. Secondly, MT-I/II has a strong antioxidant capacity (Maret and Vallee 1998) and the redox status of macrophages can determine whether

they take on a caMΦ or aaMΦ phenotype (Gordon et al. 2003). However, the antioxidant capacity of MT-I/II would be more likely to preserve reduced conditions inside cells but this would favour a caMΦ response so this mechanism is unlikely. Thirdly, MT-I/II has been shown to affect the function of the transcription factor, NF-κB (Abdel-Mageed and Agrawal 1998, Butcher et al 2004, Kanekiyo et al. 2002b, Kim et al. 2003, Sakurai et al. 1999) which is important for the activation of immune cells (Blackwell and Christman 1997). The absence of MT-I/II may affect transcriptional signalling required for activation of caMΦ or aaMΦ responses. Fourthly, extracellular application of MT-I/II to the injured brain shifts the IDO pathway towards kynurenic acid production and away from quinolinic acid production (Chung et al. 2009). Macrophage quinolinic acid production is induced by the same conditions that generate caMΦs and kynurenic acid production is induced by the conditions that generate aaMΦs (Kwidzinski and Bechmann 2007, Yadav et al. 2007) which may indicate that extracellular MT-I/II affects the IDO pathway by modulating the ratio of caMΦs/aaMΦs. MT-I/II has the potential to interact with several important immune system pathways and further study is required to determine how MT-I/II affects the immune system *in vivo*.

One of the disadvantages to the cryolesion model has been the lack of systemic immune response to brain injury, and this has meant that study of the Th1/Th2 response in wild type and MT-I/II$^{-/-}$ mice has been difficult using this model. An altered Th1/Th2 response may be the cause of changes in Ym1 expression in MT-I/II$^{-/-}$ mice but lowered Ym1 mRNA expression was observed in the brain and PBMCs of MT-I/II$^{-/-}$ mice before brain injury occurred. *In vitro* experiments will be important to determine whether there is an intrinsic difference between the activation phenotype of MT-I/II$^{-/-}$ macrophages and wild type macrophages, once isolated from the animal. A distinction that is required to better understand how MT-I/II functions is whether MT-I/II expression within the cell is most important for the immune modulation of MT-I/II or whether MT-I/II has systemic and developmental effects that affect the immune system of the entire animal.

7.1.4 Hepatic Liver MT-I/II expression is maximal at 7 DPI and may affect zinc homeostasis

Hepatic MT-I/II expression is a common response to a systemic crisis (Cho et al. 2004, Coyle et al 1995, Ding et al. 2002, Hernández et al. 1999, Jacob et al. 1999, Philcox et al. 1995, Swapan et al. 1990, Zhou et al. 2003) and results in a decrease in plasma zinc

concentrations (Philcox et al. 1995, Coyle et al. 1995). This response has not been previously reported to occur after brain injury, hence the ability of hepatic MT-I/II expression to modulate labile zinc concentration after injury was investigated as a possible cause of the differences between wild type and MT-I/II$^{-/-}$ mice after brain injury. It was shown that MT-I/II protein is maximally up-regulated in the liver 7 days after injury. MT-I/II$^{-/-}$ mice had significantly lower liver zinc content which implies that hepatic MT-I/II expression has some control over zinc homeostasis.

At 7 DPI in MT-I/II$^{-/-}$ mice there was also an increase in circulating leukocyte numbers, increased T cell infiltration into the injury site and prolonged neuron death. One hypothesis to explain these correlations is that altered zinc homeostasis in MT-I/II$^{-/-}$ mice is caused by an inability to moderate labile zinc concentrations, which subsequently affects immune system function. In chapter 6, the parenteral administration of zinc to wild type and MT-I/II$^{-/-}$ mice induced an increase in circulating leukocytes similar to the increase observed in MT-I/II$^{-/-}$ mice 7 days after cryolesion. Dietary zinc deficiency is known to cause decreases in the numbers of circulating leukocytes (DePasquale and Fraker 1979, DePasquale and Fraker 1980, King and Fraker 2000, King and Fraker 2002, King et al. 2005) and increasing zinc by dietary supplement can augment the function of leukocytes (Aydemir et al. 2006). In the present study, there was no change to zinc in the dietary composition after cryolesion so any changes in labile zinc would likely occur via changes in zinc-homeostasis mechanisms. There is evidence to suggest that brain injury causes disruption to zinc homeostasis in brain injured patients (McClain et al. 1986) and it is possible that MT-I/II expression contributes to the maintenance of zinc homeostasis after brain injury. Therefore changes in zinc homeostasis is a feasible, but not proven, mechanism by which MT-I/II$^{-/-}$ mice have altered immune function after brain injury. The creation of a transgenic mouse expressing a luciferase gene has been used previously to observe the systemic activity of transcription factors acting at the luciferase gene promoter by measuring the light emitted from the transgenic mouse ***in situ*** (Campbell et al. 2008). The MTF-1 transcription factor is activated when free zinc levels increase in the cytoplasm. Therefore a luciferase gene with a response element to MTF-1 in its promoter could indicate regions a mouse with high levels of free cytoplasmic zinc, assuming such a transgenic mouse could be created. The magnitude by which MT-I/II affects zinc homeostasis after brain injury will be dependent on the

degree of MT-I/II expression after injury which may vary in different experimental models of brain injury and in a clinical setting.

7.1.5 Future directions to determine the role of MT-I/II in zinc homeostasis after brain injury

Because zinc is an essential trace metal involved in many cellular processes it is not straight-forward to remove zinc from an animal in an experimental system. Dietary zinc deficiency has been demonstrated to have a detrimental effect on the progression of brain injury (Penkowa et al. 2001, Yeiser et al. 2002). However, zinc deficiency is a systemic manipulation that could be affecting many processes simultaneously which makes interpretation of the effects of zinc deficiency in specific tissues difficult. Additionally, administering a zinc deficient diet is countered by the fact that intestinal zinc absorption becomes increased and zinc supplementation is also complicated because zinc absorption and excretion are regulated to appropriately maintain stable zinc levels (reviewed by Walsh et al. 1994). Under normal conditions MT-I/II$^{-/-}$ mice have normal plasma zinc concentrations and it is not until the system is altered either due to activation of the acute phase response, or pharmacological zinc administration that differences in zinc levels in various organs between MT-I/II$^{-/-}$ and wild type mice become apparent (Philcox et al. 1995, Coyle et al. 1995). This suggests that MT-I/II plays a role in zinc regulation when there is a deviation from homeostatic zinc levels.

In addition to their lack of hepatic zinc sequestration, MT-I/II$^{-/-}$ mice have altered pancreatic zinc secretion (Rofe et al. 1999). The hypothesis that altered zinc homeostasis affects the outcome from brain injury would be supported by further experiments that investigate MT-I/II expression and zinc uptake by other organs after brain injury and zinc secretion and excretion in MT-I/II$^{-/-}$ mice after brain injury. However, it has not been confirmed that MT-I/II acts on the immune system via zinc dependent mechanisms and a more generic approach would help determine the location in which MT-I/II exerts its beneficial effects after brain injury. A conditional knockout mouse that is unable to express MT-I/II in all cells except hepatocytes would be useful tool to investigate MT-I/II in a zinc regulatory role. Alternatively, the same approach could be used to express MT-I/II in astrocytes alone. Possible experiments with such a mouse strain could include cryolesion to the brain to determine if parameters such as neuron death, T cell infiltration or circulating leukocyte counts were most affected by brain-derived MT-I/II or liver derived MT-I/II. It remains possible that MT-I/II has effects in the injured brain and some effects peripherally.

7.1.6 Final considerations

There are known differences in the immune responses of mice and humans which may affect the direct comparison of the effects that MT-I/II has in the brain injury of mice to that of humans. One example is that there is no known Ym1 gene in humans hence future study should consider whether extracellular MT-I/II has the same ability to induce changes in human macrophage phenotype as those observed in this thesis, in mice, and those of Chung et al. (2009), in rats. There are several other questions that need to be answered to assess the role of MT-I/II in brain injured human patients; whether MT-I/II is up-regulated in the liver in the same fashion as in mice and whether zinc trafficking after brain injury relies as heavily on MT-I/II in humans as it does in mice. A potential role of MT-III should be considered in the CNS of MT-I/II$^{-/-}$ mice. MT-III up-regulation as a compensatory response to the lack of MT-I/II expression in MT-I/II$^{-/-}$ mice could affect the injured brain given the neurotoxic and inhibitory effects of MT-III that have been observed ***in vitro*** (Chung et al. 2002, Uchida et al. 1991). These possibilities should be considered when interpreting the data presented in this thesis.

7.1.7 Conclusions

The main aim of this thesis was to test the hypothesis that MT-I/II expressed in non-neurological organs could be affecting the progression of brain injury. This hypothesis was synthesised to explain the differences in the inflammatory response in the injured brain of MT-I/II$^{-/-}$ mice when compared to wild type mice. The quantification of the aaMΦ marker Ym1 reveals that there are some differences in the immune functions of MT-I/II$^{-/-}$ mice inherent before injury. There are other differences between wild type and MT-I/II$^{-/-}$ mice that were only found after brain injury such as the increased T cell infiltration into the injured brain, the increased number of circulating leukocytes and the MT-I/II dependent sequestration of zinc into the liver. All of these differences occurred at 7 DPI and the relationship between them, and elevated levels of neuronal death at this time in MT-I/II$^{-/-}$ mice requires further investigation. The correlation does not identify a direct causal relationship between these phenomena but the research detailed in this thesis demonstrates that there is a systemic MT-I/II response to brain injury. It is now necessary to determine the relative contribution of CNS-derived, and entraneural organ-derived MT-I/II to the beneficial effect of MT-I/II after brain injury. Such information

will help to determine the mechanism by which mice with transgenic alterations in MT-I/II expression have altered responses to brain injury.

References

Abdel-Mageed AB, Agrawal KC (1998) Activation of nuclear factor kappa B: Potential role in metallothionein-mediated mitogenic response. Cancer Research 58:2335-2338.

Abdel-Mageed AB, Zhao FS, Rider BJ, Agrawal KC (2003) Erythropoietin-induced metallothionein gene expression: Role in proliferation of K562 cells. Experimental Biology and Medicine 228:1033-1039.

Aharoni R, Kayhan B, Eilam R, Sela M, Arnon R (2003) Glatiramer acetate-specific T cells in the brain express T helper 2/3 cytokines and brain-derived neurotrophic factor in situ. Proceedings of the National Academy of Sciences of the United States of America 100:14157-14162.

Aizenman E, Stout AK, Harnett KA, Dineley KE, McLaughlin B, Reynolds IJ (2000) Induction of neuronal apoptosis by thiol oxidation: Putative role of intracellular zinc release. Journal of Neurochemistry 75:1878-1888.

Alberati-Giani D, Cesura AM (1998) Expression of the kynurenine enzymes in macrophages and microglial cells: regulation by immune modulators. Amino Acids 14:251-255.

Aloisi F (2001) Immune function of microglia. Glia 36:165-179.

Aloisi F, De Simone R, Columba-Cabezas S, Penna G, Adorini L (2000) Functional maturation of adult mouse resting microglia into an APC is promoted by granulocyte-macrophage colony-stimulating factor and interaction with Th1 cells. Journal of Immunology 164:1705-1712.

Amrani N, Sachs MS, Jacobson A (2006) Early nonsense: mRNA decay solves a translational problem. Nature Reviews Molecular Cell Biology 7:415-425.

Ancuta P, Rao R, Moses A, Mehle A, Shaw SK, Luscinskas FW, Gabuzda D (2003) Fractalkine preferentially mediates arrest and migration of CD16+ monocytes. Journal of Experimental Medicine 197:1701-1707.

Apostolova M, Nachev C, Koleva M, Bontchev PR, Kehaiov I (1998) New competitive enzyme-linked immunosorbent assay for determination of metallothionein in tissue and sera. Talanta 46:325-333.

Archambault AS, Sim J, Gimenez MAT, Russell JH (2005) Defining antigen-dependent stages of T cell migration from the blood to the central nervous system parenchyma. European Journal of Immunology 35:1076-1085.

Arora M, Chen L, Paglia M, Gallagher I, Allen JE, Vyas YM, Ray A, Ray P (2006) Simvastatin promotes Th2-type responses through the induction of the chitinase family member Ym1 in dendritic cells. Proceedings of the National Academy of Sciences of the United States of America 103:7777-7782.

Aydemir TB, Blanchard RK, Cousins RJ (2006) Zinc supplementation of young men alters metallothionein, zinc transporter, and cytokine gene expression in leukocyte populations. Proceedings of the National Academy of Sciences of the United States of America 103:1699-1704.

Babcock AA, Kuziel WA, Rivest S, Owens T (2003) Chemokine expression by glial cells directs leukocytes to sites of axonal injury in the CNS. Journal of Neuroscience 23:7922-7930.

Bajetto A, Bonavia R, Barbero S, Florio T, Schettini G (2001) Chemokines and their receptors in the central nervous system. Frontiers in Neuroendocrinology 22:147-184.

Ballabh P, Braun A, Nedergaard M (2004) The blood-brain barrier: an overview - Structure, regulation, and clinical implications. Neurobiology of Disease 16:1-13.

Baltus T, von Hundelshausen P, Mause SF, Buhre W, Rossaint R, Weber C (2005) Differential and additive effects of platelet-derived chemokines on monocyte arrest on inflamed endothelium under flow conditions. Journal of Leukocyte Biology 78:435-441.

Banci L, Bertini I, Ciofi-Baffoni S, Kozyreva T, Zovo K, Palumaa P (2010) Affinity gradients drive copper to cellular destinations. Nature 465:645-U145.

Banks WA (2005) Blood-brain barrier transport of cytokines: A mechanism for neuropathology. Current Pharmaceutical Design 11:973-984.

Bansal V, Costantini T, Ryu SY, Peterson C, Loomis W, Putnam J, Elicieri B, Baird A, Coimbra R (2010) Stimulating the Central Nervous System to Prevent Intestinal Dysfunction After Traumatic Brain Injury. Journal of Trauma-Injury Infection and Critical Care 68:1059-1064.

Bartholomäus I, Kawakami N, Odoardi F, Schlager C, Miljkovic D, Ellwart JW, Klinkert WEF, Flugel-Koch C, Issekutz TB, Wekerle H, Flugel A (2009) Effector T cell interactions with meningeal vascular structures in nascent autoimmune CNS lesions. Nature 462:94-U104.

Beattie JH, Wood AM, Newman AM, Bremner I, Choo KHA, Michalska AE, Duncan JS, Trayhurn P (1998) Obesity and hyperleptinemia in metallothionein (-I and -II) null mice. Proceedings of the National Academy of Sciences of the United States of America 95:358-363.

Becher B, Prat A, Antel JP (2000) Brain-immune connection: Immune-regulatory properties of CNS-resident cells. Glia 29:293-304.

Belmadani A, Tran PB, Ren DJ, Miller RJ (2006) Chemokines regulate the migration of neural progenitors to sites of neuroinflammation. Journal of Neuroscience 26:3182-3191.

Beltramini M, Zambenedetti P, Wittkowski W, Zatta P (2004) Effects of steroid hormones on the Zn, Cu and MTI/II levels in the mouse brain. Brain Research 1013:134-141.

Bennett GD, Kay MMB (1981) Homeostatic removal of senescent murine erythrocytes by splenic macrophages. Experimental Hematology 9:297-307.

Bernardino L, Xapelli S, Silva AP, Jakobsen B, Poulsen FR, Oliveira CR, Vezzani A, Malva JO, Zimmer J (2005) Modulator effects of interleukin-1 beta and tumor necrosis factor-alpha on AMPA-induced excitotoxicity in mouse organotypic hippocampal slice cultures. Journal of Neuroscience 25:6734-6744.

Bezzi P, Domercq M, Brambilla L, Galli R, Schols D, De Clercq E, Vescovi A, Bagetta G, Kollias G, Meldolesi J, Volterra A (2001) CXCR4-activated astrocyte glutamate release via TNFa: amplification by microglia triggers neurotoxicity. Nature Neuroscience 4:702-710.

Blackwell TS, Christman JW (1997) The role of nuclear factor-kappa B in cytokine gene regulation. American Journal of Respiratory Cell and Molecular Biology 17:3-9.

Blouin A, Bolender RP, Weibel ER (1977) Distribution of organelles and membranes between hepatocytes and non-hepatocytes in rat-liver parenchyma – stereological study. Journal of Cell Biology 72:441-455.

Borghesi LA, Lynes MA (1996) Nonprotective effects of extracellular metallothionein. Toxicology and Applied Pharmacology 139:6-14.

Borghesi LA, Youn J, Olson EA, Lynes MA (1996) Interactions of metallothionein with murine lymphocytes: Plasma membrane binding and proliferation. Toxicology 108:129-140.

Boulton M, Flessner M, Armstrong D, Mohamed R, Hay J, Johnston M (1999) Contribution of extracranial lymphatics and arachnoid villi to the clearance of a CSF tracer in the rat. American Journal of Physiology-Regulatory Integrative and Comparative Physiology 276:R818-R823.

Bozic CR, Kolakowski LF, Gerard NP, Garciarodriguez C, Vonuexkullguldenband C, Conklyn MJ, Breslow R, Showell HJ, Gerard C (1995) Expression and biologic characterisation of the murine chemokine KC. Journal of Immunology 154:6048-6057.

Bradford MM (1976) Rapid and sensitive method for quantitation of microgram quantities of protein utilizing principle of protein-dye binding. Analytical Biochemistry 72:248-254.

Brettingham-Moore KH, Rao S, Juelich T, Shannon MF, Holloway AF (2005) GM-CSF promoter chromatin remodelling and gene transcription display distinct signal and transcription factor requirements. Nucleic Acids Research 33:225-234.

Buchmullerrouiller Y, Corradin SB, Smith J, Schneider P, Ransijn A, Jongeneel CV, Mauel J (1995) Role of glutathione in macrophage activation – effect of cellular glutathione depletion on nitrite production and Leishmanicidal activity. Cellular Immunology 164:73-80.

Butcher H, Kennette W, Collins O, Demoor J, Koropatnick J (2003) A sensitive time-resolved fluorescent immunoassay for metallothionein protein. Journal of Immunological Methods 272:247-256.

Butcher HL, Kennette WA, Collins O, Zalups RK, Koropatnick J (2004) Metallothionein mediates the level and activity of nuclear factor kappa B in murine fibroblasts. Journal of Pharmacology and Experimental Therapeutics 310:589-598.

Butovsky O, Talpalar AE, Ben-Yaakov K, Schwartz M (2005) Activation of microglia by aggregated beta-amyloid or lipopolysaccharide impairs MHC-II expression and renders them cytotoxic whereas IFN-gamma and IL-4 render them protective. Molecular and Cellular Neuroscience 29:381-393.

Byram SC, Carson MJ, DeBoy CA, Serpe CJ, Sanders VM, Jones KJ (2004) CD4-positive T cell-mediated neuroprotection requires dual compartment antigen presentation. Journal of Neuroscience 24:4333-4339.

Cai YP, Kumar RK, Zhou JS, Foster PS, Webb DC (2009) Ym1/2 Promotes Th2 Cytokine Expression by Inhibiting 12/15(S)-Lipoxygenase: Identification of a Novel Pathway for Regulating Allergic Inflammation. Journal of Immunology 182:5393-5399.

Campagnolo DI, Dixon D, Schwartz J, Bartlett JA, Keller SE (2008) Altered innate immunity following spinal cord injury. Spinal Cord 46:477-481.

Campbell SJ, Wilcockson DC, Butchart AG, Perry VH, Anthony DC (2002) Altered chemokine expression in the spinal cord and brain contributes to differential interleukin-1 beta-induced neutrophil recruitment. Journal of Neurochemistry 83:432-441.

Campbell SJ, Deacon RMJ, Jiang YJ, Ferrari C, Pitossi FJ, Anthony DC (2007a) Overexpression of IL-1 beta by adenoviral-mediated gene transfer in the rat brain causes a prolonged hepatic chemokine response, axonal injury and the suppression of spontaneous behaviour. Neurobiology of Disease 27:151-163.

Campbell SJ, Jiang Y, Davis AEM, Farrands R, Holbrook J, Leppert D, Anthony DC (2007b) Immunomodulatory effects of etanercept in a model of brain injury act through attenuation of the acute-phase response. Journal of Neurochemistry 103:2245-2255.

Campbell SJ, Anthony DC, Oakley F, Carlsen H, Elsharkawy AM, Blomhoff R, Mann DA (2008a) Hepatic nuclear factor kappa B regulates neutrophil recruitment to

the injured brain. Journal of Neuropathology and Experimental Neurology 67:223-230.

Campbell SJ, Hughes PM, Iredale JP, Wilcockson DC, Waters S, Docagne F, Perry VH, Anthony DC (2003) CINC-1 is identified as an acute-phase protein induced by focal brain injury causing leukocyte mobilization and liver injury. Faseb Journal 17:1168-+.

Campbell SJ, Perry VH, Pitossi FJ, Butchart AG, Chertoff M, Waters S, Dempster R, Anthony DC (2005) Central nervous system injury triggers hepatic CC and CXC chemokine expression that is associated with leukocyte mobilization and recruitment to both the central nervous system and the liver. American Journal of Pathology 166:1487-1497.

Campbell SJ, Zahid I, Losey P, Law S, Jiang YY, Bilgen M, van Rooijen N, Morsali D, Davis AEM, Anthony DC (2008b) Liver Kupffer cells control the magnitude of the inflammatory response in the injured brain and spinal cord. Neuropharmacology 55:780-787.

Candelario-Jalil E, Yang Y, Rosenberg GA (2009) Diverse roles of matrix metalloproteinases and tissue inhibitors of metalloproteinases in neuroinflammation and cerebral ischemia. Neuroscience 158:983-994.

Canpolat E, Lynes MA (2001) In vivo manipulation of endogenous metallothionein with a monoclonal antibody enhances a T-dependent humoral immune response. Toxicological Sciences 62:61-70.

Carrasco J, Penkowa M, Hadberg H, Molinero A, Hidalgo J (2000) Enhanced seizures and hippocampal neurodegeneration following kainic acid-induced seizures in metallothionein-I plus II-deficient mice. European Journal of Neuroscience 12:2311-2322.

Carrasco J, Penkowa M, Giralt M, Camats J, Molinero A, Campbell IL, Palmiter RD, Hidalgo J (2003) Role of metallothionein-III following central nervous system damage. Neurobiology of Disease 13:22-36.

Carson MJ, Doose JM, Melchior B, Schmid CD, Ploix CC (2006) CNS immune privilege: hiding in plain sight. Immunological Reviews 213:48-65.

Chan HM, Pringle GA, Cherian MG (1992) Heterogeneity of antibodies to metallothionein isomers and development of a simple enzyme-linked-immunosorbent-assay. Journal of Biochemical Toxicology 7:219-227.

Chapman KZ, Dale VQ, Denes A, Bennett G, Rothwell NJ, Allan SM, McColl BW (2009) A rapid and transient peripheral inflammatory response precedes brain inflammation after experimental stroke. Journal of Cerebral Blood Flow and Metabolism 29:1764-1768.

Chen G, Shi J, Qi M, Yin H, Hang C (2008) Glutamine decreases intestinal nuclear factor kappa B activity and pro-inflammatory cytokine expression after traumatic brain injury in rats. Inflammation Research 57:57-64.

Cho K, Adamson L, Jeong J, VanHook T, Rucker R, Greenhalgh D (2004) Alterations in the levels of metallothionein and metals in the liver, and unique serum liver enzyme response in metallothionein knock-out mice after burn injury. Pathobiology 71:223-230.

Choi C, Park JY, Lee J, Lim JH, Shin EC, Ahn YS, Kim CH, Kim SJ, Kim JD, Choi IS, Choi IH (1999) Fas ligand and Fas are expressed constitutively in human astrocytes and the expression increases with IL-1, IL-6, TNF-alpha, or IFN-gamma. Journal of Immunology 162:1889-1895.

Chung RS, Chung RS, Vickers JC, Chuah MI, Eckhardt BL, West AK (2002). Metallothionein-III inhibits initial neurite formation in developing neurons as well as postinjury, regenerative neurite sprouting. Experimental Neurology 178: 1–12.

Chung RS, Vickers JC, Chuah MI, West AK (2003) Metallothionein-IIA promotes initial neurite elongation and postinjury reactive neurite growth and facilitates healing after focal cortical brain injury. Journal of Neuroscience 23:3336-3342.

Chung RS, Adlard PA, Dittmann J, Vickers JC, Chuah MI, West AK (2004) Neuron-glia communication: metallothionein expression is specifically up-regulated by astrocytes in response to neuronal injury. Journal of Neurochemistry 88:454-461.

Chung RS, Leung YK, Butler CW, Chen Y, Eaton ED, Pankhurst MW, West AK, Guillemin GJ (2009) Metallothionein Treatment Attenuates Microglial Activation and Expression of Neurotoxic Quinolinic Acid Following Traumatic Brain Injury. Neurotoxicity Research 15:381-389.

Chung RS, Howells C, Eaton ED, Shabala L, Zovo K, Palumaa P, Sillard R, Woodhouse A, Bennett WR, Ray S, Vickers JC, West AK (2010) The native copper- and zinc-binding protein metallothionein blocks copper-mediated Abeta aggregation and toxicity in rat cortical neurons. PLoS One 5:e12030.

Clausen F, Lorant T, Lewen A, Hillered L (2007) T lymphocyte trafficking: A novel target for neuroprotection in traumatic brain injury. Journal of Neurotrauma 24:1295-1307.

Coyle P, Philcox JC, Rofe AM (1993) Corticosterone enhances the zinc and interleukin-6 - mediated induction of metallothionein in cultured rat hepatocytes. Journal of Nutrition 123:1464-1470.

Coyle P, Philcox JC, Rofe AM (1995) Hepatic zinc in metallothionein-null mice following zinc challenge - in-vivo and in-vitro studies. Biochemical Journal 309:25-31.

Crowthers KC, Kline V, Giardina C, Lynes MA (2000) Augmented humoral immune function in metallothionein-null mice. Toxicology and Applied Pharmacology 166:161-172.

Cuajungco MP, Lees GJ (1997) Zinc metabolism in the brain: Relevance to human neurodegenerative disorders. Neurobiology of Disease 4:137-169.

Czigner A, Mihaly A, Farkas O, Buki A, Krisztin-Peva B, Dobo E, Barzo P (2007) Kinetics of the cellular immune response following closed head injury. Acta Neurochirurgica 149:281-289.

Dabrio M, Rodriguez AR, Bordin G, Bebianno MJ, De Ley M, Sestakova I, Vasak M, Nordberg M (2002) Recent developments in quantification methods for metallothionein. Journal of Inorganic Biochemistry 88:123-134.

Danks DM (1988) Copper deficiency in humans. Annual Review of Nutrition 8:235-257.

Davis MM, Krogsgaard M, Huppa JB, Sumen C, Purbhoo MA, Irvine DJ, Wu LC, Ehrlich L (2003) Dynamics of cell surface molecules during T cell recognition. Annual Review of Biochemistry 72:717-742.

de Jong EC, Vieira PL, Kalinski P, Schuitemaker JHN, Tanaka Y, Wierenga EA, Yazdanbakhsh M, Kapsenberg ML (2002) Microbial compounds selectively induce Th1 cell-promoting or Th2 cell-promoting dendritic cells in vitro with diverse Th cell-polarizing signals. Journal of Immunology 168:1704-1709.

De SK, McMaster MT, Andrews GK (1990) Endotoxin induction of murine metallothionein gene-expression. Journal of Biological Chemistry 265:15267-15274.

DeFelipe J, Alonso-Nanclares L, Arellano JI (2002) Microstructure of the neocortex: Comparative aspects. Journal of Neurocytology 31:299-316.

Denker SP, Ji SQ, Dingman A, Lee SY, Derugin N, Wendland MF, Vexler ZS (2007) Macrophages are comprised of resident brain microglia not infiltrating

peripheral monocytes acutely after neonatal stroke. Journal of Neurochemistry 100:893-904.
Depasqualejardieu P, Fraker PJ (1979) Role of corticosterone in the loss in immune function in the zinc-deficient A-J mouse. Journal of Nutrition 109:1847-1855.
Depasqualejardieu P, Fraker PJ (1980) Further characterization of the role of corticosterone in the loss of humoral immunity in zinc-deficient A-J mice as determined by adrenalectomy. Journal of Immunology 124:2650-2655.
Desagher S, Glowinski J, Premont J (1996) Astrocytes protect neurons from hydrogen peroxide toxicity. Journal of Neuroscience 16:2553-2562.
Dineley KE, Scanlon JM, Kress GJ, Stout AK, Reynolds IJ (2000) Astrocytes are more resistant than neurons to the cytotoxic effects of increased [Zn2+](i). Neurobiology of Disease 7:310-320.
Ding HQ, Zhou BJ, Liu L, Cheng S (2002) Oxidative stress and metallothionein expression in the liver of rats with severe thermal injury. Burns 28:215-221.
Dobashi K, Aihara M, Araki T, Shimizu Y, Utsugi M, Iizuka K, Murata Y, Hamuro J, Nakazawa T, Mori M (2001) Regulation of LPS induced IL-12 production by IFN-gamma and IL-4 through intracellular glutathione status in human alveolar macrophages. Clinical and Experimental Immunology 124:290-296.
Donnelly DJ, Popovich PG (2008) Inflammation and its role in neuroprotection, axonal regeneration and functional recovery after spinal cord injury. Experimental Neurology 209:378-388.
Dustin ML, Shaw AS (1999) Immunology - Costimulation: Building an immunological synapse. Science 283:649-650.
El Hendy HA, Yousef MI, El-Naga NIA (2001) Effect of dietary zinc deficiency on hematological and biochemical parameters and concentrations of zinc, copper, and iron in growing rats. Toxicology 167:163-170.
Emeny RT, Marusov G, Lawrence DA, Pederson-Lane J, Yin X, Lynes MA (2009) Manipulations of metallothionein gene dose accelerate the response to Listeria monocytogenes. Chemico-Biological Interactions 181:243-253.
Emerson JF, Ngo G, Emerson SS (2003) Screening for interference in immunoassays. Clinical Chemistry 49:1163-1169.
Falsig J, Latta M, Leist M (2004) Defined inflammatory states in astrocyte cultures: correlation with susceptibility towards CD95-driven apoptosis. Journal of Neurochemistry 88:181-193.
Faulkner JR, Woo MJ, Sislak MD, Safroniew MV (2004) Genetically targeted astrocyte scar ablation results in modest local growth of axons after spinal cord injury. Journal of Neurotrauma 21:P310.
Findlay JWA, Dillard RF (2007) Appropriate calibration curve fitting in ligand binding assays. Aaps Journal 9:E260-E267.
Fitzgerald M, Nairn P, Bartlett CA, Chung RS, West AK, Beazley LD (2007) Metallothionein-IIA promotes neurite growth via the megalin receptor. Experimental Brain Research 183:171-180.
Fox PL (2003) The copper-iron chronicles: The story of an intimate relationship. Biometals 16:9-40.
Fraker PJ, King LE (2004) Reprogramming of the immune system during zinc deficiency. Annual Review of Nutrition 24:277-298.
Gasull T, Rebollo DV, Romero B, Hidalgo J (1993) Development of a competitive double antibody-radioimmunoassay for rat metallothionein. Journal of Immunoassay 14:209-225.
Gauthier MA, Eibl JK, Crispo JAG, Ross GM (2008) Covalent Arylation of Metallothionein by Oxidized Dopamine Products: a Possible Mechanism for

Zinc-mediated Enhancement of Dopaminergic Neuron Survival. Neurotoxicity Research 14:317-328.

Gerszten RE, Garcia-Zepeda EA, Lim YC, Yoshida M, Ding HA, Gimbrone MA, Luster AD, Luscinskas FW, Rosenzweig A (1999) MCP-1 and IL-8 trigger firm adhesion of monocytes to vascular endothelium under flow conditions. Nature 398:718-723.

Ghirnikar RS, Lee YL, Eng LF (1998) Inflammation in traumatic brain injury: Role of cytokines and chemokines. Neurochemical Research 23:329-340.

Ghirnikar RS, Lee YL, He TR, Eng LF (1996) Chemokine expression in rat stab wound brain injury. Journal of Neuroscience Research 46:727-733.

Giles GI, Tasker KM, Collins C, Giles NM, O'Rourke E, Jacob C (2002) Reactive sulphur species: an in vitro investigation of the oxidation properties of disulphide S-oxides. Biochemical Journal 364:579-585.

Gimsa U, Oren A, Pandiyan P, Teichmann D, Bechmann I, Nitsch R, Brunner-Weinzierl MC (2004) Astrocytes protect the CNS: antigen-specific T helper cell responses are inhibited by astrocyte-induced upregulation of CTLA-4 (CD152). Journal of Molecular Medicine-Jmm 82:364-372.

Giralt M, Penkowa M, Lago N, Molinero A, Hidalgo J (2002) Metallothionein-1+2 protect the CNS after a focal brain injury. Experimental Neurology 173:114-128.

Giuliani F, Goodyer CG, Antel JP, Yong VW (2003) Vulnerability of human neurons to T cell-mediated cytotoxicity. Journal of Immunology 171:368-379.

Gordon S (2003) Alternative activation of macrophages. Nature Reviews Immunology 3:23-35.

Gouwy M, Struyf S, Catusse J, Proost P, Van Damme J (2004) Synergy between proinflammatory ligands of G protein-coupled receptors in neutrophil activation and migration. Journal of Leukocyte Biology 76:185-194.

Grider A, Bailey LB, Cousins RJ (1990) Erythrocyte metallothionein as an index of zinc status in humans. Proceedings of the National Academy of Sciences of the United States of America 87:1259-1262.

Gris D, Hamilton EF, Weaver LC (2008) The systemic inflammatory response after spinal cord injury damages lungs and kidneys. Experimental Neurology 211:259-270.

Guillemin GJ, Brew BJ (2004) Microglia, macrophages, perivascular macrophages, and pericytes: a review of function and identification. Journal of Leukocyte Biology 75:388-397.

Guillemin GJ, Smythe G, Takikawa O, Brew BJ (2005) Expression of indoleamine 2,3-dioxygenase and production of quinolinic acid by human microglia, astrocytes, and neurons. Glia 49:15-23.

Haase H, Rink L (2007) Signal transduction in monocytes: the role of zinc ions. Biometals 20:579-585.

Haase H, Maret W (2008) Partial oxidation and oxidative polymerization of metallothionein. Electrophoresis 29:4169-4176.

Habgood MD, Bye N, Dziegielewska KM, Ek CJ, Lane MA, Potter A, Morganti-Kossmann C, Saunders NR (2007) Changes in blood-brain barrier permeability to large and small molecules following traumatic brain injury in mice. European Journal of Neuroscience 25:231-238.

Hammarberg H, Lidman O, Lundberg C, Eltayeb SY, Gielen AW, Muhallab S, Svenningsson A, Linda H, van der Meide PH, Cullheim S, Olsson T, Piehl F (2000) Neuroprotection by encephalomyelitis: Rescue of mechanically injured neurons and neurotrophin production by CNS-infiltrating T and natural killer cells. Journal of Neuroscience 20:5283-5291.

Hanisch UK, Kettenmann H (2007) Microglia: active sensor and versatile effector cells in the normal and pathologic brain. Nature Neuroscience 10:1387-1394.
Hausmann EHS, Berman NEJ, Wang YY, Meara JB, Wood GW, Klein RM (1998) Selective chemokine mRNA expression following brain injury. Brain Research 788:49-59.
Hawkins BT, Davis TP (2005) The blood-brain barrier/neurovascular unit in health and disease. Pharmacological Reviews 57:173-185.
He LS, Yan XS, Wu DC (1991) Age-dependent variation of Zn-65 metabolism in LACA mice. International Journal of Radiation Biology 60:907-916.
Heinrich PC, Castell JV, Andus T (1990) INTERLEUKIN-6 AND THE ACUTE PHASE RESPONSE. Biochemical Journal 265:621-636.
Hendrix S, Nitsch R (2007) The role of T helper cells in neuroprotection and regeneration. Journal of Neuroimmunology 184:100-112.
Hernández J, Carrasco J, Belloso E, Giralt M, Bluethmann H, Lee DK, Andrews GK, Hidalgo J (2000) Metallothionein induction by restraint stress: Role of glucocorticoids and IL-6. Cytokine 12:791-796.
Hess DC, Abe T, Hill WD, Studdard AM, Carothers J, Masuya M, Fleming PA, Drake CJ, Ogawa M (2004) Hematopoietic origin of microglial and perivascular cells in brain. Experimental Neurology 186:134-144.
Hickey WF, Hsu BL, Kimura H (1991) Lymphocyte-T entry into the central-nervous-system. Journal of Neuroscience Research 28:254-260.
Hirauchi T, Okabe M, Nagashima T, Niioka T (1999) Metallothionein quantitation in biological materials by enzyme-linked immunosorbent assay (ELISA) using a commercial monoclonal antibody. Trace Elements and Electrolytes 16:177-182.
Hou TJ, An Y, Ru BG, Bi RC, Xu XJ (2000) Cysteine-independent polymerization of metallothioneins in solutions and in crystals. Protein Science 9:2302-2312.
Hu JR, Ferreira A, VanEldik LJ (1997) S100 beta induces neuronal cell death through nitric oxide release from astrocytes. Journal of Neurochemistry 69:2294-2301.
Huber KL, Cousins RJ (1993) Zinc-metabolism and metallothionein expression in bone-marrow during erythropoiesis. American Journal of Physiology 264:E770-E775.
Hughes PM, Allegrini PR, Rudin M, Perry VH, Mir AK, Wiessner C (2002) Monocyte chemoattractant protein-1 deficiency is protective in a murine stroke model. Journal of Cerebral Blood Flow and Metabolism 22:308-317.
Huh S, Lee K, Yun HS, Paik DJ, Kim JM, Youn J (2007) Functions of metallothionein generating interleukin-10-producing regulatory CD4(+) T cells potentiate suppression of collagen-induced arthritis. Journal of Microbiology and Biotechnology 17:348-358.
Hung SL, Chang AC, Kato I, Chang NCA (2002) Transient expression of Ym1, a heparin-binding lectin, during developmental hematopoiesis and inflammation. Journal of Leukocyte Biology 72:72-82.
Inoue K, Takano H, Shimada A, Wada E, Yanagisawa R, Sakurai M, Satoh M, Yoshikawa T (2005) Role of metallothionein in coagulatory disturbance and systemic inflammation induced by lipopolysaccharide in mice. Faseb Journal 19:533-+.
Ismail AAA, Walker PL, Cawood ML, Barth JH (2002) Interference in immunoassay is an underestimated problem. Annals of Clinical Biochemistry 39:366-373.
Iszard MB, Liu J, Liu YP, Dalton T, Andrews GK, Palmiter RD, Klaassen CD (1995) Characterization of metallothionein-i-transgenic mice. Toxicology and Applied Pharmacology 133:305-312.
Itoh N, Shibayama H, Kanekiyo M, Namphung D, Nakanishi T, Matsuyama A, Odani T, Tanaka K (2005) Reduced bactericidal activity and nitric oxide production in

metallothionein-deficient macrophages in response to lipopolysaccharide stimulation. Toxicology 216:188-196.
Iuchi Y, Okada F, Onuma K, Onoda T, Asao H, Kobayashi M, Fujii J (2007) Elevated oxidative stress in erythrocytes due to a SOD1 deficiency causes anaemia and triggers autoantibody production. Biochemical Journal 402:219-227.
Jacob C, Maret W, Vallee BL (1998) Control of zinc transfer between thionein, metallothionein, and zinc proteins. Proceedings of the National Academy of Sciences of the United States of America 95:3489-3494.
Jacob ST, Ghoshal K, Sheridan JF (1999) Induction of metallothionein by stress and its molecular mechanisms. Gene Expression 7:301-310.
Johnson TV, Camras CB, Kipnis J (2007) Bacterial DNA confers neuroprotection after optic nerve injury by suppressing CD4(+) CD25(+) regulatory T-Cell activity. Investigative Ophthalmology & Visual Science 48:3441-3449.
Jones TB, Hart RP, Popovich PG (2005) Molecular control of physiological and pathological T-cell recruitment after mouse spinal cord injury. Journal of Neuroscience 25:6576-6583.
Jones TB, Ankeny DP, Guan Z, McGaughy V, Fisher LC, Basso DM, Popovich PG (2004) Passive or active immunization with myelin basic protein impairs neurological function and exacerbates neuropathology after spinal cord injury in rats. Journal of Neuroscience 24:3752-3761.
Kanekiyo M, Itoh N, Kawasaki A, Matsuda K, Nakanishi T, Tanaka K (2002a) Metallothionein is required for zinc-induced expression of the macrophage colony stimulating factor gene. Journal of Cellular Biochemistry 86:145-153.
Kanekiyo M, Itoh N, Kawasaki A, Matsuyama A, Matsuda K, Nakanishi T, Tanaka K (2002b) Metallothionein modulates lipopolysaccharide-stimulated tumour necrosis factor expression in mouse peritioneal macrophages. Biochemical Journal 361:363-369.
Káradóttir R, Hamilton NB, Bakiri Y, Attwell D (2008) Spiking and nonspiking classes of oligodendrocyte precursor glia in CNS white matter. Nature Neuroscience 11:450-456.
Kauppinen TM, Higashi Y, Suh SW, Escartin C, Nagasawa K, Swanson RA (2008) Zinc triggers microglial activation. Journal of Neuroscience 28:5827-5835.
Kaur C, Hao AJ, Wu CH, Ling EA (2001) Origin of microglia. Microscopy Research and Technique 54:2-9.
Kelly EJ, Quaife CJ, Froelick GJ, Palmiter RD (1996) Metallothionein I and II protect against zinc deficiency and zinc toxicity in mice. Journal of Nutrition 126:1782-1790.
Khatai L, Goessler W, Lorencova H, Zangger K (2004) Modulation of nitric oxide-mediated metal release from metallothionein by the redox state of glutathione in vitro. European Journal of Biochemistry 271:2408-2416.
Kiefer CR, Snyder LM (2000) Oxidation and erythrocyte senescence. Current Opinion in Hematology 7:113-116.
Kigerl KA, Gensel JC, Ankeny DP, Alexander JK, Donnelly DJ, Popovich PG (2009) Identification of Two Distinct Macrophage Subsets with Divergent Effects Causing either Neurotoxicity or Regeneration in the Injured Mouse Spinal Cord. Journal of Neuroscience 29:13435-13444.
Kim CH, Kim JH, Lee J, Ahn YS (2003) Zinc-induced NF-kappa B inhibition can be modulated by changes in the intracellular metallothionein level. Toxicology and Applied Pharmacology 190:189-196.
Kimura M, Koizumi S, Otsuka F (1991) Detection of carboxymethylmetallothionein by sodium dodecyl sulfate-polyacrylamide gel-electrophoresis. Methods in Enzymology 205:114-119.

Kimura T, Itoh N (2008) Function of metallothionein in gene expression and signal transduction: Newly found protective role of metallothionein. Journal of Health Science 54:251-260.

King LE, Fraker PJ (2000) Variations in the cell cycle status of lymphopoietic and myelopoietic cells created by zinc deficiency. Journal of Infectious Diseases 182:S16-S22.

King LE, Fraker PJ (2002) Zinc deficiency in mice alters myelopoiesis and hematopoiesis. Journal of Nutrition 132:3301-3307.

King LE, Frentzel JW, Mann JJ, Fraker PJ (2005) Chronic zinc deficiency in mice disrupted T cell lymphopoiesis and erythropoiesis while B cell lymphopoiesis and myelopoiesis were maintained. Journal of the American College of Nutrition 24:494-502.

Kipnis J, Avidan H, Caspi RR, Schwartz M (2004) Dual effect of CD4(+)CD25(+) regulatory T cells in neurodegeneration: A dialogue with microglia. Proceedings of the National Academy of Sciences of the United States of America 101:14663-14669.

Kipnis J, Mizrahi T, Hauben E, Shaked I, Shevach E, Schwartz M (2002) Neuroprotective autoimmunity: Naturally occurring CD4(+)CD25(+) regulatory T cells suppress the ability to withstand injury to the central nervous system. Proceedings of the National Academy of Sciences of the United States of America 99:15620-15625.

Kipnis J, Nevo U, Panikashvili D, Alexandrovich A, Yoles E, Akselrod S, Shohami E, Schwartz M (2003) Therapeutic vaccination for closed head injury. Journal of Neurotrauma 20:559-569.

Kirchhoff F, Dringen R, Giaume C (2001) Pathways of neuron-astrocyte interactions and their possible role in neuroprotection. European Archives of Psychiatry and Clinical Neuroscience 251:159-169.

Knoch ME, Hartnett KA, Hara H, Kandler K, Aizenman E (2008) Microglia induce neurotoxicity Zn2+ release and a K+ current via intraneuronal surge. Glia 56:89-96.

Køhler LB, Berezin V, Bock E, Penkowa M (2003) The role of metallothionein II in neuronal differentiation and survival. Brain Research 992:128-136.

Koike Y, Hisada T, Utsugi M, Ishizuka T, Shimizu Y, Ono A, Murata Y, Hamuro J, Mori M, Dobashi K (2007) Glutathione redox regulates airway hyperresponsiveness and airway inflammation in mice. American Journal of Respiratory Cell and Molecular Biology 37:322-329.

Kostianovsky AM, Maier LM, Anderson RC, Bruce JN, Anderson DE (2008) Astrocytic regulation of human monocytic/microglial activation. Journal of Immunology 181:5425-5432.

Krężel A, Maret WG (2008) Thionein/metallothionein control Zn(II) availability and the activity of enzymes. Journal of Biological Inorganic Chemistry 13:401-409.

Kukačka J, Vajtr D, Huska D, Prusa R, Houstava L, Samal F, Diopan V, Kotaska K, Kizek R (2006) Blood metallothionein, neuron specific enolase, and protein S100B in patients with traumatic brain injury. Neuroendocrinology Letters 27:116-120.

Kwidzinski E, Bechmann I (2007) IDO expression in the brain: a double-edged sword. Journal of Molecular Medicine-Jmm 85:1351-1359.

Lalancette-Hébert M, Gowing G, Simard A, Weng YC, Kriz J (2007) Selective ablation of proliferating microglial cells exacerbates ischemic injury in the brain. Journal of Neuroscience 27:2596-2605.

Lambertsen KL, Gregersen R, Finsen B (2002) Microglial-macrophage synthesis of tumor necrosis factor after focal cerebral ischemia in mice is strain dependent. Journal of Cerebral Blood Flow and Metabolism 22:785-797.

Lambertsen KL, Clausen BH, Babcock AA, Gregersen R, Fenger C, Nielsen HH, Haugaard LS, Wirenfeldt M, Nielsen M, Dagnaes-Hansen F, Bluethmann H, Faergeman NJ, Meldgaard M, Deierborg T, Finsen B (2009) Microglia Protect Neurons against Ischemia by Synthesis of Tumor Necrosis Factor. Journal of Neuroscience 29:1319-1330.

Lansdown ABG, Mirastschijski U, Stubbs N, Scanlon E, Agren MS (2007) Zinc in wound healing: Theoretical, experimental, and clinical aspects. Wound Repair and Regeneration 15:2-16.

Lau JC, Cherian MG (1998) Developmental changes in hepatic metallothionein, zinc, and copper levels in genetically altered mice. Biochemistry and Cell Biology-Biochimie Et Biologie Cellulaire 76:615-623.

Laurino L, Wang XXX, de la Houssaye BA, Sosa L, Dupraz S, Caceres A, Pfenninger KH, Quiroga S (2005) PI3K activation by IGF-1 is essential for the regulation of membrane expansion at the nerve growth cone. Journal of Cell Science 118:3653-3662.

Lazarov-Spiegler O, Solomon AS, ZeevBrann AB, Hirschberg DL, Lavie V, Schwartz M (1996) Transplantation of activated macrophages overcomes central nervous system regrowth failure. Faseb Journal 10:1296-1302.

Lee J, Cacalano G, Camerato T, Toy K, Moore MW, Wood WI (1995) CHEMOKINE BINDING AND ACTIVITIES MEDIATED BY THE MOUSE IL-8 RECEPTOR. Journal of Immunology 155:2158-2164.

Leidenfrost (1966) On fixation of water in diverse fire. International Journal of Heat and Mass Transfer 9:1153-1166.

Lenzlinger PM, Hans VHJ, Joller-Jemelka HI, Trentz O, Morganti-Kossmann MC, Kossmann T (2001) Markers for cell-mediated immune response are elevated in cerebrospinal fluid and serum after severe traumatic brain injury in humans. Journal of Neurotrauma 18:479-489.

Ley K (2003) Arrest chemokines. Microcirculation 10:289-295.

Ley K, Laudanna C, Cybulsky MI, Nourshargh S (2007) Getting to the site of inflammation: the leukocyte adhesion cascade updated. Nature Reviews Immunology 7:678-689.

Li XK, Cai L, Feng WK (2007) Diabetes and metallothionein. Mini-Reviews in Medicinal Chemistry 7:761-768.

Liberto CM, Albrecht PJ, Herx LM, Yong VW, Levison SW (2004) Pro-regenerative properties of cytokine-activated astrocytes. Journal of Neurochemistry 89:1092-1100.

Liesz A, Suri-Payer E, Veltkamp C, Doerr H, Sommer C, Rivest S, Giese T, Veltkamp R (2009) Regulatory T cells are key cerebroprotective immunomodulators in acute experimental stroke. Nature Medicine 15:192-199.

Ling CY, Sandor M, Suresh M, Fabry Z (2006) Traumatic injury and the presence of antigen differentially contribute to T-cell recruitment in the CNS. Journal of Neuroscience 26:731-741.

Little AR, Benkovic SA, Miller DB, O'Callaghan JP (2002) Chemically induced neuronal damage and gliosis: Enhanced expression of the proinflammatory chemokine, monocyte chemoattractant protein (MCP)-1, without a corresponding increase in proinflammatory cytokines. Neuroscience 115:307-320.

Liu J, Liu YP, Habeebu SS, Klaassen CD (1999) Metallothionein-null mice are highly susceptible to the hematotoxic and immunotoxic effects of chronic CdCl2 exposure. Toxicology and Applied Pharmacology 159:98-108.

Liu Y, Zheng JH, Dang WW, Ren HW, Yu MM, Ru BG (2000) The study of direct ELISA and competitive ELISA for rabbit metallothionein: correlation of induction with zinc. Analusis 28:361-366.

Lumpkins K, Bochicchio GV, Zagol B, Ulloa K, Simard JM, Schaub S, Meyer W, Scalea T (2008) Plasma levels of the beta chemokine regulated upon activation, normal T cell expressed, and secreted (RANTES) correlate with severe brain injury. Journal of Trauma-Injury Infection and Critical Care 64:358-361.

Lynes MA, Borghesi LA, Youn JH, Olson EA (1993) Immunomodulatory activities of extracellular metallothionein .1. Metallothionein effects on antibody-production. Toxicology 85:161-177.

Madrigal JLM, Leza JC, Polak P, Kalinin S, Feinstein DL (2009) Astrocyte-Derived MCP-1 Mediates Neuroprotective Effects of Noradrenaline. Journal of Neuroscience 29:263-267.

Mahad DJ, Ransohoff RM (2003) The role of MCP-1 (CCL2) and CCR2 in multiple sclerosis and experimental autoimmune encephalomyelitis (EAE). Seminars in Immunology 15:23-32.

Malaiyandi LM, Dineley KE, Reynolds IJ (2004) Divergent consequences arise from metallothionein overexpression in astrocytes: Zinc buffering and oxidant-induced zinc release. Glia 45:346-353.

Man S, Ubogu EE, Williams KA, Tucky B, Callahan MK, Ransohoff RM (2008) Human brain microvascular endothelial cells and umbilical vein endothelial cells differentially facilitate leukocyte recruitment and utilize chemokines for T cell migration. Clinical & Developmental Immunology:1-8.

Maret W, Vallee BL (1998) Thiolate ligands in metallothionein confer redox activity on zinc clusters. Proceedings of the National Academy of Sciences of the United States of America 95:3478-3482.

Maret W, Jacob C, Vallee BL, Fischer EH (1999) Inhibitory sites in enzymes: Zinc removal and reactivation by thionein. Proceedings of the National Academy of Sciences of the United States of America 96:1936-1940.

Martin R, McFarland HF, McFarlin DE (1992) Immunological aspects of demyelinating diseases. Annual Review of Immunology 10:153-187.

Martinon S, Garcia E, Flores N, Gonzalez I, Ortega T, Buenrostro M, Reyes R, Fernandez-Presas AM, Guizar-Sahagun G, Correa D, Ibarra A (2007) Vaccination with a neural-derived peptide plus administration of glutathione improves the performance of paraplegic rats. European Journal of Neuroscience 26:403-412.

Masters BA, Kelly EJ, Quaife CJ, Brinster RL, Palmiter RD (1994) Targeted disruption of metallothionein-i and metallothionein-ii genes increases sensitivity to cadmium. Proceedings of the National Academy of Sciences of the United States of America 91:584-588.

Mazzeo AT, Kunene NK, Gilman CB, Hamm RJ, Hafez N, Bullock MR (2006) Severe human traumatic brain injury, but not cyclosporin A treatment, depresses activated T lymphocytes early after injury. Journal of Neurotrauma 23:962-975.

McClain C, Cohen D, Phillips R, Ott L, Young B (1991) Increased plasma and ventricular fluid interleukin-6 levels in patients with head-injury. Journal of Laboratory and Clinical Medicine 118:225-231.

McClain CJ, Twyman DL, Ott LG, Rapp RP, Tibbs PA, Norton JA, Kasarskis EJ, Dempsey RJ, Young B (1986) Serum and urine zinc response in head-injured patients. Journal of Neurosurgery 64:224-230.

Medvedeva YV, Lin B, Shuttleworth CW, Weiss JH (2009) Intracellular Zn2+ Accumulation Contributes to Synaptic Failure, Mitochondrial Depolarization, and Cell Death in an Acute Slice Oxygen-Glucose Deprivation Model of Ischemia. Journal of Neuroscience 29:1105-1114.

Michalska AE, Choo KHA (1993) Targeting and germ-line transmission of a null mutation at the metallothionein I-loci and II-loci in mouse. Proceedings of the National Academy of Sciences of the United States of America 90:8088-8092.

Mills CD, Kincaid K, Alt JM, Heilman MJ, Hill AM (2000) M-1/M-2 macrophages and the Th1/Th2 paradigm. Journal of Immunology 164:6166-6173.

Milnerowicz H, Bizon A (2010) Determination of metallothionein in biological fluids using enzyme-linked immunoassay with commercial antibody. Acta Biochimica Polonica 57:99-104.

Mita M, Imura N, Kumazawa Y, Himeno S (2002) Suppressed proliferative response of spleen T cells from metallothionein null mice. Microbiology and Immunology 46:101-107.

Mita M, Satoh M, Shimada A, Okajima M, Azuma S, Suzuki JS, Sakabe K, Hara S, Himeno S (2008) Metallothionein is a crucial protective factor against Helicobacter pylori-induced gastric erosive lesions in a mouse model. American Journal of Physiology-Gastrointestinal and Liver Physiology 294:G877-G884.

Moalem G, Leibowitz-Amit R, Yoles E, Mor F, Cohen IR, Schwartz M (1999a) Autoimmune T cells protect neurons from secondary degeneration after central nervous system axotomy. Nature Medicine 5:49-55.

Moalem G, Gdalyahu A, Shani Y, Otten U, Lazarovici P, Cohen IR, Schwartz M (2000) Production of neurotrophins by activated T cells: Implications for neuroprotective autoimmunity. Journal of Autoimmunity 15:331-345.

Moalem G, Gdalyahu A, Leibowitz-Amit R, Yoles E, Muller-Gilor S, Shani Y, Mor F, Otten U, Lazarovici P, Cohen IR, Schwartz M (1999b) Neuroprotection by autoimmune T cells in injured central nervous system involves T cell-derived neurotrophins. Neuroscience Letters:S30-S30.

Morgan PN, Wehr CM, Macgregor JT, Woodhouse LR, King JC (1995) Zinc-deficiency, erythrocyte production, and chromosomal damage in pregnant rats and their fetuses. Journal of Nutritional Biochemistry 6:263-268.

Moritz KM, Lim GB, Wintour EM (1997) Developmental regulation of erythropoietin and erythropoiesis. American Journal of Physiology-Regulatory Integrative and Comparative Physiology 273:R1829-R1844.

Mosmann TR, Cherwinski H, Bond MW, Giedlin MA, Coffman RL (1986) 2 types of murine helper T-cell clone .1. Definition according to profiles of lymphokine activities and secreted proteins. Journal of Immunology 136:2348-2357.

Mullally AM, Vogelsang GB, Moliterno AR (2004) Wasted sheep and premature infants: the role of trace metals in hematopoiesis. Blood Reviews 18:227-234.

Murata Y, Shimamura T, Hamuro J (2002) The polarization of T(h)1/T(h)2 balance is dependent on the intracellular thiol redox status of macrophages due to the distinctive cytokine production. International Immunology 14:201-212.

Natale JE, Knight JB, Cheng Y, Rome JE, Gallo V (2004) Metallothionein I and II mitigate age-dependent secondary brain injury. Journal of Neuroscience Research 78:303-314.

Neumann J, Sauerzweig S, Roenicke R, Gunzer F, Dinkel K, Ullrich O, Gunzer M, Reymann KG (2008) Microglia cells protect neurons by direct engulfment of invading neutrophil granulocytes: A new mechanism of CNS immune privilege. Journal of Neuroscience 28:5965-5975.

Nielson KB, Winge DR (1983) Order of metal-binding in metallothionein. Journal of Biological Chemistry 258:3063-3069.

Ott L, McClain CJ, Gillespie M, Young B (1994) Cytokines and metabolic dysfunction after severe head-injury. Journal of Neurotrauma 11:447-472.

Palmiter RD (1998) The elusive function of metallothioneins. Proceedings of the National Academy of Sciences of the United States of America 95:8428-8430.

Palmiter RD (2004) Protection against zinc toxicity by metallothionein and zinc transporter 1. Proceedings of the National Academy of Sciences of the United States of America 101:4918-4923.

Palmiter RD, Sandgren EP, Koeller DM, Brinster RL (1993) Distal regulatory elements from the mouse metallothionein locus stimulate gene-expression in transgenic mice. Molecular and Cellular Biology 13:5266-5275.

Pankhurst NW, Ludke SL, King HR, Peter RE (2008) The relationship between acute stress, food intake, endocrine status and life history stage in juvenile farmed Atlantic salmon, Salmo salar. Aquaculture 275:311-318.

Pardridge WM (1998) CNS drug design based on principles of blood-brain barrier transport. Journal of Neurochemistry 70:1781-1792.

Pearson VL, Rothwell NJ, Toulmond S (1999) Excitotoxic brain damage in the rat induces interleukin-1 beta protein in microglia and astrocytes: Correlation with the progression of cell death. Glia 25:311-323.

Penkowa M, Moos T (1995) Disruption of the blood-brain interface in neonatal rat neocortex induces a transient expression of metallothionein in reactive astrocytes. Glia 13:217-227.

Penkowa M, Hidalgo J (2000) Metallothionein I+II expression and their role in experimental autoimmune encephalomyelitis. Glia 32:247-263.

Penkowa M, Hidalgo J (2001) Metallothionein treatment reduces proinflammatory cytokines IL-6 and TNF-alpha and apoptotic cell death during experimental autoimmune encephalomyelitis (EAE). Experimental Neurology 170:1-14.

Penkowa M, Carrasco J, Giralt M, Moos T, Hidalgo J (1999a) CNS wound healing is severely depressed in metallothionein I and II-deficient mice. Journal of Neuroscience 19:2535-2545.

Penkowa M, Giralt M, Thomsen PS, Carrasco J, Hidalgo J (2001a) Zinc or copper deficiency-induced impaired inflammatory response to brain trauma may be caused by the concomitant metallothionein changes. Journal of Neurotrauma 18:447-463.

Penkowa M, Espejo C, Martinez-Caceres EM, Montalban X, Hidalgo J (2003) Increased demyelination and axonal damage in metallothionein I+II-deficient mice during experimental autoimmune encephalomyelitis. Cellular and Molecular Life Sciences 60:185-197.

Penkowa M, Giralt M, Moos T, Thomsen PS, Hernandez J, Hidalgo J (1999b) Impaired inflammatory response to glial cell death in genetically metallothionein-I- and -II-deficient mice. Experimental Neurology 156:149-164.

Penkowa M, Espejo C, Martinez-Caceres EM, Poulsen CB, Montalban X, Hidalgo J (2001b) Altered inflammatory response and increased neurodegeneration in metallothionein I plus II deficient mice during experimental autoimmune encephalomyelitis. Journal of Neuroimmunology 119:248-260.

Penkowa M, Moos T, Carrasco J, Hadberg H, Molinero A, Bluethmann H, Hidalgo J (1999c) Strongly compromised inflammatory response to brain injury in interleukin-6-deficient mice. Glia 25:343-357.

Penkowa M, Florit S, Giralt M, Quintana A, Molinero A, Carrasco J, Hidalgo J (2005) Metallothionein reduces central nervous system inflammation, neuro degeneration, and cell death following kainic acid-induced epileptic seizures. Journal of Neuroscience Research 79:522-534.

Penkowa M, Tio L, Giralt M, Quintana A, Molinero A, Atrian S, Vasak M, Hidalgo J (2006a) Specificity and divergence in the neurobiologic effects of different metallothioneins after brain injury. Journal of Neuroscience Research 83:974-984.

Penkowa M, Caceres M, Borup R, Nielsen FC, Poulsen CB, Quintana A, Molinero A, Carrasco J, Florit S, Giralt M, Hidalgo J (2006b) Novel roles for metallothionein-I plus II (MT-I plus II) in defense responses, neurogenesis, and tissue restoration after traumatic brain injury: Insights from global gene expression profiling in wild-type and MT-I plus II knockout mice. Journal of Neuroscience Research 84:1452-1474.

Peterson JD, Herzenberg LA, Vasquez K, Waltenbaugh C (1998) Glutathione levels in antigen-presenting cells modulate Th1 versus Th2 response patterns. Proceedings of the National Academy of Sciences of the United States of America 95:3071-3076.

Philcox JC, Coyle P, Michalska A, Choo KHA, Rofe AM (1995) Endotoxin-induced inflammation does not cause hepatic zinc accumulation in mice lacking metallothionein gene-expression. Biochemical Journal 308:543-546.

Piccio L, Rossi B, Scarpini E, Laudanna C, Giagulli C, Issekutz AC, Vestweber D, Butcher EC, Constantin G (2002) Molecular mechanisms involved in lymphocyte recruitment in inflamed brain microvessels: Critical roles for P-selectin glycoprotein ligand-1 and heterotrimeric G(i)-linked receptors. Journal of Immunology 168:1940-1949.

Ponomarev ED, Maresz K, Tan Y, Dittel BN (2007) CNS-Derived interleukin-4 is essential for the regulation of autoimmune inflammation and induces a state of alternative activation in microglial cells. Journal of Neuroscience 27:10714-10721.

Potter EG, Cheng Y, Natale JE (2009) Deleterious Effects of Minocycline After In Vivo Target Deprivation of Thalamocortical Neurons in the Immature, Metallothionein-deficient Mouse Brain. Journal of Neuroscience Research 87:1356-1368.

Potter EG, Cheng Y, Knight JB, Gordish-Dressman H, Natale JE (2007) Metallothionein I and II attenuate the thalamic microglial response following traumatic axotomy in the immature brain. Journal of Neurotrauma 24:28-42.

Prasad AS (2007) Zinc: mechanisms of host defense. Journal of Nutrition 137:1345-1349.

Raes G, De Baetselier P, Noel W, Beschin A, Brombacher F, Hassanzadeh G (2002) Differential expression of FIZZ1 and Ym1 in alternatively versus classically activated macrophages. Journal of Leukocyte Biology 71:597-602.

Rahman MT, De Ley M (2001) Metallothionein isogene transcription in red blood cell precursors from human cord blood. European Journal of Biochemistry 268:849-856.

Rahman MT, Vandingenen A, De Ley M (2000) Metallothionein biosynthesis in human RBC precursors. Cellular Physiology and Biochemistry 10:237-242.

Raivich G (2005) Like cops on the beat: the active role of resting microglia. Trends in Neurosciences 28:571-573.

Rancan M, Bye N, Otto VI, Trentz O, Kossmann T, Frentzel S, Morganti-Kossmann MC (2004) The chemokine fractalkine in patients with severe traumatic brain injury and a mouse model of closed head injury. Journal of Cerebral Blood Flow and Metabolism 24:1110-1118.

Reeves PG (1998) Copper metabolism in metallothionein null mice fed a high-zinc diet. Journal of Nutritional Biochemistry 9:598-601.

Rhodes JKJ, Sharkey J, Andrews PJD (2009) The Temporal Expression, Cellular Localization, and Inhibition of the Chemokines MIP-2 and MCP-1 after Traumatic Brain Injury in the Rat. Journal of Neurotrauma 26:507-525.

Robertson CL, Scafidi S, McKenna MC, Fiskum G (2009) Mitochondrial mechanisms of cell death and neuroprotection in pediatric ischemic and traumatic brain injury. Experimental Neurology 218:371-380.

Rofe AM, Winters N, Hinskens B, Philcox JC, Coyle P (1999) The role of the pancreas in intestinal zinc secretion in metallothionein-null mice. Pancreas 19:69-75.

Ryu MS, Lichten LA, Liuzzi JP, Cousins RJ (2008) Zinc transporters ZnT1 (Slc30a1), Zip8 (Slc39a8), and Zip10 (Slc39a10) in mouse red blood cells are differentially regulated during erythroid development and by dietary zinc deficiency. Journal of Nutrition 138:2076-2083.

Saito S, Kojima Y (1997) Differential role of metallothionein on Zn, Cd and Cu accumulation in hepatic cytosol of rats. Cellular and Molecular Life Sciences 53:267-270.

Sakurai A, Hara S, Okano N, Kondo Y, Inoue J, Imura N (1999) Regulatory role of metallothionein in NF-kappa B activation. Febs Letters 455:55-58.

Sandhir R, Puri V, Klein RM, Berman NE (2004) Differential expression of cytokines and chemokines during secondary neuron death following brain injury in old and young mice. Neuroscience Letters 369:28-32.

Sankarapandi S, Zweier JL, Mukherjee G, Quinn MT, Huso DL (1998) Measurement and characterization of superoxide generation in microglial cells: Evidence for an NADPH oxidase-dependent pathway. Archives of Biochemistry and Biophysics 353:312-321.

Santambrogio L, Belyanskaya SL, Fischer FR, Cipriani B, Brosnan CF, Ricciardi-Castagnoli P, Stern LJ, Strominger JL, Riese R (2001) Developmental plasticity of CNS microglia. Proceedings of the National Academy of Sciences of the United States of America 98:6295-6300.

Savaridas T, Andrews PJD, Harris B (2004) Cortisol dynamics following acute severe brain injury. Intensive Care Medicine 30:1479-1483.

Saxena RK, Khandelwal S (2009) Aging and destruction of blood erythrocytes in mice. Current Science 97:500-507.

Schmued LC, Stowers CC, Scallet AC, Xu LL (2005) Fluoro-Jade C results in ultra high resolution and contrast labeling of degenerating neurons. Brain Research 1035:24-31.

Schnell L, Fearn S, Klassen H, Schwab ME, Perry VH (1999) Acute inflammatory responses to mechanical lesions in the CNS: differences between brain and spinal cord. European Journal of Neuroscience 11:3648-3658.

Schwartz M, Butovsky O, Bruck W, Hanisch UK (2006) Microglial phenotype: is the commitment reversible? Trends in Neurosciences 29:68-74.

Sedgwick JD, Schwender S, Imrich H, Dorries R, Butcher GW, Termeulen V (1991) Isolation and direct characterization of resident microglial cells from the normal and inflamed central-nervous-system. Proceedings of the National Academy of Sciences of the United States of America 88:7438-7442.

Séguin R, Biernacki K, Prat A, Wosik K, Kim HJ, Blain M, McCrea E, Bar-Or A, Antel JP (2003) Differential effects of Th1 and Th2 lymphocyte supernatants on human microglia. Glia 42:36-45.

Selby C (1999) Interference in immunoassay. Annals of Clinical Biochemistry 36:704-721.

Semple BD, Bye N, Rancan M, Ziebell JM, Morganti-Kossmann MC (2010) Role of CCL2 (MCP-1) in traumatic brain injury (TBI): evidence from severe TBI

patients and CCL2$^{-/-}$ mice. Journal of Cerebral Blood Flow and Metabolism 30:769-782.

Serpe CJ, Coers S, Sanders VM, Jones KJ (2003) CD4+ T, but not CD8+ or B, lymphocytes mediate facial motoneuron survival after facial nerve transection. Brain Behavior and Immunity 17:393-402.

Serpe CJ, Kohm AP, Hupperbauer CB, Sanders VM, Jones KJ (1999) Exacerbation of Facial Motoneuron Loss after Facial Nerve Transection in Severe Combined Immunodeficient (scid) Mice. Journal of Neuroscience 19.

Sharma HS, Nyberg F, Westman J, Alm P, Gordh T, Lindholm D (1998) Brain derived neurotrophic factor and insulin like growth factor-1 attenuate upregulation of nitric oxide synthase and cell injury following trauma to the spinal cord - An immunohistochemical study in the rat. Amino Acids 14:121-129.

Shaw CF, Savas MM, Petering DH (1991) Ligand substitution and sulfhydryl reactivity of metallothionein. Methods in Enzymology 205:401-414.

Shechter R, London A, Varol C, Raposo C, Cusimano M, Yovel G, Rolls A, Mack M, Pluchino S, Martino G, Jung S, Schwartz M (2009) Infiltrating Blood-Derived Macrophages Are Vital Cells Playing an Anti-inflammatory Role in Recovery from Spinal Cord Injury in Mice. Plos Medicine 6.

Sherman DL, Brophy PJ (2005) Mechanisms of axon ensheathment and myelin growth. Nature Reviews Neuroscience 6:683-690.

Shohami E, Gati I, Beit-Yannai E, Trembovler V, Kohen R (1999) Closed head injury in the rat induces whole body oxidative stress: Overall reducing antioxidant profile. Journal of Neurotrauma 16:365-376.

Siddiqui AH (2008) Increased intestinal permeability in rats subjected to traumatic frontal lobe percussion brain injury - Comment. Journal of Trauma-Injury Infection and Critical Care 64:137-138.

Simpson E (2006) A historical perspective on immunological privilege. Immunological Reviews 213:12-22.

Skabo SJ, Holloway AF, West AK, Chuah MI (1997) Metallothioneins 1 and 2 are expressed in the olfactory mucosa of mice in untreated animals and during the regeneration of the epithelial layer. Biochemical and Biophysical Research Communications 232:136-142.

Skihar V, Silva C, Chojnacki A, Doring A, Stallcup WB, Weiss S, Yong VW (2009) Promoting oligodendrogenesis and myelin repair using the multiple sclerosis medication glatiramer acetate. Proceedings of the National Academy of Sciences of the United States of America 106:17992-17997.

Smith DF, Galkina E, Ley K, Huo YQ (2005) GRO family chemokines are specialized for monocyte arrest from flow. American Journal of Physiology-Heart and Circulatory Physiology 289:H1976-H1984.

Sorrells SF, Caso JR, Munhoz CD, Sapolsky RM (2009) The Stressed CNS: When Glucocorticoids Aggravate Inflammation. Neuron 64:33-39.

Spahl DU, Berendji-Grun D, Suschek CV, Kolb-Bachofen V, Kroncke KD (2003) Regulation of zinc homeostasis by inducible NO synthase-derived NO: Nuclear translocation and intranuclear metallothionein Zn2+ release. Proceedings of the National Academy of Sciences of the United States of America 100:13952-13957.

Span PN, Grebenchtchikov N, Geurts-Moespot J, Sweep CGJ (2003) Screening for interference in immunoassays. Clinical Chemistry 49:1708-1709.

Sredni-Kenigsbuch D (2002) Th1/Th2 cytokines in the central nervous system. International Journal of Neuroscience 112:665-703.

Sroga JM, Jones TB, Kigerl KA, McGaughy VM, Popovich PG (2003) Rats and mice exhibit distinct inflammatory reactions after spinal cord injury. Journal of Comparative Neurology 462:223-240.

Stirling DP, Yong VW (2008) Dynamics of the inflammatory response after murine spinal cord injury revealed by flow cytometry. Journal of Neuroscience Research 86:1944-1958.

Stirling DP, Liu SH, Kubes P, Yong VW (2009) Depletion of Ly6G/Gr-1 Leukocytes after Spinal Cord Injury in Mice Alters Wound Healing and Worsens Neurological Outcome. Journal of Neuroscience 29:753-764.

Sudo S, Tanaka J, Toku K, Desaki J, Matsuda S, Arai T, Sakanaka M, Maeda N (1998) Neurons induce the activation of microglial cells in vitro. Experimental Neurology 154:499-510.

Suemori S, Shimazawa M, Kawase K, Satoh M, Nagase H, Yamamoto T, Hara H (2006) Metallothionein, an endogenous antioxidant, protects against retinal neuron damage in mice. Investigative Ophthalmology & Visual Science 47:3975-3982.

Sullivan VK, Burnett FR, Cousins RJ (1998) Metallothionein expression is increased in monocytes and erythrocytes of young men during zinc supplementation. Journal of Nutrition 128:707-713.

Summer KH, Klein D (1991) Determination of metallothionein in biological-materials. Methods in Enzymology 205:57-60.

Suzuki S, Yamamoto M, Sato M (2009) Modulated Responses to Restraint Stress and Inflammation in Metallothionein-Null Mice. Journal of Health Science 55:554-559.

Suzuki T, Dale GL (1987) Biotinylated erythrocytes - Invivo survival and invitro recovery. Blood 70:791-795.

Suzuki Y, Apostolova MD, Cherian MG (2000) Astrocyte cultures from transgenic mice to study the role of metallothionein in cytotoxicity of tert-butyl hydroperoxide. Toxicology 145:51-62.

Swierzcek S, Abuknesha RA, Chivers I, Baranovska I, Cunningham P, Price RG (2004) Enzyme-immunoassay for the determination of metallothionein in human urine: application to environmental monitoring. Biomarkers 9:331-340.

Szitanyi Z, Nemes C, Rozlosnik N (1996) Metallothionein and heavy metal concentration in blood. Microchemical Journal 54:246-251.

Takano H, Inoue K, Yanagisawa R, Sato M, Shimada A, Morita T, Sawada M, Nakamura K, Sanbongi C, Yoshikawa T (2004) Protective role of metallothionein in acute lung injury induced by bacterial endotoxin. Thorax 59:1057-1062.

Tan AM, Zhang WB, Levine JM (2005) NG2: a component of the glial scar that inhibits axon growth. Journal of Anatomy 207:717-725.

Tanaka K, Min KS, Onosaka S, Fukuhara C, Ueda M (1985) The origin of metallothionein in red blood-cells. Toxicology and Applied Pharmacology 78:63-68.

Tang WF, Kido T, Gross WA, Nogawa K, Sabbioni E, Shaikh ZA (1999) Measurement of cadmium-induced metallothionein in urine by ELISA and prevention of overestimation due to polymerization. Journal of Analytical Toxicology 23:153-158.

Terao S, Yilmaz G, Stokes KY, Russell J, Ishikawa M, Kawase T, Granger DN (2008) Blood cell-derived RANTES mediates cerebral microvascular dysfunction, inflammation, and tissue injury after focal ischemia-reperfusion. Stroke 39:2560-2570.

Testa U (2004) Apoptotic mechanisms in the control of erythropoiesis. Leukemia 18:1176-1199.

Thomas DG, Linton HJ, Garvey JS (1986) Fluorometric ELISA for the detection and quantitation of metallothionein. Journal of Immunological Methods 89:239-247.

Tontsch U, Rott O (1993) Cortical-neurons selectively inhibit MHC class-II induction in astrocytes but not in microglial cells. International Immunology 5:249-254.

Ubogu EE, Callahan MK, Tucky BH, Ransohoff RM (2006a) CCR5 expression on monocytes and T cells: Modulation by transmigration across the blood-brain barrier in vitro. Cellular Immunology 243:19-29.

Ubogu EE, Callahan MK, Tucky BH, Ransohoff RM (2006b) Determinants of CCL5-driven mononuclear cell migration across the blood-brain barrier. Implications for therapeutically modulating neuroinflammation. Journal of Neuroimmunology 179:132-144.

Uchida Y, Takio K, Titani K, Ihara Y, Tomonaga M (1991) the growth inhibitory factor that is deficient in the Alzheimer's-disease brain is a 68-amino acid metallothionein-like protein. Neuron 7:337-347.

Upender MB, Naegele JR (1999) Activation of microglia during developmentally regulated cell death in the cerebral cortex. Developmental Neuroscience 21:491-505.

van Lookeren Campagne M, Thibodeaux H, van Bruggen N, Cairns B, Gerlai R, Palmer JT, Williams SP, Lowe DG (1999) Evidence for a protective role of metallothionein-1 in focal cerebral ischemia. Proceedings of the National Academy of Sciences of the United States of America 96:12870-12875.

Vasto S, Mocchegiani E, Malavolta M, Cuppari I, Listi F, Nuzzo D, Ditta V, Candore G, Caruso C (2007) Zinc and inflammatory/immune response in aging. Biogerontology: Mechanisms and Interventions 1100:111-122.

Voskuhl RR, Peterson RS, Song BB, Ao Y, Morales LBJ, Tiwari-Woodruff S, Sofroniew MV (2009) Reactive Astrocytes Form Scar-Like Perivascular Barriers to Leukocytes during Adaptive Immune Inflammation of the CNS. Journal of Neuroscience 29:11511-11522.

Waelput W, Broekaert D, Vandekerckhove J, Brouckaert P, Tavernier J, Libert C (2001) A mediator role for metallothionein in tumor necrosis factor-induced lethal shock. Journal of Experimental Medicine 194:1617-1624.

Wake H, Moorhouse AJ, Jinno S, Kohsaka S, Nabekura J (2009) Resting Microglia Directly Monitor the Functional State of Synapses In Vivo and Determine the Fate of Ischemic Terminals. Journal of Neuroscience 29:3974-3980.

Walsh CT, Sandstead HH, Prasad AS, Newberne PM, Fraker PJ (1994) Zinc - health-effects and research priorities for the 1990s. Environmental Health Perspectives 102:5-46.

Walter BA, Valera VA, Takahashi S, Ushiki T (2006) The olfactory route for cerebrospinal fluid drainage into the peripheral lymphatic system. Neuropathology and Applied Neurobiology 32:388-396.

Wang FA, Wang LY, Wright D, Parmely MJ (1999) Redox imbalance differentially inhibits lipopolysaccharide-induced macrophage activation in the mouse liver. Infection and Immunity 67:5409-5416.

Wastney ME, House WA (2008) Development of a Compartmental Model of Zinc Kinetics in Mice. Journal of Nutrition 138:2148-2155.

Weiss S, Kotsch K, Francuski M, Reutzel-Selke A, Mantouvalou L, Klemz R, Kuecuek O, Jonas S, Wesslau C, Ulrich F, Pascher A, Volk HD, Tullius SG, Neuhaus P, Pratschke J (2007) Brain death activates donor organs and is associated with a worse I/R injury after liver transplantation. American Journal of Transplantation 7:1584-1593.

Wekerle H, Sun D, Oropezawekerle RL, Meyermann R (1987) Immune reactivity in the nervous-system - modulation of lymphocyte-T activation by glial-cells. Journal of Experimental Biology 132:43-57.

Welch JS, Escoubet-Lozach L, Sykes DB, Liddiard K, Greaves DR, Glass CK (2002) T(H)2 cytokines and allergic challenge induce YM1 expression in macrophages by a STAT6-dependent mechanism. Journal of Biological Chemistry 277:42821-42829.

Werner C, Engelhard K (2007) Pathophysiology of traumatic brain injury. British Journal of Anaesthesia 99:4-9.

Whalen MJ, Carlos TM, Kochanek PM, Wisniewski SR, Bell MJ, Clark RSB, DeKosky ST, Marion DW, Adelson PD (2000) Interleukin-8 is increased in cerebrospinal fluid of children with severe head injury. Critical Care Medicine 28:929-934.

Wilkins A, Chandran S, Compston A (2001) A role for oligodendrocyte-derived IGF-1 in trophic support of cortical neurons. Glia 36:48-57.

Wong CP, Song Y, Elias VD, Magnusson KR, Ho E (2009) Zinc supplementation increases zinc status and thymopoiesis in aged mice. Journal of Nutrition 139:1393-1397.

Xie L, Poteet1 EC, Li W, Scott AE, Liu R, Wen Y, Ghorpade A, Simpkins JW, Yang S (2010) Modulation of polymorphonuclear neutrophil functions by astrocytes. Journal of Neuroinflammation epub ahead of print.

Yadav MC, Burudi EME, Alirezaei M, Flynn CC, Lanigan CM, Fox HS (2007) IFN-gamma-induced IDO and WRS expression in microglia is differentially regulated by IL-4. Glia 55:1385-1396.

Yang Y, Maret W, Vallee BL (2001) Differential fluorescence labeling of cysteinyl clusters uncovers high tissue levels of thionein. Proceedings of the National Academy of Sciences of the United States of America 98:5556-5559.

Yeiser EC, Vanlandingham JW, Levenson CW (2002) Moderate zinc deficiency increases cell death after brain injury in the rat. Nutritional Neuroscience 5:345-352.

Young B, Ott L, Kasarskis E, Rapp R, Moles K, Dempsey RJ, Tibbs PA, Kryscio R, McClain C (1996) Zinc supplementation is associated with improved neurologic recovery rate and visceral protein levels of patients with severe closed head injury. Journal of Neurotrauma 13:25-34.

Zangger K, Shen G, Oz G, Otvos JD, Armitage IM (2001) Oxidative dimerization in metallothionein is a result of intermolecular disulphide bonds between cysteines in the alpha-domain. Biochemical Journal 359:353-360.

Zeng J, Heuchel R, Schaffner W, Kagi JHR (1991) Thionein (apometallothionein) can modulate dna-binding and transcription activation by zinc finger containing factor-Sp1. Febs Letters 279:310-312.

Zhou ZB, Ding HQ, Qin FJ, Liu L, Cheng S (2003) Effect of Zn-7-metallothionein on oxidative stress in liver of rats with severe thermal injury. Acta Pharmacologica Sinica 24:764-770.

Zhou ZX, Wang LP, Song ZY, Saari JT, McClain CJ, Kang YJ (2004) Abrogation of nuclear factor-kappa B activation is involved in zinc inhibition of lipopolysaccharide-induced tumor necrosis factor-alpha production and liver injury. American Journal of Pathology 164:1547-1556.

Zimmer H, Riese S, Regnier-Vigouroux A (2003) Functional characterization of mannose receptor expressed by immunocompetent mouse microglia. Glia 42:89-100.

Zygun DA, Kortbeek JB, Fick GH, Laupland KB, Doig CJ (2005) Non-neurologic organ dysfunction in severe traumatic brain injury. Critical Care Medicine 33:654-660.